Pontifícia Universidade Católica
do Rio de Janeiro

Vinícius Lionel Mateus

Multivariate and interdisciplinary air pollution case studies at rural, urban-coastal, and protected sites: An endeavor to advance the public and environmental health comprehension

Tese de Doutorado

Thesis presented to the Programa de Pós–graduação em Química of PUC-Rio in partial fulfillment of the requirements for the degree of Doutor em Química.

Advisor: Prof. Adriana Gioda

Rio de Janeiro
April 2017

Pontifícia Universidade Católica
do Rio de Janeiro

Vinícius Lionel Mateus

Multivariate and interdisciplinary air pollution case studies at rural, urban-coastal, and protected sites: An endeavor to advance the public and environmental health comprehension

Thesis presented to the Programa de Pós–graduação em Química of PUC-Rio in partial fulfillment of the requirements for the degree of Doutor. Approved by the undersigned Examination Committee.

Prof. Adriana Gioda
Advisor
Departamento de Química – PUC-Rio

Prof. Tatiana Dillenburg Saint'Pierre
Pontifícia Universidade Católica do Rio de Janeiro – PUC-Rio

Prof. Sérgio Machado Corrêa
Universidade do Estado do Rio de Janeiro – UERJ

Prof. Luiz Francisco Pires Guimarães Maia
Universidade Federal do Estado do Rio de Janeiro – UFRJ

Prof. Ricardo Queiroz Aucélio
Pontifícia Universidade Católica do Rio de Janeiro – PUC-Rio

Prof. Márcio da Silveira Carvalho
Vice Dean of Graduate Studies
Centro Técnico Científico – PUC-Rio

Rio de Janeiro, April 28th, 2017

Vinícius Lionel Mateus

Holds a BSc degree in Chemistry (Fundação Técnico- Educacional Souza Marques, 2009) and a MSc degree in Analytical Chemistry (Pontifícia Universidade Católica do Rio de Janeiro, 2012).

Bibliographic data

Lionel Mateus, Vinícius

Multivariate and interdisciplinary air pollution case studies at rural, urban-coastal, and protected sites: An endeavor to advance the public and environmental health comprehension / Vinícius Lionel Mateus; orientador: Adriana Gioda. – 2017.

v., 202 f: il. color. ; 30 cm

Tese (doutorado) - Pontifícia Universidade Católica do Rio de Janeiro, Departamento de Química.

Inclui bibliografia

1. Química - Teses – Teses. 2. Poluição do ar;. 3. Material particulado;. 4. Saúde ambiental;. 5. R. I. Gioda, Adriana. II. Pontifícia Universidade Católica do Rio de Janeiro. Departamento de Química. III. Título.

CDD: 540

I would like to dedicate this work to my loving parents, Cláudio (*In memorian*) and Eliana, and to my loved uncles, Hélio (*In memorian*) and Helena, for their support and care which forged my emotional intelligence.

But as a work of science, I dedicate it to whoever is hunger and thirsty for knowledge.

Acknowledgements

I would like to thank my supervisor, Prof. Adriana Gioda, for providing me with the research support, flexibility, and research coaching. I am so thankful to God for your very existence.

I would like to thank CAPES (specially Prof. Luiz Drude, the coordinator of the INCT-TMCOCEAN Project, which provided my initial months of scholarship).

I would like to thank CNPq for my Science without Borders (SwB) scholarship (200426/2014-1), which allowed me to develop my research during 1 year in the University of Southern Denmark.

I would like to thank Prof. Tatiana Dillenburg Saint'Piere (LABSPECTRO) for the collaboration in the ICP-MS and ICP OES analysis, congresses fees, and for sharing all their lab infrastructure.

I would like to thank Prof. Ricardo Aucélio (LEEA), the technicians Paulo and Júlio for the collaboration in the TOC analyses and for providing ultrapure water as needed.

I would like to thank Prof. José Marcus Godoy (LABAGUAS), Dr. Ana and the technicians Diogo and Mônica for providing assistance with the setting process of our IC equipment as well as for providing ultrapure water as needed.

I would like to thank Dr. Rosa I. Rodríguez-Cotto and Prof. Braulio D. Jiménez-Vélez from the University of Puerto Rico (UPR) for the toxicological analyses of my samples.

I would like to thank Prof. Juliane Ventura-Lima, Prof. Carolina R. Gioda, and Prof. Jose Montserrat from the Federal University of the Rio Grande (FURG) for providing me all the infrastructure at the lab and outside, during my 2 weeks stay for the white shrimp bioaccumulation experiments.

I would like to thank Prof. Luiz F. P. G. Maia from the Federal University of Rio de Janeiro (UFRJ) for providing the samples from the protected areas and for travel support.

I would like to thank Prof. Victoria Blanes-Vidal, Prof. Esmaeil S. Nadimi, and Dr. Mohammed-Hossein Ramezani from the University of Southern Denmark (SDU) for hosting me at the πSec group of signal processing and providing me research guidance during my 1 year SwB stay at SDU.

I would like to thank the jury for kindly accept the invitation, for their flexibility and great contributions to this thesis.

I would like to thank the Department of Chemistry at PUC-Rio (specially our secretary Fátima Almeida).

Last but not least, I would to thank all my friends specially the ones from the research front (LQA, LABSPECTRO, FURG, and University of Southern Denmark) for keeping me sane and nurtured with healthy relationships.

Abstract

Lionel Mateus, Vinícius; Gioda, Adriana (Advisor). **Multivariate and interdisciplinary air pollution case studies at rural, urban-coastal, and protected sites: An endeavor to advance the public and environmental health comprehension**. Rio de Janeiro, 2017. 202p. Tese de Doutorado – Departamento de Química, Pontifícia Universidade Católica do Rio de Janeiro.

Air pollution is a worldwide concern that relates to multiple pollutants and its complex relationships with many factors such as local meteorology and land use. Numerous studies state that exposure to air pollution increases the risk of mortality, respiratory symptoms, lung inflammation, and oxidative stress. However, some studies examining public and environmental health adverse effects associated with air pollution consider only criteria pollutant levels (e.g., particulate matter, PM). This work builds mostly on the non-criteria pollutants using the following approaches: 1) long-term monitoring; 2) toxicological and bioaccumulation essays; 3) application of state-of-the-art statistical models; and 4) a closer look at the increased exposure to which rural residents have been exposed.

Keywords

Air pollution; Particulate matter; Environmental health; R

Resumo

Lionel Mateus, Vinícius; Gioda, Adriana. **Estudo de casos multivariados e interdisciplinares de poluição atmosférica em zonas rural, costeira-urbana e áreas preservadas: Um esforço para melhorar a compreensão da saúde pública e ambiental**. Rio de Janeiro, 2017. 202p. Tese de Doutorado – Departamento de Química, Pontifícia Universidade Católica do Rio de Janeiro.

A poluição do ar é um assunto de preocupação mundial que se relaciona com poluentes múltiplos e suas relações complexas com muitos fatores, tais como meteorologia local e uso da terra. Numerosos estudos afirmam que a exposição à poluição do ar aumenta o risco de mortalidade, sintomas respiratórios, inflamação pulmonar e estresse oxidativo. No entanto, alguns estudos que examinam os efeitos adversos para a saúde pública e ambiental associados à poluição atmosférica consideram apenas os níveis de poluentes legislados (por exemplo, material particulado, MP). Este trabalho baseia-se principalmente nos poluentes ainda não legislados usando as seguintes abordagens: 1) monitoramento de longo período; 2) ensaios toxicológicos e de bioacumulação; 3) aplicação de modelos estatísticos de complexos; e 4) um olhar mais atento à exposição aumentada a que os residentes rurais têm sido expostos.

Palavras-chave

Poluição do ar; Material particulado; Saúde ambiental; R

Table of Contents

List of Figures

List of Tables

List of Abreviations

AD – Aerodynamic Diameter
CIT – Conditional Inference Trees
CMB – Chemical Mass Balance
DF – Deferoxamine Mesylate
FLONA – National Forest Mario Xávier
HCA – Hierarchical Cluster Analysis
IC – Ion Chromatography
ICP-MS – Inductively Coupled Plasma Optical Emission Spectrometry
ICP OES – Inductively Coupled Plasma Mass Spectrometry
INEA – Environmental Institute of Rio de Janeiro
INMET – National Institute of Meteorology
PCA – Principal Component Analysis
PAH – Polycyclic Aromatic Hydrocarbons
PM – Particulate Matter
PMF – Positive Matrix Factorization
DL – Detection Limit
MRRJ – Metropolitan Region of Rio de Janeiro
PARNASO/PARNA – Serra dos Órgãos National Park
QA/QC – Quality Assurance/Quality Control
RJ – Rio de Janeiro
RF – Random Forests
SEM – Structural Equation Modelling
SRM® – Standard Reference Material
TSP – Total Suspended Particles
TWSC – Total Water-Soluble Carbon
UNMIX – EPA Receptor Model Unmix
WSIC – Water-Soluble Inorganic Carbon
WSIS – Water-Soluble Inorganic Species
WSOC – Water-Soluble Organic Carbon

"Leave your simple ways and you will live;
walk in the way of insight."

King Solomon, *Proverbs 9:6 (NIV).*

1
Introduction

1.0.1
Atmospheric pollution

Aerosols are at the core of many questions in the environmental sciences. This importance is due to its implication on climate, public health, and the atmosphere per se. Given their size, chemical composition, and form, they can absorb or scatter radiation, elicit or enhance health symptoms as well as alter the distribution of atmospheric chemicals and dynamic of atmospheric reactions (1). Aerosols (also known as particulate matter, PM) are defined as a suspension of solid or liquid particles in a gas. These particles can be generated by human activities (i.e., anthropogenic) or by natural processes (i.e., primary biological aerosol particles) (2).

Particulate matter is often classified according to its aerodynamic diameter (AD) as: Total suspended particles (TSP, AD $<$ 100 μm), particulate matter with AD $<$ 10 μm (PM_{10}), particulate matter with AD $<$ 2.5 μm ($PM_{2.5}$), and particulate matter with AD $<$ 1 μm (PM_1) (1, 3).

1.0.2
Toxicological effects of particulate matter

There is strong evidence in the literature that support an increased degree of toxicity associated to PM as the AD decreases (4). The formation of the so-called fine particulate ($PM_{2.5}$) is mainly associated to anthropogenic sources, which result in particles that reach deeper into the respiratory system and trigger toxicological effects due to its chemical composition (1, 3, 5). Recently, there is an increased interest in the identification of the individual components of $PM_{2.5}$ and its association with human health effects (6).

The chemical composition of PM varies as a function of multiple variables. However, its commonly reported components are inorganic species (sulfates, nitrates, ammonium, sea-salts), organic compounds (carboxylic acids, aminoacids, PAH - polycyclic aromatic hydrocarbons), and metals. These compound were already associated with adverse health effects (7, 8).

It is documented that epithelial cells take part in allergic/inflammatory processes (9). However, the chronic inflammation can yield to diseases (10). Aqueous extracts of $PM_{2.5}$ were associated to the increase of IL-6 (11), an inflammatory cytokine. Gioda et al. (11), reported V levels as the most important PM component to the increase of cytokines.

1.0.3 Ecotoxicology

Due to the presence of metals associated to the generation of reactive oxygen species (ROS) (e.g., Fe and Cu), the exposure of the fauna and flora to PM represents an environmental risk (12, 13). The exposure of animals to metals can also affect the reproductive functions as well as produce pro-inflammatory and systemic vascular effects (14, 15).

1.0.3.1 Toxic effects of metals to aquatic organisms

Lesions in different aquatic organisms were reported as consequence of metal exposure: fishes (16), molluscs (17), and shrimps (18). In fishes, there is a concerning about the absorption and metabolism of metals, via gills, before reaching the liver (19). Besides that, authors reported histological damages to gills, but these findings are related to higher concentration of single metals (Cd, Cu, Pb, and Zn) in different species of shrimps (18, 20, 21).

1.0.4 Source apportionment

A common task in the field of atmospheric chemistry studies, is to draw conclusions about sources based on ambient data, which is called source apportionment. According to Viana et al. (22), there are three main groups of source apportionment techniques:

a: Methods based on the evaluation of monitoring data (e.g., correlation of gaseous pollutants with PM)

b: Methods based on emission inventories and/or dispersion models to simulate aerosol emission, formation, transport and deposition

c: Methods based on the statistical evaluation of PM chemical data acquired at receptor sites (receptor models) (e.g., CMB and PMF)

Receptor models can be divided in two main groups: 1) the chemical mass balance (CMB) model; and 2) the factor analytic family. The factor analytic family includes models as positive matrix factorization (PMF) and EPA Unmix (UNMIX). Principal component analysis (PCA) is disregarded as a member of the factor analytic family for the aim of source apportionment for multiple reasons including unrealistic sources (23, 24). Recently developed methods associated to data mining and machine learning seem promising alternatives to replace some receptor models in the future, since they are mostly open source and cross platform, which allow them to become widespread. Besides that, methods related to these new branches of computer science have been implemented with successful outcomes including in the atmospheric sciences (25, 26, 27, 28).

1.0.5 Air pollution and health at rural sites

A plethora of air contaminants potentially hazardous is associated with handling, storage, treatment and disposal of agricultural, animal and municipal biodegradable wastes, including ammonia, hydrogen sulfide, phenols, indoles, volatile fatty acids, carbon dioxide, methane, particulate matter, and endotoxins (29). These pollutants can have adverse health effects on the local populations and some of them may lead to the perception of malodors. Therefore, citizens living in rural areas are exposed to a series of air pollutants that are originated from local sources. This scenario presents a case to the evaluation of the concept of health and also environmental health in its full sense. According to the World Health Organization (WHO), health is a "State of physical, mental and social well-being not merely the absence of disease and infirmity" (30).

Not only the chemical composition of pollution sources associated to the rural environment, but also the high frequency in which residents complain make a case for a careful evaluation of health symptoms associated to odor pollution. Although some studies were carried out they did not objectively estimate the pollution levels, which result in a degree of skepticism by some scholars (31, 32). More than a theoretical exercise, the investigation of the relationships between odor pollution and health symptoms is an act of social justice towards non-urban communities. An effective way to test previous findings (33, 34, 35) and look for further insights is to use structural equation models to test hypothesis about the pathway from exposure to health symptoms.

1.0.6
About the layout of this manuscript

This PhD thesis is an article-based one, which means that the section "Results and discussion" is an adaptation of journal papers already submitted or yet to submit. For the sake of simplicity, the material and methods are introduced in the traditional way and the reader is just referred backwards, when one reaches this section in the papers (Section 3 to Section 7).

2
Material and Methods

Since this thesis is based on an article layout for the presentation of the section 'Results and discussion', the methods will be presented here and omitted in the respective articles.

2.1
Toxicological assessment

The following description of material and methods refer to chapter 3, page 60.

2.1.1
Sample collection and sites description

Particulate matter samples (PM_{10} in 2009 and $PM_{2.5}$ in 2010) were collected by the Environmental Institute of Rio de Janeiro (INEA). Standard Brazilian method for inhalable particles sampling was used. These methods are consistent with the USEPA. The collectors were placed at a height of approximately 2 m in a large open area. Samples were collected over 24 h every 6 days on fiberglass filters (203 $\times$ 254 mm, 0.21 mm thickness, 0.3 μm diameter, Millipore, USA) using high-volume samplers (AGV-PM_{10} and AGV-$PM_{2.5}$, Energética, Rio de Janeiro, Brazil) at an average flow rate of 1.14 m^3 min^{-1}. The average temperature in the MRRJ ranged from 25 to 26 °C for Spring-Summer and from 22 to 23 °C for Autumn-Winter. The total rainfall in the studied period was about 1000 mm distributed between the hottest months, Spring-Summer, coinciding with the seasonal wet period. The predominant wind direction is from the southwest. PM_{10} samples were collected in June and $PM_{2.5}$ samples in August-September, during wintertime in Brazil. No rain occurred during or 24 h before samplings.

2.1.2
PM10

Three sites of different socio-economic background were chosen (Fig.1). Two sites are located in the MRRJ: one is Centro shown as urban (22°54′10"S and 43°12′28" W, GMT - 3) and the other is in the industrial area of Duque de Caxias (22°47′09"S 43°18′43" O, GMT - 3), which is marked in the map as

industrial (Ind) 1. The reference site was selected in the county of Seropédica marked as rural reference (Ref) 1 (22°44′38"S and 43°42′28" W, GMT - 3). Centro urban site is located in the downtown area of Rio de Janeiro City (RJ) and its main influence is heavy vehicular traffic. Duque de Caxias is an industrial area which houses about 800 industries including chemical, metallurgical, gas, plastics, furniture, textiles and clothing. In addition one of the largest refineries of the country is located in this area. Seropédica is a county whose main activity used to be agriculture. However, it has diversified as a food sector and mineral extraction for civil construction. The distance between Centro and Duque de Caxias to the rural area is about 75 km and 52 km, respectively.

2.1.3 PM2.5

Santa Cruz enclosed by a red line in Fig. 2.1 (22°55′13"S and 43°41′6"W, GMT - 3) is another important industrial area with several industries such as paint and solvent production, leather manufacture, printing, structural steel manufacture and metallurgy. In 2010, the biggest steel mill in Brazil was settled. Due to its importance to the environment and population around the industrial region, two sampling sites were chosen: a school area (CIEP João XXIII represented as Ind 2a) and a residential area (Conjunto Alvorada marked as Ind 2b). Seropédica was again chosen as rural reference Ref 2. The distance between the sampling sites (CIEP João XXIII, Conjunto Alvorada and Seropédica) to the industrial area is about 3 km, 8 km and 15 km, respectively.

2.2 Extraction procedure

2.2.1 PM10 samples

An aliquot of the filter (1/4) was cut and weighted in an analytical balance (Shimadzu, Brazil, ± 0.0002 g). The filters were subsequently extracted using the following steps: 1) 120 mL of n-hexane (Vetec, Brazil) and sonication for 2 h; 2) re-extraction with 120 mL of acetone (Vetec, Brazil) and sonication for 2 h; 3) re-extraction with 120 mL of ultrapure water (Millipore, USA) and sonication for 2 h. An aliquot of the aqueous extract was analyzed by inductively coupled plasma or – optical emission spectrometry (ICP-MS or OES) to determine the metal concentrations. The organic extracts were not analyzed due to the difficulty of analyzing metals inorganic extracts since the

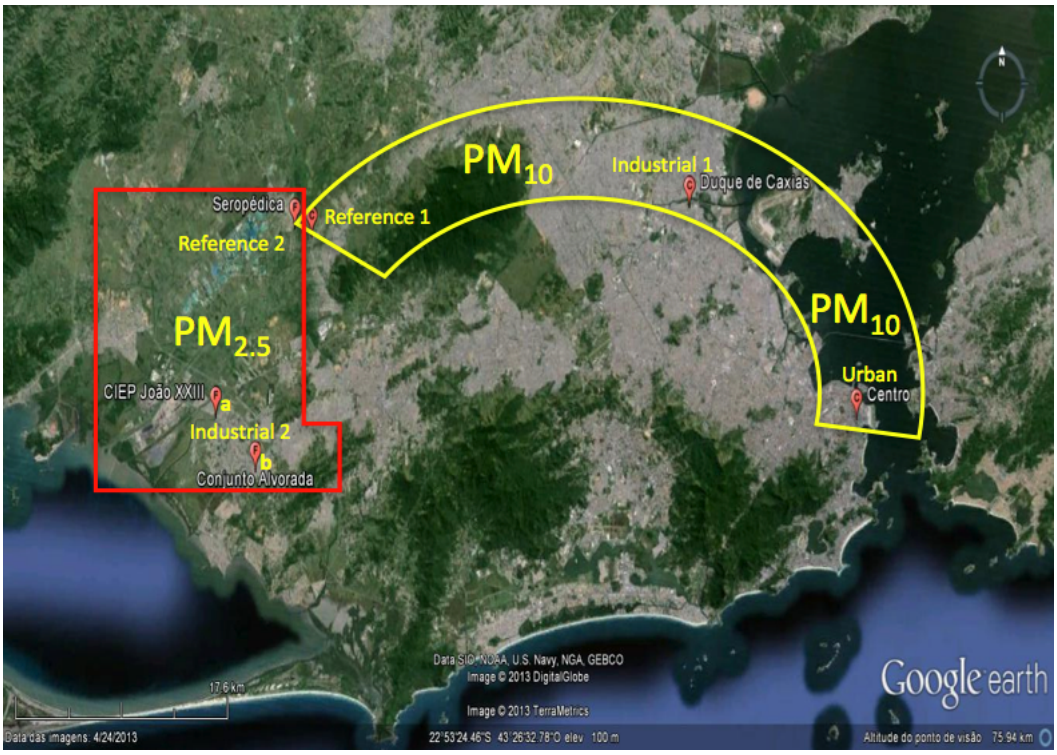

Figure 2.1: Geographical locations of PM_{10} and $PM_{2.5}$ sampling sites in Rio de Janeiro: PM_{10} stations are contained within the yellow semicircle these are: Duque de Caxias (Industrial 1), Centro (Urban) and Seropédica (Reference/Ref 1). The $PM_{2.5}$ locations are within the red rectangle: Santa Cruz (CIEP João XXII as Industrial 2a, Conjunto Alvorada as Industrial 2b and Seropédica as Reference/Ref 2. The Map was obtained from: `https://www.googlemaps.com`

ICP flame is extinguished. For cells exposure organic extracts were dried with a nitrogen stream and aqueous extracts with a Centrivap console (Labconco). The extract mass was determined gravimetrically, subsequently the organic fractions were dissolved in DMSO and the aqueous fractions in water to a concentration of 100 mg mL^{-1}. Blank filters were analyzed in the same manner.

2.2.2 PM2.5 samples

A portion of the filter (¼) was cut and weighed in an analytical balance (Shimadzu, Brazil, ± 0.0002 g). Extraction was performed in 45.0 mL ultrapure water (Millipore, USA), which was sonicated for 2 h. Aliquots of the aqueous extracts were analyzed by ICP OES to study metal composition of the samples. Heating reduced extracts volume and the samples were lyophilized and weighted. Blank filters were analyzed in the same order.

2.2.3
Chemical analysis

Determinations of trace elements (Cd, Cr, Cu, Mn, Ni, Pb, Ti, and V) were performed using an ICP-MS model DRC II (PerkinElmer-Sciex, USA) and major elements (Al, Fe, and Zn) using Optima DV 4300 model (Perkin Elmer, USA), which is able to perform analyses in axial or radial mode of observation. This tool makes it possible to choose the best operational mode to analyze an element in function of background and concentration levels. The analytical solutions were prepared by diluting multi-elemental standards (Titrisol®- Merck, Germany) with concentrations of 1000 mg L^{-1}, with water and acidified with HNO3 (30-35 % w/w) to avoid precipitations. The calibration curves ranged from 5 to 50 mg L^{-1} (ICP OES) and from 50 μg L^{-1} to 100 μg L^{-1} (ICP-MS). External calibration was employed using the Linear Throw Zero statistical model. Duplicates and calibration controls were performed at fifteen samples. A calibration check with external standards was performed to ensure a relative error no more than 10 %. The limit of detection (LOD) was calculated based on three times the standard deviation of the blanks. LOD values ranged from 0.11 to 65.8 μg L^{-1}. The methodology is further discussed and explained in previous papers (10, 36).

2.2.4
Cell culture and exposures

Human bronchial epithelial cells (BEAS-2B) were obtained from the American Type Culture Collection (ATCC®CRL-9609^{TM}). Cells were cultured according to ATCC protocols in Keratinocyte growth medium (KGM-2, Lonza, Walkersville, MD, USA), maintained at 37 °C in humidified atmosphere of 5 % CO_2 and used at passages 44-59. The cells were seeded at a density of 5 $\times$ 104 cells per well onto 96-well plates and incubated for 24 h. $PM_{2.5}$ and PM_{10} extracts were diluted in cell media at concentrations ranging from 5 to 250 μg mL^{-1} and used to expose cells for 24 h. An additional set of cells ($n = 3$ dishes) was also concurrently exposed to PM extracts pre- treated with deferoxamine mesylate (DF, Sigma, Cat No D9533), a metal chelator, at a final concentration of 50 μM. Cell supernatants were collected after each exposure and used for cytokine analyses while the adhered cells to the plates were processed to study cell viability.

2.2.5
Cytotoxicity

The Neutral Red bioassay was used to measure cell viability. After a 24 h cell exposure to PM extracts, the treatments were removed and BEAS-2B cells incubated with Neutral Red dye (Sigma, Cat No N2889) at a final concentration of 100 μg mL^{-1} for 3 h. The dye was then removed; cells were fixed in 1 % calcium chloride, 0.5 % formaldehyde, rinsed with phosphate buffered saline (PBS) and lysed using 1 % acetic acid and 50 % ethanol. Cell viability was spectrophotometrically determined at 540 nm using an Ultramark microplate reader (Bio Rad, Richmond, CA, USA). Triton-X (25 μg mL^{-1}) was used as a positive control for cell toxicity. The following negative controls were simultaneously employed in each experiment: media, media with deferoxamine (DF) and water. Cell viability less than 80 % was the cut off considered for cytotoxicity.

2.2.6
Cytokine measurements

The levels of IL-6, IL-8 and IL-10 were analyzed using a Fluorokine Multi-analyte Profiling Kit from R & D Systems, Minneapolis, MN, USA according to the manufacturer's instructions. Lipopolysacharide (LPS), a positive control was used at a final concentration of 10 μg mL^{-1}. The same negative controls used for the cytotoxicity experiments were also employed. Cytokine concentrations were determined using the dual laser flow analyzer Luminex 200 (Luminex Corp, Austin, TX, USA). Standard curves for each cytokine were plotted employing a 5-paremeter logistic fit (5-PL). This procedure has been previously used and reported by our laboratory (37, 38).

2.2.7
Statistical analyses

To evaluate differences among groups ANOVA statistical analyses were performed followed by the non-parametric Tukey test for multiple comparisons. Differences between individual groups were evaluated using the unpaired Student's t Test. The criterion for statistical significance was set at $p \leq 0.05$. Statistical analyses were performed using the Graph Pad InStat 3 software. Analyses were based on 3 independent experiments per cell response.

2.3
Bioaccumulation assessment

The following description of material and methods refer to chapter 4, page 76.

2.3.1
Sample collection and sites description

Samples of total suspended particulate matter (TSP) were collected in the state of Rio de Janeiro, Brazil. Two sampling sites were chosen. Santa Cruz (SC, 22°55′13"S and 43°41′6"W) is an industrial district, whose main activities are related to metallurgy. SC is nearby Sepetiba Bay area, an important ecosystem about 100 km west from Rio de Janeiro city. Seropédica (SE, 22°44′38"S and 43°42′28"W) was chosen as a reference site. SE has a lower influence of industries, in comparison with SC, and the site is well ventilated. The TSP sampling sites are showed in Figure 2.2.

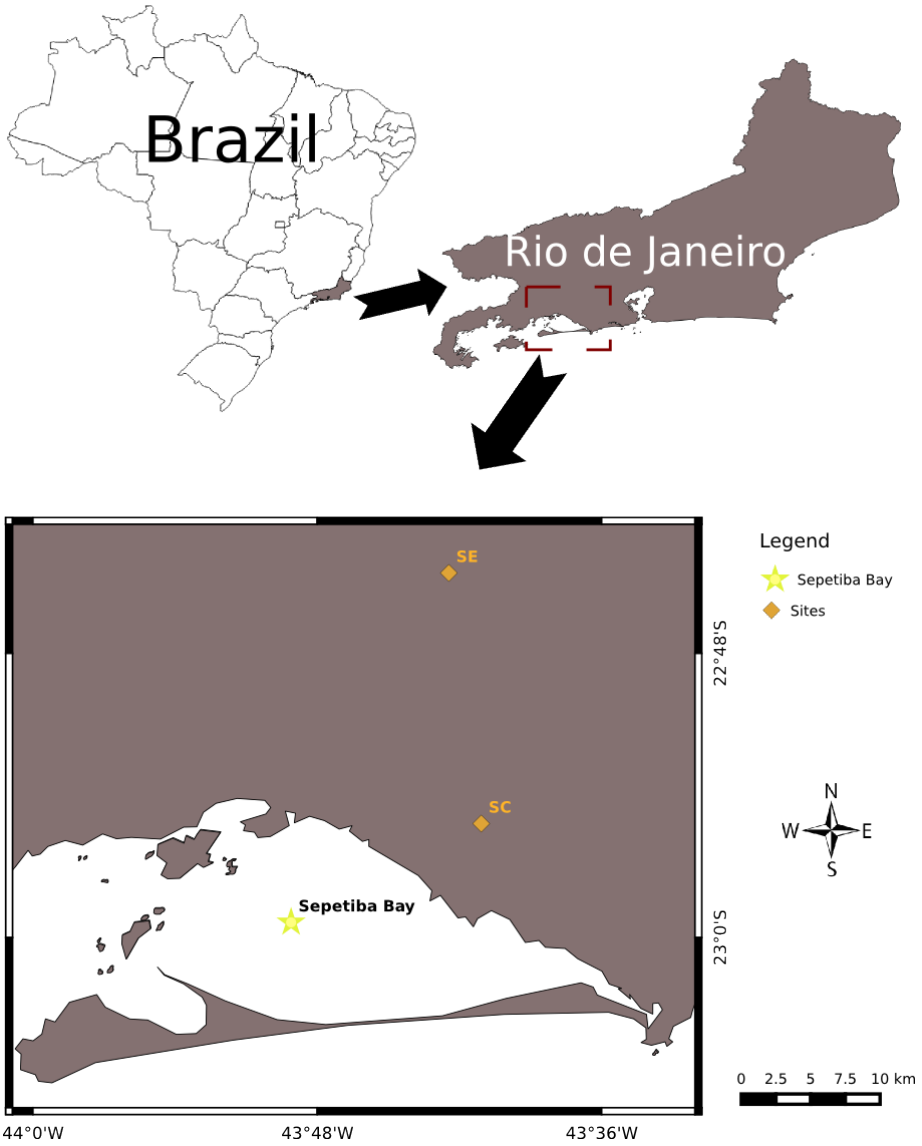

Figure 2.2: Sampling sites locations: Santa Cruz (SC), industrial area, and Seropédica (SE), reference area.

Particulate matter samples were collected by the Environmental Institute of Rio de Janeiro State (INEA) for 24 h, every sixth day, using glass fiber

filters (203 × 254 mm, 0.21 thickness, 0.3 μm diameter, Millipore, USA) in high-volume samplers (Energética, Brazil) with an average flow of 1.14 m^3 min^{-1} (36). The sampling occurred in two campaigns between August 2010 and September 2011. The campaigns are related to low (1) and high (2) rainfall periods. For each period, twelve samples were collected per site, resulting in 48 samples.

2.3.2
Extraction procedure

Sample filters (1/2 of each filter) were cut and weighed. All filters were extracted together (composite) in about 1,550 mL of saline water under mechanical stirring for about 1 h. Four blank filters (1/2 each filter) were also cut, weighed, and extracted with saline water as a control. Saline water used for extraction was prepared using a commercial sea-salt (Redcoral Aquatech, China) and based on the characteristics of Sepetiba Bay, such as: salinity (surface: $21 - 30$ ‰, bottom: $29 - 30$ ‰) and pH (surface: 6.8-8.2) (39, 40) (Table 2.1).

Table 2.1: Mean concentration levels ± standard deviation (mg kg^{-1}) for the saline extracts of PM samples and certified elements in the CRM DORM-3 (n = 2), LOD (mg kg^{-1}), LOQ (mg kg^{-1}). (The percentual recovery for the analysis of the CRM DORM-3 is between parentheses.)

Element	Blank filter	SE-2	SE-1	SC-2	SC-1	LOD		LOQ		Recovery
						SW[b]	ST	SW	ST	
Al	12.2 ± 0.6	-	-	-	-	12.89	1.94	3.14	6.41	n.a.
Ba	11.4 ± 0.08	3.62 ± 0.16	3.03 ± 0.05	3.35 ± 0.11	4.73 ± 0.09	4.89	0.13	1.19	0.43	n.a.
Cd	-	-	-	-	0.23 ± 0.01	0.86	0.07	0.21	0.24	0.23 ± 0.007 (78)
Cr	-	-	-	-	-	3.96	0.17	0.97	0.56	1.61 ± 0.02 (85)
Cu	-	24.89 ± 0.26	19.87 ± 0.06	11.19 ± 0.09	10.48 ± 0.08	1.67	0.03	0.41	0.10	15.2 ± 1.32 (98)
Fe	0.23 ± 0.11	0.68 ± 0.04	0.62 0.03	0.36 ± 0.02	1.18 ± 0.03	0.88	0.08	0.21	0.25	355 ± 5 (102)
Mn	-	4.29 ± 0.13	3.44 ± 0.01	4.11 ± 0.08	6.75 ± 0.09	2.67	0.05	0.65	0.10	n.a.
Ni	-	-	-	-	-	3.42	0.33	0.83	1.09	0.97 ± 0.07 (76)
Pb	-	-	-	-	-	15.28	0.05	3.72	0.18	0.520 ± 0.08 (132)
Sb	n.a.	n.a.	n.a.	n.a.	n.a.	n.a.	3[a]	n.a.	12[a]	n.a.
Si	n.a.	n.a.	n.a.	n.a.	n.a.	n.a.	1.26	n.a.	3.34	n.a.
Ti	-	0.08 ± 0.01	-	0.09 ± 0.01	0.12 ± 0.01	0.21	1.99	0.05	0.14	n.a.
V	-	-	-	-	1.46 ± 0.04	3.34	3.73[a]	0.81	12.31[a]	n.a.
Zn	2.41 ± 0.23	23860 ± 210[a]	17690 ± 90[a]	18960 ± 130[a]	32850 ± 170[a]	3.51	0.30	0.85	0.99	54 ± 3 (106)

n.a.: not available; SW: Saline water extract; ST: Shrimp tissue

-: lower than the LOD (mg kg^{-1}); [a]: µg kg^{-1}; b: instrumental LOD (µg L^{-1})

2.4
Source apportionment: Urban-coastal and rural sites

The following description of material and methods refer to chapter 5, page 82.

2.4.1
The area of study

The Environmental Institute of Rio de Janeiro State (INEA) defined a network for monitoring fine inhalable particles ($PM_{2.5}$). In this study, three sampling sites in the metropolitan region of Rio de Janeiro (MRRJ) were investigated. The urban-industrial characteristics are given by Conjunto Alvorada (CA, 22°55′31.1"S and 43°41′26.7"W) and Centro Integrado de Educação Pública João XXIII (CJ, 22°54′81"S and 43°42′14.81"W). Both sites are located in the industrial district of Santa Cruz. Santa Cruz is worthy of special attention due to its big industrial matrix as well as busy roads. Among the reported sources, there are solvent and paint production, metallurgical and structural steel manufacture, printing facilities, leather manufacture, power plants, and an integrated steelworks (41, 42). The reference site is located in Seropédica (SE, 22°44′38"S and 43°42′28"W) whose main activity used to be agriculture. In the recent history of the region, there is an industrial expansion which added new activities including power plants (42, 43). Besides, SE is nearby to a busy road, which connects the states of Rio de Janeiro and São Paulo (Figure 2.3).

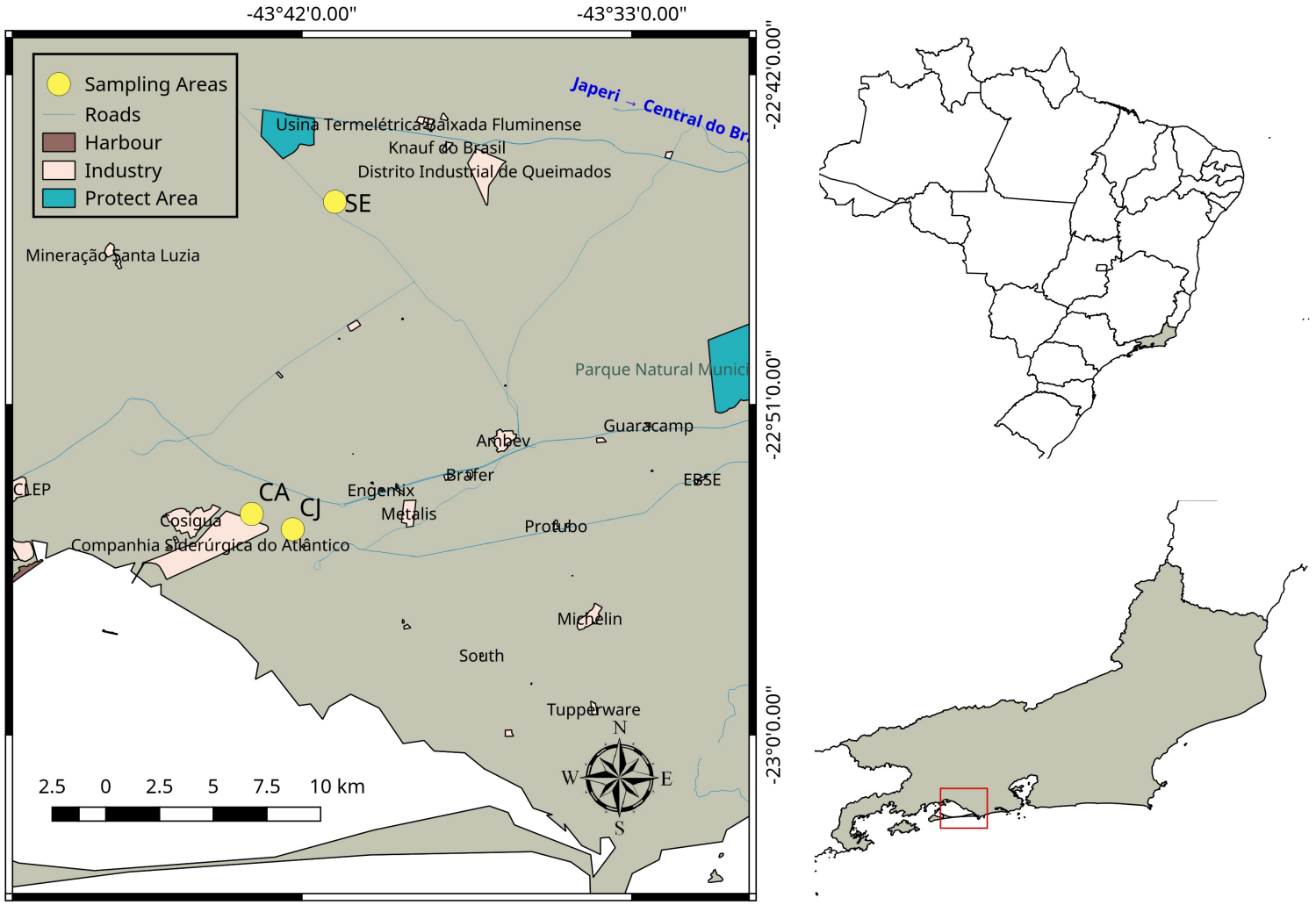

Figure 2.3: Map showing the location of the monitoring sites and emission sources. © OpenStreetMap contributors

Since 2010, there is a continuous monitoring of airborne particles and gaseous pollutants in the region that was carried out by INEA. This study comprehends a 5-year monitoring of $PM_{2.5}$, 3-year monitoring of gaseous pollutants (NO_2, O_3, SO_2), and two speciation campaigns based upon elemental, water-soluble ions, and water-soluble organic carbon (WSOC) analyses. In the first evaluation (Aug/10 - Jul/11), twelve chemical elements (Al, Cr, Cu, Cd, Fe, Mn, Ni, Pb, Sb, Ti, V, and Zn), cations (Na^+, Mg^{2+}, K^+, Ca^{2+}), anions (NO_3^-, SO_4^{2-}, Cl^-), and WSOC were determined. In the second evaluation (Jan - Dec/13), eighteen chemical elements (Ag, Al, Bi, Co, Cr, Cu, Cd, Fe, Mn, Ni, Pb, Sb, Sn, Th, Ti, Tl, V, and Zn), cations (Li^+, Na^+, NH_4^+, K^+, Mg^{2+}, Ca^{2+}), anions (F^-, Cl^-, NO_2^-, Br^-, NO_3^-, SO_4^{2-}, $C_2O_4^{2-}$, PO_4^{3-}), and WSOC were determined.

2.4.2
Particulate matter sampling

Fine inhalable particulate matter samples ($PM_{2.5}$) were collected by INEA from Aug/10 to Dec/15, according to the Brazilian method (ABNT-NBR 13412/95), which is in fully agreement with the USEPA method. Samples were collected over 24 h every 6 days using fiberglass filters (203 × 254 mm, 0.21 mm thickness, 0.3 μm diameter, Millipore, USA) in high-volume samplers (Energética, Brazil) at an average flow rate of 1.17 m^3 min^{-1}.

2.4.3
Aqueous extraction

In order to determine major water-soluble components, aqueous extraction was performed in both first and second speciation campaigns. The method used in the first evaluation was previously described in Mateus et al. (36). An aliquot of the filter (9 cm^2) was cut and weighed in an analytical balance (Shimadzu, Brazil, ± 0.0002 g). Extraction was performed in 10.0 mL of ultrapure water (Millipore, USA), which was sonicated for 10 min. The extract-was filtered through a 0.45 μm cellulose acetate membrane (Macherey-Nagel, Germany) to eliminate insoluble material. Subsequently, the extract was further analyzed by an ion chromatography system (IC), a total organic carbon analyzer (TOC) system, and an inductively coupled plasma optical emission system (ICP OES).

In the second evaluation, the method had significant improvements. One strip (2.54 × 20.32 cm) of loaded filter was used. The aliquot was transferred to a 50 mL conical flask and weighed. Twenty milliliters of ultrapure water were added to each flask, shaken using a vortex mixer for 1 min, and centrifuged

at 2000 rpm for 4 min. The extract were filtered through a 0.45 μm cellulose acetate membrane (Macherey-Nagel, Germany) to eliminate insoluble material. The water-soluble ionic composition was determined using only an IC system. In the case of the TOC system, fifty milliliters of ultrapure water were used for the extraction. Concerning the changes in the filter aliquot, the adjustments were motivated by the USEPA recommendations for PM collected in fiberglass filter (44).

2.4.4 Acid extraction

In order to investigate the elemental composition, mostly metals, an acid extraction was performed. In the first evaluation, a higher dilution factor was used, which was acceptable due to the high concentration of PM (36). Twelve elements were determined (Al, Cr, Cu, Cd, Fe, Mn, Ni, Pb, Sb, Ti, V, and Zn).

In the second evaluation, a strip of loaded filter (2.54 $\times$ 20.32 cm) was cut, added to a 50 mL conical flask and weighed. Five milliliters of concentrated HNO_3 were added to each flask. After an overnight pre-extraction, the flasks were heated in a hot plate at 95 °C for 4 h. Samples were analyzed for a total of 18 elements (Ag, Al, Bi, Co, Cr, Cu, Cd, Fe, Mn, Ni, Pb, Sb, Sn, Th, Ti, Tl, V, and Zn). In both campaigns, the certified reference material SRM 1648a (Urban dust, NIST, USA) was used to check the analytical procedure applied, which includes the sample dissolution as well as the inductively coupled plasma mass spectrometry (ICP-MS) analysis.

2.4.5 Analyses

2.4.5.1 ICP-MS determinations

ICP-MS determinations were performed using a DRC II (PerkinElmer-Sciex, USA). Operational conditions were optimized based upon daily performance. Calibration solutions were prepared in ultrapure water (5 % v/v) acidified with twice-distilled HNO_3. The chosen internal standard was Rh (400 μg L^{-1}), injected on line and the quantification was based on an external calibration.

2.4.5.2

Water-soluble ions determinations

First campaign IC determinations were performed just for a few major anions (NO_3^-, SO_4^{2-}, Cl^-) using an IC system with a Supp5 column (Metrohm, USA) and a micromembrane supressor, eluted with Na_2CO_3 (1.0 mmol L^{-1})/ $NaHCO_3$ (3.2 mmol L-1) (10). The quantification was based on an external calibration.

Major cations (Na^+, Mg^{2+}, K^+, Ca^{2+}) were determined by an ICP OES system Optima DV 4300 (PerkinElmer, USA). This equipment performs analysis in axial or radial mode, which helps to determine elements according to the best relation background-concentration. All calibration solutions were prepared in ultrapure water, acidified with twice-distilled HNO_3 (10 % v/v). The quantification was based on an external calibration (36).

Since only major cations and anions were determined by an ICP OES and IC system, respectively, the analytical omissions of important source tracers (i.e., organic acids and NH_4^+) were caused by an instrumental difficulty.

Second campaign In the second evaluation, a very sophisticated system which allows the simultaneous determination of cations, inorganic, and organic anions was used. The dual-system ICS 5000 (Thermo Scientific Dionex, USA) is equipped with a cation isocratic component, an anion gradient component, and an AS-AP autosampler. Cations were analyzed using a Dionex IonPac CS 12A (Thermo Scientific Dionex, USA) while a Dionex IonPac AS19 (Thermo Scientific Dionex, USA) was used to analyze anions. The AS-AP temperature was set to 10 °C in order to improve the quantification of volatile species.

2.4.5.3 Total organic carbon (TOC) determinations

Water-soluble organic carbon was estimated based on total water-soluble carbon (TWSC) and water-soluble inorganic carbon (WSIC) measurements (WSOC = TWSC - WSIC) using a total carbon analyzer (TOC-V, Shimadzu Corp., Japan). Standards were prepared in ultrapure water from reagent-grade potassium hydrogen phthalate for TWSC while sodium hydrogen carbonate/sodium carbonate anhydrous were used for WSIC (10).

2.4.5.4 Quality assurance and quality control (QA/QC)

Blank filters were processed simultaneously with sample filters. Ultrapure water, both unfiltered and filtered, and HNO_3 were also analyzed. After

removing outliers based on the Grubbs criteria, the average value for trace elements, water-soluble ions, and WSOC in the blanks were subtracted from those obtained for each sample filter.

In every 15 samples, a calibration check was performed to ensure a relative standard deviation no more than 10 % as well as one sample was analyzed in duplicate. For both the elemental determination and the water-soluble fraction (i.e., ions and WSOC), the DL was calculated based on 3 times the standard deviation of the blank filters (n = 7) plus the mean concentration (Table E.1). The efficiency of the acid extraction was evaluated by analysis of the certified reference material by ICP-MS.

2.4.6
Gaseous pollutants and meteorological variables

From 2010 to 2013, gaseous pollutants data (NO_2, SO_2, and O_3) were provided by INEA. The measurements were registered every hour and averaged for each day. The employed methodologies were based on chemiluminescence, fluorescence UV, and UV photometry, respectively.

From 2010 to 2015, the following meteorological data with hourly resolution were provided by the national institute of meteorology (INMET): barometric pressure (Pressure), wind speed (WS), accumulated precipitation (Precipitation), wind direction (WD), Temperature, and Relative Humidity (RH). The measurements were averaged for each day.

2.4.7
Source Apportionment Framework

Data analyses were carried out using the language and environment for statistical computing R (45).

2.4.7.1
Statistical tests

Differences among pollutants (i.e., $PM_{2.5}$ and WSOC) levels at CA, CJ, and SE were determined based on Kruskal-Wallis analysis considering 95 % of confidence level ($\alpha = 0.05$).

2.4.7.2
Left-censored and missing data

A common issue in environmental datasets is the presence of missing values and/or left-censored (e.g., lower than the detection limit - "<DL"). Missing values may represent failures in automatic measurement systems

or an instrumental difficulty. In general, they are either removed or simply substituted by the geometric mean, depending on their proportion in the dataset. Perhaps, left-censored data are even more common and more strategies were developed to overcome this issue. In this paper, a new strategy is applied, based on the imputation of left-censored under a compositional approach.

The aim of compositional data analysis is to investigate the relative variation structure, given a multivariate dataset that represents fractions of a same total. If there are left-censored values, the analysis becomes more complex. It is well documented that simple replacement of these values may corrupt the multivariate structure (46, 47). Therefore, an approach that considers both the multivariate structure of the data and the compatibility with the compositional question is implemented via the R package *zCompositions* (47, 48).

2.4.7.3 Data groups

In the speciation campaigns, four groups of predictors were used for investigating the $PM_{2.5}$ sources: (**1**) site and season, which includes a variable for site location and another to describe the season as dry or wet; (**2**)trace gases, which is represented by NO_2, SO_2, and O_3; (**3**) speciated PM, which includes variables obtained through chemical analyses of PM (e.g., metals and water-soluble ions); (**4**) meteorology, which includes the variables Pressure, WS, Precipitation, WD, Temperature, and RH. Three predictors were categorical (i.e., Local, Season, and WD). The sites were classified in three categories (CA, CJ, and SE) which are linked to the previous knowledge about the land use. The season is also a categorical variable with two levels (Dry and Wet). The variable WD is a 16-point compass obtained from the daily scalar WD. The average of scalar WD was calculated using the R package *circular* (49), which considered the principles of directional statistics.

2.4.7.4 Estimation of non-sea-salt particles: Equations

Given that the sites are located in a coastal region, the magnitude of non-sea-salt (nss) particles was estimated using the following equations:

$$nss - Ca^{2+} = C_{Ca^{2+}} - 0.038 * C_{Na^{+}} \tag{2-1}$$

$$nss - Mg^{2+} = C_{Mg^{2+}} - 0.12 * C_{Na^{+}} \tag{2-2}$$

$$nss - K^{+} = C_{K^{+}} - 0.035 * C_{Na^{+}} \tag{2-3}$$

$$nss - SO_4^{2-} = C_{SO_4^{2-}} - 0.250 * C_{Na^+} \quad (2\text{-}4)$$

The equation 2-2 is an attempt to apportion some extent of the $nss - Mg^{2+}$ without the total decomposition of Mg (e.g., (50)). The choice for fiberglass filters limits an acid decomposition of major cations such as Mg, since they are also major elements in the blanks.

2.4.7.5 CIT

The association between the predictors and the mass concentration of $PM_{2.5}$ is given by CIT. CIT is an advanced development of a class of models for regression and classification known as "recursive binary partitioning" or "trees". CIT performs as good as optimally pruned trees based on the strong conditional inference theory (51). Given a response variable Y, a conditional distribution can be written by the m-dimensional covariate $X = (X_1, X_2, ..., X_m)$:

$$D(Y|X) = D(Y|X_1, X_2, ..., X_m) = D(Y|f(X_1, X_1, X_2, ..., X_m)) \quad (2\text{-}5)$$

where $f(X_1, X_1, X_2, ..., X_m)$ is a function of the covariate. For a given population ϕ_n with n samples $(\phi_n = (Y_i, X_{1i}, ..., X_{mi}); i = 1, 2, ..., n)$, the binary partitioning algorithm is constructed using the nonnegative integer valued case weight vector $W = (w_1, w_2, ..., w_n)$. For each node of the tree, there is a case weight vector W that assumes zero value for observations which are not elements of the node and nonzero integers otherwise. The analysis is implemented via the function ctree from the R package *party* (51).

2.4.7.6 Random Forests

Random forests is a further development of the so-called bagging or bootstrap aggregation. This method has become a major tool for problems in many areas (52). Random forests is suitable for classification or regression problems. The relevance of random forests may be related to at least two reasons: 1) dealing with nonlinear and complex high-order interaction effects; and 2) capability to estimate variable importance for predictors. The development of the method is attributed to Breiman (53).

Although the original idea of Breiman performs similarly to methods like discriminant analysis, artificial neural networks (ANN) and support vector machines (SVM) (53), random forests may be biased when predictors vary in scale of measurement or number of categories (54). In this work, the importance

of predictors was evaluated by random forests; however, the variable selection was based on CIT rather than classification and regression trees (CART). Our analysis was based on a subsampling without replacement (54) and a conditional permutation design ensures the preference of correlated predictors (52). The analysis is implemented via the function cforest from the R package *party* (52, 54, 55).

2.4.7.7 CBPF

An extension of the conditional probability function (CPF) model (56) known as conditional bivariate probability function (CBPF) (57) was applied through the R package *openair*.

Given a wind sector, the basic CPF calculates the probability of a measured concentration exceeds a set threshold criterion. CPF is defined as:

$$CPF_{\Delta\theta} = \frac{m_{\Delta\theta}|_{C \geq X}}{n_{\Delta\theta}} \tag{2-6}$$

where $m_{\Delta\theta}$ refers to the number of samples in a given wind sector θ which concentration is equal or above a threshold value X, and the total number of samples from the wind sector $\Delta\theta$ is equal to $n_{\Delta\theta}$. In general, the used threshold relates to the contribution of a source to high pollution events (75th or 90th percentile).

Recently, Uria-Tellaetxe and Carslaw (57) have developed a new receptor modelling technique, CBPF. The model adds wind speed as a third variable and allocates the observed pollutant concentration in cells defined by wind direction-speed. Mathematically, CBPF is defined as follows:

$$CBPF_{\Delta\theta,\Delta u} = \frac{m_{\Delta\theta,\Delta u}|_{C \geq X}}{n_{\Delta\theta,\Delta u}} \tag{2-7}$$

where $m_{\Delta\theta,\Delta u}$ is the number of samples in the wind sector $\Delta\theta$ with wind speed interval Δu which concentration C is greater than the threshold X, the denominator $n_{\Delta\theta,\Delta u}$ is the total number of samples in the given wind direction-speed interval. The functionality of CBPF is caused by the different wind speed from different sources. The CBPF unveil which wind direction-speed is associated with high concentrations and estimates the probability of such relation (58). However, other variables can also compose the radial axis (57). In this paper, the sources of daily levels of gaseous pollutants and $PM_{2.5}$ are evaluated by means of CBPF. This model was implemented through the function polarPlot of the R package *openair*.

At sites with typical urban features, an expected finding is the pair high concentration associated to low wind speed. In these sites, the low wind speed

represents more stable atmospheric conditions and reduced advection (59). This is often attributed to non-buoyant ground-level sources (e.g., road traffic sources) (57). In opposition to non-buoyant ground-level sources, increases in concentration with wind speed indicate buoyant plumes (i.e., elevated sources) such as from power station and integrated steelworks (57, 60). As a consequence, the buoyant plume affects ground-level receptors as the wind speed increases (60). The atmosphere of typical urban-coastal sites may be under the influence of both ground-level and elevated sources.

2.4.7.8 Theil-Sen method for trend estimation

Although estimation trend is a key feature in air pollution exposure assessment and source apportionment, many issues such as uncertainty estimation and use of linear models can decrease the power of this tool. The basic idea of the Theil-Sen method dates before the seminal papers of Theil (61) and Sen (62). However, only through the advances in computing the method became available (58). Given a set n of x, y pairs, the method proposes the calculation of the slopes between all pairs of points. This method was implemented through the function TheilSen on the R package *openair*. Consequently, the concentration time series was estimated as a generalized additive model (GAM) (63). The advantages of using this approach are: 1) accuracy of estimation even with non-normalilty and heterocedasticity; 2) robustness to outliers; and 3) use of bootstrap-resampling to estimate p values of the slopes.

2.5 Source apportionment: Protected areas

The following description of material and methods refer to chapter 6, page 106.

2.5.1 The area of study

Two sampling sites located in the surroundings of the metropolitan region of Rio de Janeiro were investigated: the Mário Xavier National Florest (Flonamax, 22°43′21.7"S and 43°42′21.8"W) and the Serra dos Órgãos National Park (Parnaso, 22°29′16.9"S and 43°04′42.1"W), but from hereafter FLONA and PARNA, respectively (Figure 2.4). The former sampling comprehends a smaller area in comparison with the latter, but it is nearby two busy highways Presidente Dutra and Raphael de Almeida Magalhães highway (Arco Metropolitano). Besides that, the region is the habitat for an endangered specie of tree frog *Physalaemus soaresi* (64). The second sampling site is one

of the most important national parks in Brazil and the habitat for multiple endangered species(65). As observed at FLONA, PARNA is also affected by traffic related sources given the proximity of busy highways, including the Arco Metropolitano. Previous findings highlighted the susceptibility of PARNA to emissions originated from the MRRJ (66), but there are no reports of a long term monitoring which included the analysis of trace and major elements. Both sites represent fragments of the Atlantic Rain Forest, one of the most important biodiversity hotspots in the world. At the surroundings of PARNA and FLONA, the influence of traffic sources is assigned by the yellow lines labeled with "RJ". Besides that, the stationary source are represented by pins: marine sources (yellow pins), industrial zone (red pin), and an oil refinery (green pin) (Figure 2.4).

Figure 2.4: Map showing the location of the monitoring sites Flonamax and Parnaso, which from hereafter are labeled as FLONA and PARNA. The Map was obtained from `https://www.google.com/earth/`

Since 2010, there is an airborne particulate matter (PM) monitoring at both sites. The monitoring program of TSP was carried out by the laboratory of air pollution studies of the Federal University of Rio de Janeiro (LEPA/UFRJ), while the monitoring program of PM_{10} was carried out in partnership with the company that manages the road (CRT). This study presents results of the chemical characterization of TSP and PM_{10} during 4 and 5 years at

FLONA and PARNA, respectively. During this campaign, thirteen chemical elements (Al, Cd, Cr, Cu, Fe, Mn, Ni, Pb, Sb, Si, Ti, V, and Zn), cations (Li^+, Na^+, NH_4^+, K^+, Mg^{2+}, Ca^{2+}), inorganic anions (Br^-, F^-, Cl^-, NO_3^-, PO_4^{3-}, SO_4^{2-}), organic anions (Acetate, Formate, Malonate, Oxalate)and water-soluble organic carbon (WSOC) were determined.

2.5.2 Particulate matter sampling

Particulate matter samples (TSP and PM_{10}) were collected by the LEPA/UFRJ (INEA) in accordance with the standard Brazilian methods ABNT-NBR 9547/86 and ABNT-NBR 13412/95, respectively. These methods are in agreement with the USEPA methods. Samples were collected over 24 h every 6 days using fiberglass filters (203 × 254 mm, 0.21 mm thickness, 0.3 μm diameter, Energética, Brazil) in high-volume samplers (Energética, Brazil) at an average flow rate of 1.13 m^3 min^{-1}.

2.5.3 Aqueous extraction

In order to determine major water-soluble components, a strip (2.54 × 20.32 cm) of loaded filter was used. The aliquot was transferred to a 50 mL conical flask and weighed. Twenty milliliters of ultrapure water were added to each flask, shaken using a vortex mixer for 1 min, and centrifuged at 2000 rpm for 4 min. The extract was filtered through a 0.45 μm cellulose acetate membrane (Macherey-Nagel, Germany) to eliminate insoluble material. The water-soluble ionic composition was determined using only an IC system. In the case of the TOC system, fifty milliliters of ultrapure water were used for the extraction.

2.5.4 Acid extraction

A strip of loaded filter (2.54 × 20.32 cm) was cut, added to a 50 mL conical flask and weighed. Five milliliters of concentrated HNO_3 were added to each flask. After that, they were heated in a hot plate at 95 °C for 4 h. Samples were analyzed for a total of 13 elements (Al, Cd, Cr, Cu, Fe, Mn, Ni, Pb, Sb, Si, Ti, V, and Zn) In both campaigns, the certified reference material SRM 1648a (Urban dust, NIST, USA) was used to check the analytical procedure applied, which includes the sample dissolution as well as the inductively coupled plasma mass spectrometry (ICP-MS) analysis. The determination of Si was performed using an inductively coupled plasma optical emission spectrometry (ICP OES).

2.5.5 Analyses

2.5.5.1 ICP-MS determinations

ICP-MS determinations were performed using a DRC II (PerkinElmer-Sciex, USA). Operational conditions were optimized based upon daily performance. Calibration solutions were prepared in ultrapure water (5 % v/v) acidified with twice-distilled HNO_3. The chosen internal standard was Rh (400 μg L^{-1}), injected on line and the quantification was based on an external calibration.

2.5.6 ICP OES determinations

The Si levels were determined by an ICP OES system Optima DV 4300 (PerkinElmer, USA). All calibration solutions were prepared in ultrapure water, acidified with twice-distilled HNO_3 (10 % v/v). The quantification was based on an external calibration (36).

2.5.6.1 Water-soluble ions determinations

Cations, inorganic and organic anions were determined using a the dual-system ICS 5000 (Thermo Scientific Dionex, USA), which is equipped with a cation isocratic component, an anion gradient component, and an AS-AP autosampler. Cations were analyzed using a Dionex IonPac CS 12A (Thermo Scientific Dionex, USA) while a Dionex IonPac AS19 (Thermo Scientific Dionex, USA) was used to analyze anions. The AS-AP temperature was set to 10 °C in order to improve the quantification of volatile species.

2.5.6.2 Total organic carbon (TOC) determinations

WSOC was estimated based on total water-soluble carbon (TWSC) and water-soluble inorganic carbon (WSIC) measurements (WSOC = TWSC - WSIC) using a total carbon analyzer (TOC-V, Shimadzu Corp., Japan). Standards were prepared in ultrapure water from reagent-grade potassium hydrogen phthalate for TWSC while sodium hydrogen carbonate/sodium carbonate anhydrous were used for WSIC (10).

2.5.6.3 Quality assurance and quality control (QA/QC)

Blank filters were processed simultaneously with sample filters. Ultrapure water, both unfiltered and filtered, and HNO_3 were also analyzed. After removing outliers based on the Grubbs criteria, the average value for trace elements, water-soluble ions, and WSOC in the blanks were subtracted from those obtained for each sample filter.

In every 15 samples, a calibration check was performed to ensure a relative standard deviation no more than 10 % as well as one sample was analyzed in duplicate. For both the elemental determination and the water-soluble fraction (i.e., ions and WSOC), the DL was calculated based on 3 times the standard deviation of the blank filters (n = 7) plus the mean concentration. The efficiency of the acid extraction was evaluated by analysis of the certified reference material by ICP-MS (Table E.2).

2.5.7 Meteorological variables

From 2010 to 2015, the following meteorological data with hourly resolution were provided by the national institute of meteorology (INMET): accumulated precipitation (Precipitation), barometric pressure (Pressure), dew point (DP), gust wind speed (Gust), global radiation (Rad), wind speed (WS), wind direction (WD), Temperature (T), and Relative Humidity (RH). In the case a variable presented minimum and maximum values, they were used (e.g., T_Min and T_Max) in order to maximize the amount of information about the local meteorology of the sites. The measurements were averaged for each day.

Wind speed and direction A better way to use wind data either for averaging purposes or as input in mathematical models is to calculate the u (towards the E) and v (towards the N) components (58, 67). The wind components u and v can be expressed as:

$$\vec{u} = -u_i \times \sin\left(2\pi \times \frac{\theta_i}{360}\right) \tag{2-8}$$

$$\vec{v} = -u_i \times \cos\left(2\pi \times \frac{\theta_i}{360}\right) \tag{2-9}$$

where u_i is the wind speed and θ_i is the wind direction in degrees. In this paper, our wind data was decomposed in the u.WIND and v.WIND variables.

2.5.8 Source Apportionment Framework:Clustering

The reader is referred to the section 2.4.7, page 41. However, two new items were added to the source apportionment framework and will be described as follows.

2.5.8.1 Hierarchical clustering

Given a certain metric, the hierarchical cluster analysis (HCA) aims to find the distance between samples and represent it in a two-dimensional space (i.e., dendogram). The graphical output provided by HCA is appealing because it favors the human pattern skills. HCA is a widespread technique in data science and it can be used to dimension reduction in the row or variable space. However, the use of HCA brings a question about to which extent the clusters are accurate and reproducible. The use of multiscale bootstrap resampling can help to answer this question.

In this paper, the HCA was carried out using the language and environment for statistical computing R (45). The analysis used the Ward's aggregation method and the Spearman's correlation-based distance metrics. For each terminal node obtained via CIT, HCA was performed in order to investigate the relationship among the chemical variables and to enrich the interpretation of ascribable sources.

2.5.8.2 Multiscale bootstrap resampling

Multiscale bootstrap resampling is implemented in the HCA via the *R* package pvclust (68). The technique helps to ensure the reliability of interesting structures in data measuring p-values. The multiscale bootstrap resampling is a less biased way to measure p-values than the bootstrap resampling. The former estimates the approximately unbiased (AU) estimate of p-value, while the latter estimates the bootstrap probability (BP) value. The method was released recently and a further description can be found in the literature (69, 70, 71).

2.5.8.3 Polar plots and k-means clustering

Bivariate polar plots by definition show the relationship between the concentration of a given variable and wind speed and wind direction pairs in polar coordinates. The use of polar plots requires the wind decomposition in

u.WIND 2-8 and v.WIND 2-9. Polar plots analysis were carried out using the *R* package openair (59).

To model the concentration of a given pollutant as a function of wind speed and wind direction, a general additive model (GAM) is written as follows:

$$\sqrt{C_i} = \beta_0 + s(u_i, v_i) + \epsilon_i \tag{2-10}$$

where C_i is the ith pollutant concentration, β_0 is the overall mean of the response, $s(u_i, v_i)$ is the isotropic smooth function of ith value of covariate u and v, and ϵ_i is the ith residual.

k-means clustering applied to the bivariate polar plots allows one to identify and group important features, based on similarities measurements. Three variables are used to investigate regions of similar-dissimilar concentration in a bivariate polar plot: the two wind components u and v plus the concentration, C. Defining $X = x_i, i = 1, ..., n$ as set of n points to be partitioned into K clusters, $C = C_k, k = 1, ..., K$. K-means is defined by minimizing (59):

$$\sum_{k=1}^{K} \sum_{x_i \in C_k} \parallel x_i - u_k \parallel^2 \tag{2-11}$$

where the term $\parallel x_i - u_k \parallel^2$ is the distance measure and u_k represents the the mean of a cluster c_k.

In the the *R* package openair (59), the chosen distance measure is Euclidean:

$$d_{x,y} = \sqrt{\sum_{j=1}^{J} (x_j - y_j)^2} \tag{2-12}$$

where x and y are two J-dimensional standardized vectors and J has length equal to three (wind components u and v and the concentration C). The vectors were standardized by subtracting the mean and dividing by the standard deviation, since they are in different units.

A potential disadvantage of the basic k-means algorithm is the arbitrary selection of the number of clusters. After a couple of runs to check stability of the solutions, the number of clusters was set to be equal to the number of terminal nodes provided by CIT. Although the algorithms are different, we expect some agreement in the detection of major sources.

2.6 Air pollution and environmental health

The following description of material and methods refer to chapter 7, page 126.

2.6.1 Population data collection

Using a cross-sectional design, a population-based study was performed in six 12 km × 12 km non-urban Danish regions. The six regions provided feasible amplitude of exposures to animal waste/farming odors. A sum of 1120 households located in the six regions were randomly selected and a structured questionnaire, based on an indoor climate study (72), was mailed from October 2011 to February 2012. Only one adult (> 18 years old) living in each household was required to fill and return the questionnaire. The research was conducted in fully agreement with the Declaration of Helsinki. The study was notified to and registered by the Danish Data Protection Agency, Datatilsynet.

An anonymous questionnaire with three main sections was used. The first part was related to general socio-demographic and lifestyle data, i.e., age, gender, smoking habit, job (occupation), time spent at home per week, existence of household residents below 18 years old, and years living in the region. The second part referred to environmental stressors, i.e., annoyance, health risk perception, and behavioral interference experienced between the years 2010 and 2011. Participants were asked about their perception of annoyance (0 = not annoyed; 1 = annoyed). as well as their concerns about the adverse health effects of environmental perceived odor pollution (0 = no health risk perception; 1 = health risk perception). Finally, residents answered whether or not the environmental odor prevented them from either properly ventilating their homes or from performing outdoor activities as they wished (0 = no behavioral interference; 1 = behavioral interference).

The third part of the questionnaire asked individuals about physical health symptoms. In this study, six irritation/respiratory symptoms were considered: itching, dryness or irritation of eyes, itching, dryness or irritation of the nose, runny nose, cough, chest wheezing or whistling, and difficulty breathing. Besides these specific health symptoms, five non-specific health symptoms were considered: dizziness, difficulty concentrating, headache, unnatural fatigue and nausea (73, 74). Individuals gave information about the frequency of these symptoms (0 = never/very rarely; 1 = several times). Physician-diagnosed respiratory conditions, self-reported, were collected and classified into three groups: (1) acute respiratory conditions (acute infections of the respiratory tract, acute bronchitis, flu or pneumonia in the past 2 years), (2) chronic respiratory conditions (asthma, allergic rhinitis, chronic bronchitis, lung disease or other diseases of the airways), and (3) other chronic diseases.

2.6.2 Exposure assessment

Using emission-based atmospheric dispersion modeling, air pollution was objectively estimated at each household. Based on previous considerations (75), ammonia (NH_3) was chosen as a proxy gas to air pollution exposure. Firstly, processes associated to farming, animal and agricultural wastes are major emission sources and NH_3 is an ubiquitous pollutant released in such activities (76). Secondly, the processes of wastewater mixing, agitation and application are related to an acute increase in the emissions of odors as well as to a significant increase in NH_3 emissions (35). Thirdly, NH_3 is a well-known odorous and irritating gas and its correlation with farming and livestock odor was previously verified (77). Finally, the increased occurrence of PSY, RNS, and SIS has been associated with NH_3 (33, 34, 35).

Along the six regions, ammonia concentration was estimated using data from emission-dispersion models (Eulerian long-range transport model, DEHM, and the local-scale transport deposition model, OML-DEP) (33, 34, 35). At a 16 km $\times$ 16 km resolution, the DEHM estimates the background NH_3 concentration (from medium and long-range transport). Based on local point sources and surface sources, the OML-DEP is a Gaussian dispersion model based on the boundary-layer theory. Besides, the OML-DEP provided detailed annual emission inventories with hourly resolution and spatial resolution of 400 m $\times$ 400 m. Using UTM coordinates and OML-DEP results, NH_3 levels, at each household, were calculated through inverse distance weighting (IDW) multivariate interpolation. Both DEHM and OML-DEP model have been validated in previous works (76).

2.6.3 Selection and grouping of variables

First, an exploratory factor analysis (EFA) was carried out with the physical health symptoms (i.e., RNS and SIS), using the rotation methods *geomin* (oblique) and *varimax* (orthogonal) with the *psych* package (78). Second, a confirmatory factor analysis (CFA) of the structure provided by means of EFA was performed using the *lavaan* package (79), without the presence of potential confounders and including the latent variable PSY - measured by odor annoyance, behavioral interference, and health risk perception. Finally, the potential confounders were added to the previous CFA framework and the model successfully converged, supporting the use of SEM.

2.6.4 Structural equation modeling

SEM is a powerful and general framework of statistical modeling such that other traditional tools may be seen as special cases, e.g., confirmatory factor analysis (CFA) and linear ordinary least squares regression (OLS). The general SEM is is composed of: 1) a structural model component and 2) a measurement model component.

The main aim of SEM is to model the conditional distribution of observed response variables $(y_i = (y_{i,1}, ...y_{i,p})^t$, given the observed covariates $(x_i = (x_{i,1}, ..., x_{i,q})^t$. To achieve this aim, the observed variables are assumed to be indicators of other unmeasurable ones, so-called latent variables. The corresponding latent variables for x_i and y_i are often called exogenous (independent) and endogenous (dependent) variables, respectively. As a consequence of Muthén's work (80), a combination of categorical (i.e., dichotomous and ordered polytomous) and continuous can be used as observed variables.

By considering η $(m \times 1)$ and ξ $(n \times 1)$ as endogenous and exogenous latent variables, respectively, the structural model component of SEM can be written as follows:

$$\eta_i = \alpha_i + B\eta_i + \Gamma\xi_i + \zeta_i, \tag{2-13}$$

where α $(m \times 1)$ is a vector of intercepts, B $(m \times m)$ is a matrix of regression coefficient for the relationships among the η variables, Γ $(m \times n)$ is a matrix of regression coefficients for the effect of ξ on η, and ζ is a random vector of residuals. The measurement model component represents the process of linking observed variables to a concept derived from a theoretical assumption, i.e., a latent variable. This is achieved by linking the observed indicators $x_{i,j}$ and $y_{i,j}$ to latent continuous indicators $x^*_{i,j}$ and $y^*_{i,j}$, respectively. In the case of $y_{i,j}$ being continuous $y_{i,j}$ is equal to $y^*_{i,j}$, otherwise this assumption is violated, $y_{i,j} \neq y^*_{i,j}$. Categorical observed indicators can be related to latent continuous ones assuming a monotonic relation (80):

$$y_{i,j} = \begin{cases} C-1, & \text{if } \tau_{i,C-1} < y^*_{i,j}, \\ C-2, & \text{if } \tau_{i,C-2} < y^*_{i,j} \leq \tau_{i,C-1}, \\ \vdots & \\ 1, & \text{if } \tau_{i,1} < y^*_{i,j} \leq \tau_{i,2}, \\ 0, & \text{if } y^*_{i,j} \leq \tau_{i,1}, \end{cases} \tag{2-14}$$

where C is the number of categories and τ is the category threshold parameter.

Given a linear relationships between observed and latent variables, the latent indicators are defined by,

$$y^* = \nu_y + \Lambda_y\eta + \epsilon, \tag{2-15}$$

$$x^* = \nu_x + \Lambda_x \xi + \delta, \tag{2-16}$$

where ν_y $(p \times 1)$ and ν_x $(q \times 1)$ are vectors of intercepts, Λ_y $(p \times m)$ and Λ_x $(q \times n)$ are matrices of coefficients (*factor loadings*) for the regression of y_i on η and x_i on ξ, respectively. The random vectors of residuals are ϵ $(p \times 1)$ and δ $(q \times 1)$.

Muthén (80) describes two different cases related to the distribution of observed variables which are particularly important to model observed categorical variables in SEM. The case described hereafter is also known as "fixed x", where x_i is a continuous, unbiased indicator of ξ, i.e., $E(\delta) = 0$, $\Lambda_x = I$, and $\nu_x = 0$. Then, (2-16) becomes

$$x = x^* = \xi, \tag{2-17}$$

Since x_i is expressed in deviation form $\nu_x = 0$. Substituting (2-17) to (2-13) yields to

$$\eta_i = \alpha_i + B\eta_i + \Gamma x_i + \zeta_i. \tag{2-18}$$

Given the changes in the general SEM framework, the equations 2-18, 2-15, 2-14, and 2-17 summarize the most important assumptions for the modeling of dichotomous and continuous latent variable indicators according to the "fixed x" case.

2.6.4.1 Estimation

The parameters that should be estimated are collected in a vector; $\theta = (\tau_y, \nu_y, \Lambda_y, \Theta_\epsilon, \alpha, B, \Gamma, \Psi)$. A three-stage weighted least square (WLS) method for the estimation of θ has been proposed as the best practice where SEM involves observed response categorical variables (81). Although this method is not numerically efficient as the full information maximum likelihood estimator (FIML), it provides consistent and asymptotically normally distributed estimates (82). In this method, first, an intermediate population vector function of the parameter θ is defined, $\sigma(\theta)[\cdot]$. Then, the estimation of θ is performed in two steps: estimation of $\sigma(\theta)$ and subsequent estimation of θ. Defining the unrestricted format of $\sigma(\theta)$ as s, it is estimated in the first and second stages of the mentioned three-stage WLS. In order to perform this task, the elements of s are estimated in univariate and bivariate analyses of the latent continuous indicators $y^*_{i,j}$. In the third stage, θ is estimated by minimizing a WLS discrepancy function

$$F(\theta) = \{s - \sigma(\theta)\}^t W^{-1} \{s - \sigma(\theta)\} \tag{2-19}$$

between the estimated values for s and $\sigma(\theta)$. W is a positive definite weight matrix, and in the standard WLS form it conforms with V_2, a consistent estimator of the asymptotic covariance matrix of s. However, W may also be a diagonal matrix with estimated variances of s and WLS becomes the weighted least squares mean and variance adjusted (WLSMV) estimator (83), whose asymptotic covariance matrix is determined by

$$\widehat{var}(\widehat{\theta}_{WLSMV}) = n^{-1} \left(\Delta^t W^{-1} \Delta\right)^{-1} \Delta^t W^{-1} V_2 W^{-1} \Delta (\Delta^t W^{-1} \Delta)^{-1} \qquad (2\text{-}20)$$

where $\Delta = \partial\sigma(\theta)/\partial\theta$ and n is the number of p response variables y_i.

WLSMV has proved to be a robust estimator in simulation studies due to its better estimation efficiency in moderate sample sizes (84, 85). Another robust estimator found in the literature from the WLS family is mean adjusted weighted least square (WLSM).

2.6.5 Path diagram

As the number of modeled observed variables increases, a common way to simplify the hypotheses is achieved by the use of a *path diagram*. The single headed arrow connects a given cause to its effect. If no directionality (i.e., causation) is tested between two variables, a two-headed arrow represents such assumption. Given the nature of the variables, observed or latent ones, they are represented by different geometrical forms. Observed variables (x_i, y_i) are represented by squares while latent ones (ξ_i, η_i) are represented by circles (or ellipses).

2.6.6 Test of model fit

Defining Σ as the population covariance matrix of observed variables y and x, and $\Sigma(\widehat{\theta})$ as the model implied covariance matrix from SEM obtained through the estimation of θ, the fundamental hypothesis of model fit in SEM can be expressed by

$$\Sigma = \Sigma(\widehat{\theta}) \qquad (2\text{-}21)$$

In general, both Σ and $\Sigma(\widehat{\theta})$ are unknown matrices. Assuming that S is a consistent estimator of Σ (in the case of categorical indicators only the estimation of $y^*_{i,j}$ is performed), (2-21) becomes

$$S^* = \Sigma(\widehat{\theta}) \qquad (2\text{-}22)$$

where S^* is the population covariance matrix of $y^*_{i,j}$ variables. For the sake of simplicity, the superscript "*" will be removed hereafter. The aim of the model

fit assessment is to estimate a set of parameters θ (i.e., $\widehat{\theta}$) which imply the minimization of $S - \Sigma(\widehat{\theta})$. The magnitude of the discrepancy between S and $\Sigma(\widehat{\theta})$ is an indicator of the adherence of the model to the data (86).

2.6.6.1 Chi-square statistic

The degree of approximation between S and $\Sigma(\widehat{\theta})$ is called overall fit. The most important fit index for this purpose is the model χ^2 - statistic which is also scaled as a badness-of-fit index, given that a large χ^2 means a bad fit. χ^2 evaluation is based on the statistical significance of the exact-fit hypothesis, given a certain p-value. When categorical variables are modeled, it may result in a large sample χ^2 test of model fit as follows

$$2 \cdot n \cdot F_{WLS}(\widehat{\theta_{WLS}}), \tag{2-23}$$

where F_{WLS} denotes the WLS discrepancy function (2-19). To avoid this, an alternative is the *mean and variance adjusted* χ^2 test (G_{MV}) (84), which is specially appropriated to moderate sample sizes. G_{MV} is expressed by

$$G_{MV} = \{d^*/tr(UV_2)\} \cdot n \cdot F_{WLSMV}(\widehat{\theta}_{WLSMV}), \tag{2-24}$$

where $U = W^{-1} - W^{-1}\,\Delta(\Delta^t W^{-1}\Delta)^{-1}\,\Delta^t W^{-1}$, W is the weight matrix of the WLSMV estimator, $\Delta = \partial\sigma(\theta)/\partial\theta$, and d^* is the closest integer to the term $\{tr(UV_2)\}^2/tr\{(UV_2)^2\}$. This variable is approximately χ^2 distributed with d^* degrees of freedom.

2.6.6.2 Comparative fit index (CFI)

Lets define the difference between the number of observed variances and covariances and the number of estimated parameters as *degrees of freedom*, df. Given the noncentrality parameter $d = \chi^2 - df$, Bentler (87) developed a fit index to compare the difference between a null model d_{null} and the specified one $d_{specified}$,

$$CFI = \frac{d_{null} - d_{specified}}{d_{null}} \tag{2-25}$$

The fit index can be classified as a goodness-of-fit, since a value close to 1 indicates the best fit. The desired cutoff value in a well specified model is 0.90. However, CFI values do not tend to be high, if the correlation between variables is not high. Therefore, CFI is also considered an incremental or relative fit index.

2.6.6.3 Tucker-Lewis index (TLI)

Another fit index that is commonly used in SEM model fit is the TLI, which can be defined as follows,

$$TLI = \frac{(\chi^2_{null}/df_{null} - \chi^2_{specified}/df_{specified})}{(\chi^2_{null}/df_{null} - 1)} \tag{2-26}$$

TLI (88) is also reffered as NNFI and is classified as an incremental fit index. Also like CFI, TLI depends on the magnitude of the correlations between variables. A well specified model must present TLI between 0.90 and 1. The difference between CFI and TLI is that the last favors parsimonious models. Very complex models tend to present a great number of free parameters, therefore they present a low $df_{specified}$. Another observation concerning the difference between CFI and TLI is that the last generally presents smaller values than the former (86); however, the same cutoff is generally used for both fit indexes.

2.6.6.4 Root mean square error of approximation (RMSEA)

A well known alternative fit index for model fit evaluation also used in SEM is RMSEA, which is defined as follows

$$RMSEA = \sqrt{\frac{\chi^2_{specified} - df_{specified}}{df_{specified}(N-1)}} \tag{2-27}$$

where N is the sample size.

RMSEA is an index both scaled as badness-of-fit and parsimony-adjusted. It assumes a noncentral distribution, given by $\chi^2_{specified} - df_{specified}$. In the case where $\chi^2_{specified} > df_{specified}$, the index is increasingly positive, otherwise RMSEA is equal to 0. Besides model complexity, the fit index penalizes small samples, given the term $(N-1)$. The generally used cutoff values are: 0 = perfect fit; < 0.05 = close fit; $0.05 - 0.08$ = fair fit; $0.08 - 0.10$ = mediocre fit; and > 0.10 = poor fit (89). Special attention must be given when $\chi^2_{specified} \leq df_{specified}$ because RMSEA will be $= 0$, but this do not necessarily mean perfect fit.

An advantage of RMSEA in comparison with other indexes is the possibility to estimate a confidence interval (CI). In general, a well specified model has a 90% CI, asymmetric, around the RMSEA value. A null hypothesis test, where H_0 is RMSEA < 0.05, is performed based on p-value statistics. This p-value is also known as "p-value of close fit (PCLOSE)" (90).

2.6.6.5
Weighted root mean square residual (WRMR)

WRMR is a model fit index commonly reported in models where sample statistics are in different scales, for instance models with mean and/or threshold structures. WRMR is defined as (91)

$$WRMR = \sqrt{\frac{\sum_j \sum_k (s_{jk} - \widehat{\sigma}_{jk})}{\upsilon_{jk}} \times \frac{1}{e}} \tag{2-28}$$

where $(s_{jk} - \widehat{\sigma}_{jk})$ is the residual of elements in the matrices S and $\Sigma(\widehat{\theta})$, υ_{jk} is the estimated asymptotic variance of elements in the matrix S, and e is the total number of the elements in the matrix S. WRMR values equal of lower than 1.0 are indicators of good model fit (91).

2.6.7
Statistical computing

The analyses were performed in the language and environment for statistical computing R (92), using the *lavaan* package (79). This package presents a relatively easy syntax, the robust estimator WLSMV, and the robust scaled version of fit indexes (e.g., χ^2, TLI). Once the model was fitted, the existence of indirect effects in a classical mediation setup was investigated. The standard error for the parameters related to the indirect effects are estimated using the delta method (93).

3
Particle pollution in Rio de Janeiro, Brazil: increase and decrease of pro-inflammatory cytokines IL-6 and IL-8 in human lung cells

Rosa I. Rodríguez-Cotto[a,b], Mario G. Ortiz-Martínez[a,b], Evasomary Rivera-Ramírez[b,c], Vinicius L. Mateus[d], Beatriz S. Amaral[d], Braulio D. Jiménez-Vélez[a,b], Adriana Gioda[b,d]

[a]University of Puerto Rico- Medical Sciences Campus, Department of Biochemistry;
[b]Center for Environmental and Toxicological Research, San Juan, Puerto Rico 00936;
[c]University of Puerto Rico-Río Piedras Campus, Department of Biology.
[d]Pontifical Catholic University, Rio de Janeiro (PUC-Rio), Department of Chemistry, RJ, Brazil

Corresponding author: Braulio D. Jiménez-Vélez - Email: braulio.jimenez@upr.edu

Published: *Environmental Pollution 194 (2014) 112-120*

Abstract

Ambient particle pollution mostly results from human activities originating in industrialized and metropolitan urban areas. Airborne particulate matter ($PM_{2.5}$ and PM_{10}) collected from six sites in Rio de Janeiro: two industrial sites (Duque de Caxias, Ind 1 (PM_{10}) and Santa Cruz, Ind 2 ($PM_{2.5}$), the urban area of Centro (PM_{10}) and a rural site of Seropédica ($PM_{2.5}$ and PM_{10}) was used to evaluate metal constituents. Cytotoxicity and the release of pro-inflammatory cytokines (IL-6 and IL-8) were analyzed in human bronchial epithelial cells (BEAS-2B) exposed to organic and aqueous extracts. Chemical analyses of the aqueous extracts revealed the presence of Zn as the most abundant trace element. The lowest metal concentrations were obtained at the rural site (Seropédica, Ref 1 and Ref 2) excluding Al and Cu. While PM_{10} acetone extracts were highly cytotoxic they did not elicit cytokine release, conversely the aqueous extracts were less toxic and yet stimulated the secretion of pro-inflammatory mediators. The $PM_{2.5}$ aqueous extracts from Santa Cruz (Ind 2) contain elements that inhibit the release of IL-6 and IL-8. These results

demonstrate that ambient PM from Rio de Janeiro can either induce or inhibit cytokine secretion and that it is not only site specific but also dependent on time.

Keywords: particle; BEAS-2B; industry; cytokines; inhibition; metals

3.1 Introduction

Introduction Atmospheric aerosol also referred as particulate matter (PM) is an essential component of air that can influence climate, visibility, biogeochemical cycling, and atmospheric reactivity; and ultimately affect human health (6). A worldwide effort to control global PM emissions, reduce global warming and protect human health has been recently recognized and endorsed by respectable institutions. The United States Environmental Protection Agency (USEPA) has established $PM_{2.5}$ and PM_{10} National Ambient Air Quality Standards (NAAQS) in order to regulate and protect human health. The NAAQS for $PM_{2.5}$ are 35 μg m^{-3} in a 24 h period plus an annual mean of 15 μg m^{-3} and 150 μg m^{-3} for PM_{10} (94, 95). The World Health Organization (WHO) established an annual average of 10 μg m^{-3} ($PM_{2.5}$) and 20 μg m^{-3} (PM_{10}) and a 24 h average of 25 μg m^{-3} ($PM_{2.5}$) and 50 μg m^{-3} (PM_{10}) (96). The Brazilian legislation for PM has not been updated since it was initially published in 1990. It established ambient air quality standards for inhalable particulate matter (PM_{10}) but has not yet adopted any ($PM_{2.5}$) standards. The Brazilian limits for annual PM_{10} is established at 50 μg m^{-3} and daily maximum at 150 μg m^{-3} . Therefore, the PM_{10} limits are much higher than those recommended by the WHO.

Natural and anthropogenic sources contribute to the total PM global mass emissions and are critical at particular sites due to its PM environmental load. The most abundant natural source of PM (coastal environments) is sea salt followed by soil dust resuspended by wind (dust plumes) and aerosol particles derived from plant waxes, pollens, spores and other similar materials (2). Other natural sources include volcanic ash, which also contributes to increases in PM through eruption. Reports from a 2010 volcanic eruption in Iceland show a 24 h mean concentration of PM_{10} as high as 1,230 μg m^{-3} (25 times the established health limit) with a 10 min average values over 13,000 μg m^{-3} (97). Moreover, Soufrière Hills Volcano in the island of Montserrat increased background PM concentrations to a factor of 10 (98). Some heavy metals including Cd, Cu, V, F, Cl, Zn, and Pb were found enriched in PM aqueous fractions from volcanic aerosol (99). Anthropogenic sources contain combustion (black or elemental carbon and organic material such as

polycyclic aromatic hydrocarbons/PAH's) and industrial processing materials (100). The amount of compounds resulting from vehicle tire ware and the combustion of gas and diesel fuel also contribute to environmental urban PM. A variety of indoor combustion and human activity also contribute significantly to human exposure. Incinerator burning of waste and land burning are also considered additional sources contributing to local as well as global aerosols. All of these sources modulate PM to the extent of causing human respiratory and cardiovascular diseases through inhalation and (101, 102, 103, 104, 105, 106). The mechanisms associated to PM adverse health effects are not well understood, but inflammatory processes and oxidative stress are believed to play a key factor in the development of diseases (107). Current efforts are focused on the identification of specific constituents of PM from complex mixture, which are linked to human health effects (6).

In Brazil, the continuous monitoring of PM has been performed in a few regions, for example, by the Company of Environmental Sanitation Technology (Cetesb) in São Paulo (SP) and Environmental Institute of Rio de Janeiro (RJ) (INEA). São Paulo and Rio de Janeiro established the first air monitoring stations in the 70s in the metropolitan area of their capitals. Nowadays there are monitoring networks distributed throughout these states, which are the only ones tracking $PM_{2.5}$. Other states: Rio Grande do Sul (RS), Paraná (PR) and Minas Gerais (MG) have short-term monitoring stations located mainly in the metropolitan areas. Amazon region has been monitored due to biomass burning (104). The lack of continuous monitoring precludes the establishment of new standards for air quality. Due to the size of the country and the different activities of each region, as well as differences in climate, air quality varies widely as well as the chemical composition of the particles. Epidemiological studies performed in SP showed that people are exposed to high concentrations of particles (101, 102, 105, 106). São Paulo has the biggest fleet of Brazil with about 8 million vehicles as compared to 3-5 million in Mexico City, DF (108, 109). Therefore, the emissions of suspended particles are mainly from vehicular traffic. Local PM_{10} emissions (power plants, soil resuspension and road dust emissions) have been shown to impact regional air quality at Santa Catarina (SC), Brazil (110). In RJ, some studies have been performed regarding chemical analyses on PM composition (10, 36, 50, 111, 112, 113). However, studies about biological responses of specific agents using in vitro assays of these PM are scarce.

There have been various epidemiological studies conducted in RJ, which link PM exposure to various health conditions. PM exposure has been associated to mortality from lung cancer (114, 115). Respiratory diseases have

been linked to PM exposure through reduced respiratory capacity amongst children (116), and increased pediatric visits to treat symptoms of bronchial obstruction (117). The mutagenic and genotoxic activity of PM collected at three different stations in RJ was associated to PAH's found in high traffic stations (118). Although these epidemiological links to PM have been established, we do not know of any reports published characterizing toxicological responses of PM from RJ. This is the first study to report the effects of PM material on immunological responses using human lung cells. The PM from various urban/industrial (Centro, Duque de Caxias and Santa Cruz) and rural (Seropédica) sectors of RJ was tested for cytotoxic and pro-inflammatory capacity using an in vitro human bronchial epithelial cell model. The specific contribution of the effect of trace elements on these toxicological responses was evaluated for these samples by differentially testing with the chelating agent, deferoxamine mesylate (DF).

3.2 Materials and methods

The reader is referred to the description in section 2.1, page 28.

3.3 Results

3.3.1 PM levels and metal composition

The annual PM_{10} mean concentrations were 34.2 μg m^{-3} for Ref 1, 46.5 μg m^{-3} for the urban site and 71.1 μg m^{-3} for the Ind 1 (10). As expected, the lowest concentration for PM_{10} was obtained at Ref 1, followed by the urban and Ind 1 sites (10). However, the PM_{10} annual concentration at all sites exceeded the recommended standards establish by WHO (20 μg m^{-3}) which indicates that Brazil should develop a strategic plan to improve its air quality in RJ. In this study, the daily concentration at all these sites also exceeded (Table 3.1) the standard reference value established by the organization, which is 50 μg m^{-3}. The trace element analyses of all PM_{10} aqueous extracts showed that Cu and Zn were the most abundant metals at all stations. Although most metals were generally lower at the rural site Al was higher. Conversely, all other trace metals (Zn, Cu, Cd, Ti and Fe) were higher at the urban and Ind 1 sites.

The annual $PM_{2.5}$ mean was similar for all sites (12 μg m^{-3}), this is about 20 % higher than the WHO standard (10 μg m^{-3}) (Mateus et al., 2013). Correspondingly, the daily $PM_{2.5}$ concentration reported here also exceeded

Table 3.1: Trace element concentration in PM_{10} aqueous extracts at three sites in Rio de Janeiro.

Site	Urban	Industrial 1	Reference 1
PM(μg m^{-3})	84.4	63.9	86
Metals (μg mL^{-1})			
Al	0.0980	0.1313	0.1020
Cd	0.0042	0.0092	0.0007
Cr	0.000	0.0039	0.000
Cu	3.6496	0.2591	0.0808
Fe	0.1240	0.1333	0.0282
Ni	0.0109	0.0058	0.000
Pb	0.0069	0.0077	0.000
Ti	0.0038	0.0038	0.0004
V	0.0165	0.0053	0.000
Zn	2.9550	2.6361	1.5402

the value recommended by WHO (25 μg m^{-3}) (Table 3.2). Similar to what was found in PM_{10} aqueous extracts, Zn was also the most abundant element in $PM_{2.5}$. For CIEP João XXIII and Conjunto Alvorada two samples were analyzed in each case. A difference in metal concentrations was observed between the samples of the two sites (Table 3.2). The metal concentrations at Ind $2a_1$ during August 2010 were consistently higher than at the same station but at different time (Sept, Ind $2a_2$). This was also true for Ind $2b_1$ (August) and Ind $2b_2$ (September) in 2010. Industrial site Ind 1 consistently had higher concentrations of heavy metals when compared to the Ind 2 (Tables 3.1 and 3.2).

3.3.2 Cytotoxicity and Cytokines Secretion by PM10

3.3.2.1 Organic extracts

All the PM_{10} acetone extracts exhibited a toxic effect on BEAS-2B at a concentration of 10 μg mL^{-1} (Fig. 3.1). Pre-treatment with DF substantially prevented cytoxicity of both the Ind 1 and Ref 1 acetone extracts at 10 μg mL^{-1} and 15 μg mL^{-1} (Figs. 3.1B-C), respectively. At the non-toxic concentration of 5 μg L^{-1} these extracts did not inhibit the release of IL-6, IL-8 or IL-10 and neither induced them. Urban and Ref 1 hexane extracts were not toxic to cells up to 100 μg mL^{-1}. On the contrary, Ind 1 hexane extract was toxic at 100 μg mL^{-1} and pre-treatment with DF significantly increased cell viability from 76 % to 88 % (Fig. 3.2). Cytokine levels (IL-6, IL-8 and IL-10) compared

Table 3.2: Trace element concentrations in PM2.5 aqueous extracts.

Site	Industrial 2				Reference 2
Sample ID	$2a_1$	$2a_2$	$2b_1$	$2b_2$	
PM (μg m^{-3}	43.4	29.4	42.8	21.1	27.8
Metals (μg mL^{-1})					
Al	0.02	<0.06	0.01	<0.06	<0.06
Cr	<0.004	0.001	<0.004	<0.004	0.001
Cu	0.033	0.021	0.028	0.035	0.043
Fe	0.178	0.071	0.224	0.042	0.071
Mn	0.030	0.017	0.045	0.012	0.019
Ni	0.011	<0.01	0.015	0.001	<0.01
Ti	0.006	0.005	0.007	0.002	0.003
V	0.065	0.016	0.093	0.017	0.014
Zn	3.289	1.700	3.598	0.339	0.713

Ind $2a_1$ and Ind $2b_1$: collected simultaneously during August.

Ind $2a_2$ and Ind $2b_2$: collected simultaneously during September.

to controls did not change after cell exposure to these extracts at any of the concentrations tested.

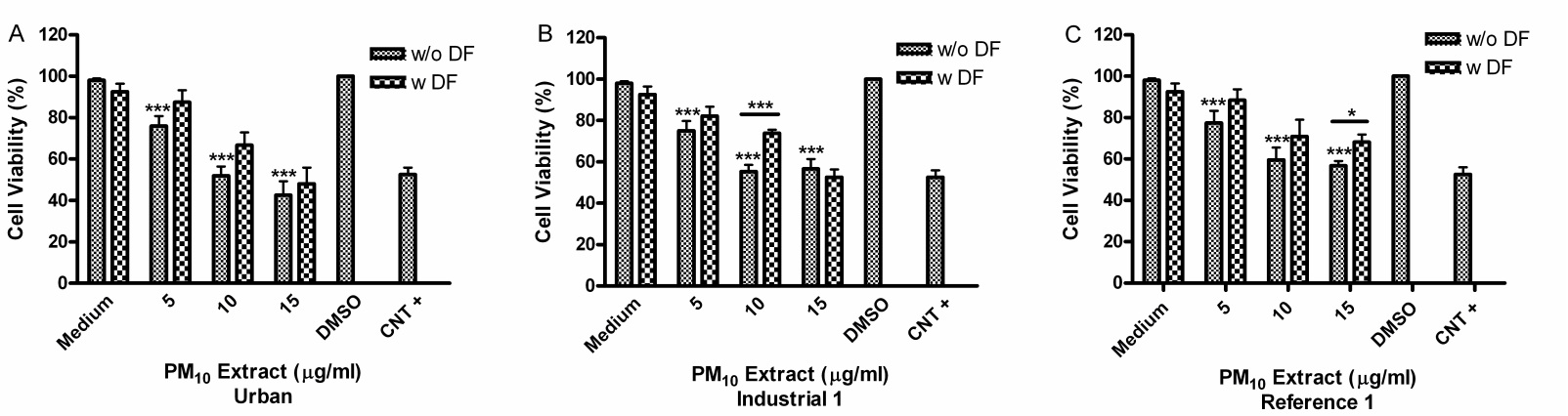

Figure 3.1: Effect of deferoxamine (DF) on BEAS-2B cytotoxicity to PM_{10} acetone extracts from: Urban (A) Ind 1 (B) and Reference Ref 1 (C) on BEAS-2B with and without 50 μM deferoxamine (DF) pre-treatment. Triton X was used as a positive control at a concentration of 25 μg mL^{-1}. A cut off value of 80 % was considered as cytotoxic. Bars represent mean % cell viability $\pm$ standard error of mean, ***: $p<0.001$, *: $p<0.05$ compared to medium or to the adjacent treatment ($n = 3$).

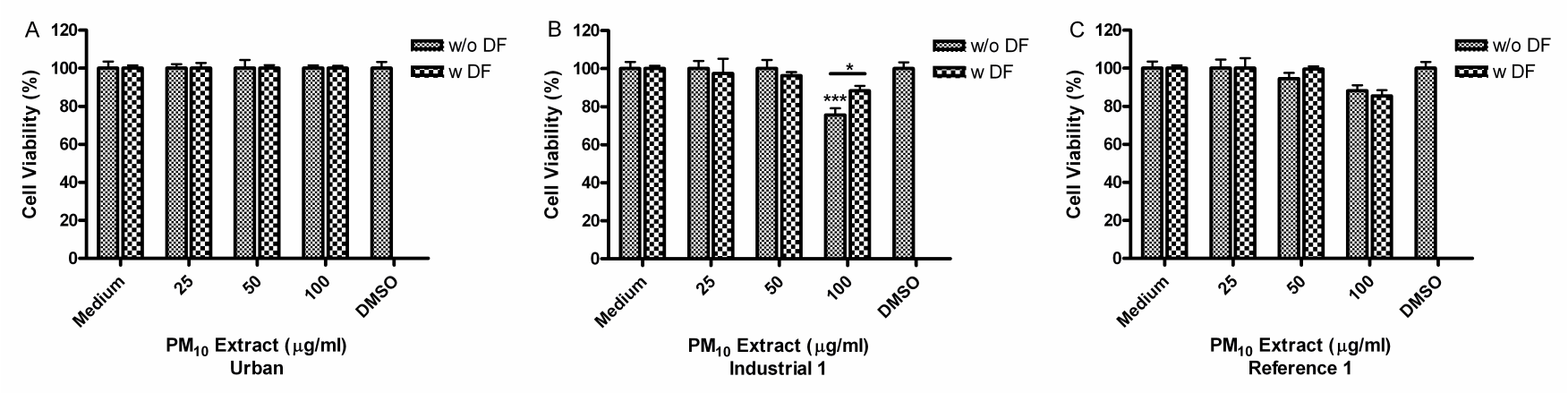

Figure 3.2: Effect of deferoxamine (DF) on BEAS-2B cytotoxicity to PM_{10} hexane extracts from: Urban (A) Industrial 1 (B) and Reference 1 (C) on BEAS-2B cells with and without 50 μM deferoxamine (DF) pre-treatment. Triton X was used as a positive control at a concentration of 25 μg mL^{-1}. A cut off value of 80 % was considered as cytotoxic. Bars represent mean % cell viability $\pm$ standard error of mean, ***: $p<0.001$, *: $p<0.05$ compared to medium or to the adjacent treatment ($n = 3$).

3.3.2.2 Aqueous extracts

The urban aqueous extract was not toxic to BEAS-2B at 25 μg mL^{-1}; however, Ind 1 and Ref 1 were not toxic even at a concentration of 250 μg mL^{-1} (Fig. 3.3). Aqueous extracts were less toxic than organic extracts and they significantly induced the release of IL-6 and IL-8 from BEAS-2B after 24 h (Fig. 3.4). The urban aqueous extract induced the release of these pro-inflammatory mediators at a concentration as low as 25 μg mL^{-1} while Ind 1 and Ref 1 required a higher concentration of 250 μg mL^{-1}. Evidence was not found for the release of IL-10 at the time point tested of 24 h.

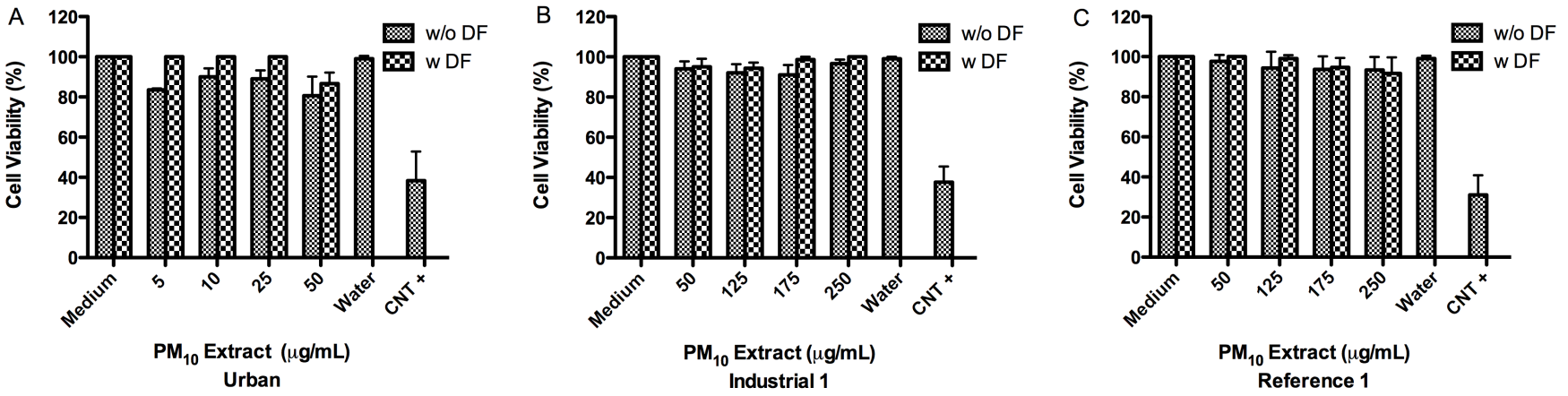

Figure 3.3: Effect of deferoxamine (DF) on BEAS-2B cytotoxicity to PM_{10} aqueous extracts from: Urban (A) Industrial 1 (B) and Reference 1 (C) on BEAS-2B cells with and without 50 µM deferoxamine (DF) pre-treatment. Triton X was used as a positive control at a concentration of 25 μg mL^{-1}. A cut off value of 80 % was considered as cytotoxic. Bars represent mean % cell viability ± standard error of mean, ***: p<0.001, *: p<0.05 compared to medium or to the adjacent treatment ($n = 3$).

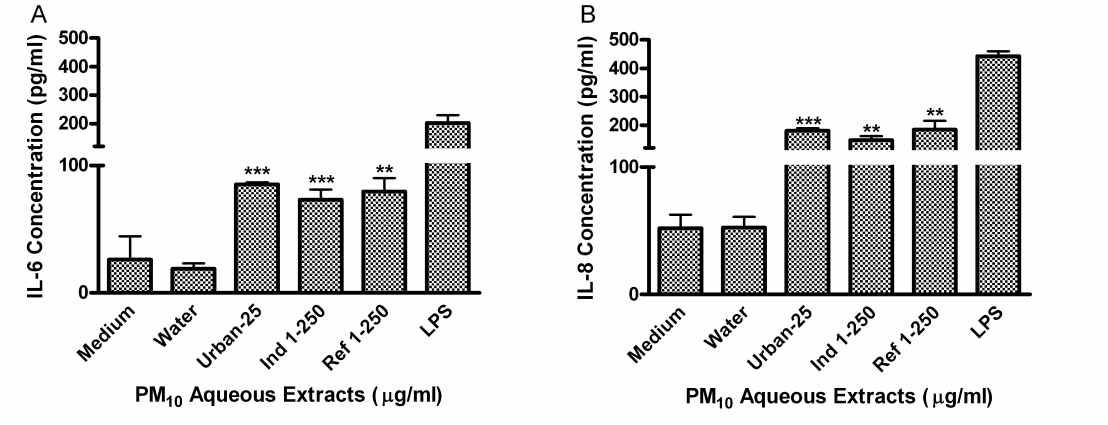

Figure 3.4: Effect of PM_{10} aqueous extracts from three sites: Urban, Industrial 1 and Reference 1 on IL-6 (A) and IL-8 (B) induction in BEAS-2B cells. Lipopolysacharides (LPS) was used as a positive control at 10 μg mL^{-1}. Bars represent cytokine mean concentration $\pm$ standard error of mean, ***: p<0.001, **: p<0.01, *: p<0.05 compared to water ($n = 3$).

3.3.3
Cytotoxicity and Cytokines Secretion by PM2.5

3.3.3.1
Aqueous extracts

Aqueous extract from Ref 2 was not toxic to BEAS-2B even at a concentration of 175 μg mL^{-1} (Fig. 3.5E). Ind 2a$_1$ extract was toxic at 50 μg mL^{-1} (Fig. 3.5A) while a similar extract from that same station (Ind 2a$_2$) taken on a different month was not toxic until 175 μg mL^{-1} (Fig. 3.5C). Extracts from samples collected at both Ind 2a$_1$ and 2b$_1$ stations at 50 μg mL^{-1} and 125 μg mL^{-1} were more toxic than Ind 2a$_2$ and 2b$_2$ extracts both at 175 μg mL^{-1} (Fig. 3.5). The concentration of metals in the air at both stations was higher during the first collection period than during the second. There are days when the airborne particulate matter collected at the Ind 2 site exhibited the same toxicity profile as that collected at the Ref 2 site. However, we also found that the material collected in August was more toxic than that collected in September (Figs. 3.5A-B).

Three of the four sample extracts tested from the Ind 2 sites inhibited the release of IL-6 (Ind 2a$_1$ at 25 μg mL^{-1}, Ind 2b$_1$ at 50 μg mL^{-1} and Ref 2 at 175 μg mL^{-1}) (Fig. 3.6A). Aqueous extracts from Ind 2a and b reduced IL-6 as much as 26 folds from that of controls while extracts from Ref 2 reduced it by 15 folds. IL-8 released was also inhibited 9 folds in extracts from both Ind 2a and 2b (Fig. 3.6B). To our surprise none of the extracts from $PM_{2.5}$

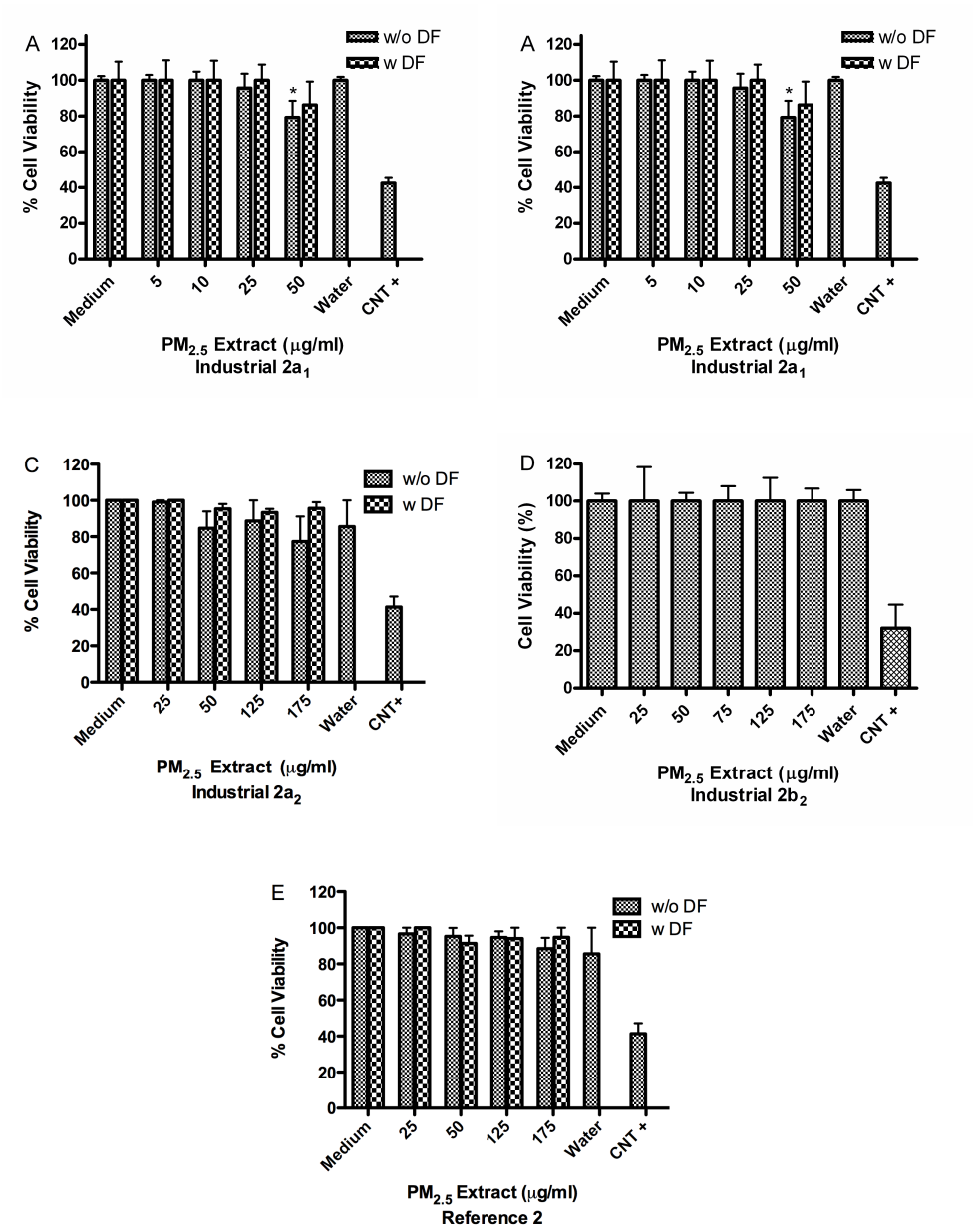

Figure 3.5: Effect of deferoxamine (DF) on BEAS-2B cytotoxicity to PM2.5 aqueous extracts from: (A) Industrial-2a1 and (B) Ind-2b1 (August), (C) Ind-2a 2 and (D) Ind-2b2 (September) and (E) Reference-2. Triton X was used as a positive control at a concentration of 25 μg mL^{-1}. DF was used at 50 μM. A cut off value of 80 % was considered as cytotoxic. Bars represent mean % cell viability $\pm$ standard error of mean, ***: $p < 0.001$, **: $p < 0.01$, *: $p < 0.05$ compared to medium ($n = 3$).

induced the release of IL-6 or IL-8 as did the PM_{10} aqueous extracts. None of the extracts induced the expression of IL-10 at the time point tested. Two samples (Ind $2a_2$ and Ind $2b_2$) were not tested for cytokine secretion.

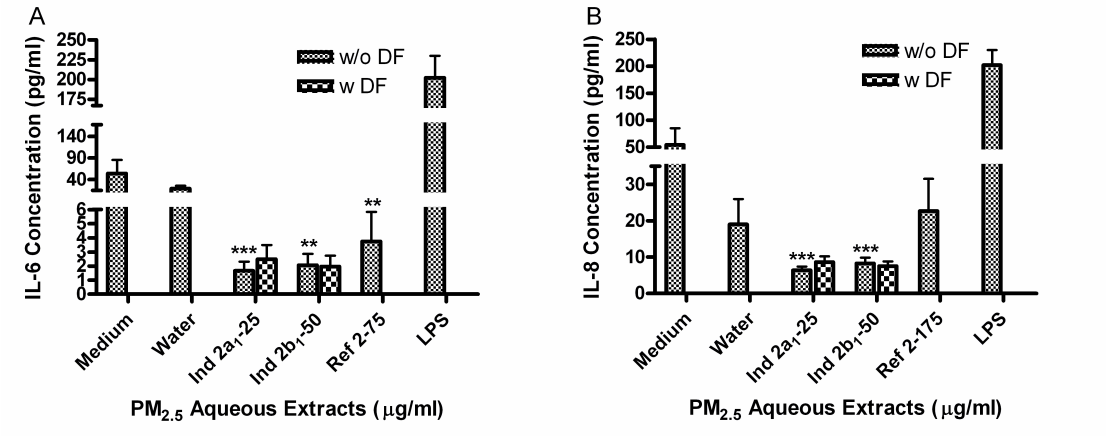

Figure 3.6: Effect of $PM_{2.5}$ aqueous extracts on BEAS-2B cytokines secretion, IL-6 (A) and IL-8 (B). Lipopolysacharides (LPS) was used as a positive control at 10 μg mL^{-1}. Bars represent cytokine mean concentration $\pm$ standard error of mean, ***: $p<0.001$, **: $p<0.01$, *: $p<0.05$ compared to water ($n = 3$).

3.4 Discussion

Increases in airborne PM levels are commonly observed from May to September in the general region of RJ (10). This is due to reduction in wind speed during winter, associated to meteorological processes such as low relative humidity and seasonal rainfall. One of the sampling periods for $PM_{2.5}$ coincided with the opening of a large steel plant in the area of Santa Cruz Ind $2a_1$. During the first months the company was under operational trials and undesirable emissions released. The differences in metal concentrations determined in $PM_{2.5}$ for CIEP João XXIII (Ind $2a_1$ and $2a_2$) compared to Conjunto Alvorada (Ind 2b1 and 2b2) can be attributed to higher levels in Cu, Fe, V, Mn, Ni, and Zn in August vs. September. The toxic characteristics of the extracts can also be attributed to the differences in collection periods, August being more toxic than September. This is evidenced by the wide difference in metal concentration between Ind $2a_1$ vs. Ind $2a_2$. The metal load in the aqueous extract can explain most of the toxicity found in Ind $2b_1$ and Ind $2a_2$, however, this is not the case for the extracts obtained in station Ind $2a_1$. The toxicity at this station is caused by additional factors other than metal alone. The results of this study reveal that Zn (available at high quantity) plays a key role in RJ environment and could be associated to toxicity and immune responses. This is consistent in part with findings of studies in downtown

and suburban areas characterized by industrial and vehicular emissions, as well as natural input. Enrichment factors found in the downtown area for Zn, Cu, Pb and Cd were in the interval 21-3237 ng m^3, indicating an important contribution of anthropogenic sources. In the suburban area, Zn levels were unusually high (596.8–5475.4 ng m^{-3}) and may be attributed to the proximity of a company that produces lubricants (112, 113). Mateus et al. (36) reported high concentrations of Zn and Al in $PM_{2.5}$ and attributed this finding to various industrial sources. Furthermore, Gioda et al. (10) showed that metal content at these industrial sites in RJ were twice as high as that of a rural site.

Organic extracts obtained from PM_{10} were highly toxic to BEAS-2B at 10 μg mL^{-1}. These extracts had a general toxic effect since it was observed for all stations even at the reference site. Much of the work performed in Brazil relates to coarse PM_{10} chemical composition and very little emphasis has been given to $PM_{2.5}$. This is evident for the lack on $PM_{2.5}$ regulations. PM_{10} composition has been previously reported at Ref 1 site and includes 9 % sea salt, 11 % NH_4NO_3 12 % $(NH_4)_2SO_4$, 13 % water-soluble organic carbon and soil as the predominant fraction with 55 % (10). Previous research performed on soil fraction showed a negative correlation with IL-8 secretion (118). The cytokine induction observed in Ref 1 can be associated with the organic fraction of PM. The PM_{10} aqueous extract obtained at the urban site induced IL-6 and IL-8 at much lower concentration than extracts from Ind 1 and Ref 1 sites. Urban PM has a strong component of fossil fuel due to the magnitude of engine emissions and energy burning in the city as compared to the other sites. It has been well established that particulate matter PM_{10}, $PM_{2.5}$ and diesel exhaust particles (DEP) can induce the production of inflammatory cytokines and chemokines in epithelial cells and macrophages (11, 37, 38, 120, 121, 122). Fuel combustion products especially from diesel are associated with IL-6 and IL-8 induction in exposed lung cells (123). Inhalation studies at high doses of urban $PM_{2.5}$ from the city of SP, showed impairment of lung function by increasing elastic and viscoelastic lung mechanistic properties (124). PM from the same city and distributed in PAH's fractions was shown to cause mutagenicity and DNA adduct formation in Salmonella strains (125). Moreover, PM from RJ was also studied and found to be mutagenic and genotoxic (126). Finally, other studies have linked ambient $PM_{2.5}$ and PM_{10} from SP to significant cardiopulmonary alterations, blood parameters in vivo and increase in blood pressure (103, 105).

Mean concentrations of PM_{10} as high as 206 μg m^{-3} have been recorded at MG (247 miles Northwest of RJ). This was attributed to the resuspension of outdoor dust blown inside and living conditions (127). This study also showed toxic and pro-inflammatory responses (IL-8 release) of high concentrations of

indoor dust particles: 250-500 μg mL^{-1} and 100-500 μg mL^{-1}, respectively. In fact some studies have shown adverse health effects in this area. Increase of symptoms (wheezing) related to asthma were reported in 28.5 % of school students (95 % confidence interval: 22.3 % to 35.3 %) (128). Another study reported that increases of 10 μg m^{-3} in PM_{10} were associated with increases in respiratory emergency room visits for children and adolescents younger than 13 years of age (129). For cardiovascular diseases, the effect was acute and mainly for the 45 to 64 age group (129).

There are very few reports on IL-6 or IL-8 inhibition due to PM exposure (11, 38, 119, 123, 130). It has been reported that exposure to PM could induce (Becker et al., 2005) or inhibit (131) IL-8 cellular production. These findings indicate that PM effects on cytokine secretion can vary depending on the nature and specific constituents in PM. Furthermore, aqueous extracts from $PM_{2.5}$ collected from RJ clearly have an inverse effect on IL-6 and IL-8 response in lung epithelial cells. All PM_{10} extracts increased the secretion of these cytokines while all $PM_{2.5}$ extracts inhibited cytokine production. There are two discrete industrial sectors the Ind 1 (PM_{10}) and the Ind 2 ($PM_{2.5}$) sites, which were separated from each other. However the Ref 1 (PM_{10}) and Ref 2 ($PM_{2.5}$) were located in the general rural area. In addition to site difference and particle size distribution we also need to consider time of the collection. The PM_{10} samples were collected in 2009 while $PM_{2.5}$ were collected in 2010. This could explain some of the difference seen between samples (providing constituent differences in PM compositions). These results suggest that the regulation of IL-6 and IL-8 expression is different between PM_{10} complex mixture in comparison to $PM_{2.5}$. The control of IL-6 and IL-8 expression is related to different factors (132). IL-6 expression is related to at least three signal-transduction pathways: protein kinase C, cAMP/protein kinase A, and calcium ionophore (119, 132). The IL-8 is upregulated by the phosphorylation of Erk 1/2. The phosphorylation of p38 reduces the phosphorylation of Erk 1/2 and this leads to a down- regulation of IL-8 secretion (119). The inhibition of EGFR is also related to a decrease in IL-8 secretion (119). The cause and reasons associated with IL-6 and IL-8 reduced secretion by $PM_{2.5}$ at the Ind 2 site is unknown. However, we have demonstrated that inhibition of both these cytokines cannot be attributed to metals alone since the basal levels of these cytokines were not restored with the pretreatment of DF (Fig. 3.6). Therefore, we propose that polar organic constituents found in the Santa Cruz $PM_{2.5}$ extract trigger this phenomenon. Other researchers have reported similar findings where high polar organic DEP-extracts suppress IL-8 responses in BEAS-2B cells; despite stimulating IL-6 responses (123). We have

also reported similar findings for polar extracts of ambient PM (38). Taking into consideration the complexity of particle pollution composition related to multiple sources, it is not easy to speculate about what mechanisms trigger the inhibition of cytokines secretion. These finding set the bases for investigating the specific constituents in PM responsible for cytokine inhibition.

Acknowledgements

This research reported in this publication was supported by the National Institute of General Medical Sciences of the National Institutes of Health under award number R25GM061838. The content is solely the responsibility of the authors and does not necessarily represent the official views of the National Institutes of Health. The authors thank FAPERJ and CNPq for financial support. Vinícius L. Mateus is especially grateful to CAPES through Professor Luiz Drude, the coordinator of the INCT-TMCOCEAN Project, which provided his scholarship. All the work was accomplished using samples provided by INEA, and we are grateful for this essential support.

Conflict of Interest Statement

We certify that none of the authors has any actual or potential conflict of interest including any financial, personal or other relationships with other people or organizations.

4
Bioaccumulation of trace elements associated with particulate matter in white shrimps Litopenaeus vannamei after in vivo exposure

Vinícius L. Mateus[1], Juliane Ventura-Lima[2], Carolina R. Gioda[2], Renan C. Machado[2], Roberta Lobato[2], José M. Monserrat[2], Wilson Wasielesky Jr.[2], Adriana Gioda[1*]

[1]Pontifical Catholic University, Rio de Janeiro (PUC-Rio), Department of Chemistry, RJ, Brazil;
[2]Federal University of Rio Grande (FURG), Institute of Biological Sciences (ICB), Rio Grande, RS, Brazil

*Corresponding author: Adriana Gioda - Email: agioda@puc-rio.br

Paper under review: *Brazilian Journal of Analytical Chemistry*

Abstract

Adverse effects of air pollution are a health concern, especially those related to particulate matter (PM) exposure. However, potential ecotoxicological effects of this complex matrix are not well understood or not even evaluated. In this study, total suspended particles (TSP) collected in two regions (Santa Cruz, SC, and Seropédica, SE, Brazil) were monitored. SC was chosen due to its proximity to the Sepetiba Bay and the presence of an industrial complex, while SE was considered as a reference site. The industrial sources have a lower impact in SE, given a priori information about local pollution sources. Taking into account its global distribution, the white shrimp (*Litopenaeus vannamei*) was chosen as a model organism. The evaluation of trace element levels associated with TSP exposure was carried out in gills, hepatopancreas, and muscle. Some elements frequently associated with toxic effects (e.g., Fe, V and Pb) were in low concentration, but they might cause damage through chronic exposure. Zn, Cu, Mn, and Ba were found in high concentration in the saline composite extracts of PM indicating more bioavailability. Confirming the great bioavailability in saline conditions, the predominant metals in all organs were Zn and

Ba. These results suggest that PM from urban areas under influence of industrial activity could represent a potential risk for aquatic organisms that can accumulate trace metals, some of which can induce toxicity.

Keywords: *Litopenaeus vannamei*, Particulate matter, Industry, Metals, Bioaccumulation

4.1 Introduction

In recent years, air pollution has increased as a result of anthropogenic activities such as urbanization and industrialization. The deterioration of air quality has consequences for human and ecosystem health (133). Many pollutants are found in the air, including particulate matter (PM). These particles have a diameter that can vary up to 100 μm (Total Suspended Particles, TSP).

PM contains many chemical components, such as inorganic species (e.g., sulfates, nitrates, ammonia, and sea salt), organic compounds (e.g., carboxylic acids, amino acids, and Polycyclic Aromatic Hydrocarbons, PAH), and metals (14). It is known that the metal fraction of PM induces several effects and damage to the aquatic environment (134). Metals can be bioaccumulated, leading to many reactions and alterations in cells and tissues of the organisms (135). Metals such as Fe, Cu, Pb, Ni, Cd have been appointed as participants in the generation of oxidative stress, since some metals catalyze Fenton reaction, producing the highly reactive hydroxyl radical (13). In addition, studies relate air pollution exposure and cellular oxidative stress, which may be attributed to the presence of redox active metals in the PM composition (136, 137).

The PM samples were collected in the two sites in the Metropolitan Region of Rio de Janeiro (MRRJ), Brazil. Santa Cruz is an industrial district with great influence of steelworks. An important marine estuary is located in its surroundings, the Sepetiba Bay (138). Trace metal inputs from rivers and atmospheric deposition are pollution sources for the Sepetiba Bay. Molisani et al. (139) reported that the bay is highly contaminated by Zn, Cd, Pb, and Hg. Seropédica is the reference site. During the period of this study, industrial and other urban sources were not predominant as in Santa Cruz.

The aim of this study is to investigate the bioaccumulation of trace elements associated with PM in white shrimps (*Litopenaeus vannamei*). Fishing is an important socio-economic activity in the region of Santa Cruz and the expansion of the industrial complex in is a potential risk. *Litopenaeus vannamei* was chosen as model organism because it is globally known as an important organisms for aquaculture, and it is widely distributed in both coastal and

estuarine/lagoon environments (140). Besides that, their biological responses are sensitive to the presence of metals in aquatic environment, including bioaccumulation (141, 142). Thus, this study evaluated the bioaccumulation of different chemical species in gills, hepatopancreas, and muscle after in vivo PM exposure.

4.2 Materials and Methods

The reader is referred to the section 2.3, page 32.

4.3 Results and Discussion

The TSP geometric mean concentration (± standard deviation) ranged from 39 (± 15) μg m^{-3} at SE to 63 (± 22) μg m^{-3} at SC. The last one exceeds the secondary annual Brazilian standard (60 μg m^{-3}), which is designed to protect the public welfare, including vegetation, animals, and material. The difference in concentrations is expected since SC has much more particles sources than SE. Besides that, particle size is another important factor because larger particles tend to be deposited near their sources.

Both the ultrapure water and the bidistilled nitric acid exhibited low levels of the monitored elements, unlike of the blank filters that presented high concentrations. The most representative elements were Al (12.2 ± 0.6 mg kg^{-1}), Ba (11.4 ± 0.08 mg kg^{-1}), Fe (0.23 ± 0.11 mg kg^{-1}), and Zn (2.41 ± 0.23 mg kg^{-1}). In general, these are the major elements in glass fiber filters (Table 2.1).

With regard to the saline extracts from PM filters, the elements can be classified in two groups: 1) major elements (Zn, Cu, Mn, and Ba); and 2) trace elements (V, Fe, and Cd). Zinc had the highest concentration (32850 ± μg kg^{-1}) among the samples and it is very often listed as one of the traffic related elements (TREs). However, in this study its concentration may also be influenced by metallurgical process (36).

Among the trace elements, Cd had the lowest concentration (0.23 ± 0.01 mg kg^{-1}). It is noteworthy the seasonality for the concentration levels of Cu, Fe, Mn, and Zn. In higher rainfall, period 2, both Zn and Cu presented higher levels in SE than in SC. In lower rainfall, period 1, Fe, Zn, and Mn levels were higher in SC than in SE. The lower rainfall corresponds to the opening of a large steel plant in SC. Given that Fe, Zn, and Mn are commonly associated with steelworks, the undesirable emission of the company may explain these results.

Due to the constant contact with external environment, the concentrations of pollutants in gills are expected to be higher than other organs (Table 4.1). Several authors have described lesions in the gills of different organisms as a result of metal exposure: 1) fishes (16), 2) molluscs (17), and 3) shrimps (18). In fishes, there is a concerning about the absorption and metabolism of metals, via gills, before reaching the liver (19). Authors reported histological damages to gills, but these findings are related to higher concentration of single metals (Cd, Cu, Pb, and Zn) in different species of shrimps (18, 19, 20). In this study, the major elements observed in gills were Si, Ba, Zn, Al, Cu, and Fe.

Table 4.1: Mean concentration ± standard deviation of the measurement of elements (mg kg^{-1}, dry weight) in a composite sample of each organ from all five shrimp: gills (G), hepatopancreas (H), and muscle (M) exposed to saline extract of TSP.

Element	Organ	Saline water	Blank filter	SE-2	SE-1	SC-2	SC-1
Al	G	335 ± 19	92 ± 6	58 ± 2	855 ± 6	-	720 ± 19
	H	26 ± 16	26 ± 0.3	-	5.47 ± 0.31	11.9 ± 0.4	13.1 ± 1.4
	M	8.20 ± 0.71	7.27 ± 0.55	-	-	-	11.5 ± 0.1
Ba	G	66 ± 0.3	47 ± 0.8	232 ± 4	904 ± 2	74 ± 1	664 ± 7
	H	4.46 ± 0.22	4.21 ± 0.24	1.94 ± 0.02	23 ± 1	22 ± 2	19 ± 1
	M	486 ± 3[a]	1.37 ± 0.04	1.01 ± 0.05	1.13 ± 0.03	139.7 ± 0.4[a]	11.4 ± 0.3
Cd	G	0.44 ± 0.10	0.26 ± 0.04	-	-	-	32 ± 2
	H	50 ± 1[a]	0.30 ± 0.02	0.25 ± 0.05	0.19 ± 0.02	0.62 ± 0.24	0.31 ± 0.04
	M	-	-	-	-	-	-
Cr	G	4.96 ± 1.25	5.32 ± 3.90	-	0.82 ± 0.17	-	-
	H	-	0.83 ± 0.13	0.05 ± 0.02	-	0.14 ± 0.04	0.51 ± 0.13
	M	0.63 ± 0.03	0.45 ± 0.03	221 ± 4[a]	-	-	34 ± 3[a]
Cu	G	213 ± 1	295 ± 4	-	421 ± 1	65 ± 0.04	54 ± 1
	H	605 ± 1	723 ± 3	-	-	-	-
	M	17.8 ± 0.1	21 ± 0.1	10.5 ± 0.1	3.83 ± 0.07	-	9.71 ± 0.10
Fe	G	313.50 ± 5.07	-	-	583 ± 7	-	396 ± 5
	H	79 ± 4	106 ± 0.6	6.34 ± 0.05	-	9.83 ± 0.08	-
	M	9.46 ± 0.04	5.23 ± 0.07	-	-	-	3.52 ± 1.14
Mn	G	33 ± 20	9.03 ± 0.73	-	-	-	-
	H	-	4.48 ± 0.41	3.45 ± 0.12	3.66 ± 0.17	9.55 ± 2.87	4.47 ± 0.33
	M	-	-	-	-	-	-

Continuation of Table 4.1

Element	Organ	Saline water	Blank filter	SE-2	SE-1	SC-2	SC-1
	G	-	-	-	-	-	-
Ni	H	-	1.76 ± 0.12	0.98 ± 0.45	1.02 ± 0.65	1.76 ± 0.53	1.91 ± 0.66
	M	-	-	-	-	-	-
	G	10.8 ± 2.8	4.47 ± 0.31	-	-	-	-
Pb	H	-	2.02 ± 0.19	0.75 ± 0.04	0.47 ± 0.03	1.31 ± 0.24	1.28 ± 0.06
	M	5.67 ± 0.02	4.53 ± 0.01	-	-	-	-
	G	1.48 ± 0.85	-	-	-	-	-
Sb	H	-	0.12 ± 0.05	0.11 ± 0.05	-	0.75 ± 0.37	0.10 ± 0.04
	M	-	-	-	-	-	-
	G	777 ± 75	420 ± 21	1013 ± 68	3070 ± 110	226 ± 13	3915 ± 136
Si	H	208 ± 63	95 ± 10	-	4.08 ± 0.25	-	36 ± 4
	M	25 ± 1	34 ± 7	11.6 ± 0.8	7.55 ± 0.35	-	-
	G	10.1 ± 0.9	2.28 ± 0.24	0.75 ± 0.05	23 ± 4	-	20 ± 1
Ti	H	-	1.01 ± 0.09	0.68 ± 0.05	0.75 ± 0.05	1.27 ± 0.40	0.87 ± 0.07
	M	13.2 ± 2.7	13.6 ± 1.8	-	-	-	-
	G	1.36 ± 0.98	0.26 ± 0.23	-	0.36 ± 0.03	-	1.27 ± 0.06
V	H	0.61 ± 0.82	0.57 ± 0.11	-	-	-	0.13 ± 0.03
	M	0.03 ± 0.04	0.04 ± 0.01	-	-	-	-
	G	114 ± 2	113 ± 0.2	155 ± 1	735 ± 57	91 ± 7	509 ± 22
Zn	H	138 ± 1	144 ± 1	-	-	33 ± 0.3	2.61 ± 0.08
	M	50 ± 0.2	47 ± 1.1	3.43 ± 0.02	-	-	27 ± 0.5

-: lower than the LOD (mg kg^{-1}); ^{a}: µg kg^{-1}

As expected, high concentration levels of known toxic metals (i.e., Mn, Ni and Pb) were found in hepatopancreas. These levels were higher than in other organs as observed in other studies (143). Crustacean hepatopancreas is important for the metabolism and storage of xenobiotics (144). Al, Ba, Si, and Zn were the highest measured elements, and their average concentration ranged from 5 to 36 mg kg^{-1} (Table 4.1). Fe, Mn, Ni, Ti, and Zn were higher at SC-2. Fe and Zn were only determined at SC treatment. Although is not common to detect exposure to high Zn concentrations, it does occurs, mainly in coastal areas, and it has already been reported (145). SE-1 period and SE-2 presented similar levels to Ni and Mn. Mn level quantified in SC-2 is higher than reported in the literature to liver tissues of intensive aquaculture (146). In period 1, Ti

did not show difference between SE and SC. Barium presents similar levels to all treatment, except for SE-2. Antimony presented similar concentration levels in three treatments. Aluminum was not detected for SE-2, while SC-2 and SC-1 were similar. Copper was not detected at any treatment.

As observed in other studies, the metal content in muscles was lower than in the other organs. The concentration of elements has the decreasing order Zn > Ba > Cu > Fe > Cr (Table 4.1). The other elements were either detected in only one composite (i.e., Al, and Fe) or not detected in any composite (i.e., Cd, Mn, Ni, Pb, Sb, and V).

In general, shrimp exposed to saline water and blank filter treatments present higher concentration than those exposed to PM extracts specially for Al, Cr, Cu, Fe, Mn, Pb, Si, Ti, and Zn. Possible reasons for this behavior are impurities from the commercial sea-salt and blank filter, the use of coarse PM, and the relatively short exposure time. These factors not only explain the fact that some PM extracts were below detection for these elements, but they also provide new possibilities for future investigations.

Our study suggests that the industrialization of coastal areas is a potential risk for aquaculture, given the exposure to TSP. In general, TSP is not associated to direct damages to human health, since they have high aerodynamic diameter and cannot penetrate in the respiratory system. However, in the context of industrialized coastal areas, these particles have the potential to affect the environment because the elements can be solubilized and transferred to the organisms. Even though some trace elements were in lower concentrations they are toxic through chronic exposure. Besides, shrimps are small and they tend to be abundant, which may imply tropic transfer of contaminants.

Acknowledgments

The authors thank CAPES (especially to Prof. Luiz Drude, INCT-TMCOCEAN Project coordinator), CNPq, and FAPERJ for research grants. The authors also thank INEA for supplying PM samples and the aquaculture marine station (EMA-FURG) that provided the shrimps. They are also grateful to Prof. Tatiana Dillenburg Saint'Pierre for the spectrometric analyses (ICP-MS and ICP OES). J.M. Monserrat and W. Wasiliesky Jr are productivity fellows from CNPq (process number PQ 307880/2013-3 and PQ 310993/2013-0).

5
A candidate framework for $PM_{2.5}$ source identification in highly industrialized urban coastal areas

Vinícius L. Mateus[a] and Adriana Gioda[a*]

[a]Pontifical Catholic University, Rio de Janeiro (PUC-Rio), Department of Chemistry, RJ, Brazil

*Corresponding author: Adriana Gioda - Email: agioda@puc-rio.br

Paper under review: *Atmospheric Environment*

Abstract

The variability of PM sources and composition are tremendous challenges for police makers in order to establish guidelines. In urban PM, sources associated with industrial processes are among the most important ones. In this study, a 5-year monitoring of $PM_{2.5}$ samples was carried out in an industrial district. Their chemical composition was strategically determined in two campaigns in order to check the effectiveness of mitigation policies. Gaseous pollutants (NO_2, SO_2, and O_3) were also monitored along with meteorological variables. The new method called Conditional Bivariate Probability Function (CBPF) was successfully applied to allocate the observed concentration of criteria pollutants (gaseous pollutants and $PM_{2.5}$) in cells defined by wind direction-speed which provided insights about ground-level and elevated pollution plumes. CBPF findings were confirmed by the Theil-Sen long trend estimations for criteria pollutants. By means of CBPF, elevated pollution plumes were detected in the range of 0.54 to 5.8 μg m^{-3} comming from a direction associated to stacks. With high interpretability, the use of Conditional Inference Trees (CIT) provided both classification and regression of the speciated $PM_{2.5}$ in the two campaigns. The combination of CIT and Random Forests (RF) point out NO_3^- and Ca^{+2} as important predictors for $PM_{2.5}$. The latter predictor mostly associated to non-sea-salt sources, given a nss-Ca^{2+} contribution equal to 96 %.

Keywords: Coastal urban atmosphere, Conditional bivariate probability function, Conditional inference trees, Secondary inorganic aerosols, $PM_{2.5}$, Steelworks

5.1 Introduction

Global awareness concerning hazards of particulate matter (PM) has been increasing. As a function of population growth and the diversification of socio-economic activities, air pollution mitigation is a worldwide effort. In this scenario, PM may represent the biggest challenge due to its multiple sources and heterogeneous composition. The United States Environmental Protection Agency (USEPA) established $PM_{2.5}$ National Ambient Air Quality Standards (NAAQS). The primary NAAQS for $PM_{2.5}$ are 35 μg m^{-3} in a daily basis (24 h) plus 12 μg m^{-3} in an annual arithmetic mean (94). Another established guidelines are provided by the World Health Organization (WHO). According to WHO, guidelines for $PM_{2.5}$ are 25 μg m^{-3} for a daily basis (24 h) and an annual arithmetic mean of 10 μg m^{-3} (96). In the late 1990s, Brazil established guidelines for PM_{10} and TSP. $PM_{2.5}$ guidelines have not been included yet.

Particulate matter global mass emissions are influenced by both natural and anthropogenic sources. The major natural sources of PM are sea salt, soil dust, and plant exuding (2). Combustion, traffic, and industrial processing materials are sources commonly associated to the anthropogenic components of PM (50, 147, 148). Anthropogenic sources such as domestic and industrial biofuel, and garbage burning contribute local and globally to PM emissions (149). In urban PM, industry-related processes are often reported as one of the most important sources(148).

As in other developing countries, there is a compelling need for quantification, identification, and apportionment of air pollutants in Brazil. In the early 1970s, São Paulo and Rio de Janeiro established their respective air monitoring networks (150). Nowadays, only these two states have $PM_{2.5}$ among criteria pollutants. In Rio de Janeiro, some studies concerning air quality monitoring and source apportionment have been reported (36, 41, 50, 111, 112, 151, 152). However, there is still a lack of continuous monitoring and source apportionment works which prevent the update of air quality guidelines. Given the continental dimensions, diverse socio-economic activities and climate, air quality in the country varies as much as the chemical composition.

Emission inventories as well as chemical transport models are certainly valuable tools for air quality, but it is a challenge to incorporate poorly quantified sources, which are mostly fugitive (148). Therefore, these tools

reinforce the importance of receptor models. Receptor models can be divided in two main groups: 1) the chemical mass balance (CMB) model; and 2) the factor analytic family. The factor analytic family includes models as positive matrix factorization (PMF) and EPA Unmix (UNMIX). Principal component analysis (PCA) is disregarded as a member of the factor analytic family for the aim of source apportionment for multiple reasons including unrealistic sources (23, 24). Recently, new alternatives which are not classified in the major families of receptor models have been used. A new extension of the conditional probability function known as conditional bivariate probability function provides important dispersion characteristic information at the local scale (56). Another alternative which is able to overcome large-scale and long-term monitoring is the recently developed algorithm conditional inference trees (CIT). The CIT algorithm was applied in the source apportionment of surface soil (26). However, to our knowledge, it has not been applied to air pollution studies yet.

The main goal of this work is to fill the gap regarding source apportionment of PM emitted from highly industrialized urban areas. $PM_{2.5}$ samples and trace gas measurements were collected during critical periods, which involved industrial expansion and infrastructure works. Two strategic campaigns were carried out in order to determine PM composition prior and after mitigation policies. The PM samples were analyzed for trace elements, water-soluble organic and inorganic species. Methods recently developed - conditional bivariate probability function (CBPF) and CIT - are applied to unveil nonlinear relationships, which are helpful to improve the knowledge of pollution sources and suggest a more realistic data-driven mitigation at a highly industrialized urban coastal area.

5.2 Materials and methods

The reader is referred to the section 2.4, page 36.

5.3 Results and discussion

5.3.1 PM levels

The annual arithmetic mean for $PM_{2.5}$, standard deviation, minimum, maximum, and number of daily PM exceedances according to the WHO standard are presented in Table 5.1. The null hypothesis that PM levels in

the three sites are similar was tested and accepted, given Kruskal-Wallis rank sum test ($\chi^2 = 1.9358$, df = 2, p-value = 0.3799). This fact can be explained by at least four factors: 1) flat terrain; 2) high residence time of $PM_{2.5}$; 3) the relative proximity of sites in the same air basin; and 4) predominant wind direction. The values observed through this five-year monitoring are comparable with other sites under influence of sources like traffic, urban-background, and industry-related (153). However, the annual average for the three sites are higher than other industrial sites influenced by integrated steelworks (154, 155). A combination of infrastructure works for great events (i.e., World Cup and Olympics), industrial expansion, and seasonality are likely to explain this finding.

Concerning the fraction of the PM dataset submitted to chemical speciation, it is noteworthy that the annual WHO guideline was exceeded in the first campaign. Besides, the daily WHO guideline was exceeded multiple times in all three sites. These events happened during the months of August and September, in the dry season. This is a well-known pattern in Rio de Janeiro (e.g., (10)), but locals and the media reported a phenomenon called "silver rain" in the industrial zone. This phenomenon stands for the undesirable emissions associated to a by-product from a blast furnace (BF). Rodríguez-Cotto et al. (150) reported a decrease of pro-inflammatory cytokine (IL-6 and IL-8) associated to aqueous extracts of $PM_{2.5}$ collected in this industrial region in August and September 2010. According to the findings of Rodríguez-Cotto et al. (150), zinc may play a key role for the toxicity of PM in RJ. Although Zn is also related to traffic and fuel emissions in urban areas (126), previous works determined higher levels of Zn in industrial areas in comparison with rural areas (10). During the first campaign of our study, these two potential Zn sources (i.e., traffic and industrial) must be taken into account, including the likelihood of steel making plants as potential sources of Zn (156). Undoubtedly, further studies which take advantage of Zn speciation and hourly PM measurements might give further insight to the question.

In the second campaign, the annual WHO guideline was exceeded except for SE. Concerning the daily WHO guideline, it was exceeded twice in CA but only once in both CJ and SE. The acute air pollution events took place during the months of August and September, in the dry season; however, there are no acute events registered by INEA associated to steelworks. Judging by the number of daily standard exceedance events, there is a slight improvement in the air quality. The integrated steelworks close to the sites adjusted its processes and this may be one of the factors for the mitigation of high concentration of $PM_{2.5}$. The problem seem to be related to the cooling practice

of slag known as open-pit practice (157). After 2012, an active emission collection system composed of capturing hoods was installed at the integrated steelworks. However, even after this improvement in the largest potential source of PM, in the year of 2014 the number of exceedances increased. Certainly, there may exist influence of seasonal factors such as speed winds, relative humidity, and precipitation at the sites.

Table 5.1: Mean, standard deviation (SD), minimum, maximum, and number of violations of the daily WHO guideline.

Year	Site	Mean	SD	Minimum	Maximum	WHO # violations
2010-	CA	12.1	8.4	2.0	43	5
2011(*)	CJ	12.1	8.6	1.0	43	6
	SE	11.8	7.3	1.0	35	3
2012	CA	6.3	4.2	0.5	23	0
	CJ	9.2	5.7	2.0	25	1
	SE	9.4	6.0	1.4	28	1
2013	CA	10.3	7.5	1.5	37	2
	CJ	10.8	7.3	2.9	35	1
	SE	9.2	6.1	2.5	26	1
2014	CA	13.6	6.7	3.3	32	4
	CJ	12.3	6.0	2.9	29	4
	SE	13.7	6.8	3.6	35	2
2015	CA	10.7	9.7	3.1	50	3
	CJ	13.3	11.7	3.5	57	5
	SE	-	-	-	-	-

*: Aug/10-Jul/11; -: data not available

5.3.1.1 WSOC

In the first speciation campaign, the arithmetic mean ± standard deviation at CA, CJ, and SE were 1.83 ± 2.50 μg m^{-3}, 1.28 ± 1.46 μg m^{-3}, and 1.67 ± 1.22 μg m^{-3}, respectively. Likewise observed for PM levels, the difference between the WSOC levels in the three sites was not statistically significant (χ^2 = 1.5119, df = 2, p-value = 0.4696).

In the second speciation campaign, the arithmetic mean ± standard deviation at CA, CJ, and SE were 1.11 ± 0.29 μg m^{-3}, 1.13 ± 0.58 μg m^{-3}, and 0.90 ± 0.63 μg m^{-3}. The null hypothesis was also accepted (χ^2 = 0.3882, df = 2, p-value = 0.8236). At the three sites, the averages are slightly lower than the ones in the first evaluation. In both evaluations, the measured WSOC is comparable with other urban costal (158) and suburban environments (159). However, a decrease in the concentration range is observed in the second

evaluation. We believe that this may be related to the relationship of WSOC with other components of $PM_{2.5}$. For instance, high concentration of SO_4^{2-} is one of the key factors for the degree of photochemical reactivity.

5.3.1.2 Water-soluble ions

In the first evaluation, the water-soluble ions are primarily composed of SO_4^{2-} (0.9 - 13 μg m^{-3}), NO_3^- (0.1 - 9.3 μg m^{-3}), Cl^- (0.1 - 6.4 μg m^{-3}), Ca^{2+} (0.07 - 0.65 μg m^{-3}), Na^+ (2.0 - 3.7 μg m^{-3}) and to a lesser extent of minor ions (less than 0.3 μg m^{-3}, in average, for K^+ and Mg^{2+})(Table E.3, Supplementary material). The median contribution of nss-Ca^{2+} (96 %), nss-K^+ (96 %), and nss-SO_4^{2-} (75 %) at the three sites suggest that the major sources for Ca^{2+}, K^+ and SO_4^{2-} were non-marine. However, the same conclusion does not apply to Mg^{2+} concentration at the three sites. The median contribution of nss-Mg^{2+} at CA, CJ, and SE were 66 %, 48 %, and 26 %.

In the second evaluation, the water-soluble ions are primarily composed of SO_4^{2-} (1.2 - 6.7 μg m^{-3}), Na^+ (2.1 - 4.1 μg m^{-3}), NO_3^- (0.1 - 4.0 μg m^{-3}), Cl^- (0.1 - 1.1 μg m^{-3}), Oxalate (0.03 - 0.8 μg m^{-3}) and to a lesser extent of minor ions (less than 0.3 μg m^{-3}, in average, for Ca^{2+}, K^+, Mg^{2+}, F^-, NH_4^+, and NO_2^-). Even though the magnitude of major ions changed in the second campaign, the concentration of SO_4^{2-} is circa 2-fold higher than other investigations (49, 160). Despite of the mitigation policies that took place in the industrial region, SO_4^{2-} concentration is comparable with scenarios of strong industrial influence (161). Furthermore, the median contribution of nss-Ca^{2+} (96 %), nss-K^+ (96 %), and nss-SO_4^{2-} (75 %) at the three sites suggest that the major sources for Ca^{2+}, K^+ and SO_4^{2-} were non-marine, as observed in the first evaluation. Differently from the first evaluation, the median contribution of nss-Mg^{2+} at the three sites suggests that the major source for Mg^{2+} is marine.

5.3.1.3 Elemental concentration

In the first speciation campaign, Cu and Mn were the highest elements in the three sites (Table 5.2). These elements are generally associated with raw materials in the steel industry, traffic as well as soil-related sources. The values observed in our evaluation were high in comparison with other sites under influence of industrial emissions (161). For instance, the city of Huelva is under influence of emission from the largest Cu-smelter operation in Europe; however, the average concentration of Cu was lower than the levels at CA. Antimony

presented the lowest levels, but it was comparable with other industrial (161) and urban-industrial areas (50). At the investigated sites, Godoy et al. (50) were the pioneers in the monitoring of $PM_{2.5}$ and it was not possible to observe a great difference between their Sb measurements and ours. Antimony is a global pollutant which genotoxicity is not clearly understood (162). Therefore, an advance of future studies would be the speciation of Sb and evaluation of its toxic potential despite of the low concentration in comparison with other industrial areas (160).

In the second speciation campaign, a greater number of elements presented concentration below the detection limit in comparison with the first evaluation. The whole set of determined species is available in the supplementary material (Table E.3). There is a difference between the levels of Cu during the first and second evaluation. The levels observed in the second campaign were lower than sites with different socio-economic activities such as urban (125) and industrial (161).

Concerning the elements with lower and below DL concentrations, an interesting remark is related to the reduction in the levels of Ni and V. Both elements are often associated with burning of fossil fuels, mainly diesel, and can also be emitted in the complex processes of integrated steelworks. The measured levels for Ti, both in the first and second evaluation, are visibly lower in comparison with other studies and they may be explained by our choice in the sample preparation. The table E.2 provides the extraction efficiency based on the ICP-MS analysis of the certified reference material SRM 1648a (NIST, USA).

Table 5.2: Elemental chemical composition (average in ng m^{-3}) determined in CA, CJ, SE (Aug/10-Jul and Jan-Dec/13) and other studies

Reference	Site	Cu	Mn	Ni	Ti	V	Sb
(160)	Urban-Industrial (Malaysia)	2.1	0.8	0.4	*	0.8	8
(161)	Industrial (Spain)	31	4.0	2.3	18	3.4	0.8
(111)	Urban (Brazil)	35	5	*	*	2	*
(50)	Urban-Industrial (Brazil)	5.5	4.6	1.0	15	1.4	1.9
This paper							
	CA (Aug/10-Jul/11)	62	22	1.8	8.0	5.1	1.1
	CA (Jan-Dec/13)	20	<DL	1.3	7.1	<DL	<DL
	CJ (Aug/10-Jul/11)	13	19	2.1	8.3	6.1	1.3
	CJ (Jan-Dec/13)	11	<DL	1.0	7.5	<DL	<DL
	SE (Aug/10-Jul/11)	51	18	1.8	7.7	4.8	1.6
	SE (Jan-Dec/13)	18	<DL	1.0	6.9	<DL	<DL

*: not analyzed; <DL: below detection limit

The use of glass fiber filters adds a degree of uncertainty due to its highly variable composition, which is mostly problematic in the analysis of some elements (e.g., Al, Cu, Mn, and Zn (44)) in the fine mode PM. Since the typical metal background for glass fiber filters varies widely, we provided more information concerning the DLs achieved in this work (Table E.1).

5.3.2 Gaseous pollutants

The annual average concentrations of gaseous pollutants and the 25th and 75th percentiles for the three sites are presented in Table 5.3. Ozone was the pollutant with the highest annual average concentration in the range of 31.7-38.6 μg m^{-3}. This could be attributed to the weather conditions, such as intense solar radiation, elevated temperatures and fairly low wind-speed (i.e., below 4 m s^{-1}), promoting photochemical reactions (50). Due to the high oxidation rate of NO to NO_2, some studies report high O_3 levels as the influence of traffic sources increases in a given site; however, this trend was not observed in our data. Across the three sites, similarity in the O_3 levels was observed.

The similarity observed to O_3 daily concentration does not hold for SO_2. The sites in the industrial area present an increase in concentration from 2010 (CA: 1.4-3.0 μg m^{-3}, CJ: 1.8-2.4 μg m^{-3}) to 2013 (CA: 4.3-6.2 μg m^{-3}, CJ: 6.1-7.6 μg m^{-3}). Surprisingly, the SO_2 mean concentration for CA and CJ were also comparable with rural sites, respectively, 2.6 and 2.2 μg m^{-3}, during the year of 2010. Industrial emissions and shipping are believed to cause the increase of SO_2 levels throughout the years. Although SE presents initial mean concentration in 2010 (1.4 μg m^{-3}) even lower than rural sites (2.2 μg m^{-3}) (163), the SO_2 concentration in the reference site also increases from 2010 (SE: 0.9-1.6 μg m^{-3}) to 2013 (SE: 4.2-5.6 μg m^{-3}). A few hypotheses could explain the increase of SO_2 at SE such as, 1) the recent changes in land use (e.g., increase in the number of industries), 2) construction works related to a big freeway (i.e., Arco Metropolitano), and to a less extent 3) the wind transport, whose magnitude may be decreased by dilution along the 16 km between the sites.

In general, a slightly inter-site variation was observed for NO_2. The highest annual average concentration was measured in 2013 at CA (27.8 μg m^{-3}) and the lowest annual average concentration measured in 2010 at SE (14.1 μg m^{-3}). Besides the industrial processes, given the localization of the sites, traffic is certainly a source with potential to affect the air quality, specially diesel powered engines, which in Brazil are represented by heavy-duty diesel vehicles (HDDV). In addition, traffic of HDDV is also an important pollution

source at industrial sites (148). Furthermore, the presence of power plants in the industrial district as well as in the reference site is also a potential source of NO_2 emissions.

Table 5.3: Mean, 25th percentile, 75th percentile (μg m^{-3}) for NO_2, SO_2, and O_3.
(The sampling year for CA, CJ, and SE is presented between parenthesis.)

Reference	Site	NO_2			SO_2			O_3		
		Mean	25th	75th	Mean	25th	75th	Mean	25th	75th
This paper	CA (2010)	12.1	4.9	18.6	2.6	1.4	3.0	33.0	21.0	42.9
	CJ (2010)	16.7	10.4	22.3	2.2	1.8	2.4	38.6	26.0	50.8
	SE (2010)	14.1	7.2	19.7	1.4	0.9	1.6	32.1	19.0	44.4
	CA (2011)	25.6	16.5	34.0	4.3	3.0	5.0	34.5	21.9	49.3
	CJ (2011)	18.0	14.1	21.6	3.0	2.6	3.1	36.8	21.9	49.3
	SE (2011)	-	-	-	2.0	1.5	2.4	36.8	25.4	47.2
	CA (2012)	22.9	18.0	26.5	4.1	2.6	5.0	31.7	20.7	42.0
	CJ (2012)	23.3	18.0	26.5	3.7	3.1	3.8	37.0	28.2	45.2
	SE (2012)	18.7	15.4	21.8	2.9	2.2	3.5	34.1	24.8	42.1
	CA (2013)	27.8	19.2	35.1	5.6	4.3	6.2	34.8	24.0	44.0
	CJ (2013)	20.7	14.5	24.4	7.5	6.1	7.6	32.7	22.9	40.2
	SE (2013)	22.1	15.0	24.4	5.0	4.2	5.6	34.3	23.8	43.2
(153)	Spain (Urban*)	14.3	7.5	19.4	6.7	3.5	8.5	62.9	48.9	77.0
(153)	Greece (Urban*)	21.6	14.3	28.0	8.1	3.0	11.1	87.1	60.6	111.0
(163)	Tanzania (Rural)	5.1	-	-	2.2	-	-	25	-	-
(151)	Brazil	-	-	-	186	-	-	-	-	-
	(Industrial)		-	-	73	-	-	-	-	-
(164)	Italy (Urban)	47.6	-	-	3.5	-	-	-	-	-
(164)	Italy (Industrial)	47.2	-	-	5.5	-	-	-	-	-
(160)	Malaysia (Industrial)	60.2	-	-	7.9	-	-	24.0	-	-

-: not available, *: influenced by industry

Ozone concentration was also evaluated according to the WHO guidelines (165), which recommends a 8-hour daily maximum equal to 100 μg m^{-3} (96). According to O_3 range observed at CA (1.23-170.5), CJ (0.25-331.3), and SE (0.13-167.0), CJ presents the highest maximum value for the time series. The number of days which exceeded the WHO guidelines is shown in Figure 5.1. According to the EU Directive2008/50/CE, the number of occasions should not occur more than 25 days in a 3-year average. Despite the decrease in daily exceedances between 2010 and 2013, the number of days are high, specially for CJ. In an annual base, the number of events are comparable to the ones observed in countries located in Southern Europe (165).

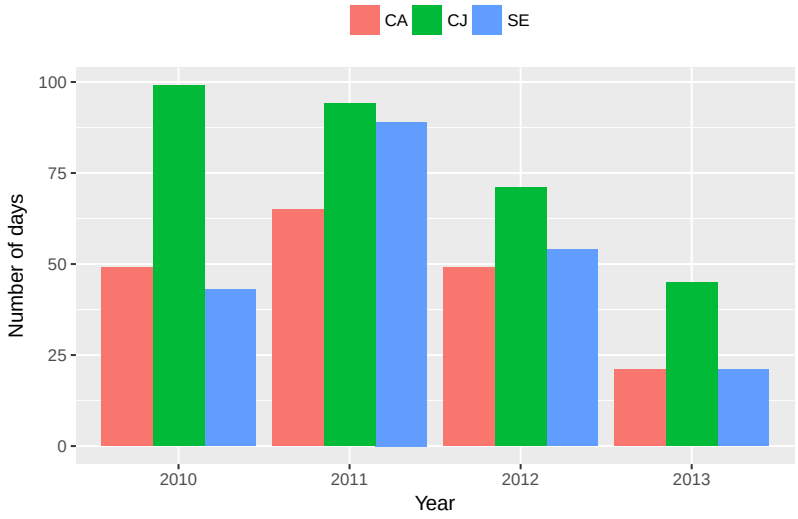

Figure 5.1: Number of daily exceedances of the 8-hour WHO guideline determined in CA, CJ, SE.

5.3.3 CBPF and bivariate polar plots

5.3.3.1 Selection of intervals

The very nature of CBPF allows the estimation of local minor sources as well as remote sources, which can be equally hard to detect. Four splits were made in our dataset in order to detect a higher number of sources: 1) $<$ 25th concentration percentile, 2) 25-50th concentration percentile, 3) 50-75th concentration percentile, and 4) $>$ 75th concentration percentile. This exploration benefits from the fact that sources tend to occupy distinct concentration intervals. The number of percentile classes was based in previous data screening and application of CBPF in areas of similar land use (57). The most relevant concentration percentiles for CBPF analyses of NO_2, SO_2, O_3, and $PM_{2.5}$ are presented in Figure 5.2 - 5.4. Additional concentration percentiles are available as supplementary information (Figure E.1 - E.11).

5.3.3.2 Exploration of sources

Although the industrial monitoring sites (CA and CJ) are relatively close to the integrated steelworks, the CBPF analyses of each site provided complementary information. Steelworks processes are per se very complex, the region has multiple other important sources (e.g., power plants), and some of them have similar signatures (e.g., metallurgic processes). However, the wind direction-speed proved to be helpful to unveil regions of high CBPF probability.

Previous works in sites close to large integrated steelworks stress that local meteorology (i.e., wind speed and mixing layer height) are essential to source apportionment (57, 157, 166). Emissions in the surroundings of steelworks are time dependent as well as height dependent (56, 154, 167). The undesirable emission of particulates tend to be intermittent, but gaseous emission are often continuous.

Exploration of sources at CA A co-emission pattern of NO_2, SO_2, O_3, and $PM_{2.5}$ is observed at CA (Figure 5.2) for different concentration percentiles. South-westerly winds with intermediate-high speeds are determining factors to the CBPF probability. NO_2 and O_3 present relatively high CBPF probability, respectively, ~ 0.6 and ~ 0.8. Single continuous dominant sources have potentially high probability while complex mixtures, e.g., some steelworks processes, have reduced probabilities. Since the probability increases in intermediate-high wind speed, this fact strongly suggests elevated sources for NO_2 and O_3. However, ground-level sources also affect the receptor site in different concentration percentiles and wind directions (Figures E.1 and E.3). At the 0-25th concentration percentile range, two sources were detected for SO_2. As observed for NO_2 and O_3, south-westerly winds influenced an elevated source, but another ground-level source is associated to low wind speeds ($\sim$ 4 m s^{-1}) from the south-east sector. This we attribute to road traffic. In Brazil, HDDV traffic may not be a major ground-level source for SO_2 in the future. A national program to mitigate vehicular pollution (PROCONVE) led to a reduction of sulfur from 2000 mg kg^{-1} (2011) to 10 mg kg^{-1} (2013) (152). For $PM_{2.5}$, the south-westerly and westerly winds showed high probability. The probability varies from circa 0.7 to 1 at the south-westerly and westerly winds, respectively. To the west of CA, other important industries are present including a smaller steelworks established long time ago, which has not been associated to episodic emissions by the state environment agency.

Exploration of sources at CJ At CJ, the co-emission pattern observed in CA for NO_2, SO_2, O_3, and $PM_{2.5}$ holds (Figure 5.3). The CBPF maximum for NO_2 remains close to 0.6, which highlights the importance of elevated sources at concentrations from 0.63 to 14 μg m^{-3} at both CA and CJ. The most important sources for the highest concentration percentiles of SO_2 are elevated given the intermediate-high wind speeds. The two main wind sectors for SO_2 are SSW and W. Ozone is associated to elevated sources from the SSW, but ground-level sources from the SSE and also SSW sectors play an important role on air quality at CJ. In the case of $PM_{2.5}$, a westerly ground-level source can

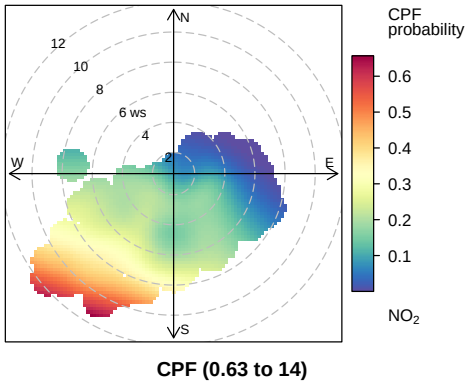

5.2(a): 0-25th percentile

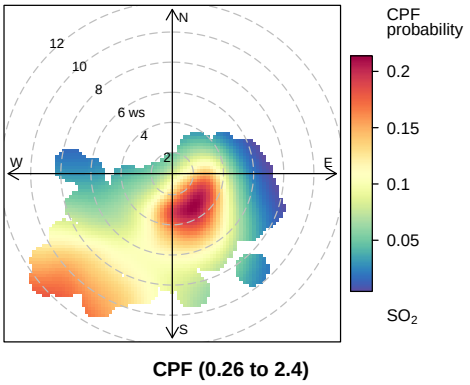

5.2(b): 0-25th percentile

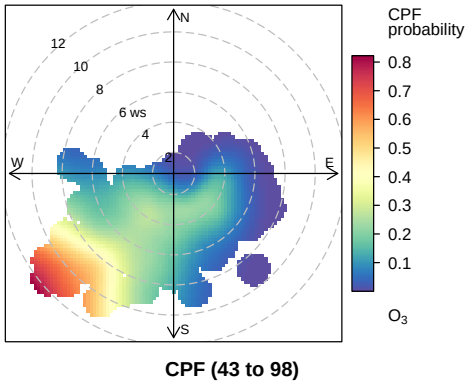

5.2(c): 75-100th percentile

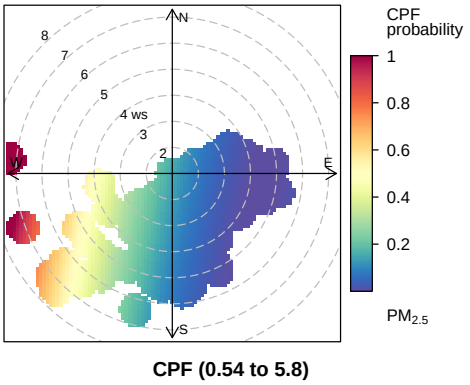

5.2(d): 0-25th percentile

Figure 5.2: Conditional bivariate probability function plot of criteria pollutants at the CA site for (a) NO_2 concentrations between 0.63 and 14 μg m^{-3}, (b) SO_2 concentrations between 0.26 and 2.4 μg m^{-3}, (c) O_3 concentrations between 43 and 98 μg m^{-3}, and (d) $PM_{2.5}$ concentrations between 0.54 and 5.8 μg m^{-3}.

be attributed to non-intermittent events given the high CBPF probability. In addition to this, elevated sources were detected for westerly and south westerly wind directions. These findings may be associated to integrated steelworks emissions. A variable particle size range has been attributed to PM and its components in samples collected nearby industrial areas (148, 154, 157). Many processes associated to steelworks are intermittent. However, in integrated steelworks some processes, e.g., the coke ovens, operate in a batch mode process, which result in regularity of subsequent steps and emissions (157).

Exploration of sources at SE Given the relative proximity ($\sim$ 16.5 km) between the industrial district of Santa Cruz and Seropédica, similar profiles were found for NO_2, SO_2, O_3, and $PM_{2.5}$ (Figure 5.4). At the 0-25th percentile range, south-westerly winds with high speeds influence both NO_2 and SO_2 concentrations. The CBPF probability is relatively high for these two gaseous

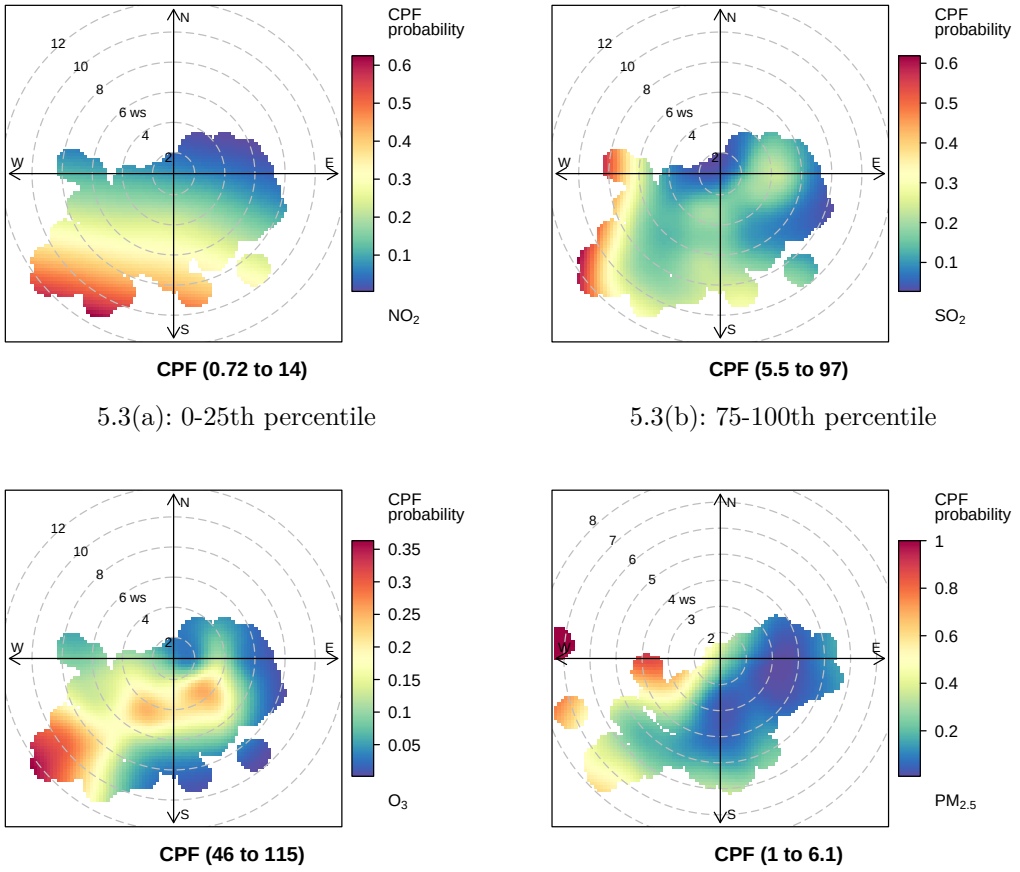

5.3(a): 0-25th percentile

5.3(b): 75-100th percentile

5.3(c): 75-100th percentile

5.3(d): 0-25th percentile

Figure 5.3: Conditional bivariate probability function plot of criteria pollutants at the CJ site for (a) NO_2 concentrations between 0.72 and 14 μg m^{-3}, (b) SO_2 concentrations between 5.5 and 97 μg m^{-3}, (c) O_3 concentrations between 46 and 115 μg m^{-3}, and (d) $PM_{2.5}$ concentrations between 1 and 6.1 μg m^{-3}.

pollutants, respectively, ~ 0.7 and ~ 0.5. At percentiles higher than the 25th, the probability decreases and low speed winds point to the predominance of ground-level sources, which seem to be related to road traffic (Figures E.8 and E.9). For O_3, two sources were identified at the 50-75th percentile range with distinct wind speed and wind direction. An elevated source is associated with the south sector while a ground-level source is associated with the north-easterly winds. To the north east, the reference site is close to a new industrial district, a thermoelectric power plant, and a busy road. To the south, the reference site receives influence from the long-range transport of the industrial region of Santa Cruz as well as road traffic. The CBPF analysis for $PM_{2.5}$ points to the significance of the southerly winds for elevated sources given a high probability (~ 0.7). However, it seems that $PM_{2.5}$ concentration is influenced by both ground-level and elevated sources related to easterly winds (Figures E.4(a), E.7(a), and E.11(c)) at the three sites.

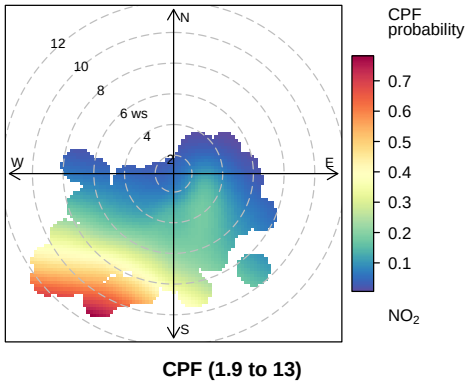

5.4(a): 0-25th percentile

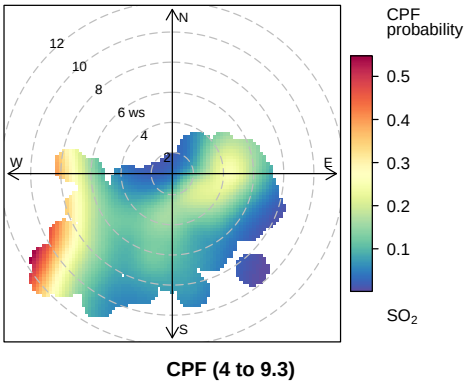

5.4(b): 75-100th percentile

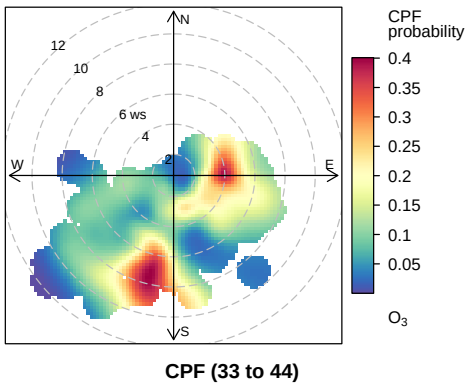

5.4(c): 50-75th percentile

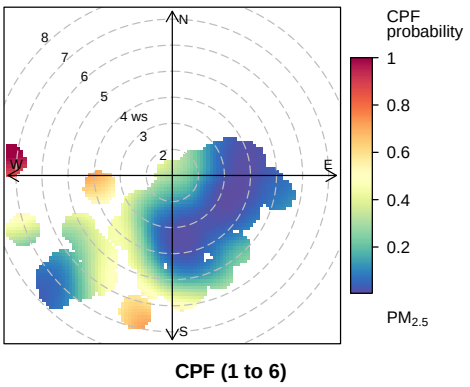

5.4(d): 0-25th percentile

Figure 5.4: Conditional bivariate probability function plot of criteria pollutants at the SE site for (a) NO_2 concentrations between 1.9 and 13 μg m^{-3}, (b) SO_2 concentrations between 4 and 9.3 μg m^{-3}, (c) O_3 concentrations between 33 and 44 μg m^{-3}, and (d) $PM_{2.5}$ concentrations between 1 and 6 μg m^{-3}.

5.3.4 Long trend evaluation

The trend for the criteria pollutants (NO_2, SO_2, O_3, and $PM_{2.5}$) was estimated based on the deseasonalized monthly mean concentrations (Figures 5.5 and 5.6). The solid red line shows the trend estimate and the dashed red lines show the 95 % confidence intervals for the trend. The figures of the trend analyses according to wind sectors are provided as supplementary material (Figure E.12 - E.19). To reinforce the confidence in the following trends, the concentrations measured at the two receptor sites in the industrial district of Santa Cruz (SC), CA and CJ, were considered in the same dataset.

5.3.4.1
Long trend of gaseous pollutants

Atmospheric NO_2 concentrations increased in the two regions specially at SE. The overall NO_2 trend at Seropédica was higher and presented a higher degree of statistical significance (3.32 μg m^{-3}/year, p $<$ 0.001) than the one at SC (2.79 μg m^{-3}/year, p $<$ 0.01) (Figures 5.5 and 5.6). Evaluating the trends according to the wind sectors, winds from south are important at the two regions (Figure E.16). Similarly, the NE winds present an increase between 2.8 and 3 μg m^{-3}/year (p $<$ 0.001) at the two regions .

For SO_2, the trend at SC was higher (1.29 μg m^{-3}/year, p $<$ 0.001) than at SE (1.08 μg m^{-3}/year, p $<$ 0.001) (Figures 5.5 and 5.6). Evaluating trends according to the wind sectors, all trends were statistical significant at both SC and SE (Figures E.13)and E.17). The higher trend estimates were observed for the west (1.37 to 1.61 μg m^{-3} / year) and south-east sectors (1.13 to 1.36μg m^{-3} / year) at the two regions. At SC, the S and SW sectors presented an increasing trend of 1.21 μg m^{-3}/year and 1.25 μg m^{-3}/year, respectively.

For O_3, there was a decreasing trend at SC (-0.47 μg m^{-3}/year) while an increasing trend was estimated at SE (0.15 μg m^{-3}/year), but there was no statistical significance for any trend (Figures 5.5 and 5.6). Evaluating the trends according to the wind sectors, the estimates at SC can be slit in two groups: 1) increasing trend (SW and NE), 2) decreasing trend (W, S, E, and SE). The decreasing trends for west (-10.81 μg m^{-3}/year, p $<$ 0.001) and south-east (-0.58 μg m^{-3}/year, p $<$ 0.01) are the most significant (Figure E.14). At SE, all trend estimates according to the wind sectors are increasing except for the W sector (-6.58 μg m^{-3}/year, p $<$ 0.1) (Figure E.18). The importance of local sources from the NE sector pointed out by CBPF matches with the increasing trend estimate for this sector (2.06 μg m^{-3}/year, p $<$ 0.01).

5.3.4.2
Long trend of $PM_{2.5}$

The overall trend analysis for $PM_{2.5}$ points to an increasing trend to SC (0.47 μg m^{-3}/per year) while a decreasing trend was estimated to SE (-0.1 μg m^{-3}/per year), but none of the trends are statistical significant (Figure 5.7). The difference in the year range between SC (2010-2015) and SE (2010-2014) is due to technical difficulties (i.e., failure in the power supply and equipment maintenance) for the sampling in the later region. Evaluating trends according to the wind sectors, the E and SW sectors have increasing trends at both regions, but the trends are only statistical significant at SC (Figure E.15). The south-east sector (0.66 μg m^{-3}/per year, p $<$ 0.05) also presents an increasing

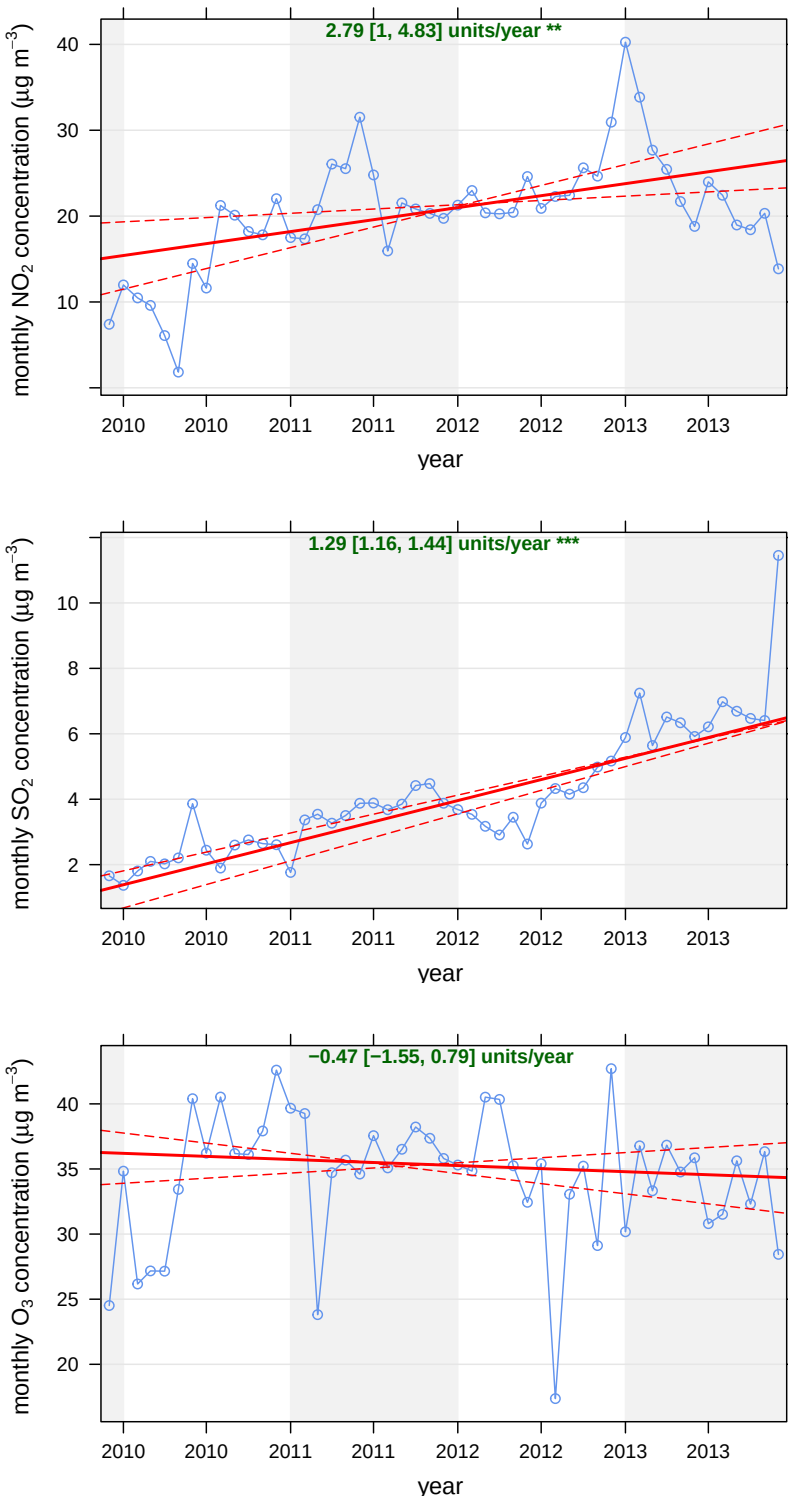

Figure 5.5: Trend analysis of NO_2, SO_2, and O_3 at the industrial region of Santa Cruz. The solid red line shows the trend estimate and the dashed red lines show the 95 % confidence intervals. The overall trend per year is shown at the top, before brackets, and the 95 % confidence intervals between brackets. $p < 0.001 = ***$, $p < 0.01 = **$

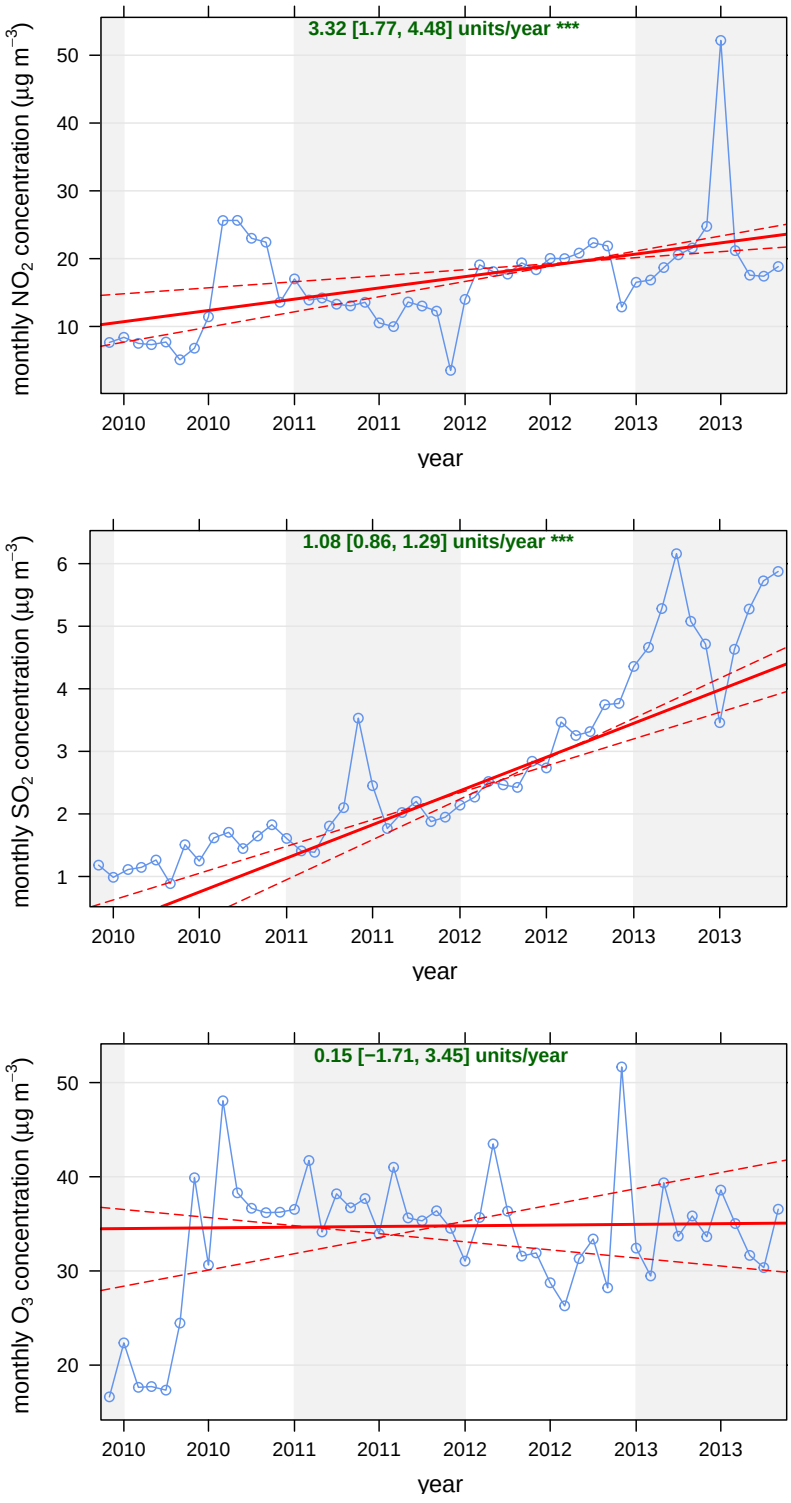

Figure 5.6: Trend analysis of NO_2, SO_2, and O_3 at the reference site (SE). The solid red line shows the trend estimate and the dashed red lines show the 95 % confidence intervals. The overall trend per year is shown at the top, before brackets, and the 95 % confidence intervals between brackets. $p < 0.001 = ***$

and statistical significant trend at SC that reinforces the impact of sources other than the steelworks at the region.

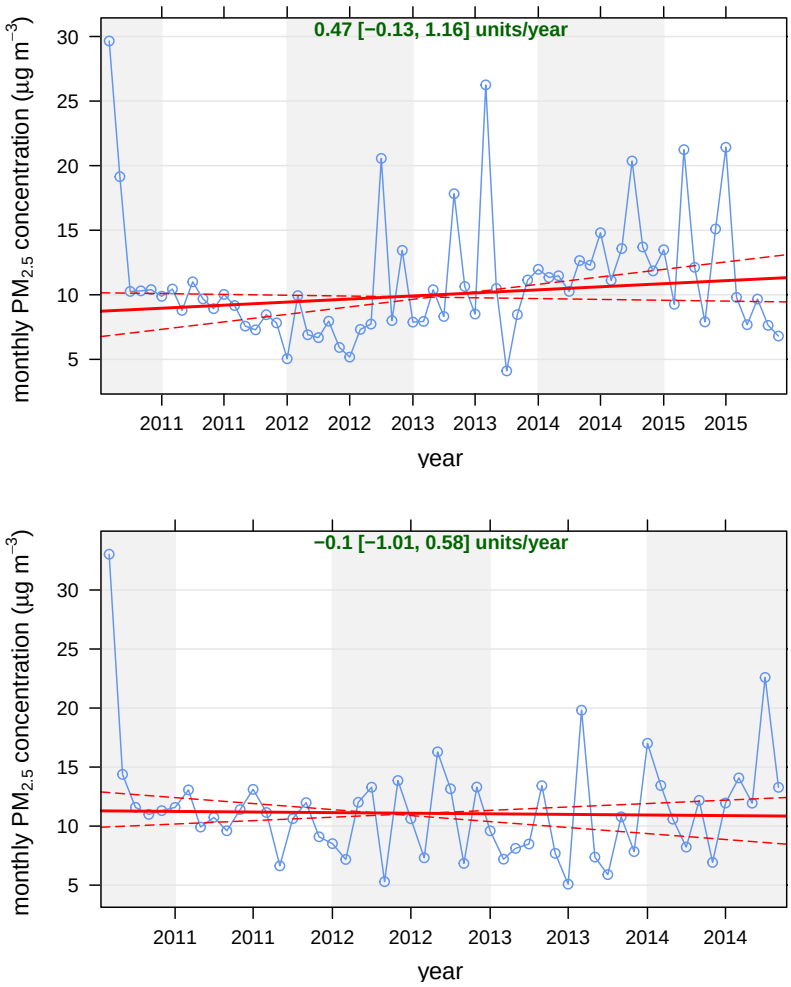

Figure 5.7: Trend analysis of $PM_{2.5}$ at the industrial region (SC) and the reference site (SE). The solid red line shows the trend estimate and the dashed red lines shows the 95 % confidence intervals. The overall trend per year is shown at the top, before brackets, and the 95 % confidence intervals between brackets.

5.3.5
Stochastic models

5.3.5.1
Speciated $PM_{2.5}$: Aug/10-Jul/11

The CIT consisted of 11 nodes including 6 terminal nodes (Figure 5.8). The most important splitting variable of the root node was the concentration of Mg (Figure 5.9). As expected, based on the statistical similarities of the $PM_{2.5}$ levels, the insights provided by CBPF, and trend estimates, the location of the

sites was not a highly important variable for predicting PM. This fact justifies the use of a single tree to classify predictors for PM samples from the three sites.

We infer that three sources mainly influence Mg and thus they influence the $PM_{2.5}$ levels. Samples exceeding the daily WHO guideline (node 11, $PM_{2.5}[_{mean}] = 30.3$ μg m^{-3}) may be related to undesirable emissions from steelworks. During this campaign, locals reported what they call "silver rain", which may be associated to the failures in the emission control of BFs. In order to remove oxide impurities from iron ores (e.g., SiO_2 and Al_2O_3), limestone ($CaCO_3$) or dolomite ($CaMg(CO_3)_2$) is added during reactions in the BFs that occur at circa 900 °C (168). The reaction forms the so-called slags. A high particle loading is generated when the molten slag produced by BFs cools down between manufacturing steps (157), with a significant fraction of fine particles (156).

The node 6 yielded to the three terminal nodes 7 ($PM_{2.5}[_{mean}] = 18.3$ μg m^{-3}), 9 ($PM_{2.5}[_{mean}] = 12.8$ μg m^{-3}), and 10 ($PM_{2.5}[_{mean}] = 20.3$ μg m^{-3}). The chemical composition of slags is similar to other sources, and they may also be used as road materials, landfill covermaterial, cement additive, and other applications (154). Elements such as Mg, Si, Al, Ca, may be present in emission originated from slags (154, 169). Potassium is used as a biomass burning tracer, but its multiple sources are a shortcoming for this assumption (170). Therefore, we attribute the terminal nodes to soil-related sources. These sources may be related to construction sites, wind-blown dust, paved and unpaved road dust.

Among the sources for Mg in coastal urban atmosphere, sea spray cannot be disregarded. Previous works in the MRRJ apportioned Mg solely to marine origin (50), but our data suggests additional sources with reasonable influence on PM based on the CIT results and median percentage of nss-Mg^{2+}. The node 3 splits in the terminal node 4 ($PM_{2.5}[_{mean}] = 5.3$ μg m^{-3}) and terminal node 5 ($PM_{2.5}[_{mean}] = 8.2$ μg m^{-3}). The partitioning criteria for node 3, Mg concentration in μg m^{-3}, is close to Mg levels determined in the MRRJ before the recent increases in both urbanization and industrialization (50). Therefore, the terminal nodes are likely related to the sea salt spray processes. In node 5, the higher $PM_{2.5}$ mean may be attributed to aged sea salt.

Apart from the importance of Mg, the rank of variable importance for the CIT add extra information to sources in the studied region (Figure 5.9). Likely due to the common sources with Mg, Ca also has a great importance for the composition of PM. The high rank of NO_3^- suggests its importance over other gas-to-particle conversion processes. The careful analysis of the variables used to predict $PM_{2.5}$ can be helpful in choosing non-trivial ways

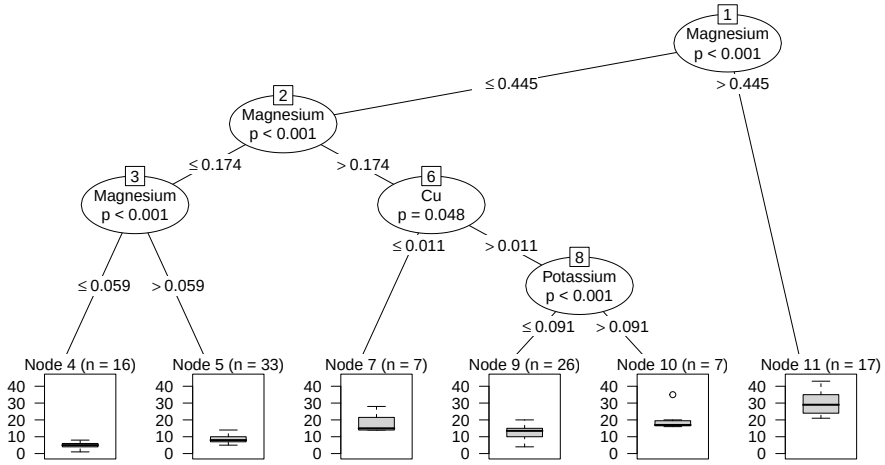

Figure 5.8: Conditional inference trees (CIT) for $PM_{2.5}$ data (Aug/10-Jul/11). In the CIT, n is the number of samples classified in a given node, and the $PM_{2.5}$ concentration is shown in the unit of μg m^{-3}.

for the best mitigation policies, since the prediction using CIT are based on nonlinear relationships, which certainly represent the case for air pollution investigations.

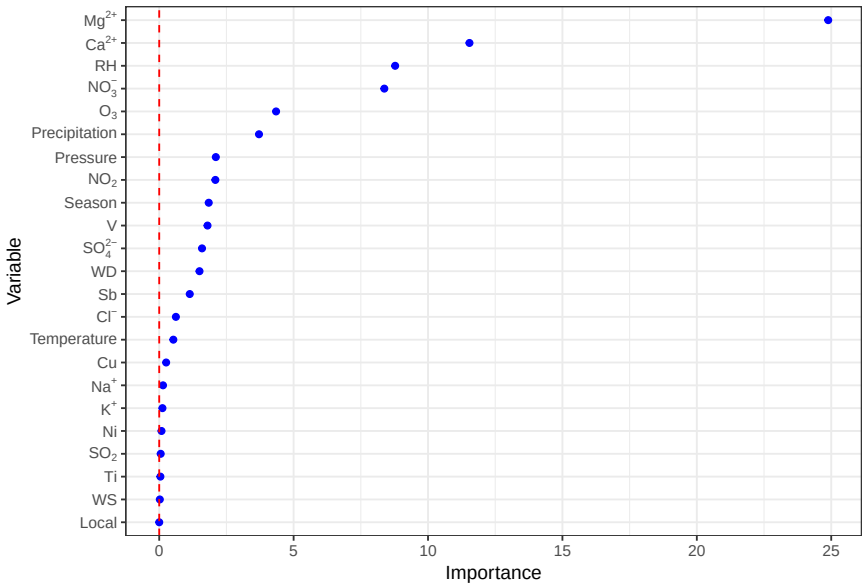

Figure 5.9: Conditional ranking variable importance: CIT for $PM_{2.5}$ (Aug/10-Jul/11). Predictors to the right of the dashed line are significant.

5.3.5.2 Speciated $PM_{2.5}$: Jan-Dec/13

Similar to the analysis for the period Aug/10-Jul/11, the CIT for the speciated $PM_{2.5}$ consisted of 11 nodes including 6 terminal nodes (Figure 5.10).

The most important splitting variable of the root node was the concentration of NO_3^- indicating strong influence of secondary inorganic aerosols (SIA) (Figure 5.11). Although the location of the sites, the differences in land use, did not play an important role on $PM_{2.5}$ prediction, during this campaign the seasonality presented great importance, given by the variable 'Season' (Figure 5.11).

After the partitioning of the root node, three main sources influence the $PM_{2.5}$ levels, which are represented by nodes 3, 6, and 9. The highest PM levels are located as terminal nodes from node 9 (node 10 - $PM_{2.5}[_{mean}]$ = 16.5 μg m^{-3} and node 11 - $PM_{2.5}[_{mean}]$ = 27.5 μg m^{-3}). Despite of any official report of episodic emission associated to the recent installed steelworks, the daily WHO guideline was exceeded in total four times. According to the INEA, there were still improvements in the processes of major pollutants industries in the region (42). In addition to that, another potential source of PM as well as NO_X are power plants located in the region. With regard to emissions from steelworks, they are a complex chain from the raw material preparation area to the fabrication of finished products and the coking and sintering plants are the first steps to consider (168). The sintering process is a pre-treatment process for iron ores which involves combustion (156) and it presents K as one of the major elements (148, 156). As other authors, we suggest a combination of soil/street dust and sintering for the significance of K (154, 167), which is supported by a median contribution of nss-K^+ equal to 96 % and the traffic of vehicles on paved as well as unpaved roads.

The node 6 yielded to the terminal nodes 7 ($PM_{2.5}[_{mean}]$ = 7.9 μg m^{-3}) and 8 ($PM_{2.5}[_{mean}]$ = 13.7 μg m^{-3}). This finding reflects the complexity of source apportionment in the surroundings of steelworks. Nodes 7 and 8 may be related to a mixture of other SIA formation processes (e.g., other industrial activities) and K sources (e.g., aged sea-salt). The higher PM level of node 8, marked by the importance of NO_3^- concentration, may be explained by the busy roads surrounding the studied sites, which can be an important factor for the SIA formation.

The node 3 yielded to the terminal nodes 4 ($PM_{2.5}[_{mean}]$ = 7.5 μg m^{-3}) and 5 ($PM_{2.5}[_{mean}]$ = 4.9 μg m^{-3}). As observed in the CIT related to the first campaign, the terminal nodes at the left seem to be related to background processes. The difference between the two apportioned nodes is influenced by the RH. RH may act like a proxy for the seasonality, given the importance of the variable 'Season' for the prediction of $PM_{2.5}$. Therefore, node 3 may represent soil-related sources, and the terminal nodes 4 and 5 are affected by the *wash-out effect*, respectively, low influence ("dry season") and high influence ("wet season").

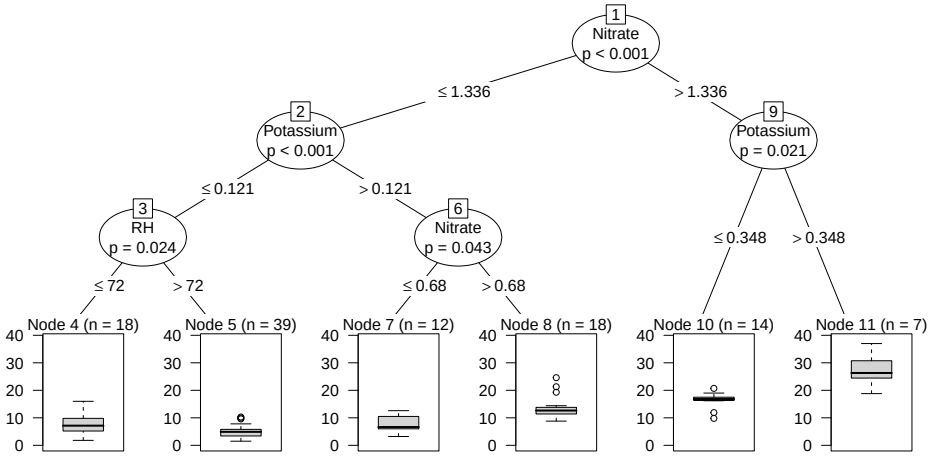

Figure 5.10: Conditional inference tree (CIT) for $PM_{2.5}$ data (Jan-Dec/13). In the CIT, n is the number of samples classified in a given node, and the $PM_{2.5}$ concentration is shown in the unit of μg m^{-3}.

The addition of new variables to the set of speciated $PM_{2.5}$ may have influenced in the ranking of variables, but some comparison with the CIT related to Aug/10-Jul/11 is possible. The addition of new variables to the set of speciated $PM_{2.5}$ was an attempt to improve the comprehension of sources even with many samples under the DL. Despite of this difference in the number of variables, some species are commonly imported in the two evaluation campaigns, such as Ca, Mg, and NO_3^- (Figure 5.11), which provide evidence for mitigation policies aiming sources associated to these species.

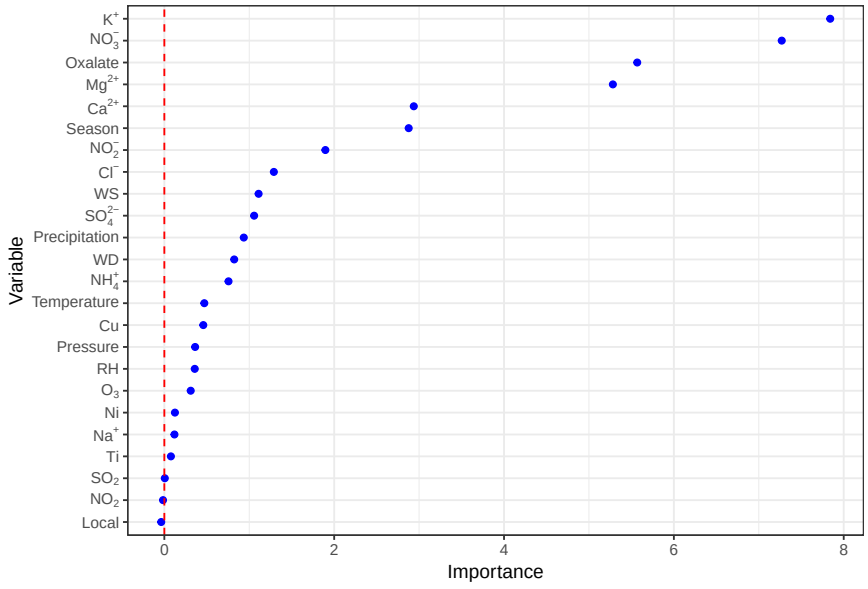

Figure 5.11: Conditional ranking variable importance: CIT for $PM_{2.5}$ (Jan-Dec/13). Predictors to the right of the dashed line are significant.

5.4 Conclusion

Stationary sources are generally well chemically characterized, but this is not the case for complex processes (e.g., integrated steelworks). Fugitive sources impose a challenge for mitigation specially when sources have similar signatures per se or co-emit. The environment state agency and the integrated steelworks are carrying out major research aiming to control releases from major sources.

The reported results represent part of the overall work that has been carried out to understand the main processes related to the generation and dispersion of pollutants in the industrial district of Santa Cruz and the reference site Seropédica. Even though we used daily data for $PM_{2.5}$ monitoring, the long term evaluation provided solid ground for trend estimates and sources contribution based on local meteorology. Ozone was the pollutant with the highest range for annual average concentration (31.7-38.6 μg m^{-3}) and presented no clear trend across the tree sites. On the contrary, SO_2 and NO_2 showed higher concentration at the industrial sites (CA and CJ). Although the trend analysis for O_3 did not provide a statistical significant trend neither for the industrial district of Santa Cruz nor for Seropédica, noticeable trends were observed for NO_2 at the former and later regions, respectively, 3.32 μg m^{-3} /year ($p < 0.001$) and 2.79 μg m^{-3} /year ($p < 0.01$). The trend estimate reveals that road-related and industry-related sources influence the two regions. With regard to non-buoyant sources, future studies should check the existence of SO_2 ground-level sources in the MRRJ. The signal of these sources may reduce due to the decrease of sulfur content in the HDDV fleet.

Concerning the $PM_{2.5}$ levels, all three sites exhibit high annual average, even after the application of mitigation policies. CBPF analyses pointed out that ground-level (mostly traffic/road-related) and elevated sources (industry-related) from south-easterly winds contribute to $PM_{2.5}$ concentration. The long trend analysis corroborated the CBPF findings, since the trend based on the E sector at the industrial district is greater (1.61 μg m^{-3} /year, $p < 0.001$) than the trend based on the sector that a priori was mostly influenced by industrial emission (0.44 μg m^{-3} /year, $p < 0.01$). At the reference site, the trend estimation according to the wind sectors does not point to statistical significance in any sector, but there is a trend for high contribution to the $PM_{2.5}$ concentration from the E sector. Comparing the speciation campaigns, the levels of SIA still are circa 2-fold levels observed in the literature, but a decrease in the concentrations of metals (Cu, Mn, Ni, and V) is observed.

It is noteworthy that this work suffered from poor detection limits as a

consequence of the choice for the fiberglass filters. Important elements (e.g., Zn) and cations (e.g., Na^+) presented a high frequency of left-censored data. However, when the left-censored data was imputed, they did not generated unrealistic interpretations under the CIT approach. In addition, CIT presented high interpretability of results by the visualization of the fitted trees. Comparing the fitted trees for the two speciated datasets, CIT highlight the most important variables for the PM source apportionment. To our knowledge, this approach has never been used before for this purpose. We believe in the suitability of this framework for other similarly complex environments such as urban coastal sites, large urban centers/PM hotspots, and megacities.

Acknowledgements

The authors thank CAPES (specially to Prof. Luiz Drude, INCT-TMCOCEAN Project coordinator), CNPq, and FAPERJ for research grants. They are also grateful to Prof. Tatiana Dillenburg Saint'Pierre and Prof. Ricardo Aucélio for sharing their technical infrastructure. The authors also thank technicians who helped in the ICP analyses: Álvaro Pereira and Rafael Christian Chávez Rocha, and in the IC analyses: Heloisa Fontenelle and Verônica Luiza. The authors also thank to all the graduation students which helped in any phase of this project. The authors thank INMET for providing the meteorological data and INEA for supplying PM samples and gaseous pollutants data.

6
Assessment of ambient aerosol sources in two important Atlantic Rain Forest hotspots in the surroundings of a megacity

Vinícius Lionel Mateus[1], Adriana Gioda[1*], Helga Ribeiro [1], Thiago Veras do Valles[1], Ana Clara Iusten Prohmann[1], Larissa Cândida[1], Alexandre Collett Solberg Leitão de Almeida[1], Tatiane Bourguignon de Oliveira[1], Fernanda Melo[1], Tatiana Dillenburg Saint'Pierre[1], Luiz F. P. G. Maia[2]

[1]Pontifical Catholic University, Rio de Janeiro (PUC-Rio), Department of Chemistry, RJ, Brazil;

[2]Federal University of Rio de Janeiro (UFRJ), Department of Meteorology, RJ, Brazil

[*]Corresponding author: Adriana Gioda - Email: agioda@puc-rio.br

Working paper: *Science of Total Environment* (Aimed journal)

Abstract

The chemical characterization of particulate matter (PM) at two Atlantic Rain Forest hotspots was evaluated during the year of 2010 and 2015. In order to further the understanding of the PM sources, local meteorology data was evaluated along with the chemically speciated PM datasets. At the Mário Xavier National Florest (FLONA), the TSP annual geometric mean concentration ranged from 43.8 μg m^{-3} to 42.9 μg m^{-3}. At the Serra dos Órgãos National Park (PARNA), the PM_{10} annual arithmetic mean concentration ranged from 26.6 μg m^{-3} to 33.1 μg m^{-3}. Bivariate polar plots, k-means clustering, and the conditional bivaritate probability function (CBPF) plots were used to disentagle sources associated to wind speed-direction pairs. The water-soluble composition of the PM at both FLONA and PARNA, revealed the importance of nss-Ca^{2+} (96 %), nss-K^{+} (96 %), and nss-SO_4^{2-} (75 %) sources. The use of the conditional probability trees (CIT) and Random Forests (RF) methods helped to estimate the key variables for the prediction of TSP (NO_3^- > Mn > Rad (Global radiation) > Ca^{2+} > Precipitation > Mg $^{2+}$) and PM_{10} (Gust wind speed > NO_3^- > Ca^{2+} > Zn > Cu > Ti) at FLONA and PARNA, respectively.

Keywords: Atmospheric pollution, Atlantic Rain Forest, Source apportionment, Secondary inorganic aerosols

6.1 Introduction

The Brazilian Atlantic Forest is among the most important biodiversity hotspots in the planet. As many developing countries, Brazil strives for a sustainable future. According to the Brazilian legislation (171), a conservation unit comprehends a territorial space and its ecosystem services. A conservation unit can be classified by the degree of human interference as: 1) Unit of Integral Protection, and 2) Unit of Sustainable Use. In this study, two sites were selected, which not only relate to different sources and its contribution, but they also connect to the indirect use of natural resources (i.e., Unit of Integral Protection) as well as the harmonizing between protection and a sustainable and fractional use of resources (i.e., Unit of Sustainable Use). The Serra dos Órgãos National Park (Parnaso - 43°04′42.1"W and 22°29′16.9"S) the Mário Xavier National Forest (Flonamax - 43°42′21.8"W and 22°43′21.7"S) are Unit of Integral Protection and Unit of Sustainable Use, respectively, located in the surroundings of the Metropolitan Region of Rio de Janeiro (MRRJ). For the sake of simplicity, hereafter Parnaso and Flonamax will be replaced by PARNA and FLONA, respectively (Figure 2.4).

The effects of atmospheric pollution are deleterious for both aquatic and terrestrial ecosystems. The composition of particulate matter associated with urban sources present high levels of SO_2 and NO_x. These trace gases yield to secondary inorganic aerosols (SIA). The deposition of SIA has the potential to cause acidification, eutrophication, and mobilization of macro and trace elements.

The main goal of this work is to evaluate ambient aerosol sources affecting the air quality of two protected areas in the surroundings of the MRRJ. Particulate matter samples (TSP and PM_{10}) were analyzed for trace elements, water-soluble organic and inorganic species. Meteorological information was coupled to the speciated PM dataset in order to improve source apportionment. This investigation builds on multi-year datasets for both TSP and PM_{10}. To our knowledge, this is the first assessment of this nature in the region.

6.2 Materials and methods

The reader is referred to the section 2.5, page 45.

6.3 Results and discussion

6.3.1 PM levels

The geometric mean of TSP as well as the number of CONAMA daily guideline exceedances determined at FLONA are presented in Table 6.1. The geometric mean of TSP does not present a strong seasonality and only one exceedance of the primary CONAMA guideline was observed during the wet season. Although the values for FLONA are in agreement with the Brazilian guidelines, the geometric mean levels are comparable to urban sites with very low greenspace (34.0 ± 4.0 μg m^{-3}, Town Hall, Australia) (172).

Table 6.1: Geometric mean (range between parentheses) concentration of PM_{10} (μg m^{-3}) and number of CONAMA daily guideline exceedances (#) at the Mário Xavier National Florest (FLONA) taking into account three data subsets: Dry season ("Dry"), Wet season ("Wet"), and Overall sampling ("Total").

Year	Dry		Wet		Total	
	mean	#	mean	#	mean	#
2010	45.0 (17.2-94.1)	0	42.7 (15.2-67.1)	0	43.8 (15.2-94.1)	0
2011	58.5 (27.5-105.7)	0	39.5 (5.67-242.6)	1[a]	48.5 (5.67-242.6)	1[a]
2012	43.4 (35.3-55.7)	0	42.5 (15.4-82.0)	0	42.8 (15.4-82.0)	0
2013	39.3 (17.7-83.3)	0	39.4 (22.9-112.3)	0	39.3 (17.7-112.3)	0
2014	39.1 (9.15-111.3)	0	63.4 (41.3-107.2)	0	42.9 (9.15-111.3)	0

[a]: Exceedance of the primary CONAMA daily guideline (240 μg m^{-3})

The overall trend analysis for TSP points to an increasing trend of 2.3 μg m^{-3}/per year, but there is not a statistical significance. However, the trend analysis classified by wind sectors points to a statistical significant trend from the south east sector of 5.13 μg m^{-3}/per year (Fig.6.1).

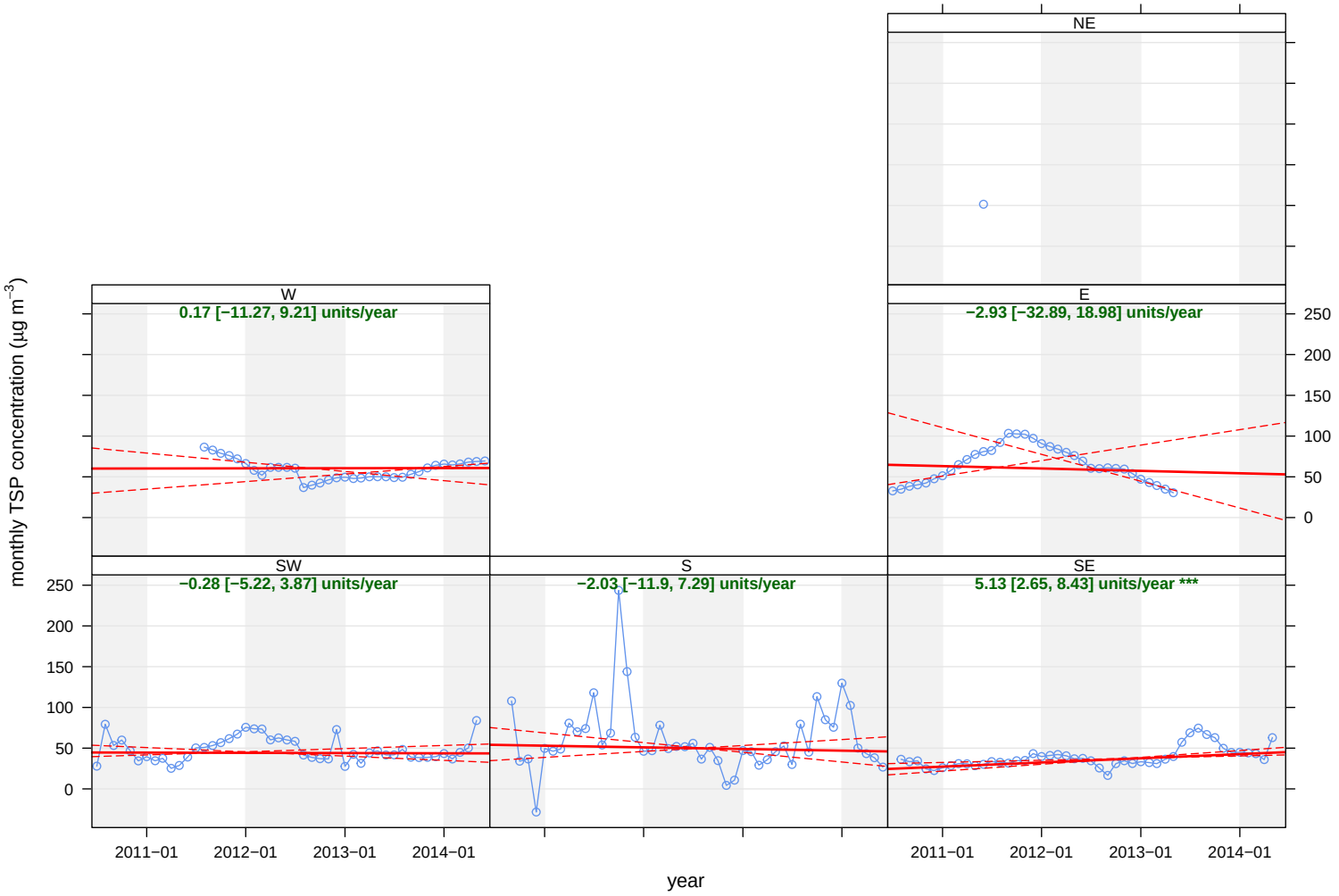

Figure 6.1: Trend analysis of TSP at the FLONA according to wind sectors. The solid red line shows the trend estimate and the dashed red lines show the 95 % confidence intervals for the trend. The overall trend per year is shown at the top, before brackets, and the 95 % confidence intervals between brackets. $p < 0.001 = ***$

The arithmetic mean of PM_{10} as well as the number of WHO daily guidelines exceedances at PARNA are presented in Table 6.2. The annual arithmetic mean ("Total") of PM_{10} varied from 22.2 μg m^{-3} to 33.1 μg m^{-3}. In total, there were nine events where the WHO guideline was exceeded. As expected, the majority of the events took place in the Dry season, which is a known pattern in Rio de Janeiro (10). The PM_{10} levels determined at PARNA are comparable with urban areas in Rio de Janeiro (111), Bloomsbury - UK (173), and Gent - Belgium (174), respectively, 22.9 μg m^{-3}, 28 μg m^{-3}, and 25 μg m^{-3}.

Table 6.2: Arithmetic mean (range between parentheses) concentration of PM_{10} (μg m^{-3}) and number of WHO daily guideline exceedances (#) at the Serra dos Órgãos National Park (PARNA) taking into account three data subsets: Dry season ("Dry"), Wet season ("Wet"), and Overall sampling ("Total").

Year	Dry		Wet		Total	
	mean	#	mean	#	mean	#
2010	41.0 (25.8-58.1)	3	13.5 (0.60-28.1)	0	26.6 (0.60-58.1)	3
2011	29.0 (6.58-78.5)	2	17.5 (2.15-39.3)	0	23.7 (2.15-78.5)	2
2012	28.4 (15.3-67.6)	1	26.0 (11.2-38.9)	0	27.5 (11.2-67.6)	1
2013	20.8 (5.31-37.6)	0	24.6 (8.02-41.0)	0	22.3 (5.31-41.0)	0
2014	19.2 (7.56-29.7)	0	24.1 (6.86-44.4)	0	22.2 (6.86-44.4)	0
2015	33.0 (17.2-71.6)	2	33.3 (21.7-64.7)	1	33.1 (17.2-71.6)	3

The overall trend analysis for PM_{10} points to an increasing trend to 0.71 μg m^{-3}/per year, but there is not a statistical significance. However, the trend analysis classified by wind sectors points to statistical significant trends from the N, NE, E, SE, S, and W sectors (Fig.6.2). It is noteworthy the similarity of the trends from the sectors W and E. The later seems to be related to the urban local traffic in the surroundings of the national park. Based on this long trend analysis, the most important wind sectors for the concentration of PM_{10} are the N (14.2 μg m^{-3}/per year; $p < 0.001$) and NE (2.57 μg m^{-3}/per year; $p < 0.05$).

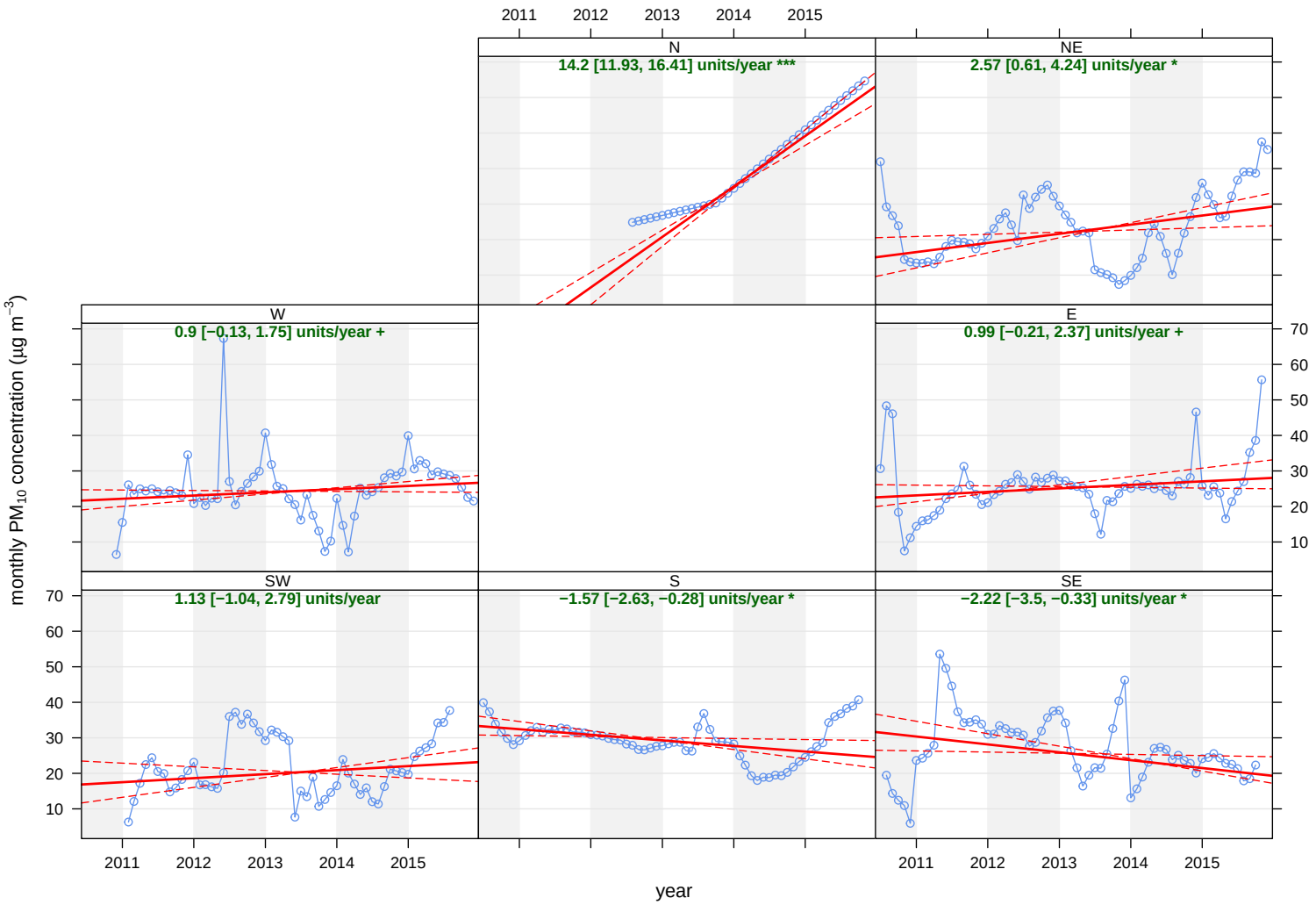

Figure 6.2: Trend analysis of PM_{10} at the PARNA according to wind sectors. The solid red line shows the trend estimate and the dashed red lines show the 95 % confidence intervals for the trend. The overall trend per year is shown at the top, before brackets, and the 95 % confidence intervals between brackets. $p < 0.001 = ***$, $p < 0.05 = *$, $p < 0.1 = +$

6.3.1.1 Water-soluble compounds

The water-soluble composition of the TSP at FLONA is primarily attributed to Na^+ (0.11 - 18.5 μg m^{-3}), SO_4^{2-} (0.75 - 13.7 μg m^{-3}), NO_3^- (0.26 - 15.0 μg m^{-3}), Cl^- (0.16 - 11.0 μg m^{-3}), WSOC (0.88 - 3.78 μg m^{-3}), Ca^{2+} (0.00 - 7.29 μg m^{-3}) and to a lesser extent of minor ions (less than 1.00 μg m^{-3}, in average, for Oxalate, K^+, Mg^{2+}, Formate, Br^-, PO_4^{3-}, Malonate, F^-, Acetate, NH_4^+, and Li^+ (Table F.1 - Supplementary Material - 2). The median contribution of nss-Ca^{2+} (96 %), nss-K^+ (96 %), and nss-SO_4^{2-} (75 %) at FLONA suggest that the major sources for Ca^{2+}, K^+ and SO_4^{2-} were non-marine. However, the same conclusion does not apply to Mg^{2+} sources, since the median contribution of nss-Mg^{2+} was 43 %.

The water-soluble composition of the speciated PM_{10} at PARNA primarily attributed to SO_4^{2-} (0.03 - 25.6 μg m^{-3}), Na^+ (0.10 - 16.2 μg m^{-3}), WSOC (1.32 - 4.69 μg m^{-3}), NO_3^- (0.26 - 15.0 μg m^{-3}), Cl^- (0.16 - 11.0 μg m^{-3}), and to a lesser extent of minor ions (less than 1.00 μg m^{-3}, in average, for Oxalate, Ca^+ K^+, Mg^{2+}, PO_4^{3-}, Br^-, Malonate, F^-, Formate, NH_4^+, and Li^+ (Table F.1 - Supplementary Material - 2) As observed at FLONA, the median contribution of nss-Ca^{2+} (96 %), nss-K^+ (96 %), and nss-SO_4^{2-} (75 %) at PARNA suggest that the major sources for Ca^{2+}, K^+ and SO_4^{2-} were non-marine. The magnitude of nss-Mg^{2+} (53 %) sources is slightly higher than observed at FLONA. The atmospheric deposition of NH_4^+, NO_3^-, and SO_4^{2-} was previously studied at PARNA (66). The contribution of nss sources to SO_4^{2-} was 97 %. The nss-SO_4^{2-} contribution determined by Rodrigues et al. 2007 (66) is higher than ours because the authors determined the total wet and dry deposition. The connection between their evaluation and ours is the idea that PARNA might be influenced not only by the great number of atmospheric pollution sources in the MRRJ, but also due to favorable meteorological conditions such as prevailing winds and high accumulated precipitation.

6.3.1.2 Elemental composition

Table F.1 (Supplementary material - 2) presents the concentration of elements extracted from TSP at FLONA. Zinc and Al presented the highest concentration ranges from 0.17 to 44.4 μg m^{-3} and from 0.24 to 22.9 μg m^{-3}, respectively. In average, the levels of Zn (7.01 μg m^{-3}) and Al (4.24 μg m^{-3}) were high in comparison with other studies (175, 176), including one evaluation of TSP chemical composition under similar characteristics (111). Among elements often regarded as trace level in PM, Ti and Cd presented

the highest concentration ranges from 3.21 to 221.9 ng m^{-3} and from 0.06 to 77.4 ng m^{-3}, respectively. Similar to the trend observed to major elements, the average concentration of Ti (53.9 ng m^{-3}) and Cd (31.7 ng m^{-3}) were also high in comparison with the ones reported in (111, 175, 176).

Zinc and Al were also major elements in the speciated PM_{10} at PARNA (Table F.1, Supplementary material - 2), as observed in the speciated TSP, ranging from 0.14 to 26.6 μg m^{-3} and from 0.05 to 18.4 μg m^{-3}, respectively. In average, the levels of Zn (4.43 μg m^{-3}) and Al (3.39 μg m^{-3}) were high in comparison with other studies (111, 174). Despite of the distance between FLONA and PARNA as well as the different particle size, it is noteworthy the apparent similarity in the average levels of Zn and Al. With regard to the trace elements at PARNA, Ti (0.93 - 74.2 ng m^{-3}), Mn (0.33 - 47.9 ng m^{-3}), and Pb (0.90 - 51.7 ng m^{-3}) presented the highest levels. The average Ti (20.3 ng m^{-3}), Mn (17.1 ng m^{-3}), and Pb (16.5 ng m^{-3}) levels at PARNA are higher than other urban sites also influenced by natural sources (111, 174). This fact may suggest that anthropogenic sources like roadside soil and road dust play an important role in the chemical composition of PM_{10} at PARNA.

6.3.2
k-means clustering

The cluster analysis of TSP concentration for three clusters is shown in Fig. 6.3. The number of clusters was based on exploratory data analysis and previous knowledge about sources at FLONA. According to the bivariate plot (Fig. 6.3(a)), the maximum of mean concentration is associated to southerly intermediate winds (4 m s^{-1}). This may be associated to the road traffic and other local anthropogenic sources in the region. Besides that, there is some overlap between clusters 1 and 3 at the S sector.

A time series analysis shows the proportional contribution of clusters identified at FLONA to the mean concentration of TSP (Fig. 6.4). Based on Fig. 6.4, one can observe that the cluster 1 presented low importance and this agrees with the number of samples related to this clusters ($n = 7$). In comparison with cluster 1 and 2, cluster 3 was the most representative along the time series, which agrees with its little overlap with other clusters (Fig. 6.3(b)).

At PARNA, three clusters were identified, which were also supported by initial exploratory analysis (Figure 6.5). Among the three identified clusters, the cluster 1 presented at least two sources: 1) a ground-level source from all sectors associated to air stagnation; and 2) a source associated to the circulation of low wind speed (1.5 m s^{-1}) from the S sector. The increase of PM

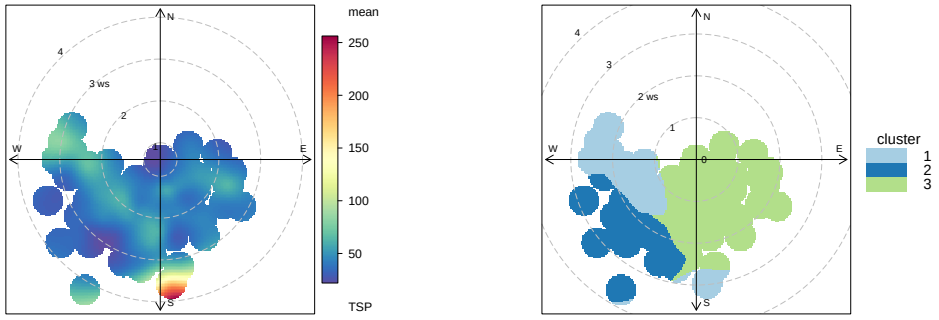

6.3(a): 6.3(b):

Figure 6.3: Characterizing TSP emission sources using bivariate plots and k-means clustering. for (a) Bivariate polar plot for TSP concentrations at FLONA. The color scale shows the concentration of TSP in μg m^{-3} and the radial scale shows the wind speed, which increases the center of the plot radially outwards. (b) Clusters identified at FLONA.

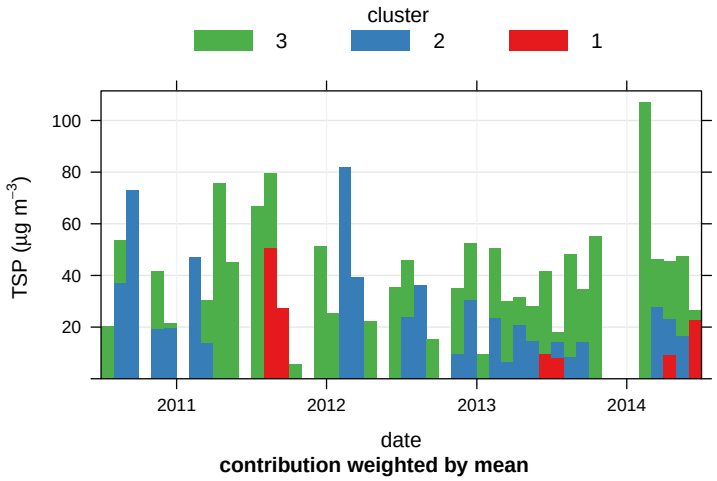

Figure 6.4: Time series of identified clusters at FLONA.

levels associated to air stagnation is an expected feature in urban background atmospheres, but the second source may be associated to traffic influence, which is also a ground-level type of source. The cluster 2, associated to the direction of the National Park, may be associated to biogenic emissions.

The time series analysis of clusters identified at PARNA shows a more balanced contribution of sources (Fig. 6.6). The cluster 2 and 3 showed similar contribution between the years of 2012 and 2014, while the cluster 1 contributed mostly in the end of 2010 and towards the end of 2015.

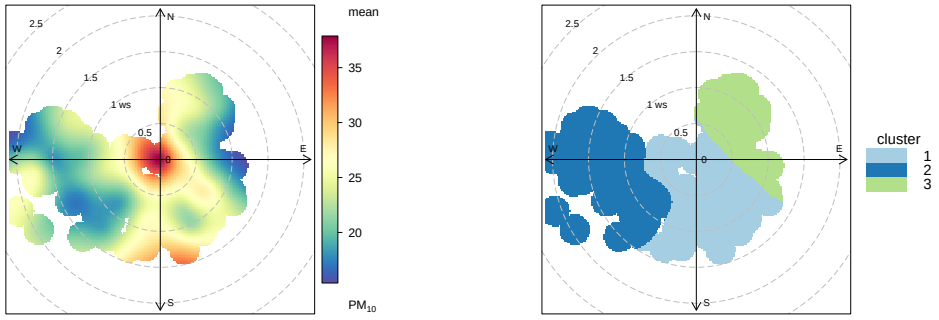

6.5(a): 6.5(b):

Figure 6.5: Characterizing PM_{10} emission sources using bivariate plots and k-means clustering. for (a) Bivariate polar plot for PM_{10} concentrations at PARNA. The color scale shows the concentration of PM_{10} in μg m^{-3} and the radial scale shows the wind speed, which increases the center of the plot radially outwards. (b) Clusters identified at PARNA.

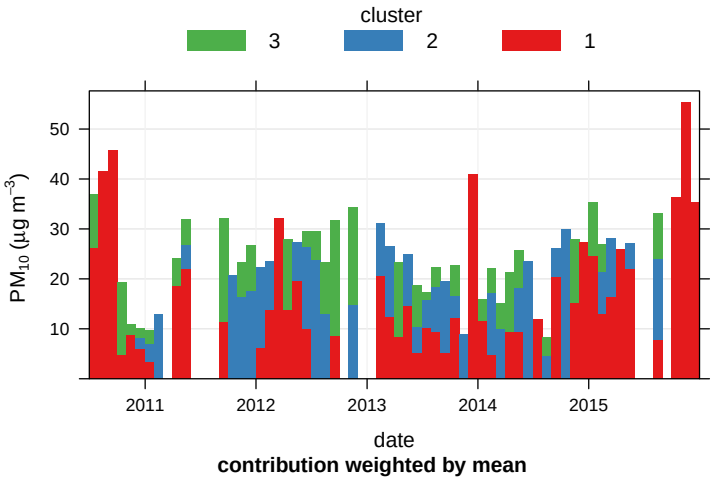

Figure 6.6: Time series of identified clusters at PARNA.

6.3.3 CBPF

6.3.3.1 Selection of intervals

The very nature of CBPF allows the estimation of local minor sources as well as remote sources, which can be equally hard to detect. Four splits were made in our dataset in order to detect a higher number of sources: 1) $<$ 25th concentration percentile, 2) 25-50th concentration percentile, 3) 50-75th concentration percentile, and 4) $>$ 75th concentration percentile. This exploration benefits from the fact that sources tend to occupy distinct concentration intervals.

6.3.3.2 Exploration of sources at FLONA

The CBPF plots for the TSP concentration at FLONA complemented the k-means clustering by disentangling substructures inside the clusters (Fig. 6.7). For instance, based on the CBPF findings, there is reasonable evidence to believe that the cluster 1 is associated to both intermittent (Fig. 6.7(c)) and continuous processes (Fig. 6.7(d)). The magnitude of CBPF probability is the criteria to classify emission as intermittent or continuous (57). In this sense, continuous emissions sources at FLONA are not only associated to high concentration (Fig. 6.7(d)), but also to low-to-moderate pollution signals (Fig. 6.7(b)) from the SW and E sectors.

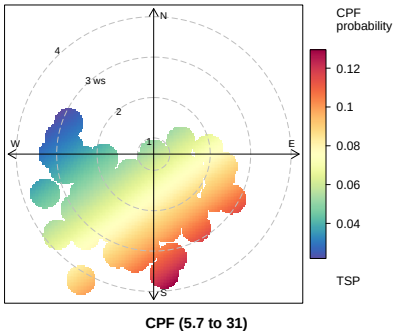

6.7(a): 0-25th percentile

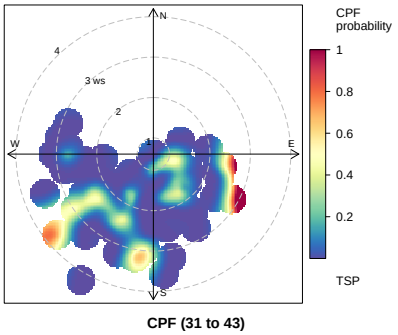

6.7(b): 25-50th percentile

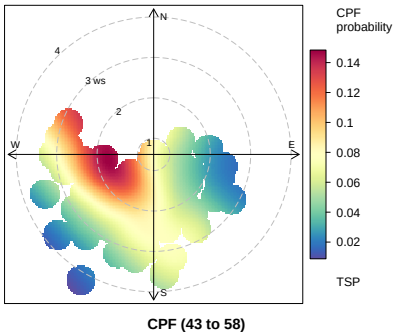

6.7(c): 50-75th percentile

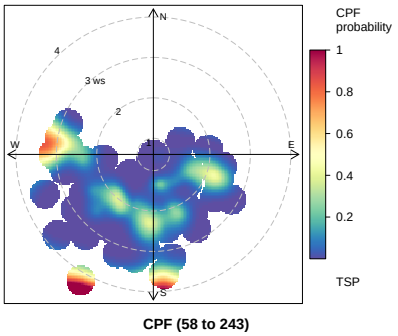

6.7(d): 75-100th percentile

Figure 6.7: Conditional bivariate probability function plot of TSP at the FLONA site for (a) TSP concentrations between 5.7 and 31 μg m^{-3}, (b) TSP concentrations between 31 and 43 μg m^{-3}, (c) TSP concentrations between 43 and 58 μg m^{-3}, and (d) TSP concentrations between 58 and 243 μg m^{-3}.

6.3.3.3 Exploration of sources at PARNA

As observed at FLONA, the CBPF plots for PARNA were also useful to highlight substructures in the sources apportioned via k-means clustering.

The Figs. 6.8(b) and 6.8(c) shown that cluster 3 6.5 is strongly influenced by intermittent sources. By means of CBPF, the sharp signal of the cluster 1 6.5(a) can be attributed to intermittent signals as well. Given a high probability, the analysis of the concentration percentile range 0-25th reinforced the importance of sources from the W and SW sectors (Fig. 6.8(a)).

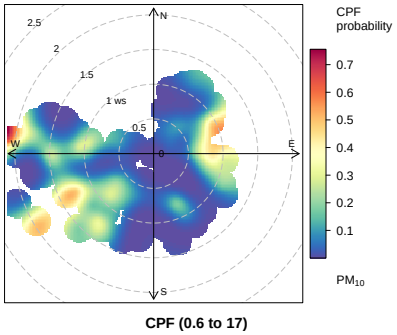

6.8(a): 0-25th percentile

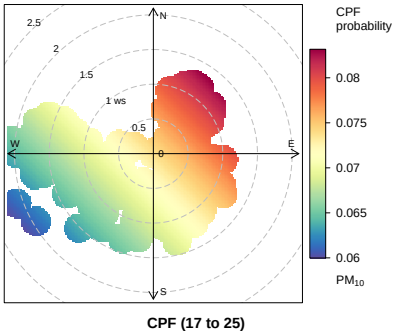

6.8(b): 25-50th percentile

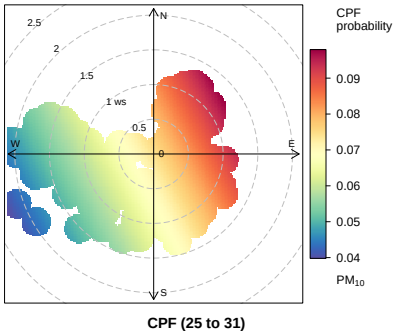

6.8(c): 50-75th percentile

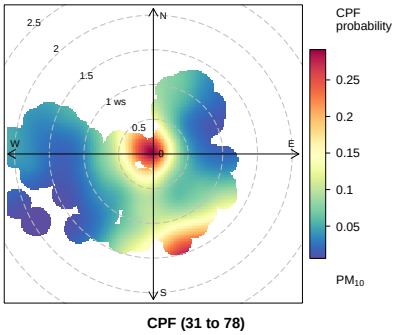

6.8(d): 75-100th percentile

Figure 6.8: Conditional bivariate probability function plot of PM_{10} at the PARNA site for (a) PM_{10} concentrations between 0.6 and 17 μg m^{-3}, (b) PM_{10} concentrations between 17 and 25 μg m^{-3}, (c) PM_{10} concentrations between 25 and 31 μg m^{-3}, and (d) PM_{10} concentrations between 31 and 78 μg m^{-3}.

6.3.4 Stochastic models

6.3.4.1 Key variables for PM prediction at FLONA

The CIT consisted of 5 nodes including 3 terminal nodes (Figure 6.9). The most important splitting variable of the root node was the concentration of Ca. Despite the difference in both algorithms k-means clustering, implemented by the *R* package openair, and CIT, a small group of observations ($n = 7$) with a common feature was identified using the two approaches. This finding confirms

the definition of the two methods as "robust" tools. The node 5 presented a TSP$[_{mean}]$ = 98.3 μg m^{-3})

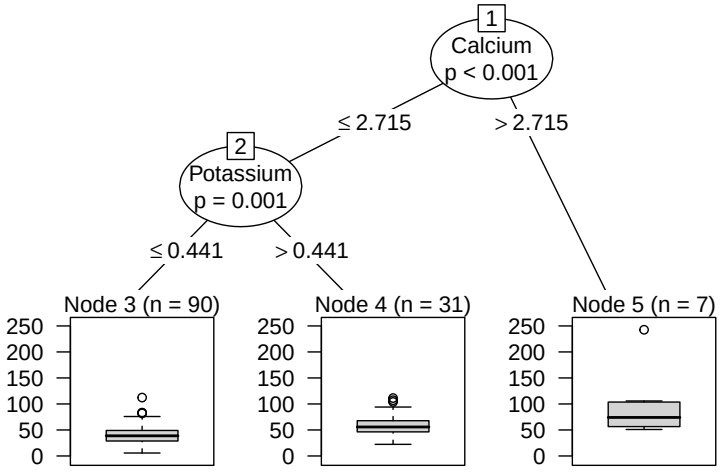

Figure 6.9: Conditional inference trees (CIT) for TSP data. In the CIT, n is the number of samples classified in a given node, and the TSP concentration is in μg m^{-3}.

The node 2 yielded to the terminal nodes 3 (TSP$[_{mean}]$ = 40.9 μg m^{-3}) and 4 (TSP$[_{mean}]$ = 59.2 μg m^{-3}). Potassium is used as a biomass burning tracer, but its multiple sources are a shortcoming for this assumption (170). Given the high median contribution of nss-K^+ sources as well as the particle size, we attribute difference between the two terminal nodes to soil-related sources. These sources may be related to construction sites, wind-blown dust, paved and unpaved road dust. The cluster analysis for the terminal nodes 3 and 4 shown a quite similar relationship between the chemical variables (Fig. 6.10. However, the terminal node 4 presents significant relationships between Ti and Mn, Zn and Al.

The overall importance of variables to predict TSP, considering the conditional correlation between them, is shown in Fig. 6.11. As expected, Ca^{2+} and K^+ are one of the most important chemical species, but other chemical variables like NO_3^- and Mn are also very important to predict PM concentration at FLONA. It is noteworthy that the seasonality demonstrated low prediction power, while the variable precipitation was one of the most high ranked variables.

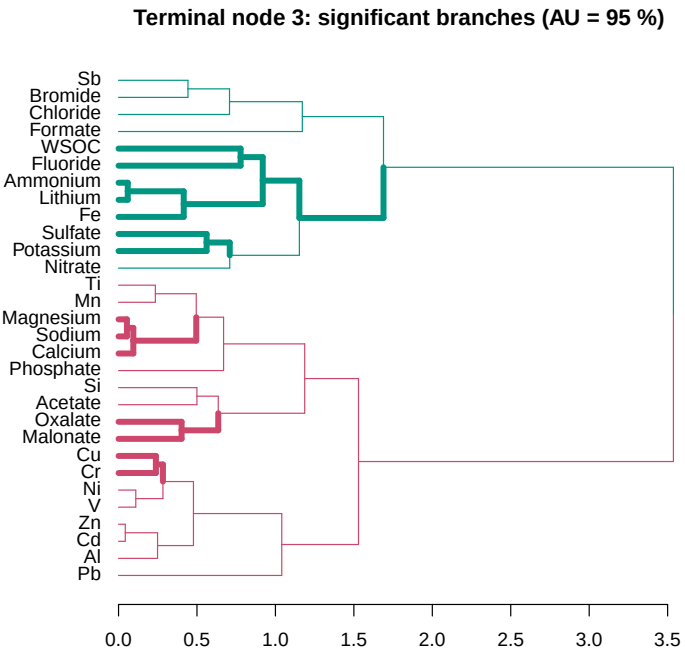

6.10(a):

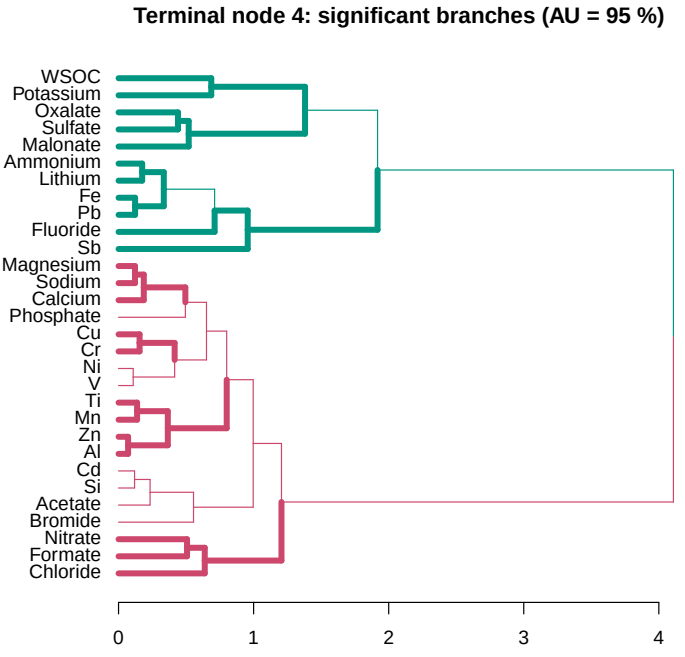

6.10(b):

Figure 6.10: Hierarchical clustering of speciated TSP with uncertainty estimate using multiscale bootstrap resampling. for (a) CIT terminal node 3. (b) CIT terminal node 4. Variables associated in clusters with AU = 0.95 are highlighted. The different colors in the dendograms point to potential substructures in the CIT terminal nodes.

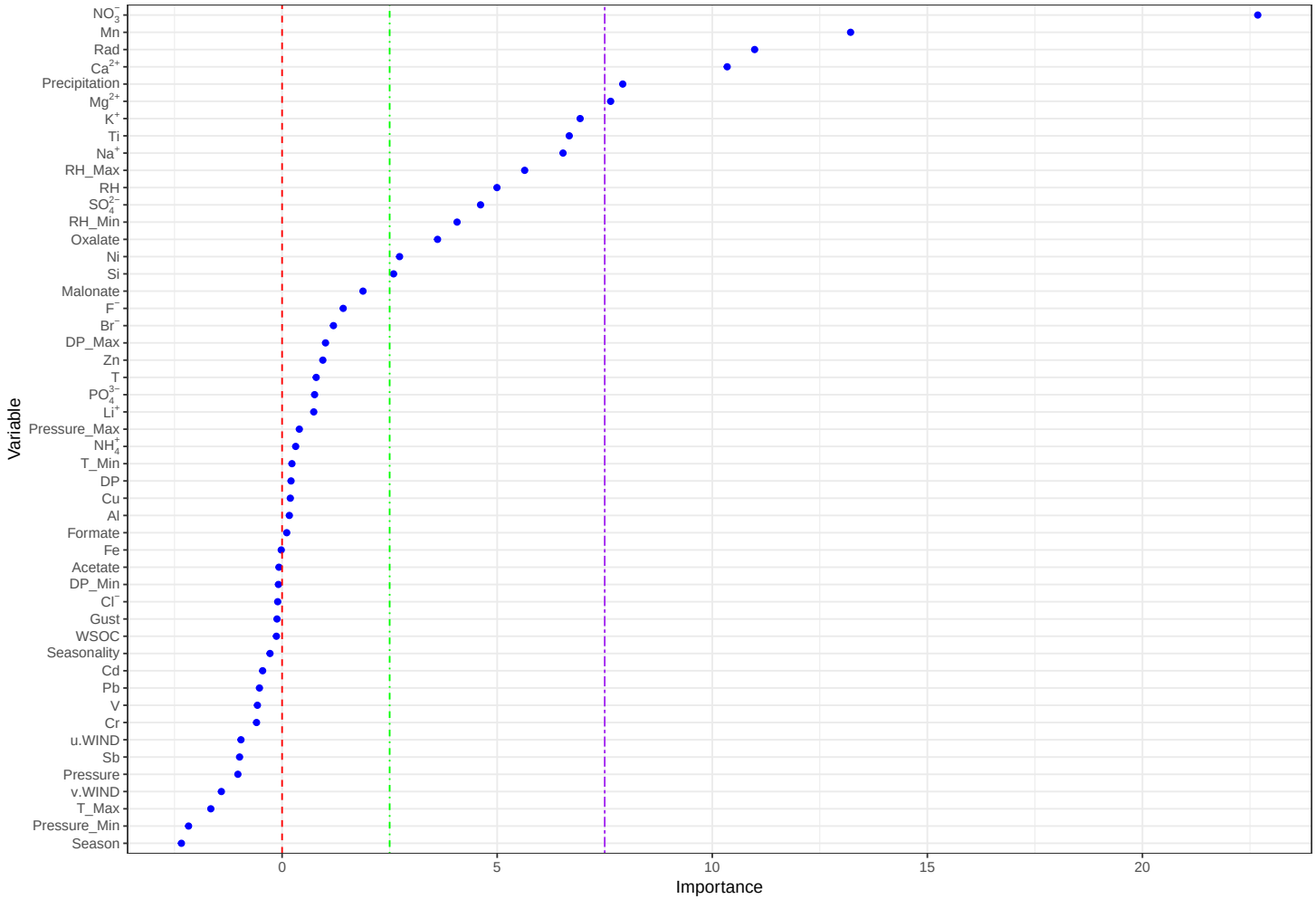

Figure 6.11: Conditional ranking variable importance: CIT for TSP. Predictors to the right of the red dashed line are significant.

6.3.4.2 Key variables for PM prediction at PARNA

The CIT consisted of 5 nodes including 3 terminal nodes (Figure 6.12). The most important splitting variable of the root node was the Gust speed. The concentration of Ca^{2+} was another important variable to predict PM. The node 1 yielded to the terminal node 2 ($PM_{10}[_{mean}] = 35.4$ μg m^{-3}), while the node 3 yielded to the terminal nodes 4 ($PM_{10}[_{mean}] = 22.4$ μg m^{-3}) and ($PM_{10}[_{mean}] = 31.2$ μg m^{-3}). Although a direct connection of the results from the k-means clustering analysis of PM_{10} with the CIT plot is not possible, the classification of samples in node 2, based on low Gust speed, agreed with the existence of one of the apportioned sources at cluster 1, associated to air stagnation (Fig. 6.5(a)).

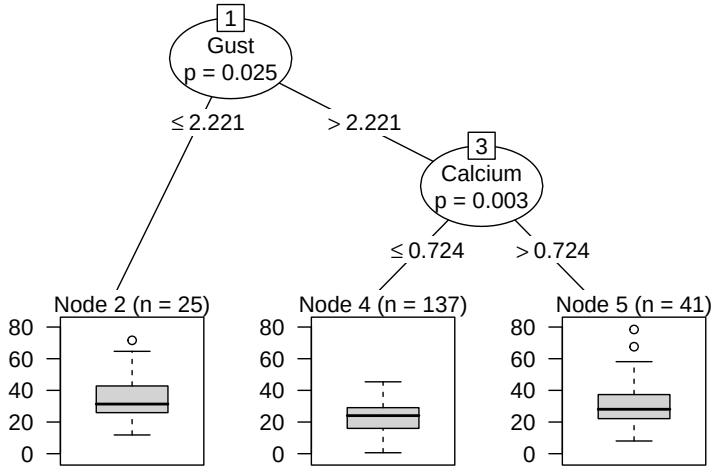

Figure 6.12: Conditional inference trees (CIT) for PM_{10} data. In the CIT, n is the number of samples classified in a given node, and the PM_{10} concentration is in μg m^{-3}.

According to the hierarchical analysis of the nodes 4 and 5, as the concentration of Ca^{2+} decreased, there were more significant association between species such as, Oxalate-Malonate, Zn-Fe, Cu-Al, and Mn-Pb. We believe that this may be due to emissions of the so-called traffic related elements (TREs). The TREs (e.g., Cu, Sb, Cr, Pb, and Zn) are elements associated to a broad range of processes from tail-pipe emissions to wear products (e.g, tyres and breaks) as well as from corrosion in general of vehicle components to plants growing on the roadsides (111, 177).

The overall importance of variables to predict PM_{10}, considering the conditional correlation between them, is shown in Fig. 6.14. As observed at FLONA, Ca^{2+} was an important variable to predict PM_{10}. Nitrate also was ranked among the most important predictors, which is in agreement with the

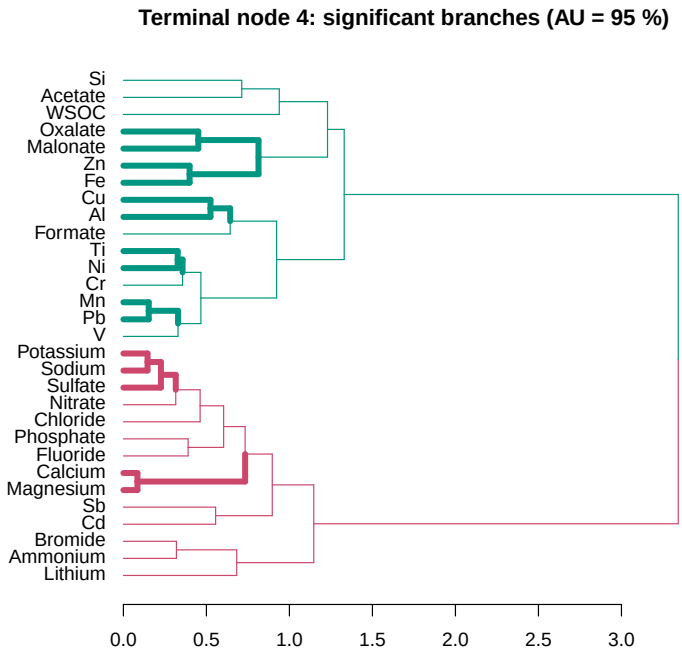

6.13(a):

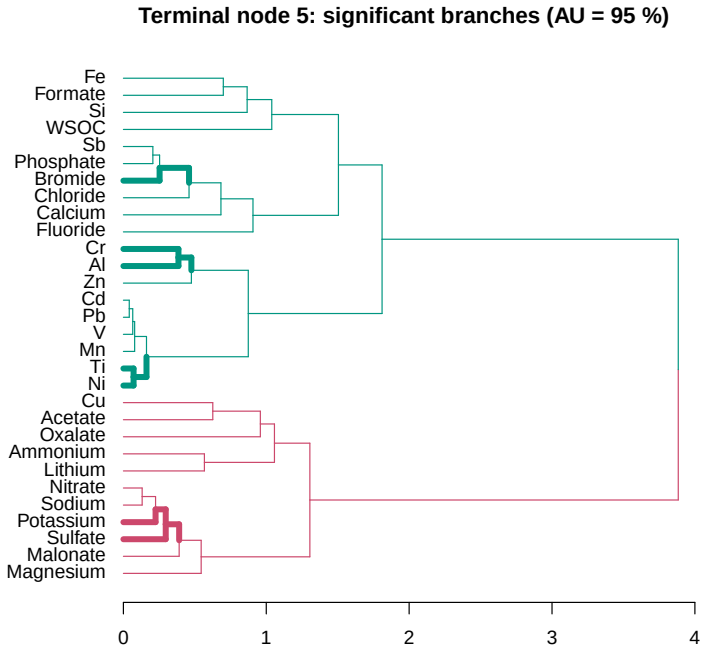

6.13(b):

Figure 6.13: Hierarchical clustering of speciated PM_{10} with uncertainty estimate using multiscale bootstrap resampling. for (a) CIT terminal node 4. (b) CIT terminal node 5. Variables associated in clusters with AU = 0.95 are highlighted. The different colors in the dendograms point to potential substructures in the CIT terminal nodes.

importance of secondary inorganic aerosols (SIA) at PM_{10}. As seen in the CIT plot, Gust was the most important PM predictor. Titanium, Cu, and Zn were also important predictors, which agree with the initial idea about the importance of TREs at the PARNA site. In agreement with the importance of Gust, the seasonality plays an important role in the prediction of PM_{10} at PARNA.

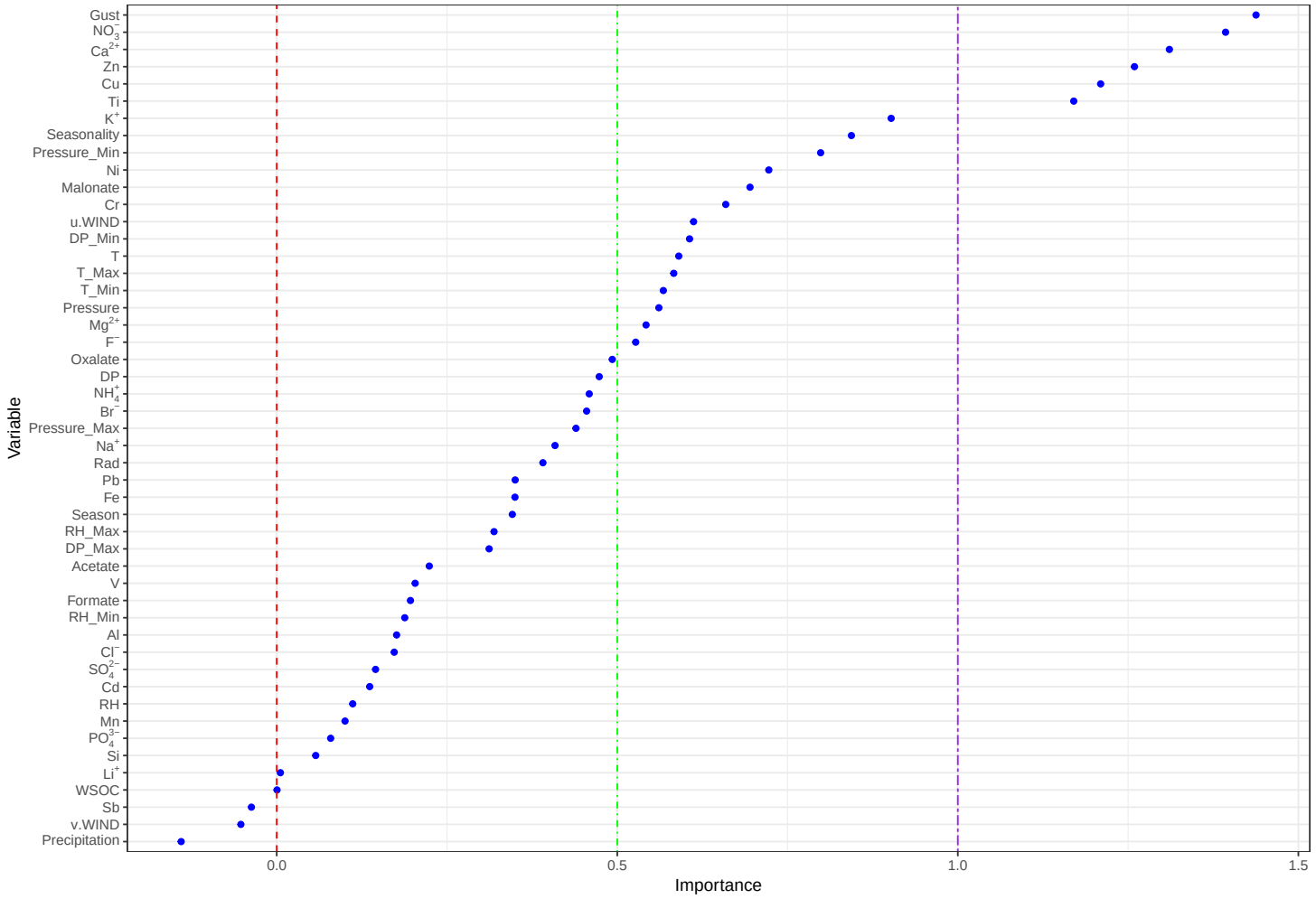

Figure 6.14: Conditional ranking variable importance: CIT for PM_{10}. Predictors to the right of the red dashed line are significant.

6.4 Conclusion

The evaluation of ambient aerosol sources in two Atlantic Rain Forest hotspots in the surroundings of Rio de Janeiro was carried based on chemically speciated PM datasets. The results for TSP and PM_{10} source apportionment used novel approaches in environmental sciences. Previous findings were confirmed concerning the importance of non-sea-salt sources at the Serra dos Órgãos National Park, while the ambient aerosol sources at the Mário Xavier National Florest were evaluated for the first time. For TSP, the main predictors were NO_3^- > Mn > Rad (Global radiation) > Ca^{2+} > Precipitation > Mg^{2+}. For PM_{10}, the main predictors were Gust (Gust wind speed) > NO_3^- > Ca^{2+} > Zn > Cu > Ti. The CBPF and k-means clustering analyses reinforced the importance of measuring and characterizing the frequency of both natural and anthropogenic sources, which can contribute to the development of appropriated mitigation policies in the surroundings of the studied protected areas.

Acknowledgements

The authors thank CAPES (specially to Prof. Luiz Drude, INCT-TMCOCEAN Project coordinator), CNPq, and FAPERJ for research grants. They are also grateful to Prof. Ricardo Aucélio for sharing his technical infrastructure for the TOC analyses. The authors also thank technicians who helped in the ICP-MS analyses: Álvaro Pereira and Rafael Christian Chávez Rocha; ICP OES analyses: Maurício Dupim and André Vechi; and IC analyses: Heloisa Fontenelle and Verônica Luiza. The authors also thank to the research coordination of the Serra dos Órgãos National Park and the INMET for providing meteorological information.

7
A preliminary test on the use of structural equation modeling to study the relationship between air pollution exposure and health symptoms

Vinícius L. Mateus[a], Mohammed-Hossein Ramezani[b], Esmaeil S. Nadimi[b], Per Løfstrøm[c], Adriana Gioda[a], Victoria Blanes-Vidal[b]

[a]Pontifical Catholic University, Rio de Janeiro (PUC-Rio), Department of Chemistry, RJ, Brazil;
[b]University of Southern Denmark, The Mærsk McKinney Møller Institute, Odense, Denmark;
[c]Aarhus University, Department of Environmental Science, Roskilde, Denmark

Working paper: *Chemosphere* (Aimed journal)

Abstract

In the last years, non-urban residents have experienced a significant increasing in exposure to air pollutants from biodegradable waste sites. Although the exposure to high levels of air pollutants presents a solid body of knowledge, there is still a lack of contributions in low-to-moderate levels and its association with psychosocial and physical health symptoms. Most studies have ranked the degree of exposure based on the distance between site and residents' household. In this work, ammonia (NH_3) was considered a proxy of exposure to biodegradable waste. Using emission-dispersion models, NH_3 concentration was objectively estimated during the period 2005-2010. A total of 454 individuals were randomly selected, and their self-reported health symptoms were combined with estimation of the proxy gas. The general SEM framework was used to analyze the pathways between air pollution exposure and health symptoms, properly adjusted for confounding variables. Previous results reported mediation effects of odor annoyance on health symptoms, but they were not conceived as a single model. These results were confirmed, but evidences of borderline association suggest the inclusion of more psychosocial symptoms to a proper model estimation. A second alternative model reinforces the findings about the mediation role of psychosocial health symptoms, measured by odor

annoyance, behavioral interference, and health risk perception. Strong mediated effects of biodegradable waste exposure on physical health symptoms were found. This study provides robust indicatives of psychosocial health symptoms in predicting environmental induced physical health symptoms, among non-urban residents exposed to low-to-moderate air pollution from biodegradable wastes.

Keywords: Air pollutants, Structural equation modeling, Environmental health, Biodegradable waste, Psychosocial health symptoms

7.1 Introduction

Rural air quality has become a matter of global concern. Citizens living in rural areas are exposed to a series of air pollutants that are originated from local sources. Typical local sources include agricultural and animal production activities, mainly concentrated animal feeding operations (CAFOs) (178, 179), e.g., swine (180, 181), and field applications of animal manure (33, 181, 182). A abundance of potentially hazardous air contaminants is associated with handling, storage, treatment and disposal of agricultural, animal and municipal biodegradable wastes, including ammonia, hydrogen sulfide, phenols, indoles, volatile fatty acids, carbon dioxide, methane, particulate matter, and endotoxins (29). These pollutants can have adverse health effects on the local populations and some of them may lead to the perception of malodors.

Acting as an environmental stressor, odor is able to induce psychosocial responses, i.e., annoyance, that are related with health symptoms also experienced by healthy individuals (183). Annoyance is a feeling of displeasure related to an observed or hypothesized agent or condition, which affects a community or individual (184). Annoyance can be considered a health effect based on the WHO definition of health, a "State of physical, mental and social well-being not merely the absence of disease and infirmity" (30).

Communities in the surroundings of biodegradable wastes facilities complain more frequently about annoyance and health symptoms, which can be related with malodorous components (185). In biodegradable wastes, the exposition always includes remarkable toxic compounds along with strong malodor (29, 182). Odorous compounds are commonly related to physical health symptoms even below the levels where a priori toxicity would be expected (186). A consistent literature supports the relationships between odor pollution, annoyance, and health symptoms.

Some scholars affirm that scientific findings do not support connection between odor exposure and health outcomes (32). Using controversial concepts,

this point of view finds support in occupational environments where individuals are assumed to be healthy and have some tolerance to exposure. In addition, they argue about anecdotal reports and the lack of causal relation provided by epidemiological studies (31). As a matter of fact, it is doubtful that individuals will complain about odor annoyance at their workplaces. Not only the healthy worker assumption, but also the different context can be ascribed to the failure of occupational studies regard to the assessment of adverse effects among communities living near biodegradable wastes (187).

Previous studies have used adjusted logistic regression models and formal mediation analyzes, to separately investigate the associations between air pollution exposure, measured by the proxy gas NH_3, and: 1) non-specific health symptoms (33), 2) respiratory and sensory irritation symptoms (34), 3) psychosocial health symptoms (35). Odor annoyance was related to full (indirect effects only) and partial mediation (either direct or indirect). Given the complexity of these associations, the entire pathway from air pollution exposure to health symptoms cannot be assessed without the use of a more comprehensive analysis method. On the other hand, previous studies investigating these associations have important limitations since they have been ecological studies, or they have used distances as surrogates of individual exposures. Due to the high variability of concentration between the sites, ecological studies cannot provide good estimates of individual exposures (188).

Structural equation modeling (SEM) is a family of techniques, an extension of the general linear model, that combine aspects from multiple regression and factor analysis (189). SEM has been used successfully to test complex hypotheses on environmental health (90, 190). In the early 1970's, SEM was conceptualized from the integration of classical pathway analysis (structural component) and the confirmatory factor analysis (measurement component), which is attributed to K. Jöreskog, J. Keesling, and D. Wiley (191). Using the concept of latent variables, SEM provides estimation of the measurement errors, and can be used to clarify the pathways between air pollution and different classes of health symptoms.

The aim of this work is to carry out a comprehensive analysis of the relationships between air pollution, psychosocial health symptoms (PSY) - measured by odor annoyance, behavioral interference, and health risk perception - respiratory and non-specific health symptoms (RNS), and sensory irritation symptoms (SIS) through structural equation modeling (SEM) and based on individual exposures to a proxy chemical. It is not possible to establish an only mediation model. Successfully, two mediation models were selected from a series of hypothesized path-analytic models and their results will be presented.

7.2 Material and methods

The reader is referred to the section 2.6, page 51.

7.3 Results

A total of 454 individuals (40.5%) returned the completed questionnaire. The residential level of exposure as well as the socio-demographic information are provided in the Appendix section (Table G.1). Non-response analyses (i.e., gender, age, and exposure) did not show statistically significant differences between respondents and non-respondents (34).

7.3.1 Model development

The symptoms were grouped in two latent variables: SIS (itching, dryness or irritation of eyes, itching, dryness or irritation of the nose, runny nose) and RNS (cough, chest wheezing or whistling, difficulty breathing, dizziness, difficulty concentrating, headache, unnatural fatigue, and nausea).

7.3.2 PSY - measured by odor annoyance

Considering odor annoyance as a mediator of health symptoms, a set of hypotheses was formulated in a SEM framework (Fig. 7.1).

Firstly, using selected fit indexes the model fit was evaluated (Table 7.1). Secondly, the evaluation of the theoretical relevance of the path estimation was carried out. Finally, both the theoretical consistence of the measurement structure of SEM model and the degree of explanation explained for each variable were investigated (Table 7.2 and Table G.2 - Appendix).

Taking into account the previous work on the topic, odor annoyance has already been associated with respiratory and sensory, and non-specific health symptoms. However, the use of a SEM framework makes possible to conceptualize these symptoms as dimensions of latent variables. Therefore, this work proposes new structures for the physical health symptoms grouping. In the current approach, odor annoyance is considered a proxy of the latent variable PSY.

The air pollution effect on PSY was statiscally significant ($p < 0.0001$) while both pathways directly linking AP to SIS and RNS were not statiscally supported. The partially mediated effect was not significant for RNS ($p = 0.196$) while the fully mediated effect was borderline significant ($p = 0.048$).

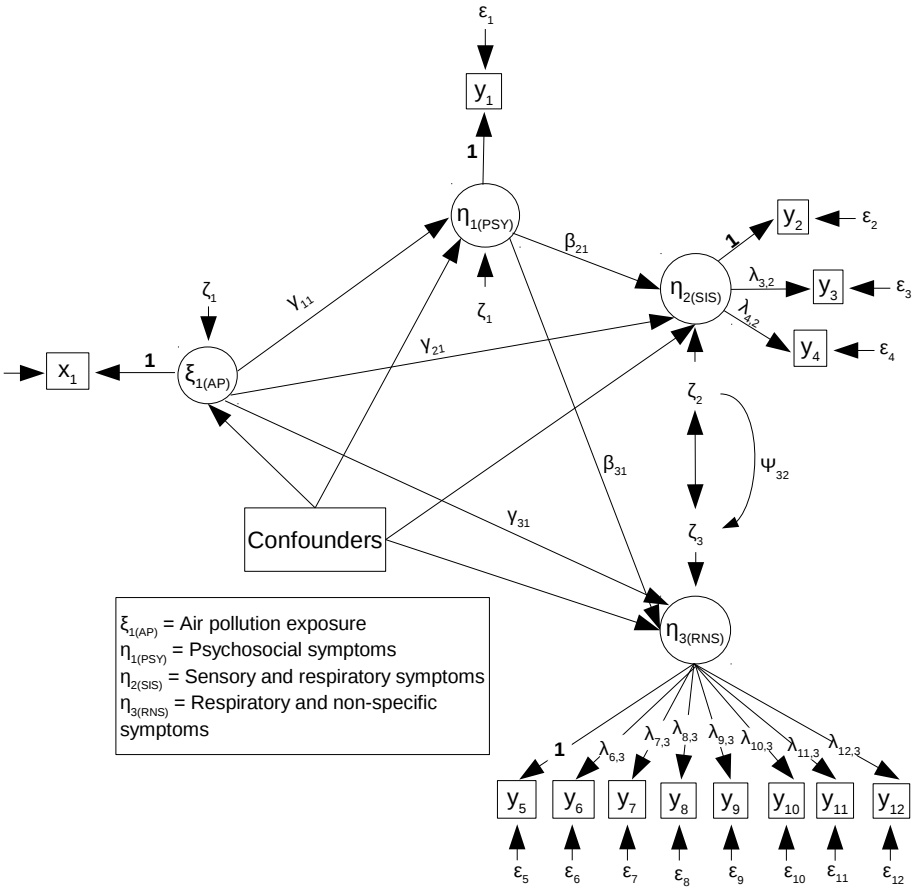

Figure 7.1: Path diagram for the mediation effect of AP through PSY - measured only by odor annoyance - on SIS and RNS.

Table 7.1: Model fit for the investigation of PSY, measured by one indicator.

Fit index	Value	Criterion status
$\chi^2(df)$	180.984 (128.000)	Failed (χ^2 should be equal to df.)
p-value (χ^2)	0.001	Failed (p-value should not be significant at the 95% confidence level.)
CFI	0.981	Succeeded (Should be > 0.90.)
TLI	0.971	Succeeded (Should be > 0.90.)
RMSEA (CI)	0.030 (0.019 - 0.040)	Succeeded (Close fit is indicated by values < 0.05.)
PCLOSE	1.000	Succeeded (The p-value must be nonsignificant at the 95% confidence level.)
WRMR	0.675	Succeeded (Must be ≤ 1.0)

Table 7.2: Measurement structure: PSY measured by one indicator. (Estimation values in bold face represent fixed parameters.)

Latent variable	Indicator	Estimation	Standard error	*p*-value	Standardized estimation value
AP					
	NH_3 exposure	**1.000**	0.000		1.000
SIS					
	Eyes itching dryness or irritation	**1.000**	0.000		0.919
	Nose itching dryness or irritation	1.007	0.046	0.000	0.925
	Runny nose	0.896	0.051	0.000	0.823
RNS					
	Nausea	**1.000**	0.000		0.876
	Cough	0.919	0.069	0.000	0.805
	Chest wheezing or whistling	0.808	0.085	0.000	0.708
	Difficulty breathing	0.857	0.086	0.000	0.750
	Fatigue	1.005	0.062	0.000	0.880
	Headache	0.956	0.066	0.000	0.837
	Difficulty concentrating	1.027	0.071	0.000	0.899
	Dizziness	0.953	0.064	0.000	0.834
PSY					
	Odor annoyance	**1.000**	0.000		0.949

Regarding SIS, both the partially ($p = 0.004$) and fully mediated effects ($p = 0.011$) were significant (Table 7.3).

7.3.3 PSY - measured by odor annoyance, behavioral interference, and health risk perception

Measuring PSY with three indicators, a slight difference is seen in the model fit (Table 7.4, Fig. 7.2) and some hypotheses could be more precisely evaluated. The new indicators of PSY, odor annoyance, behavioral interference and health risk perception (Table 7.5), yielded improvement in the degree of explanation for the endogenous latent variable RNS, according to the adjusted coefficient of determination (R^2) (Table G.3 - Appendix). The R^2 for each one of the observed modeled variables were higher than 0.500. This model successfully supports the importance of including more dimensions, i.e., indicators, while evaluating the mediating capacity of the psychosocial health symptoms.

The model derived from PSY's measurement by odor annoyance, behavioral interference, and health risk perception achieves findings similar to the previous one where PSY is only measured by odor annoyance. For in-

Table 7.3: Pathways for model represented by Fig. 7.1

Parameter (Fig. 1)	Path	Estimation	Standard error	p-value	Standardized estimation value
γ_{21}	AP $\rightarrow$ SIS	-0.038	0.097	0.691	-0.042
γ_{31}	AP $\rightarrow$ RNS	-0.036	0.088	0.681	-0.041
γ_{11}	AP $\rightarrow$ PSY	0.466	0.056	0.000	0.490
β_{21}	PSY $\rightarrow$ SIS	0.409	0.165	0.013	0.423
β_{31}	PSY $\rightarrow$ RNS	0.247	0.128	0.054	0.268
$\gamma_{11} \times \beta_{21}$	AP $\rightarrow$ SIS (fully mediated)	0.190	0.075	0.011	0.207
$\gamma_{11} \times \beta_{31}$	AP $\rightarrow$ RNS (fully mediated)	0.115	0.058	0.048	0.131
$\gamma_{21} + (\gamma_{11} \times \beta_{21})$	AP $\rightarrow$ SIS (partially mediated)	0.152	0.053	0.004	0.165
$\gamma_{31} + (\gamma_{11} \times \beta_{31})$	AP $\rightarrow$ RNS (partially mediated)	0.079	0.061	0.196	0.090

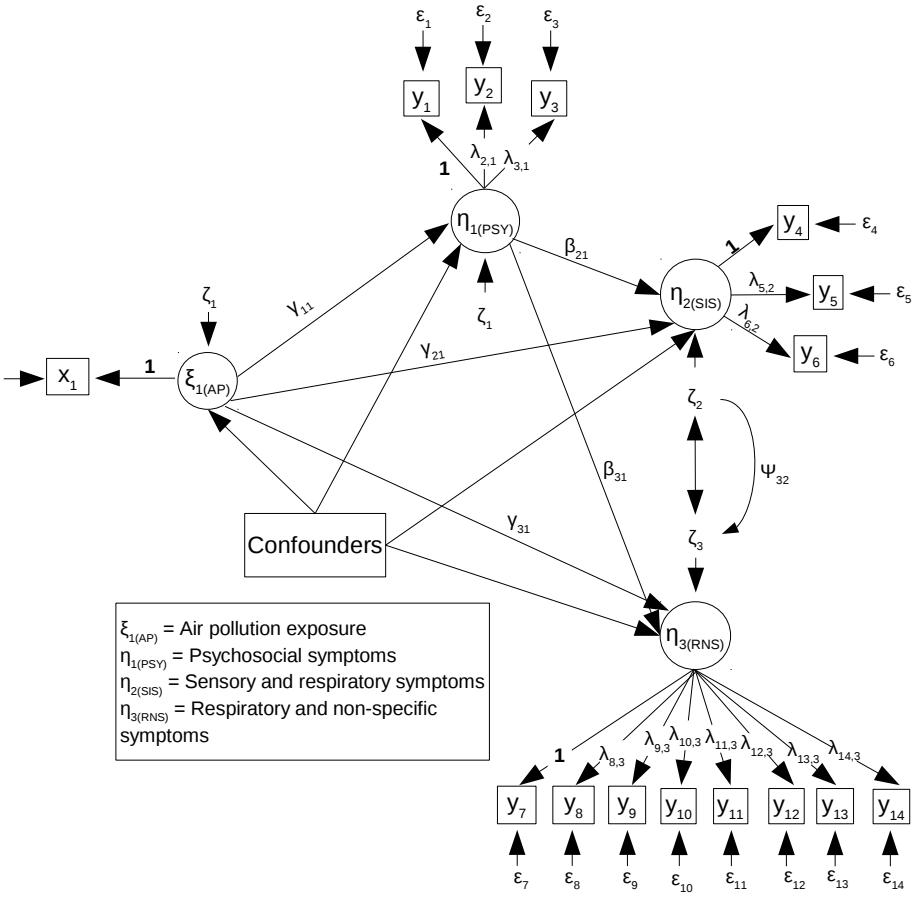

Figure 7.2: Path diagram for the mediation effect of AP through PSY - measured by odor annoyance, behavioral interference, and health risk perception - on SIS and RNS.

Table 7.4: Model fit for investigation of PSY, measured by three indicators.

Fit index	Value	Criterion status
$\chi^2(df)$	219.559 (167.000)	Failed (χ^2 should be equal to df.)
p-value (χ^2)	0.001	Failed (p value should not be significant at the 95% confidence level.)
CFI	0.981	Succeeded (Must be > 0.90.)
TLI	0.974	Succeeded (Must be > 0.90.)
RMSEA (CI)	0.026 (0.016 - 0.035)	Succeeded (Close fit is indicated by values < 0.05.)
PCLOSE	1.000	Yes (The p-value must be nonsignificant at the 95% confidence level.)
WRMR	0.705	Succeeded (Must be ≤ 1.0)

Table 7.5: Measurement structure: PSY measured by three indicators. (Estimation values in bold face represent fixed parameters.)

Latent variable	Indicator	Estimation	Standard error	p-value	Standardized estimation value
AP					
	NH_3 exposure	**1.000**	0.000		1.000
SIS					
	Eyes itching dryness or irritation	**1.000**	0.000		0.921
	Nose itching dryness or irritation	1.001	0.046	0.000	0.922
	Runny nose	0.893	0.051	0.000	0.822
RNS					
	Nausea	**1.000**	0.000		0.872
	Cough	0.925	0.071	0.000	0.806
	Chest wheezing or whistling	0.821	0.086	0.000	0.716
	Difficulty breathing	0.854	0.089	0.000	0.745
	Fatigue	1.008	0.065	0.000	0.878
	Headache	0.957	0.067	0.000	0.834
	Difficulty concentrating	1.034	0.071	0.000	0.901
	Dizziness	0.960	0.065	0.000	0.837
PSY					
	Odor annoyance	**1.000**	0.000		0.860
	Behavioral interference	0.986	0.131	0.000	0.848
	Health risk perception	1.055	0.169	0.000	0.908

stance, the direct effect of AP on both SIS and RNS were not statistical significant ($p = 0.596$ and $p = 0.177$, respectively). However, the model provides clearly statistical significance for the direct pathway linking PSY and RNS ($p = 0.001$). Furthermore, these results suggest full mediation of AP effect on RNS ($p = 0.001$), given the non significance of the partially mediated effect of AP on RNS ($p = 0.176$) (Table 7.6).

Table 7.6: Pathways for model represented by Fig. 7.2

Parameter (in Fig. 2)	Path	Estimation	Standard error	p-value	Standardized estimation value
γ_{21}	AP $\rightarrow$ SIS	-0.044	0.083	0.596	-0.048
γ_{31}	AP $\rightarrow$ RNS	-0.112	0.083	0.177	-0.128
γ_{11}	AP $\rightarrow$ PSY	0.430	0.058	0.000	0.499
β_{21}	PSY $\rightarrow$ SIS	0.465	0.146	0.001	0.435
β_{31}	PSY $\rightarrow$ RNS	0.451	0.133	0.001	0.445
$\gamma_{11} \times \beta_{21}$	AP $\rightarrow$ SIS (fully mediated)	0.200	0.062	0.001	0.217
$\gamma_{11} \times \beta_{31}$	AP $\rightarrow$ RNS (fully mediated)	0.194	0.056	0.001	0.222
$\gamma_{21} + (\gamma_{11} \times \beta_{21})$	AP $\rightarrow$ SIS (partially mediated)	0.156	0.053	0.003	0.169
$\gamma_{31} + (\gamma_{11} \times \beta_{31})$	AP $\rightarrow$ RNS (partially mediated)	0.082	0.060	0.176	0.094

7.4 Discussion

The aim of the present study was to evaluate interrelations between air pollution exposure and health symptoms in a low-to-moderate level of exposure to NH_3. Previously, these data were analyzed by means of adjusted logistic regression models, but due to the complex nature of the problem a re-analysis using structural equation modeling was needed. The present results weakly support the relationship of low-to-moderate air pollution exposure to adverse physical health symptoms through the psychosochial health symptoms.

In a cross sectional approach, SEM is successfully used for testing measurement, interrelations hypotheses, and functional analysis. Confirming previous expectations, the psychosocial health latent variable, PSY, measured by odor annoyance allowed to draw conclusions about the mediation role of the latent variable PSY . However, the measurement of PSY by addition of health risk perception and behavioral interference strengthened the confidence in the model. Considering previous studies in the topic, we believe that odor annoyance may be a predictor of risk perception and behavioral interference. Given the multivariate capabilities of SEM, it was confirmed that in low-to-moderate levels air pollution from biodegradable wastes does not directly

affect RNS and SIS. Traditional statistical techniques are somehow inflexible, given the assumption of measurements without errors. In this work, the latent variables were properly adjusted for confounders and their associated measurement error were estimated.

Structural equation modeling allowed researchers to successfully test hypotheses in many fields. In environmental health, SEM models framework are applied from investigation of health effects of prenatal mercury exposure to (192) the role of environmental smoking (193). In exposure to air pollutants, many works are related to urban pollution sources (194, 195, 196, 197, 198). One the one hand studies performed in such environments are important, on other hand exposure to environmental substances at high level have already a significant body of knowledge. At a non- toxic level of exposure, a few relevant works can be enumerated in the last years (90, 190, 199).

In a methodological sense, both works of Stelund et al. (199) and Claeson et al. (90) are similar to the one here presented. Both studies provide interesting findings about the role of psychosocial health symptoms in predicting environmentally induced health symptoms. However, they assume the categorization of exposure level (i.e., high, medium, low) based on the distance from the pollution source. Although this assumption gives good approximation of exposure, they lack chemical measurements to support it.

The present study has some limitations. First, the local air pollution exposure was evaluated by a proxy gas, NH_3, while the air pollution associated to biodegradable wastes is understood as a complex mixture of pollutants. Second, the direction of the effects in the proposed model must be carefully considered. For instance, the hypothesis that both latent variables SIS and RNS affect PSY should not be disregarded. Finally, some covariates were able to perfectly or *quasi*-perfectly predict desired outcomes.

In conclusion, the relationship between odorous pollution hold, even when adjusted for person- specific factors. Using SEM, the relationships among a high dimensional data set with dichotomous covariates were disentangled. Besides the theoretical purpose of understanding the pathways from air pollution exposure to health symptoms, we propose a new way to evaluate the psychosocial effects of exposure to NH_3 from biodegradable waste sites, given the latent variable PSY. We believe that further studies with a longitudinal design and bigger sample size may provide causal relation proves to the interrelations here presented. Besides the individual exposure assessment, one of the strengths of this work is to use SEM to build a complex information- processing model. A model able to congregate the sensory, physiological signals and psychological processes involved in perception, memory and self-assessment-reports (183).

Acknowledgments

This study was supported by the Department of Chemical Engineering, Biotechnology and Environmental Technology (University of Southern Denmark, Odense, Denmark) and the authors are thankful. The first author specially thanks Brazilian National Council for Scientific and Technological Development (CNPq) for his Science without Borders scholarship (200426/2014-1).

8
Conclusion and future perspective

Although very few reports on inhibition of IL-6 or IL-8 due to PM exposure, our findings clearly shown an inverse effect on the two cytokines. This finding is supported by other two studies (38, 131). Our findings suggest that the regulation of IL-6 and IL-8 expression is different between PM_{10} and $PM_{2.5}$. The mechanisms behind the secretion of IL-6 and IL-8 by the fine particulate remains unknown, but this study provides evidence that this inhibition cannot be ascribable to metals. Based on previous studies (38, 123), high polar organic content is proposed as a cause for the suppresion of the IL-6 and IL-8 responses in BEAS-2B cells. This toxicological data reinforces the challenges to determine the organic composition of the $PM_{2.5}$.

With regard to the bioaccumulation of trace elements associated with PM in white shrimps, we believe that this pilot experiment could be tested for a longer exposure time to a sharp definiton of the accumulated levels in the organs and biochemical measurements. Despite of the low levels of some elements, they are toxic through chronic exposure.

In the context of urban-coastal areas under strong industrialization, the use of CBPF to investigate sources for criteria pollutants (NO_2, SO_2, O_3, and $PM_{2.5}$) was insightful, but it could have been even more powerful, if there were hourly measurements of PM in the region. In spite of that, sources associated to industrial emission were detected at the concentration percentile range of 0.54 to 5.8 μg m^{-3}. The combination of CIT and RF pointed out that NO_3^- and Ca^{+2} were the most important predictors for $PM_{2.5}$. The high median contribution of nss-Ca^{2+} (96 %) in the region suggests a strong influence of anthropogenic sources.

Using the R package openair, the use of CBPF and k-means clustering disentangled the importance of natural sources in two Atlantic Rain Forest hotspots in the surroundings of Rio de Janeiro. Besides that, the combination of CIT and RF estimate that the main predictors for TSP were NO_3^- > Mn > Rad (Global radiation) > Ca^{2+} > Precipitation > Mg^{2+}. For PM_{10}, the main predictors were Gust (Gust wind speed) > NO_3^- > Ca^{2+} > Zn > Cu > Ti. Further studies should benefit from the direct comparison of the importance of $PM_{2.5}$ in the coarse mode, since NO_3^- and Ca^{2+} are common main predictors

for TSP, PM_{10}, and $PM_{2.5}$ mass concentration in the MRRJ.

In conclusion, the analysis of the multiple health symptoms associated to the exposure to low-to-moderate NH_3 levels from biodegradable provided an objectively way to prove the importance of the environmental health question. Although the sample size was not large enough to test more hypotheses, it provided two models that confirm previsou individual findings and congregate the sensory, physiological signals and psychological processes involved in perception, memory and self-assessment-reports (183). Most certainly, this model is applicable to other contexts and not only to the six Danish regions studied, as long as there is an objectively measured pollutant.

References

[1] PÖSCHL, U.. **Atmospheric aerosols: composition, transformation, climate and health effects.** Angewandte Chemie (International ed. in English), 44(46):7520–40, nov 2005.

[2] DESPRÉS, V. R.; ALEX HUFFMAN, J.; BURROWS, S. M.; HOOSE, C.; SAFATOV, A. S.; BURYAK, G.; FRÖHLICH-NOWOISKY, J.; ELBERT, W.; ANDREAE, M. O.; PÖSCHL, U. ; JAENICKE, R.. **Primary biological aerosol particles in the atmosphere: a review**. Tellus B, 64, feb 2012.

[3] COLBECK, I.; LAZARIDIS, M.. **Aerosols and environmental pollution.** Die Naturwissenschaften, 97(2):117–31, feb 2010.

[4] KIM, K., KABIR, E., KABIR, S.. **A review on the human health impact of airborne particulate matter**. Environment International, 74:136–143, 2015.

[5] RIBEIRO, J. D. P.; KALB, A. C.; CAMPOS, P. P.; CRUZ, A. R. H. D. L.; MARTINEZ, P. E.; GIODA, A.; DE SOUZA, M. M. ; GIODA, C. R.. **Toxicological effects of particulate matter (PM2.5) on rats: Bioaccumulation, antioxidant alterations, lipid damage, and ABC transporter activity**. Chemosphere, 163:569–577, nov 2016.

[6] GRIFFIN, R. J.. **The Sources and Impacts of Tropospheric Particulate Matter**. Nature Education Knowledge, 1(4(5)), 2013.

[7] DELFINO, R. J.; SIOUTAS, C. ; MALIK, S.. **Potential Role of Ultrafine Particles in Associations between Airborne Particle Mass and Cardiovascular Health**. Environmental Health Perspectives, 113(8):934–946, mar 2005.

[8] MAUDERLY, J. L.; CHOW, J. C.. **Health effects of organic aerosols.** Inhalation toxicology, 20(3):257–88, feb 2008.

[9] SALTINI, C.; AMICOSANTE, M.; FRANCHI, A.; LOMBARDI, G. ; RICHELDI, L.. **Immunogenetic basis of environmental lung disease: lessons from the berylliosis model**. European Respiratory Journal, 12(6):1463–1475, dec 1998.

[10] GIODA, A.; AMARAL, B. S.; MONTEIRO, I. L. G. ; SAINT'PIERRE, T. D.. **Chemical composition, sources, solubility, and transport of aerosol trace elements in a tropical region.** Journal of environmental monitoring : JEM, 13(8):2134–42, aug 2011.

[11] GIODA, A.; FUENTES-MATTEI, E. ; JIMENEZ-VELEZ, B.. **Evaluation of cytokine expression in BEAS cells exposed to fine particulate matter (PM2.5) from specialized indoor environments.** International journal of environmental health research, 21(2):106–19, apr 2011.

[12] PUNTARULO, S.. **Iron, oxidative stress and human health.** Molecular aspects of medicine, 26(4-5):299–312, 2005.

[13] KOIVULA, M. J.; EEVA, T.. **Metal-related oxidative stress in birds.** Environmental pollution (Barking, Essex : 1987), 158(7):2359–70, jul 2010.

[14] KELLY, F. J.; FUSSELL, J. C.. **Size, source and chemical composition as determinants of toxicity attributable to ambient particulate matter**. Atmospheric Environment, 60:504–526, dec 2012.

[15] FORTOUL, T.; RODRIGUEZ-LARA, V.; GONZÁLEZ-VILLALVA, A.; ROJAS-LEMUS, M.; CANO-GUTIÉRREZ, G.; USTARROZ-CANO, M.; COLÍN-BARENQUE, L.; BIZARRO-NEVARES, P.; GARCÍA-PEALEZ, I.; MONTAÑO, L.; JIMENEZ-MARTINEZ, R.; LOPEZ-VALDEZ, N.; RUIZ-GUERRERO, M.; MELÉNDEZ-GARCÍA, N.; GARCÍA-IBARRA, F.; MARTÍNEZ-BAEZ, V.; ALFARO, D. Z.; MUÑIZ-RIVERA-CAMBAS, A.; LÓPEZ-ZEPEDA, L.; QUEZADA-MALDONADO, E. ; CERVANTES-YÉPEZ, S.. **Inhalation of vanadium pentoxide and its toxic effects in a mouse model**. Inorganica Chimica Acta, 420:8–15, aug 2014.

[16] VAN HEERDEN, D.; VOSLOO, A. ; NIKINMAA, M.. **Effects of short-term copper exposure on gill structure, metallothionein and hypoxia-inducible factor-1alpha (HIF-1alpha) levels in rainbow trout (Oncorhynchus mykiss).** Aquatic toxicology (Amsterdam, Netherlands), 69(3):271–80, aug 2004.

[17] RODRÍGUEZ DE LA RUA, A.; ARELLANO, J. M.; GONZÁLEZ DE CANALES, M. L.; BLASCO, J. ; SARASQUETE, C.. **Accumulation of copper and histopathological alterations in the oyster Crassostrea angulata**. Ciencias Marinas, 31(3):455–466, 2005.

[18] FRÍAS-ESPERICUETA, M. G.; ABAD-ROSALES, S.; NEVÁREZ-VELÁZQUEZ, A. C.; OSUNA-LÓPEZ, I.; PÁEZ-OSUNA, F.; LOZANO-

OLVERA, R. ; VOLTOLINA, D.. **Histological effects of a combination of heavy metals on Pacific white shrimp Litopenaeus vannamei juveniles.** Aquatic toxicology (Amsterdam, Netherlands), 89(3):152–7, sep 2008.

[19] VENTURA-LIMA, J.; FATTORINI, D.; REGOLI, F. ; MONSERRAT, J. M.. **Effects of different inorganic arsenic species in Cyprinus carpio (Cyprinidae) tissues after short-time exposure: bioaccumulation, biotransformation and biological responses.** Environmental pollution (Barking, Essex : 1987), 157(12):3479–84, dec 2009.

[20] YANG, Z.-B.; ZHAO, Y.-L.; LI, N. ; YANG, J.. **Effect of waterborne copper on the microstructures of gill and hepatopancreas in Eriocheir sinensis and its induction of metallothionein synthesis.** Archives of environmental contamination and toxicology, 52(2):222–8, feb 2007.

[21] LI, N.; ZHAO, Y. ; YANG, J.. **Impact of waterborne copper on the structure of gills and hepatopancreas and its impact on the content of metallothionein in juvenile giant freshwater prawn Macrobrachium rosenbergii (Crustacea: Decapoda).** Archives of environmental contamination and toxicology, 52(1):73–9, jan 2007.

[22] VIANA, M.; KUHLBUSCH, T.; QUEROL, X.; ALASTUEY, A.; HARRISON, R.; HOPKE, P.; WINIWARTER, W.; VALLIUS, M.; SZIDAT, S.; PRÉVÔT, A.; HUEGLIN, C.; BLOEMEN, H.; WÅHLIN, P.; VECCHI, R.; MIRANDA, A.; KASPER-GIEBL, A.; MAENHAUT, W. ; HITZENBERGER, R.. **Source apportionment of particulate matter in Europe: A review of methods and results**. Journal of Aerosol Science, 39(10):827–849, oct 2008.

[23] HOPKE, P. K.. **It is time to drop principal components analysis as a "receptor model"**. Journal of Atmospheric Chemistry, 72(2):127–128, jun 2015.

[24] ZHANG, R.; WANG, G.; GUO, S.; ZAMORA, M. L.; YING, Q.; LIN, Y.; WANG, W.; HU, M. ; WANG, Y.. **Formation of urban fine particulate matter.** Chemical reviews, 115(10):3803–55, may 2015.

[25] YEGANEH, B.; MOTLAGH, M. S. P.; RASHIDI, Y. ; KAMALAN, H.. **Prediction of CO concentrations based on a hybrid Partial Least Square and Support Vector Machine model**. Atmospheric Environment, 55:357–365, aug 2012.

[26] HU, Y.; CHENG, H.. **Application of Stochastic Models in Identification and Apportionment of Heavy Metal Pollution Sources in the Surface Soils of a Large-Scale Region**. Environmental Science & Technology, 47(8):3752–3760, apr 2013.

[27] PANDEY, G.; ZHANG, B. ; JIAN, L.. **Predicting submicron air pollution indicators: a machine learning approach**. Environmental Science: Processes & Impacts, 15(5):996, 2013.

[28] LUNA, A.; PAREDES, M.; DE OLIVEIRA, G. ; CORRÊA, S.. **Prediction of ozone concentration in tropospheric levels using artificial neural networks and support vector machine at Rio de Janeiro, Brazil**. Atmospheric Environment, 98:98–104, dec 2014.

[29] BLANES-VIDAL, V.; HANSEN, M.; ADAMSEN, A.; FEILBERG, A.; PETERSEN, S. ; JENSEN, B.. **Characterization of odor released during handling of swine slurry: Part I. Relationship between odorants and perceived odor concentrations**. Atmospheric Environment, 43(18):2997–3005, jun 2009.

[30] WHO. **WHO definition of Health**. Preamble to the constitution of the world health organization as adopted by the international health conference, New York, NY, 19 June– 22 July 1946; signed on 22 July 1946 by the representatives of 61 states (Official Records of the World Health Organization), 1946.

[31] NRC. **Biosolids applied to land: Advancing standards and practives**. Número July. National Academy of Sciences, Washington, DC, 2002. URL: https://goo.gl/VUlmjd (accessed on sep 01, 2015).

[32] CAIN, W. S.; COMETTO-MUÑIZ, J. E.. **Identifying and controlling odor in the municipal wastewater environment: Health effects of biosolids odors: A literature review and analysis**. WERF, Alexandria, VA, 2004.

[33] BLANES-VIDAL, V.; BÆLUM, J.; NADIMI, E. S.; LØFSTRØM, P. ; CHRISTENSEN, L. P.. **Chronic exposure to odorous chemicals in residential areas and effects on human psychosocial health: dose-response relationships.** The Science of the total environment, 490:545–54, aug 2014.

[34] BLANES-VIDAL, V.; BÆLUM, J.; SCHWARTZ, J.; LØFSTRØM, P. ; CHRISTENSEN, L. P.. **Respiratory and sensory irritation symp-**

toms among residents exposed to low-to-moderate air pollution from biodegradable wastes. Journal of exposure science & environmental epidemiology, 24(4):388–97, jul 2014.

[35] BLANES-VIDAL, V.. **Air pollution from biodegradable wastes and non-specific health symptoms among residents: Direct or annoyance-mediated associations?** Chemosphere, 120C:371–377, sep 2015.

[36] MATEUS, V. L.; MONTEIRO, I. L. G.; ROCHA, R. C. C.; SAINT'PIERRE, T. D. ; GIODA, A.. **Study of the chemical composition of particulate matter from the Rio de Janeiro metropolitan region, Brazil, by inductively coupled plasma-mass spectrometry and optical emission spectrometry**. Spectrochimica Acta Part B: Atomic Spectroscopy, 86(0):131–136, 2013.

[37] RODRÍGUEZ-COTTO, R. I.; ORTIZ-MARTÍNEZ, M. G.; RIVERA-RAMÍREZ, E.; MÉNDEZ, L. B.; DÁVILA, J. C. ; JIMÉNEZ-VÉLEZ, B. D.. **African Dust Storms Reaching Puerto Rican Coast Stimulate the Secretion of IL-6 and IL-8 and Cause Cytotoxicity to Human Bronchial Epithelial Cells (BEAS-2B)**. Health, 05(10):14–28, 2013.

[38] FUENTES-MATTEI, E.; RIVERA, E.; GIODA, A.; SANCHEZ-RIVERA, D.; ROMAN-VELAZQUEZ, F. R. ; JIMENEZ-VELEZ, B. D.. **Use of human bronchial epithelial cells (BEAS-2B) to study immunological markers resulting from exposure to PM2.5 organic extract from Puerto Rico**. Toxicology and Applied Pharmacology, 243(3):381–389, mar 2010.

[39] ARAÚJO, F. G.; DA CRUZ-FILHO, A. G.; DE AZEVEDO, M. C. C. ; SANTOS, A. C. D. A.. **Estrutura da comunidade de peixes demersais da Baía de Sepetiba, RJ**. Revista Brasileira de Biologia, 58(3):417–430, 1998.

[40] LACERDA, L. D.; MARINS, R. V.; MOUNIER, S.; BENAIM, J. ; FEVRIER, D.. **Mercury Distribution and Reactivity in Waters of a Subtropical Coastal Lagoon, Sepetiba Bay, SE Brazil**. Journal of the Brazilian Chemical Society, 12(1):93–98, 2001.

[41] QUITERIO, S. L.; SOUSA DA SILVA, C. R.; ARBILLA, G. ; ESCALEIRA, V.. **Metals in airborne particulate matter in the industrial district**

of Santa Cruz, Rio de Janeiro, in an annual period. Atmospheric Environment, 38(2):321–331, jan 2004.

[42] INEA. **Relatório da qualidade do ar do estado do Rio de Janeiro-Ano Base 2013**. Technical report, Instituto Estadual do Ambiente (Document in Portuguese), Rio de Janeiro, 2015. URL: https://goo.gl/JxxkQK (accessed on may 19, 2016).

[43] INEA. **Relatório da Qualidade do Ar do Estado do Rio de Janeiro - Anos Base 2010 e 2011**. Technical report, Instituto Estadual do Ambiente (Document in Portuguese), Rio de Janeiro, 2013. URL: https://goo.gl/tOUa8R (accessed on jun 11, 2014).

[44] USEPA. **Method IO-3.1, Selection, preparation and extraction of filter Material.** Technical report, US EPA, Washington DC, 1999. URL: https://goo.gl/Bxtdcg (accessed on mar 29, 2016).

[45] R CORE TEAM. **R: A language and environment for statistical computing**, 2016. URL: https://www.r-project.org/ [versions 3.2.5, 3.3.1 and 3.3.2].

[46] BOLKS, A.; DEWIRE, A. ; HARCUM, J.. **Baseline Assessment of Left-Censored Environmental Data Using R**. Technical Report June, Developed for U.S. Environmental Protection Agency by Tetra Tech, Inc., Fairfax, VA, 2014. URL: https://goo.gl/wmXTA5 (accessed on jun 19, 2015).

[47] PALAREA-ALBALADEJO, J.; MARTÍN-FERNÁNDEZ, J. A.. **zCompositions — R package for multivariate imputation of left-censored data under a compositional approach**. Chemometrics and Intelligent Laboratory Systems, 143(0):85–96, 2015.

[48] PALAREA-ALBALADEJO, J.; MARTÍN-FERNÁNDEZ, J. A.. **Values below detection limit in compositional chemical data.** Analytica chimica acta, 764:32–43, mar 2013.

[49] AGOSTINELLI, C.; LUND, U.. **R package circular: Circular Statistics (version 0.4-7)**. CA: Department of Environmental Sciences, Informatics and Statistics, Ca' Foscari University, Venice, Italy. UL: Department of Statistics, California Polytechnic State University, San Luis Obispo, California, USA, 2013. URL: https://goo.gl/cBb8a6 (accessed on sep 05, 2016).

[50] GODOY, M. L. D.; GODOY, J. M.; ROLDÃO, L. A.; SOLURI, D. S. ; DONAGEMMA, R. A.. **Coarse and fine aerosol source apportionment in**

Rio de Janeiro, Brazil. Atmospheric Environment, 43(14):2366–2374, may 2009.

[51] HOTHORN, T.; HORNIK, K. ; ZEILEIS, A.. **Unbiased Recursive Partitioning: A Conditional Inference Framework**. Journal of Computational and Graphical Statistics, 15(3):651–674, sep 2006.

[52] STROBL, C.; BOULESTEIX, A.-L.; KNEIB, T.; AUGUSTIN, T. ; ZEILEIS, A.. **Conditional Variable Importance for Random Forests**. BMC Bioinformatics, 9(1):307, 2008.

[53] BREIMAN, L.. **Random Forests**. Machine Learning, 45(1):5–32, 2001.

[54] STROBL, C.; BOULESTEIX, A.-L.; ZEILEIS, A. ; HOTHORN, T.. **Bias in random forest variable importance measures: Illustrations, sources and a solution**. BMC Bioinformatics, 8(1):25, 2007.

[55] HOTHORN, T.; BUHLMANN, P.; DUDOIT, S.; MOLINARO, A. ; LAAN, M. J. V. D.. **Survival ensembles**. Biostatistics, 7(3):355–373, dec 2005.

[56] ASHBAUGH, L. L.; MALM, W. C. ; SADEH, W. Z.. **A residence time probability analysis of sulfur concentrations at grand Canyon National Park**. Atmospheric Environment (1967), 19(8):1263–1270, jan 1985.

[57] URIA-TELLAETXE, I.; CARSLAW, D. C.. **Conditional bivariate probability function for source identification**. Environmental Modelling & Software, 59:1–9, sep 2014.

[58] CARSLAW, D.. **The openair manual open-source tools for analysing air pollution data**. King's College London, (January):287, 2015.

[59] CARSLAW, D. C.; BEEVERS, S. D.. **Characterising and understanding emission sources using bivariate polar plots and k-means clustering**. Environmental Modelling & Software, 40:325–329, feb 2013.

[60] CARSLAW, D.; BEEVERS, S.; ROPKINS, K. ; BELL, M.. **Detecting and quantifying aircraft and other on-airport contributions to ambient nitrogen oxides in the vicinity of a large international airport**. Atmospheric Environment, 40(28):5424–5434, sep 2006.

[61] THEIL, H.. **A rank invariant method of linear and polynomial regression analysis, I, II, III**. In: PROCEEDINGS OF THE KONINKLIJKE NEDERLANDSE AKADEMIEWETENSCHAPPEN, SERIES A – MATHEMATICAL SCIENCES, 1950.

[62] SEN, P. K.. **Estimates of the Regression Coefficient Based on Kendall's Tau**. Journal of the American Statistical Association, 63(324):1379–1389, dec 1968.

[63] HASTIE, T.; TIBSHIRANI, R.. **Generalized Additive Models**. Chapman and Hall, London, 1990.

[64] ICMBIO. **Instituto Chico Mendes de Conservação da Biodiversidade - Flona Mario Xavier**. URL: https://goo.gl/kbRj5R (accessed on dec 09, 2013).

[65] ICMBIO. **Instituto Chico Mendes de Conservação da Biodiversidade - Parna da Serra dos Orgãos**. URL: https://goo.gl/kbRj5R (accessed on dec 09, 2013).

[66] RODRIGUES, R. D. A. R.; MELLO, W. Z. D. ; SOUZA, P. A. D.. **Aporte atmosférico de amônio, nitrato e sulfato em área de floresta ombrófila densa montana na Serra dos Órgãos, RJ**. Química Nova, 30(8):1842–1848, 2007.

[67] GRANGE, S. K.. **Technical note: Averaging wind speeds and directions**. Technical Report October, University of Auckland, Auckland, New Zealand, 2014. URL: https://goo.gl/1JVPu8 (accessed on jan 24, 2017).

[68] SUZUKI, R.; SHIMODAIRA, H.. **Pvclust: an R package for assessing the uncertainty in hierarchical clustering**. Bioinformatics, 22(12):1540–1542, jun 2006.

[69] EFRON, B.; HALLORAN, E. ; HOLMES, S.. **Bootstrap confidence levels for phylogenetic trees. TL - 93**. Proceedings of the National Academy of Sciences of the United States of America, 93 VN - r(23):13429–13434, 1996.

[70] SUZUKI, R.; SHIMODAIRA, H.. **An application of multiscale bootstrap resampling to hierarchical clustering of microarray data: How accurate are these clusters**. In: FIFTEENTH INTERNATIONAL CONFERENCE ON GENOME INFORMATICS, p. P034, 2004. URL: https://goo.gl/p51ZKE (accessed on apr, 2017).

[71] SHIMODAIRA, H.. **An Approximately Unbiased Test of Phylogenetic Tree Selection**. Systematic Biology, 51(3):492–508, may 2002.

[72] BRAUER, C.; MIKKELSEN S. ; SKOV, P.. **Reliability and validity of a new questionnaire for investigation of symptoms related to "The Sick Building Syndrome" and perceived Indoor Air Quality [document in Danish, Report, own print]**. Technical report, Department of Occupational Medicine, Copenhagen University Hospital, Glostrup, Denmark, 2000.

[73] SCHIFFMAN, S. S.; WILLIAMS, C. M.. **Science of odor as a potential health issue.** Journal of environmental quality, 34(1):129–38, jan 2005.

[74] SCHIFFMAN, S. S.; WALKER, J. M.; DALTON, P.; LORIG, T. S.; RAYMER, J. H.; SHUSTERMAN, D. ; WILLIAMS, C. M.. **Potential Health Effects of Odor from Animal Operations, Wastewater Treatment, and Recycling of Byproducts**. Journal of Agromedicine, 7(1):7–81, dec 2000.

[75] BLANES-VIDAL, V.; NADIMI, E. S.; ELLERMANN, T.; ANDERSEN, H. V. ; LØFSTRØM, P.. **Perceived annoyance from environmental odors and association with atmospheric ammonia levels in non-urban residential communities: a cross-sectional study.** Environmental health : a global access science source, 11(1):27, jan 2012.

[76] GEELS, C.; ANDERSEN, H. V.; AMBELAS SKJØTH, C.; CHRISTENSEN, J. H.; ELLERMANN, T.; LØFSTRØM, P.; GYLDENKÆRNE, S.; BRANDT, J.; HANSEN, K. M.; FROHN, L. M. ; HERTEL, O.. **Improved modelling of atmospheric ammonia over Denmark using the coupled modelling system DAMOS**. Biogeosciences, 9(7):2625–2647, jul 2012.

[77] MUKHTAR, S.; ULLMAN, J. L.; CAREY, J. B. ; LACEY, R. E.. **A Review of Literature Concerning Odors, Ammonia, and Dust from Broiler Production Facilities: 3. Land Application, Processing, and Storage of Broiler Litter**. The Journal of Applied Poultry Research, 13(3):514–520, sep 2004.

[78] REVELLE, W.. **psych: Procedures for Psychological, Psychometric, and Personality Research [version 1.5.1]**. Northwestern University, Evanston, Illinois, 2015.

[79] ROSSEEL, Y.. **lavaan : An R Package for Structural Equation**. Journal of Statistical Software, 48(2):1–36, 2012.

[80] MUTHÉN, B.. **Latent variable structural equation modeling with categorical data**. Journal of Econometrics, 22(1-2):43–65, may 1983.

[81] MUTHÉN, B.. **A general structural equation model with ordered categorical and continuous latent variable indicators**. Technical report, Department of Psychology, University of California, Los Angeles, CA, 1981.

[82] ARMINGER, G.; SCHOENBERG, R. J.. **Pseudo maximum likelihood estimation and a test for misspecification in mean and covariance structure models**. Psychometrika, 54(3):409–425, sep 1989.

[83] MUTHÉN, B.. **A general structural equation model with dichotomous, ordered categorical, and continuous latent variable indicators**. Psychometrika, 49(1):115–132, mar 1984.

[84] MUTHÉN, B.; DU TOIT, S. H. C. ; SPISIC, D.. **Robust inference using weighted least squares and quadratic estimating equations in latent variable modeling with categorical and continous outcome**. Psychometrika, 1997.

[85] MUTHÉN, L.; MUTHÉN, B.. **MPlus. The Comprehensive Modeling Program for Applied Researchers. User's Guide**, 1998.

[86] WANG, J.; WANG, X.. **Structural equation modeling: application using Mplus**, volumen 1. John Wiley & Sons, Ltd., 2012.

[87] BENTLER, P. M.. **Comparative fit indexes in structural models.** Psychological Bulletin, 107(2):238–246, 1990.

[88] TUCKER, L. R.; LEWIS, C.. **A reliability coefficient for maximum likelihood factor analysis**. Psychometrika, 38(1):1–10, mar 1973.

[89] MACCALLUM, R. C.; BROWNE, M. W. ; SUGAWARA, H. M.. **Power analysis and determination of sample size for covariance structure modeling.** Psychological Methods, 1(2):130–149, 1996.

[90] CLAESON, A.-S.; LIDÉN, E.; NORDIN, M. ; NORDIN, S.. **The role of perceived pollution and health risk perception in annoyance and health symptoms: a population-based study of odorous air pollution.** International archives of occupational and environmental health, 86(3):367–74, apr 2013.

[91] YU, C.. **Evaluating cutoff criteria of model fit indices for latent variable models with binary and continuous outcomes**. Unpublished doctoral dissertation, University of California, 2002. URL: https://goo.gl/O18AO1 (accessed on sep 14, 2015).

[92] R CORE TEAM. **R: A Language and Environment for Statistical Computing**, 2015. URL: https://www.r-project.org/ [version 3.2.1].

[93] SOBEL, M. E.. **Asymptotic Confidence Intervals for Indirect Effects in Structural Equation Models**. Sociological Methodology, 13:pp. 290–312, 1982.

[94] USEPA. **Particulate Matter (PM) Standards, Table of Historical PM NAAQS, History of the National Ambient Air Quality Standards for Particulate Matter during the Period 1971-2012**, 2016. URL: https://goo.gl/lsJzfa (accessed on may 04, 2016).

[95] ESWORTHY, R.. **Air Quality: EPA's 2013 Changes to the Particulate Matter (PM) Standard**. Technical report, Congressional Research Service, 2013. [CRS Report for Congress] URL: https://goo.gl/fW6ZxG (accessed on apr 9, 2017).

[96] KRZYZANOWSKI, M.; COHEN, A.. **Update of WHO air quality guidelines**. Air Quality, Atmosphere & Health, 1(1):7–13, may 2008.

[97] THORSTEINSSON, T.; JÓHANNSSON, T.; STOHL, A. ; KRISTIANSEN, N. I.. **High levels of particulate matter in Iceland due to direct ash emissions by the Eyjafjallajökull eruption and resuspension of deposited ash**. Journal of Geophysical Research: Solid Earth, 117(B9), sep 2012.

[98] MOORE, K. R.; DUFFELL, H.; NICHOLL, A. ; SEARL, A.. **Monitoring of airborne particulate matter during the eruption of Soufrière Hills Volcano, Montserrat**. Geological Society, London, Memoirs, 21(1):557–566, 2002.

[99] SMITH, D. B.; ZIELINSKI, R. A.; ROSE, W. I. ; HUEBERT, B. J.. **Water-soluble material on aerosols collected within volcanic eruption clouds**. Journal of Geophysical Research, 87(C7):4963, 1982.

[100] BOND, T. C.; BHARDWAJ, E.; DONG, R.; JOGANI, R.; JUNG, S.; RODEN, C.; STREETS, D. G. ; TRAUTMANN, N. M.. **Historical emissions**

of black and organic carbon aerosol from energy-related combustion, 1850-2000. Global Biogeochemical Cycles, 21(2):n/a–n/a, jun 2007.

[101] LIN, C. A.; MARTINS, M. A.; FARHAT, S. C.; POPE, C. A.; CONCEIÇÃO, G. M.; ANASTÁCIO, V. M.; HATANAKA, M.; ANDRADE, W. C.; HAMAUE, W. R.; BÖHM, G. M. ; SALDIVA, P. H.. **Air pollution and respiratory illness of children in São Paulo, Brazil.** Paediatric and perinatal epidemiology, 13(4):475–88, oct 1999.

[102] CONCEIÇÃO, G. M.; MIRAGLIA, S. G.; KISHI, H. S.; SALDIVA, P. H. ; SINGER, J. M.. **Air pollution and child mortality: a time-series study in São Paulo, Brazil.** Environmental health perspectives, 109 Suppl:347–50, jun 2001.

[103] RIVERO, D. H. R. F.; SOARES, S. R. C.; LORENZI-FILHO, G.; SAIKI, M.; GODLESKI, J. J.; ANTONANGELO, L.; DOLHNIKOFF, M. ; SALDIVA, P. H. N.. **Acute Cardiopulmonary Alterations Induced by Fine Particulate Matter of Sao Paulo, Brazil**. Toxicological Sciences, 85(2):898–905, feb 2005.

[104] IGNOTTI, E.; VALENTE, J. G.; LONGO, K. M.; FREITAS, S. R.; HACON, S. D. S. ; ARTAXO NETTO, P.. **Impact on human health of particulate matter emitted from burnings in the Brazilian Amazon region**. Revista de Saúde Pública, 44(1):121–130, feb 2010.

[105] SÉRGIO CHIARELLI, P.; AMADOR PEREIRA, L. A.; DO NASCIMENTO SALDIVA, P. H.; FERREIRA FILHO, C.; BUENO GARCIA, M. L.; FERREIRA BRAGA, A. L. ; CONCEIÇÃO MARTINS, L.. **The association between air pollution and blood pressure in traffic controllers in Santo André, São Paulo, Brazil**. Environmental Research, 111(5):650–655, jul 2011.

[106] NASCIMENTO, L. F. C.; FRANCISCO, J. B.. **Particulate matter and hospital admission due to arterial hypertension in a medium-sized Brazilian city**. Cadernos de Saúde Pública, 29(8):1565–1571, aug 2013.

[107] DONALDSON, K.; TRAN, C. L.. **Inflammation caused by particles and fibers**. Inhalation Toxicology, 14(1):5–27, jan 2002.

[108] **Fideicomiso para el mejoramiento de las vias de comunicacion del Distrito Federal, Ciudad de Mexico**, 2013. URL: https://goo.gl/A6cKeo (accessed on nov, 2013).

[109] UNIVERSIA. **Demasiados vehículos circulan en el DF**, 2013. URL: https://goo.gl/MUT2uq (accessed on nov, 2013).

[110] HOINASKI, L.; FRANCO, D.; STUETZ, R. M.; SIVRET, E. C. ; DE MELO LISBOA, H.. **Investigation of PM 10 sources in Santa Catarina, Brazil through graphical interpretation analysis combined with receptor modelling**. Environmental Technology, 34(17):2453–2463, sep 2013.

[111] LOYOLA, J.; ARBILLA, G.; QUITERIO, S. L.; ESCALEIRA, V. ; MINHO, A. S.. **Trace Metals in the Urban Aerosols of Rio de Janeiro City**. Journal of the Brazilian Chemical Society, 23(4):628–638, 2012.

[112] PAULINO, S. A.; QUITERIO, S. L.; ESCALEIRA, V. ; ARBILLA, G.. **Evolution of particulate matter and associated metal levels in the urban area of Rio de Janeiro, Brazil.** Bulletin of environmental contamination and toxicology, 84(3):315–8, mar 2010.

[113] QUITERIO, S. L.; ESCALEIRA, V.; SOUSA, C. R. S.; MAIA, L. F. P. G. ; ARBILLA, G.. **Metals in Airborne Particulate Matter in Downtown Rio de Janeiro, Brazil**. Bulletin of Environmental Contamination and Toxicology, 72(5):916–922, may 2004.

[114] GOUVEIA, N.; MENDONÇA, G. A. E. S.; DE LEON, A. P.; CORREIA, J. E. D. M.; JUNGER, W. L.; DE FREITAS, C. U.; DAUMAS, R. P.; MARTINS, L. C.; GIUSSEPE, L.; CONCEIÇÃO, G. M.; MANERICH, A. ; CUNHA-CRUZ, J.. **Poluição do ar e efeitos na saúde nas populações de duas grandes metropóles brasileiras**. Epidemiologia e Serviços de Saúde, 12(1):29–40, mar 2003.

[115] JUNGER, W. L.; LEON, A. P. D. ; MENDONÇA, G. A. E. S.. **Associação entre mortalidade diária por câncer de pulmão e poluição do ar no município do Rio de Janeiro: um estudo ecológico de séries temporais**. Revista Brasileira de Cancerologia, 51(2):111–115, 2001.

[116] DE CASTRO, H. A.; DA CUNHA, M. F.; MENDONÇA, G. A. E. S.; JUNGER, W. L.; CUNHA-CRUZ, J. ; DE LEON, A. P.. **Efeitos da poluição do ar na função respiratória de escolares, Rio de Janeiro, RJ**. Revista de Saúde Pública, 43(1):26–34, feb 2009.

[117] MOURA, M.; JUNGER, W. L.; MENDONÇA, G. A. E. S. ; DE LEON, A. P.. **Air quality and emergency pediatric care for symptoms**

of bronchial obstruction categorized by age bracket in Rio de Janeiro, Brazil. Cadernos de Saúde Pública, 25(3):635–644, mar 2009.

[118] RAMOS DE RAINHO, C.; MACHADO CORRÊA, S.; LUIZ MAZZEI, J.; ALESSANDRA FORTES AIUB, C. ; FELZENSZWALB, I.. **Genotoxicity of Polycyclic Aromatic Hydrocarbons and Nitro-Derived in Respirable Airborne Particulate Matter Collected from Urban Areas of Rio de Janeiro (Brazil)**. BioMed Research International, 2013:1–9, 2013.

[119] ALFARO-MORENO, E.; TORRES, V.; MIRANDA, J.; MARTÍNEZ, L.; GARCÍA-CUELLAR, C.; NAWROT, T. S.; VANAUDENAERDE, B.; HOET, P.; RAMÍREZ-LÓPEZ, P.; ROSAS, I.; NEMERY, B. ; OSORNIO-VARGAS, A. R.. **Induction of IL-6 and inhibition of IL-8 secretion in the human airway cell line Calu-3 by urban particulate matter collected with a modified method of PM sampling**. Environmental Research, 109(5):528–535, 2009.

[120] HIRAIWA, K.; VAN EEDEN, S. F.. **Contribution of Lung Macrophages to the Inflammatory Responses Induced by Exposure to Air Pollutants**. Mediators of Inflammation, 2013:1–10, 2013.

[121] ORTIZ-MARTÍNEZ, M., RIVERA-RAMÍREZ, E., MÉNDEZ-TORRES, L., JIMÉNEZ-VÉLEZ, B.. **Role of chemical and biological constituents of PM10 from Saharan Dust in the exacerbation of asthma in Puerto Rico**. In: Theophanides, M.; Theophanides, T., editors, BIODIVERSITY SCIENCE FOR HUMANITY, número 300, p. 101–118. Athens Institute for Education and Research (ATINER), 2010.

[122] BECKER, S.; MUNDANDHARA, S.; DEVLIN, R. B. ; MADDEN, M.. **Regulation of cytokine production in human alveolar macrophages and airway epithelial cells in response to ambient air pollution particles: Further mechanistic studies**. Toxicology and Applied Pharmacology, 207(2):269–275, 2005.

[123] SCHWARZE, P. E.; TOTLANDSDAL, A. I.; LÅG, M.; REFSNES, M.; HOLME, J. A. ; ØVREVIK, J.. **Inflammation-Related Effects of Diesel Engine Exhaust Particles: Studies on Lung Cells In Vitro**. BioMed Research International, 2013:1–13, 2013.

[124] RIVA, D.; MAGALHÃES, C.; LOPES, A.; LANÇAS, T.; MAUAD, T.; MALM, O.; VALENÇA, S.; SALDIVA, P.; FAFFE, D. ; ZIN, W.. **Low dose of fine particulate matter (PM2.5) can induce acute oxidative**

stress, inflammation and pulmonary impairment in healthy mice. Inhalation Toxicology, 23(5):257–267, apr 2011.

[125] UMBUZEIRO, G. A.; FRANCO, A.; MARTINS, M. H.; KUMMROW, F.; CARVALHO, L.; SCHMEISER, H. H.; LEYKAUF, J.; STIBOROVA, M. ; CLAXTON, L. D.. **Mutagenicity and DNA adduct formation of PAH, nitro-PAH, and oxy-PAH fractions of atmospheric particulate matter from São Paulo, Brazil**. Mutation Research/Genetic Toxicology and Environmental Mutagenesis, 652(1):72–80, mar 2008.

[126] MIGUEL, A. G.; DAISEY, J. M. ; SOUSA, J. A.. **Comparative study of the mutagenic and genotoxic activity associated with inhalable particulate matter in Rio de Janeiro air**. Environmental and Molecular Mutagenesis, 15(1):36–43, 1990.

[127] DESCHAMPS, E.; WEIDLER, P. G.; FRIEDRICH, F.; WEISS, C. ; DIABATÉ, S.. **Characterization of indoor dust from Brazil and evaluation of the cytotoxicity in A549 lung cells**. Environmental Geochemistry and Health, 36(2):225–233, apr 2014.

[128] CAMARGOS, P. A. M.; CASTRO, R. M. ; FELD-MAN, J. S.. **Prevalencia de síntomas relacionados con el asma en escolares de Campos Gerais (MG), Brasil**. Rev Panam Salud Publica/Pan Am J Public Health, 6(1), 1999.

[129] BRAGA, A. L. F.; PEREIRA, L. A. A.; PROCÓPIO, M.; DE ANDRÉ, P. A. ; SALDIVA, P. H. D. N.. **Associação entre poluição atmosférica e doenças respiratórias e cardiovasculares na cidade de Itabira, Minas Gerais, Brasil**. Cadernos de Saúde Pública, 23:S570–S578, 2007.

[130] ALFARO-MORENO, E.; NAWROT, T. S.; NEMMAR, A. ; NEMERY, B.. **Particulate matter in the environment: pulmonary and cardiovascular effects**. Current Opinion in Pulmonary Medicine, 13(2):98–106, mar 2007.

[131] VERANTH, J. M.; MOSS, T. A.; CHOW, J. C.; LABBAN, R.; NICHOLS, W. K.; WALTON, J. C.; WATSON, J. G. ; YOST, G. S.. **Correlation of in Vitro Cytokine Responses with the Chemical Composition of Soil-Derived Particulate Matter**. Environmental Health Perspectives, 114(3):341–350, 2006.

[132] MARTIN, L.; ROCHELLE, L.; FISCHER, B.; KRUNKOSKY, T. ; ADLER, K.. **Airway epithelium as an effector of inflammation: molecular**

regulation of secondary mediators. European Respiratory Journal, 10(9), 1997.

[133] VANOS, J. K.; CAKMAK, S.. **Changing air mass frequencies in Canada: potential links and implications for human health.** International journal of biometeorology, 58(2):121–35, mar 2014.

[134] METIAN, M.; HÉDOUIN, L.; ELTAYEB, M. M.; LACOUE-LABARTHE, T.; TEYSSIÉ, J.-L.; MUGNIER, C.; BUSTAMANTE, P. ; WARNAU, M.. **Metal and metalloid bioaccumulation in the Pacific blue shrimp Litopenaeus stylirostris (Stimpson) from New Caledonia: laboratory and field studies.** Marine pollution bulletin, 61(7-12):576–84, jan 2010.

[135] ZUYKOV, M.; PELLETIER, E. ; HARPER, D. A. T.. **Bivalve mollusks in metal pollution studies: from bioaccumulation to biomonitoring.** Chemosphere, 93(2):201–8, sep 2013.

[136] KIM, J.-B.; KIM, C.; CHOI, E.; PARK, S.; PARK, H.; PAK, H.-N.; LEE, M.-H.; SHIN, D. C.; HWANG, K.-C. ; JOUNG, B.. **Particulate air pollution induces arrhythmia via oxidative stress and calcium calmodulin kinase II activation.** Toxicology and applied pharmacology, 259(1):66–73, feb 2012.

[137] RISOM, L.; MØLLER, P. ; LOFT, S.. **Oxidative stress-induced DNA damage by particulate air pollution.** Mutation research, 592(1-2):119–37, dec 2005.

[138] DE SOUZA, P. S. A.; MARQUES, M. R. C.; SOARES, M. L. G. ; PÉREZ, D. V.. **Trace Metals Concentrations in Mangrove Sediments of Sepetiba Bay (Rio de Janeiro, Brazil): Microwave Assisted Digestion with Nitric Acid and Aqua Regia**. Revista Virtual de Química, 4(4):464–473, 2012.

[139] MOLISANI, M. M.; MARINS, R. V.; MACHADO, W.; PARAQUETTI, H. H. M.; BIDONE, E. D. ; LACERDA, L. D.. **Environmental changes in Sepetiba Bay, SE Brazil**. Regional Environmental Change, 4(1):17–27, mar 2004.

[140] LIU, Y.; WANG, W.-N.; WANG, A.-L.; WANG, J.-M. ; SUN, R.-Y.. **Effects of dietary vitamin E supplementation on antioxidant enzyme activities in Litopenaeus vannamei (Boone, 1931) exposed to acute salinity changes**. Aquaculture, 265(1-4):351–358, may 2007.

[141] WANG, Z.; DONG, X.; ZHOU, S.; YAN, C.; YAN, Y. ; CHI, Q.. **Contamination assessments of surface water in coastal lagoon (Maluan Bay , China) incorporating biomarker responses and bioaccumulation in hepatopancreas of exposed shrimp (Litopenaeus vannamei) — an integrative approach**. Environmental Science and Pollution Research International, 21:205–219, 2014.

[142] LOBATO, R. O.; NUNES, S. M.; WASIELESKY, W.; FATTORINI, D.; REGOLI, F.; MONSERRAT, J. M. ; VENTURA-LIMA, J.. **The role of lipoic acid in the protection against of metallic pollutant effects in the shrimp Litopenaeus vannamei (Crustacea, Decapoda).** Comparative biochemistry and physiology. Part A, Molecular & integrative physiology, 165(4):491–7, aug 2013.

[143] LAVRADAS, R. T.. **Determination of metals (Cu, Fe, Zn, Pb, Cd and Ni) in tissues of marine organisms of the Bay of Ilha Grande, RJ, Brazil.** PhD thesis, Pontifical Catholic University of Rio de Janeiro (document in Portuguese), 2012.

[144] WU, J.-P.; CHEN, H.-C. ; HUANG, D.-J.. **Histopathological and biochemical evidence of hepatopancreatic toxicity caused by cadmium and zinc in the white shrimp, Litopenaeus vannamei.** Chemosphere, 73(7):1019–26, oct 2008.

[145] WU, J.-P.; CHEN, H.-C.. **Metallothionein induction and heavy metal accumulation in white shrimp Litopenaeus vannamei exposed to cadmium and zinc.** Comparative biochemistry and physiology. Toxicology & pharmacology : CBP, 140(3-4):383–94, jan 2005.

[146] WU, X.-Y.; YANG, Y.-F.. **Heavy metal (Pb, Co, Cd, Cr, Cu, Fe, Mn and Zn) concentrations in harvest-size white shrimp Litopenaeus vannamei tissues from aquaculture and wild source**. Journal of Food Composition and Analysis, 24(1):62–65, feb 2011.

[147] GUÉGUEN, F.; STILLE, P.; LAHD GEAGEA, M. ; BOUTIN, R.. **Atmospheric pollution in an urban environment by tree bark biomonitoring–part I: trace element analysis.** Chemosphere, 86(10):1013–9, mar 2012.

[148] TAIWO, A. M.; HARRISON, R. M. ; SHI, Z.. **A Review of Receptor Modelling of Industrially Emitted Particulate Matter**. Atmospheric Environment, 97:109–120, aug 2014.

[149] CHRISTIAN, T. J.; YOKELSON, R. J.; MOLINA, L. T.; ENGLING, G. ; HSU, S. C.. **Trace gas and particle emissions from domestic and industrial biofuel use and garbage burning in central Mexico**. Atmos. Chem. Phys., p. 565–584, 2010.

[150] RODRÍGUEZ-COTTO, R. I.; ORTIZ-MARTÍNEZ, M. G.; RIVERA-RAMÍREZ, E.; MATEUS, V. L.; AMARAL, B. S.; JIMÉNEZ-VÉLEZ, B. D. ; GIODA, A.. **Particle pollution in Rio de Janeiro, Brazil: increase and decrease of pro-inflammatory cytokines IL-6 and IL-8 in human lung cells.** Environmental pollution (Barking, Essex : 1987), 194:112–20, nov 2014.

[151] GIODA, A.; CAVALCANTI, P. M. S.; MAIA, M. F.; MAIA, L. F. P. G. ; NETO, F. R. A.. **Evaluation of Air Quality in Volta Redonda, the Main Metallurgical Industrial City in Brazil**. Journal of the Brazilian Chemical Society, 15(6):856–864, 2004.

[152] GIODA, A.; VENTURA, L. M. B.; RAMOS, M. B. ; SILVA, M. P. R.. **Half Century Monitoring Air Pollution in a Megacity: a Case Study of Rio de Janeiro**. Water, Air, & Soil Pollution, 227(3):86, feb 2016.

[153] KARANASIOU, A.; QUEROL, X.; ALASTUEY, A.; PEREZ, N.; PEY, J.; PERRINO, C.; BERTI, G.; GANDINI, M.; POLUZZI, V.; FERRARI, S.; DE LA ROSA, J.; PASCAL, M.; SAMOLI, E.; KELESSIS, A.; SUNYER, J.; ALESSANDRINI, E.; STAFOGGIA, M. ; FORASTIERE, F.. **Particulate matter and gaseous pollutants in the Mediterranean Basin: Results from the MED-PARTICLES project**. Science of The Total Environment, 488-489:297–315, aug 2014.

[154] TAIWO, A. M.; BEDDOWS, D. C. S.; SHI, Z. ; HARRISON, R. M.. **Mass and number size distributions of particulate matter components: comparison of an industrial site and an urban background site.** The Science of the total environment, 475:29–38, mar 2014.

[155] KIM, Y. H.; KRANTZ, Q. T.; MCGEE, J.; KOVALCIK, K. D.; DUVALL, R. M.; WILLIS, R. D.; KAMAL, A. S.; LANDIS, M. S.; NORRIS, G. A. ; GILMOUR, M. I.. **Chemical composition and source apportionment of size fractionated particulate matter in Cleveland, Ohio, USA**. Environmental Pollution, sep 2016.

[156] HLEIS, D.; FERNÁNDEZ-OLMO, I.; LEDOUX, F.; KFOURY, A.; COURCOT, L.; DESMONTS, T. ; COURCOT, D.. **Chemical profile identification of fugitive and confined particle emissions from an**

integrated iron and steelmaking plant. Journal of Hazardous Materials, 250-251:246–255, apr 2013.

[157] DALL'OSTO, M.; DREWNICK, F.; FISHER, R. ; HARRISON, R. M.. **Real-Time Measurements of Nonmetallic Fine Particulate Matter Adjacent to a Major Integrated Steelworks**. Aerosol Science and Technology, 46(6):639–653, jun 2012.

[158] WOZNIAK, A. S.; SHELLEY, R. U.; SLEIGHTER, R. L.; ABDULLA, H. A.; MORTON, P. L.; LANDING, W. M. ; HATCHER, P. G.. **Relationships among aerosol water soluble organic matter, iron and aluminum in European, North African, and Marine air masses from the 2010 US GEOTRACES cruise**. Marine Chemistry, 154:24–33, aug 2013.

[159] KUMAGAI, K.; IIJIMA, A.; TAGO, H.; TOMIOKA, A.; KOZAWA, K. ; SAKAMOTO, K.. **Seasonal characteristics of water-soluble organic carbon in atmospheric particles in the inland Kanto plain, Japan**. Atmospheric Environment, 43(21):3345–3351, jul 2009.

[160] AMIL, N.; LATIF, M. T.; KHAN, M. F. ; MOHAMAD, M.. **Seasonal variability of PM_{2.5} composition and sources in the Klang Valley urban-industrial environment**. Atmospheric Chemistry and Physics, 16(8):5357–5381, apr 2016.

[161] FERNÁNDEZ-CAMACHO, R.; RODRÍGUEZ, S.; DE LA ROSA, J.; SÁNCHEZ DE LA CAMPA, A.; ALASTUEY, A.; QUEROL, X.; GONZÁLEZ-CASTANEDO, Y.; GARCIA-ORELLANA, I. ; NAVA, S.. **Ultrafine particle and fine trace metal (As, Cd, Cu, Pb and Zn) pollution episodes induced by industrial emissions in Huelva, SW Spain**. Atmospheric Environment, 61:507–517, dec 2012.

[162] SMICHOWSKI, P.. **Antimony in the environment as a global pollutant: a review on analytical methodologies for its determination in atmospheric aerosols.** Talanta, 75(1):2–14, mar 2008.

[163] MMARI, A. G.; POTGIETER-VERMAAK, S. S.; BENCS, L.; MCCRINDLE, R. I. ; VAN GRIEKEN, R.. **Elemental and ionic components of atmospheric aerosols and associated gaseous pollutants in and near Dar es Salaam, Tanzania**. Atmospheric Environment, 77:51–61, oct 2013.

[164] SQUIZZATO, S.; MASIOL, M.; BRUNELLI, A.; PISTOLLATO, S.; TARABOTTI, E.; RAMPAZZO, G. ; PAVONI, B.. **Factors determining the formation of secondary inorganic aerosol: a case study in the Po Valley (Italy)**. Atmospheric Chemistry and Physics, 13(4):1927–1939, feb 2013.

[165] **WHO | Air quality guidelines - global update 2005**, 2011. URL: https://goo.gl/FzKQmk (accessed on nov 11, 2016).

[166] WEITKAMP, E. A.; LIPSKY, E. M.; PANCRAS, P. J.; ONDOV, J. M.; POLIDORI, A.; TURPIN, B. J. ; ROBINSON, A. L.. **Fine particle emission profile for a large coke production facility based on highly time-resolved fence line measurements**. Atmospheric Environment, 39(36):6719–6733, nov 2005.

[167] ORAVISJÄRVI, K.; TIMONEN, K.; WIIKINKOSKI, T.; RUUSKANEN, A.; HEINÄNEN, K. ; RUUSKANEN, J.. **Source contributions to PM2.5 particles in the urban air of a town situated close to a steel works**. Atmospheric Environment, 37(8):1013–1022, mar 2003.

[168] HOCKING, M. B.. **Production of Iron and Steel**. In: HANDBOOK OF CHEMICAL TECHNOLOGY AND POLLUTION CONTROL, p. 421–452. Elsevier, 2005. URL: https://goo.gl/XPybpP (accessed on sep, 2011).

[169] MACHEMER, S. D.. **Characterization of Airborne and Bulk Particulate from Iron and Steel Manufacturing Facilities**. Environmental Science & Technology, 38(2):381–389, jan 2004.

[170] CHENG, Y.; ENGLING, G.; HE, K.-B.; DUAN, F.-K.; MA, Y.-L.; DU, Z.-Y.; LIU, J.-M.; ZHENG, M. ; WEBER, R. J.. **Biomass burning contribution to Beijing aerosol**. Atmospheric Chemistry and Physics, 13(15):7765–7781, aug 2013.

[171] BRAZIL. **National System of Nature Conservation Units**, 2015. URL: https://goo.gl/2sR8Lq (accessed on aug 06, 2016).

[172] IRGA, P.; BURCHETT, M. ; TORPY, F.. **Does urban forestry have a quantitative effect on ambient air quality in an urban environment?** Atmospheric Environment, 120:173–181, nov 2015.

[173] BARMPADIMOS, I.; KELLER, J.; ODERBOLZ, D.; HUEGLIN, C. ; PRÉVÔT, A. S. H.. **One decade of parallel fine (PM2.5) and coarse (PM10–PM2.5) particulate matter measurements in Europe:**

trends and variability. Atmospheric Chemistry and Physics, 12(7):3189–3203, apr 2012.

[174] MAENHAUT, W.; VERMEYLEN, R.; CLAEYS, M.; VERCAUTEREN, J. ; ROEKENS, E.. **Sources of the PM10 aerosol in Flanders, Belgium, and re-assessment of the contribution from wood burning**. Science of The Total Environment, 562:550–560, aug 2016.

[175] XIAO, Y.-H.; LIU, S.-R.; TONG, F.-C.; KUANG, Y.-W.; CHEN, B.-F. ; GUO, Y.-D.. **Characteristics and Sources of Metals in TSP and PM2.5 in an Urban Forest Park at Guangzhou**. Atmosphere, 5(4):775–787, oct 2014.

[176] KIM, Y.-H.; KIM, K.-H.; MA, C.-J.; SHON, Z.-H.; PARK, C. G.; SONG, S.-K.; RO, C.-U. ; BROWN, R. J.. **An investigation into the relationship between the major chemical components of particulate matter in urban air**. Chemosphere, 95:387–394, jan 2014.

[177] FUJIWARA, F.; REBAGLIATI, R. J.; DAWIDOWSKI, L.; GÓMEZ, D.; POLLA, G.; PEREYRA, V. ; SMICHOWSKI, P.. **Spatial and chemical patterns of size fractionated road dust collected in a megacitiy**. Atmospheric Environment, 45(8):1497–1505, mar 2011.

[178] LAOR, Y.; PARKER, D. ; PAGE, T.. **Measurement, prediction, and monitoring of odors in the environment: a critical review.** Reviews in Chemical Engineering, 30(2):139–166, 2011.

[179] MADSEN, P. V.; HERTEL, O.; LØFSTRØM, P.; SIGSGAARD, T.; BØN-LØKKE, J.; PUPUTTI, K.; ARNOLD, M. ; BLEEKER, A.. **Abatement, control and regulation of emissions and ambient concentrations of odor and allergens from livestock farming in the Nordic countries.** Nordic Council of Ministers, Copenhagen, 2009.

[180] PARKER, D. B.; KOZIEL, J. A.; CAI, L.; JACOBSON, L. D.; AKDENIZ, N.; BEREZNICKI, S. D.; X ; HETCHLER, B. P.. **Odor and Odorous Chemical Emissions from Animal Buildings: Part 6. Odor Activity Value**. Transactions of the ASABE, 55(6):2357–2368, 2012.

[181] SPIEHS, M. J.; WHITNEY, M. H.; SHURSON, G. C.; NICOLAI, R. E.; FLORES, J. A. R. ; PARKER, D. B.. **Odor and Gas Emissions and Nutrient Excretion from Pigs Fed Diets Containing Dried Distillers Grains with Solubles**. Applied Engineering in Agriculture, 28(3):431–437, 2012.

[182] PARKER, D. B.; GILLEY, J.; WOODBURY, B.; KIM, K.-H.; GALVIN, G.; BARTELT-HUNT, S. L.; LI, X. ; SNOW, D. D.. **Odorous VOC emission following land application of swine manure slurry**. Atmospheric Environment, 66:91–100, feb 2013.

[183] SHUSTERMAN, D.. **Odor-associated Health Complaints: Competing Explanatory Models**. Chemical Senses, 26(3):339–343, apr 2001.

[184] LINDVALL, T.; RADFORD, E. P.. **Measurement of annoyance due to exposure to environmental factors**. Environmental Research, 6(1):1–36, mar 1973.

[185] WITHERSPOON, J.. **Biosolids Processing modifications for cake odor reduction.** Technical report, Water Environment Research Foundation (WERF), 2006. URL: https://goo.gl/VxCeIj (accessed on sep, 2015).

[186] SMEETS, M. A. M.; DALTON, P. H.. **Evaluating the human response to chemicals: odor, irritation and non-sensory factors.** Environmental toxicology and pharmacology, 19(3):581–8, may 2005.

[187] DALTON, P.. **Odor Perception and Beliefs about Risk**. Chemical Senses, 21(4):447–458, aug 1996.

[188] WHO. **Population Health and Waste Management: Scientific Data and Policy Options**. Technical Report March, WHO Europe, Copenhagen, 2007. URL: https://goo.gl/d67QCW (accessed on jan 08, 2015).

[189] DITLEVSEN, S.; CHRISTENSEN, U.; LYNCH, J.; DAMSGAARD, M. T. ; KEIDING, N.. **The mediation proportion: a structural equation approach for estimating the proportion of exposure effect on outcome explained by an intermediate variable.** Epidemiology (Cambridge, Mass.), 16(1):114–20, jan 2005.

[190] BRAUER, C.; BUDTZ-JØRGENSEN, E. ; MIKKELSEN, S.. **Structural equation analysis of the causal relationship between health and perceived indoor environment.** International archives of occupational and environmental health, 81(6):769–76, may 2008.

[191] KLINE, R. B.. **Principles and practice of structural equation modeling**, volumen 345. Guilford Press, New York, third edition, jul 2014.

[192] BUDTZ-JØRGENSEN, E.; KEIDING, N.; GRANDJEAN, P. ; WEIHE, P.. **Estimation of health effects of prenatal methylmercury exposure using structural equation models.** Environmental health : a global access science source, 1(1):2, 2002.

[193] SCHUCK, K.; OTTEN, R.; ENGELS, R. C. M. E. ; KLEINJAN, M.. **The role of environmental smoking in smoking-related cognitions and susceptibility to smoking in never-smoking 9-12 year-old children.** Addictive behaviors, 37(12):1400–5, dec 2012.

[194] NIKOLOV, M. C.; COULL, B. A.; CATALANO, P. J. ; GODLESKI, J. J.. **An informative Bayesian structural equation model to assess source-specific health effects of air pollution.** Biostatistics (Oxford, England), 8(3):609–24, jul 2007.

[195] DAVIS, M. E.; LADEN, F.; HART, J. E.; GARSHICK, E.; BLICHARZ, A. ; SMITH, T. J.. **Predicting changes in PM exposure over time at U.S. trucking terminals using structural equation modeling techniques.** Journal of occupational and environmental hygiene, 6(7):396–403, jul 2009.

[196] NUGROHO, S. B.; FUJIWARA, A. ; ZHANG, J.. **Spatial and Temporal Analysis of Surface Ozone in Urban Area : A Multilevel and Structural Equation Model Approach**. In: Dr. Budi Haryanto, editor, AIR POLLUTION - A COMPREHENSIVE PERSPECTIVE, chapter 8, p. 980. Intech, 2012. URL: https://goo.gl/w1UMJG (accessed on feb 21, 2014).

[197] BAJA, E. S.; SCHWARTZ, J. D.; COULL, B. A.; WELLENIUS, G. A.; VOKONAS, P. S. ; SUH, H. H.. **Structural equation modeling of parasympathetic and sympathetic response to traffic air pollution in a repeated measures study.** Environmental health : a global access science source, 12(1):81, jan 2013.

[198] MBAH, A. K.; PAOTHONG, A.; WILSON, R. E. ; SALIHU, H. M.. **Utility and application of SEM in delineating cause-effect relationship between ambient pollutant and fetal birth outcome**. Environmetrics, 25(7):548–556, nov 2014.

[199] STENLUND, T.; LIDÉN, E.; ANDERSSON, K.; GARVILL, J. ; NORDIN, S.. **Annoyance and health symptoms and their influencing factors: a population-based air pollution intervention study.** Public health, 123(4):339–45, apr 2009.

A
Published papers

Environmental Pollution 194 (2014) 112–120

Contents lists available at ScienceDirect

Environmental Pollution

journal homepage: www.elsevier.com/locate/envpol

Particle pollution in Rio de Janeiro, Brazil: Increase and decrease of pro-inflammatory cytokines IL-6 and IL-8 in human lung cells

Rosa I. Rodríguez-Cotto [a, b], Mario G. Ortiz-Martínez [a, b], Evasomary Rivera-Ramírez [b, c], Vinicius L. Mateus [d], Beatriz S. Amaral [d], Braulio D. Jiménez-Vélez [a, b, *], Adriana Gioda [b, d]

[a] University of Puerto Rico, Medical Sciences Campus, Department of Biochemistry, Puerto Rico
[b] Center for Environmental and Toxicological Research, San Juan 00936, Puerto Rico
[c] University of Puerto Rico, Río Piedras Campus, Department of Biology, Puerto Rico
[d] Pontifical Catholic University, Rio de Janeiro (PUC-Rio), Department of Chemistry, RJ, Brazil

Figure A.1: Published paper: Chapter 3.

B
Submitted papers

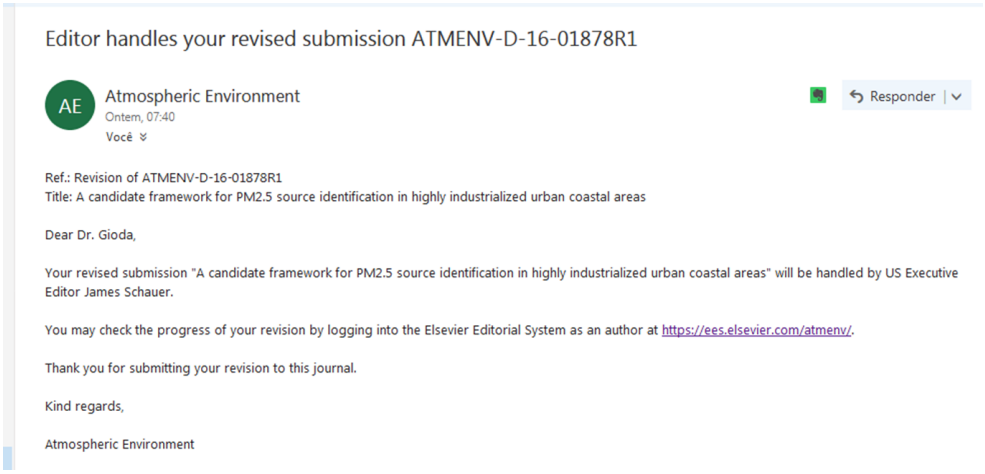

Editor handles your revised submission ATMENV-D-16-01878R1

AE Atmospheric Environment
Ontem, 07:40
Você

Responder

Ref.: Revision of ATMENV-D-16-01878R1
Title: A candidate framework for PM2.5 source identification in highly industrialized urban coastal areas

Dear Dr. Gioda,

Your revised submission "A candidate framework for PM2.5 source identification in highly industrialized urban coastal areas" will be handled by US Executive Editor James Schauer.

You may check the progress of your revision by logging into the Elsevier Editorial System as an author at https://ees.elsevier.com/atmenv/.

Thank you for submitting your revision to this journal.

Kind regards,

Atmospheric Environment

Figure B.1: Submitted paper 1: Chapter 5.

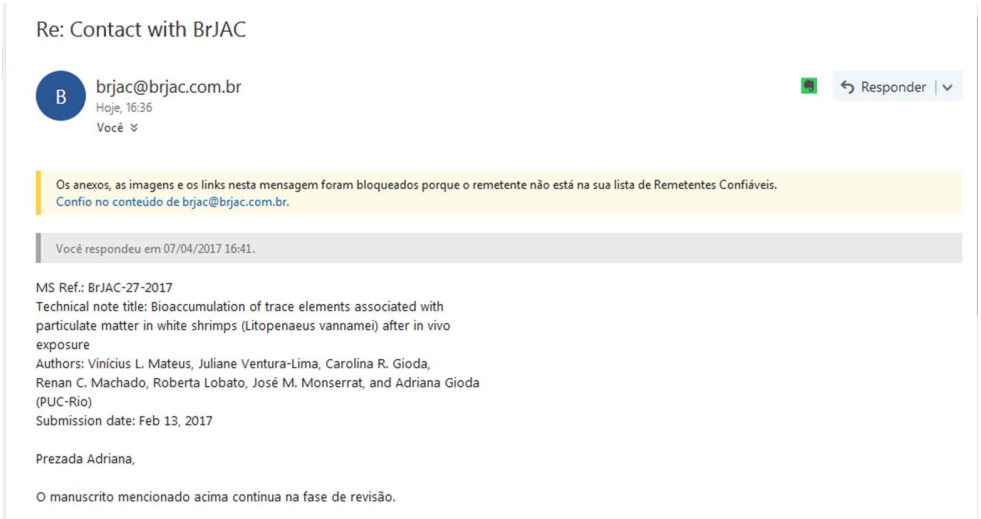

Re: Contact with BrJAC

B brjac@brjac.com.br
Hoje, 16:36
Você

Responder

Os anexos, as imagens e os links nesta mensagem foram bloqueados porque o remetente não está na sua lista de Remetentes Confiáveis.
Confio no conteúdo de brjac@brjac.com.br.

Você respondeu em 07/04/2017 16:41.

MS Ref.: BrJAC-27-2017
Technical note title: Bioaccumulation of trace elements associated with particulate matter in white shrimps (Litopenaeus vannamei) after in vivo exposure
Authors: Vinícius L. Mateus, Juliane Ventura-Lima, Carolina R. Gioda, Renan C. Machado, Roberta Lobato, José M. Monserrat, and Adriana Gioda (PUC-Rio)
Submission date: Feb 13, 2017

Prezada Adriana,

O manuscrito mencionado acima continua na fase de revisão.

Figure B.2: Submitted paper 2: Chapter 4.

C
Papers published in related topics to this thesis

Atmospheric Environment 68 (2013) 208–220

Contents lists available at SciVerse ScienceDirect

Atmospheric Environment

journal homepage: www.elsevier.com/locate/atmosenv

Chemical constituents in clouds and rainwater in the Puerto Rican rainforest: Potential sources and seasonal drivers

Adriana Gioda [a], Olga L. Mayol-Bracero [b,*], Frederick N. Scatena [c], Kathleen C. Weathers [d], Vinicius L. Mateus [a], William H. McDowell [e]

[a] Pontifical Catholic University of Rio de Janeiro (PUC-Rio), Department of Chemistry, Rio de Janeiro, Brazil
[b] Institute for Tropical Ecosystem Studies, University of Puerto Rico, San Juan, PO Box 21910, San Juan, PR 00931-1910, USA
[c] Department of Earth and Environmental Science, University of Pennsylvania, USA
[d] Cary Institute of Ecosystem Studies, Millbrook, NY, USA
[e] Department of Natural Resources and the Environment, University of New Hampshire, Durham, NH, USA

Figure C.1: Paper in collaboration 1: Source apportionment and data analysis.

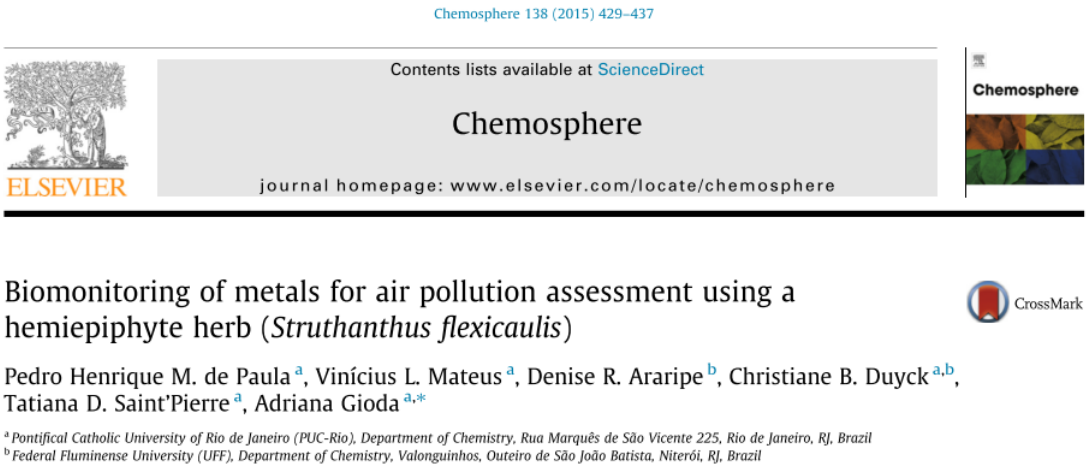

Chemosphere 138 (2015) 429–437

Contents lists available at ScienceDirect

Chemosphere

journal homepage: www.elsevier.com/locate/chemosphere

Biomonitoring of metals for air pollution assessment using a hemiepiphyte herb (*Struthanthus flexicaulis*)

Pedro Henrique M. de Paula [a], Vinícius L. Mateus [a], Denise R. Araripe [b], Christiane B. Duyck [a,b], Tatiana D. Saint'Pierre [a], Adriana Gioda [a,*]

[a] Pontifical Catholic University of Rio de Janeiro (PUC-Rio), Department of Chemistry, Rua Marquês de São Vicente 225, Rio de Janeiro, RJ, Brazil
[b] Federal Fluminense University (UFF), Department of Chemistry, Valonguinhos, Outeiro de São João Batista, Niterói, RJ, Brazil

Figure C.2: Paper in collaboration 2: Source apportionment and data analysis.

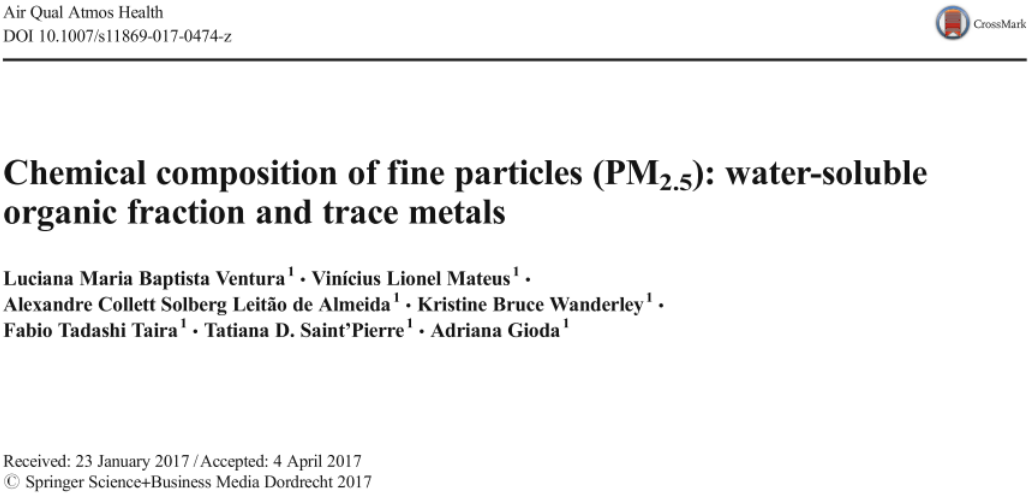

Air Qual Atmos Health
DOI 10.1007/s11869-017-0474-z

Chemical composition of fine particles ($PM_{2.5}$): water-soluble organic fraction and trace metals

Luciana Maria Baptista Ventura [1] · Vinícius Lionel Mateus [1] · Alexandre Collett Solberg Leitão de Almeida [1] · Kristine Bruce Wanderley [1] · Fabio Tadashi Taira [1] · Tatiana D. Saint'Pierre [1] · Adriana Gioda [1]

Received: 23 January 2017 / Accepted: 4 April 2017

Figure C.3: Paper in collaboration 3: Source apportionment, data handling and analysis.

D
Participation in congresses

Oral presentation

Mateus, V.L.; do Valles, T. V.; de Oliveira, T. B.; de Almeida, A. C. S. L.; Maia, L. F. P. G.; Saint' Pierre, T. D.; Gioda, A.. Atmospheric aerosol monitoring and characterization: An emission control strategy to protect tropical forests. AGU Fall Meeting 2013 (San Francisco, USA).

Conference papers and posters

GIODA, A. ; VENTURA, LUCIANA. M. ; MASSONE, CARLOS. G. ; **MATEUS, VINICIUS L.** ; WAGNER, A. . Receptor modeling in the metropolitan region of Rio de Janeiro: What is the role of PAHs, n- alkenes, meteorological conditions on source apportionment of fine aerosol?. In: 2015 Goldschmidt Conference, 2015, Praga. Goldschmidt2015 Abstracts, 2015. v. 1. p. 1047.

MAGACHO, P. H. ; NUNES, V. O. ; ARARIPE, D. B. ; DUYCK, C. B. ; Saint Pierre, T. D. ; **Mateus, V.L** ; Gioda, A. . Determination of toxic elements in plant leaves as biomonitor of air pollution.. In: TOXI-LATIN, 2014, Porto Alegre. Anais do TOXI-LATIN, 2014. v. 1. p. 28.

ALMEIDA, A. C. S. L. ; **Mateus, V.L** ; VENTURA, L. M. B. ; GIODA, A. . Air quality in Rio de Janeiro and its effects on health.. In: TOXI-LATIN, 2014, Porto Alegre. Anais do TOXI- LATIN, 2014. v. 1. p. 20.

ALMEIDA, A. C. S. L. ; **Mateus, V.L** ; VENTURA, L. M. B. ; GIODA, A. . FIRST TIME EXPLORATORY STUDY OF WATER-SOLUBLE ORGANIC CARBON RELATIONSHIPS WITH METALS AND METEOROLOGICAL CONDITIONS IN THE RIO DE JANEIRO´S ATMOSPHERE.. In: 13th IGAC Science Conference on Atmospheric Chemistry, 2014, Natal. Proceedings of 13th IGAC Science Conference on Atmospheric Chemistry, 2014. v. 1. p. 179-179.

GIODA, A. ; **Mateus, V.L** ; MONTEIRO, I. ; TAIRA, F. ; ESTEVES, V. ; SAINTPIERRE, T. ; Anthropogenic Influence on Secondary Aerosol Formation and Total Water-Soluble Carbon on Atmospheric Particles. In: European Geosciences Union General Assembly 2013, 2013, Austria. Geophysical Research Abstracts, 2013. v. 15. p. 3243.

VALLES, T. V. ; OLIVEIRA, T. B. ; **Mateus, V.L** ; Saint Pierre, T. D. ; GIODA, A. . Estudo comparativo da composição química do material particulado entre cromatografia e espectroscopia. In: 17º Encontro Nacional de Química Analítica, 2013, Belo Horizonte. 17º Encontro Nacional de Química Analítica, 2013. v. 1. p. 1.

MAGACHO, P. H. ; ARARIPE, D. R. ; DUYCK, C. B. ; **Mateus, V.L** ; Saint Pierre, T. D. . Avaliação dos níveis de elementos traços em folhas de erva de passarinho utilizadas como biomonitores de poluição atmosférica.. In: Encontro Nacional de Química Analítica, 2013, Belo Horizonte. 17º Encontro Nacional de Química Analítica, 2013. v. 1. p. 1.

OLIVEIRA, T. B. ; ALMEIDA, A. C. S. L. ; **Mateus, V.L** ; ARTAXO, P. ; GIODA, A. . Estudo da composição química de aerossóis provenientes da região Amazônica.. In: 1ª Conferencia Nacional de Mudanças Climáticas (CONCLIMA), 2013, São Paulo. Anais da 1ª Conferencia Nacional de Mudanças Climáticas (CONCLIMA), 2013. v. 1. p. 1.

MARQUES, P. E. L. ; **Mateus, V.L** ; VENTURA, L. B. ; Saint Pierre, T. D. ; Gioda, A. . Extração ácida de filtros contendo amostras de material particulado (PM2.5) coletadas no estado do Rio de Janeiro.. In: 36ª Reuniao Anual da Sociedade Brasileira de Quimica, 2013, Águas de Lindóia. 36ª Reuniao Anual da Sociedade Brasileira de Quimica, 2013. v. 1. p. 1.

VALLES, T. V. ; **Mateus, V.L** ; Gioda, A. . Avaliação da composição solúvel em água de material particulado coletado em zonas rurais e industriais do Estado do Rio de Janeiro: um estudo continuado.. In: 36ª Reuniao Anual da Sociedade Brasileira de Quimica, 2013, Águas de Lindóia. 36ª Reuniao Anual da Sociedade Brasileira de Quimica, 2013. v. 1. p. 1.

Gioda, A. ; **Mateus, V.L** ; AMARAL, B. S. ; VENTURA, L. B. . Apportionment of particulate matter sources in the Rio de Janeiro Metropolitan area.. In: AGU Meetings of the Americas, 2013, Cancun. AGU Meetings of the Americas., 2013. v. 1. p. 1.

Mateus, V.L; Monteiro, I. L. G. ; Saint' Pierre, T. D. ; GIODA, A. . Study of chemical composition of particulate matter (TSP and PM2.5) from industrial

and rural areas of the Rio de Janeiro metropolitan region, Brazil, by ICP-MS and ICP OES. In: Rio Symposium, 2012, Foz do Iguaçu. Rio Symposium, 2012. v. 1. p. 1.

E
Supplementary material - 1

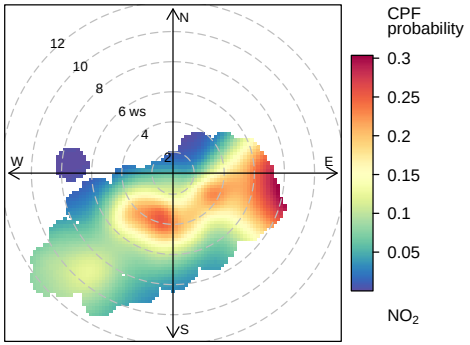

E.1(a): 25-50th percentile

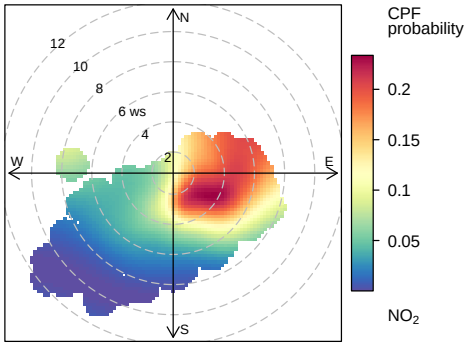

E.1(b): 50-75th percentile

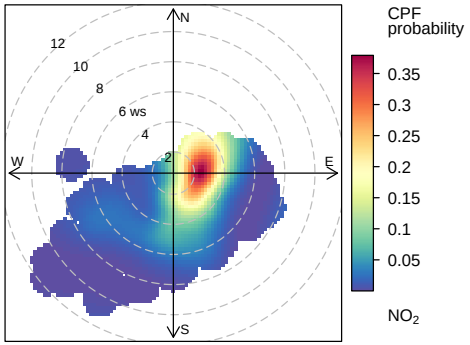

E.1(c): 50-75th percentile

Figure E.1: Conditional bivariate probability function plot of criteria pollutants at the CA site for (a) NO_2 concentrations between 14 and 21 μg m^{-3}, (b) NO_2 concentrations between 21 and 29 μg m^{-3}, and (c) NO_2 concentrations between 29 and 82 μg m^{-3}.

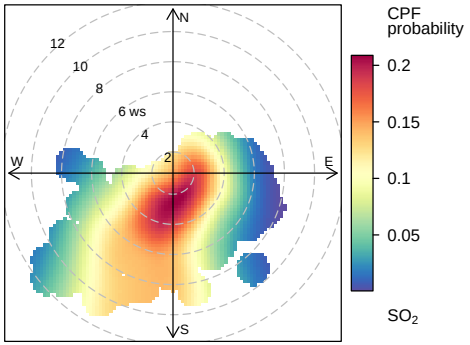

E.2(a): 25-50th percentile

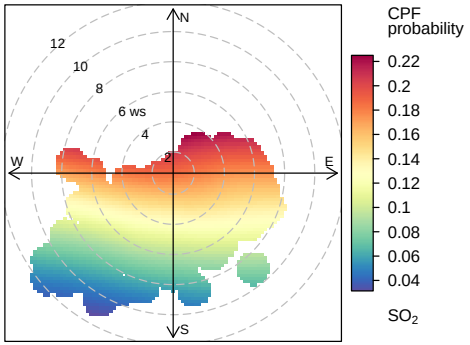

E.2(b): 50-75th percentile

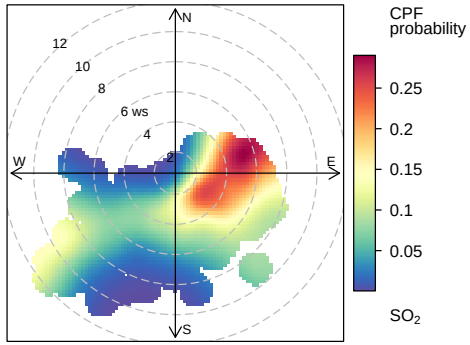

E.2(c): 50-75th percentile

Figure E.2: Conditional bivariate probability function plot of criteria pollutants at the CA site for (a) SO_2 concentrations between 2.4 and 4.2 μg m^{-3}, (b) SO_2 concentrations between 4.2 and 5.1 μg m^{-3}, and (c) SO_2 concentrations between 5.1 and 25 μg m^{-3}.

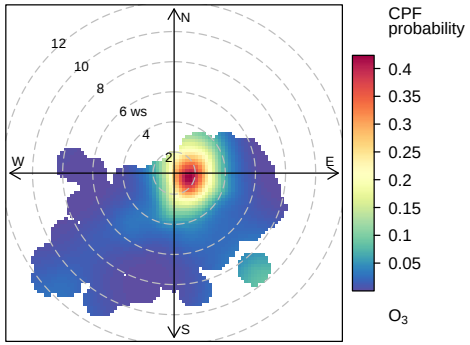

E.3(a): 0-25th percentile

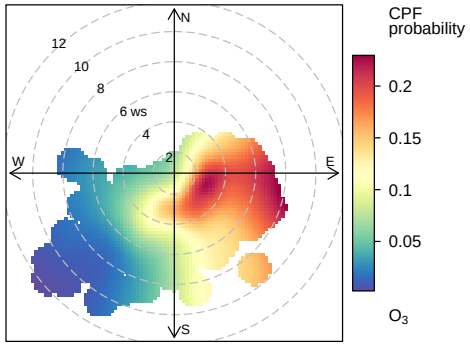

E.3(b): 25-50th percentile

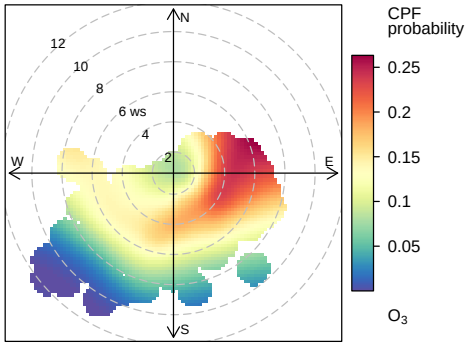

E.3(c): 50-75th percentile

Figure E.3: Conditional bivariate probability function plot of criteria pollutants at the CA site for (a) O_3 concentrations between 4.4 and 22 μg m^{-3}, (b) O_3 concentrations between 22 and 32 μg m^{-3}, and (c) O_3 concentrations between 32 and 43 μg m^{-3}.

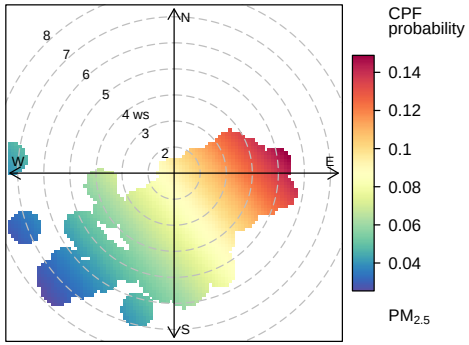

E.4(a): 25-50th percentile

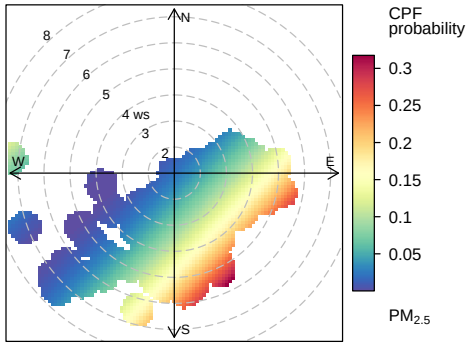

E.4(b): 50-75th percentile

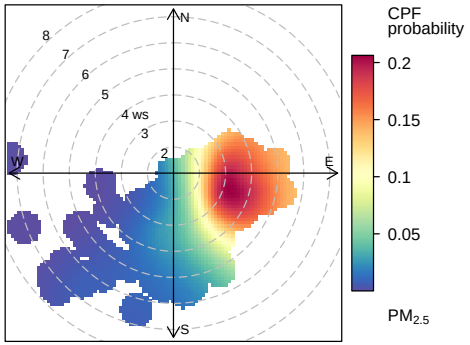

E.4(c): 75-100th percentile

Figure E.4: Conditional bivariate probability function plot of criteria pollutants at the CA site for (a) $PM_{2.5}$ concentrations between 5.8 and 8.9 μg m^{-3}, (b) $PM_{2.5}$ concentrations between 8.9 and 13 μg m^{-3}, and (c) $PM_{2.5}$ concentrations between 13 and 51 μg m^{-3}.

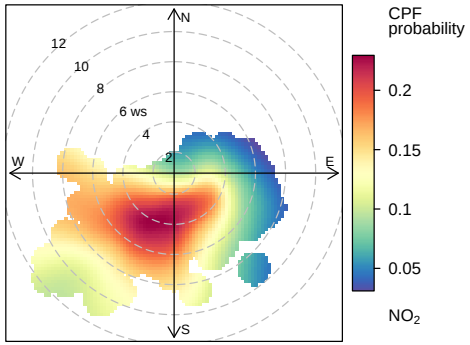

E.5(a): 25-50th percentile

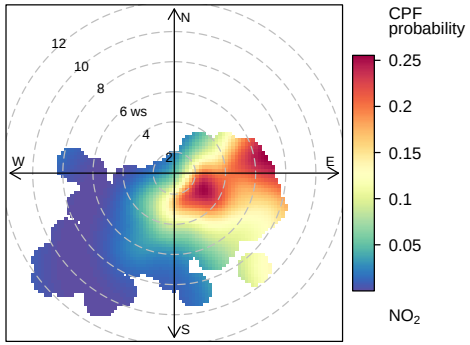

E.5(b): 50-75th percentile

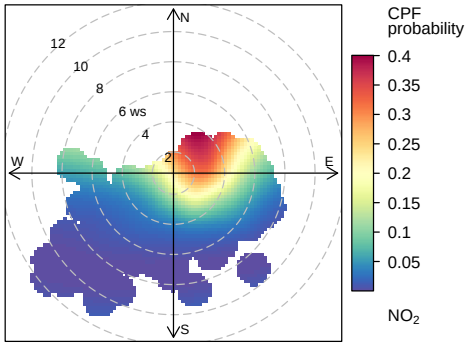

E.5(c): 75-100th percentile

Figure E.5: Conditional bivariate probability function plot of criteria pollutants at the CJ site for (a) NO_2 concentrations between 14 and 19 μg m^{-3}, (b) NO_2 concentrations between 19 and 24 μg m^{-3}, and (c) NO_2 concentrations between 24 and 60 μg m^{-3}.

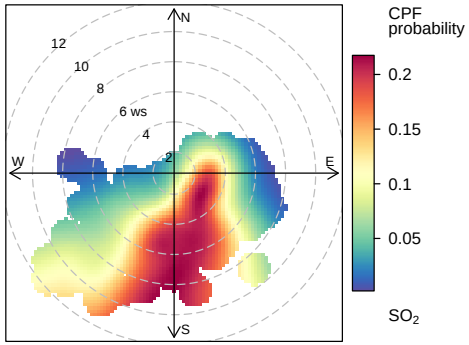

E.6(a): 0-25th percentile

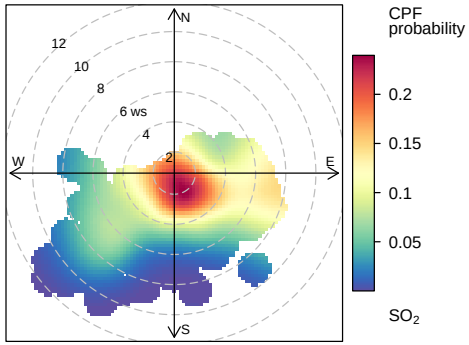

E.6(b): 25-50th percentile

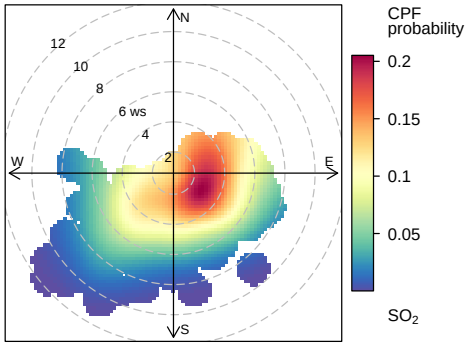

E.6(c): 50-75th percentile

Figure E.6: Conditional bivariate probability function plot of criteria pollutants at the CJ site for (a) SO_2 concentrations between 1.4 and 2.6 μg m^{-3}, (b) SO_2 concentrations between 2.6 and 3.2 μg m^{-3}, and (c) SO_2 concentrations between 3.2 and 5.5 μg m^{-3}.

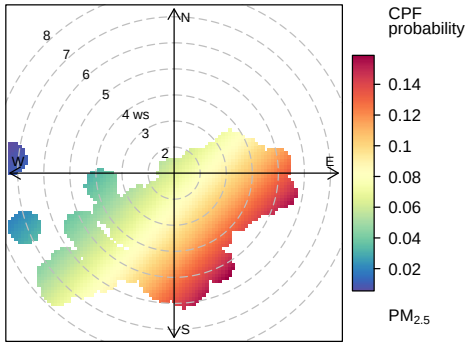

E.7(a): 25-50th percentile

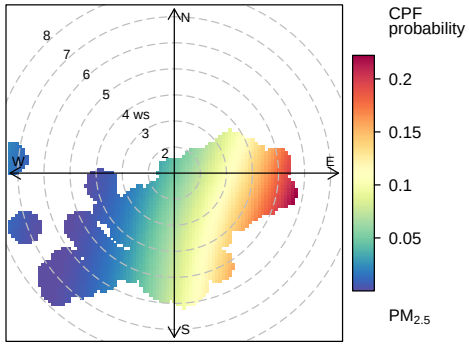

E.7(b): 50-75th percentile

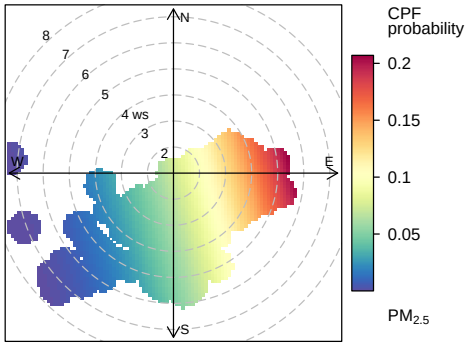

E.7(c): 75-100th percentile

Figure E.7: Conditional bivariate probability function plot of criteria pollutants at the CJ site for (a) $PM_{2.5}$ concentrations between 6.1 and 9.3 μg m^{-3}, (b) $PM_{2.5}$ concentrations between 9.3 and 14 μg m^{-3}, and (c) $PM_{2.5}$ concentrations between 14 and 57 μg m^{-3}.

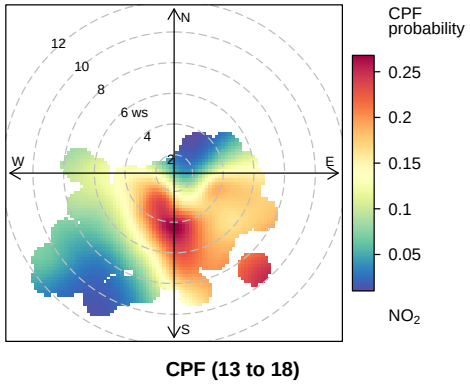

E.8(a): 25-50th percentile

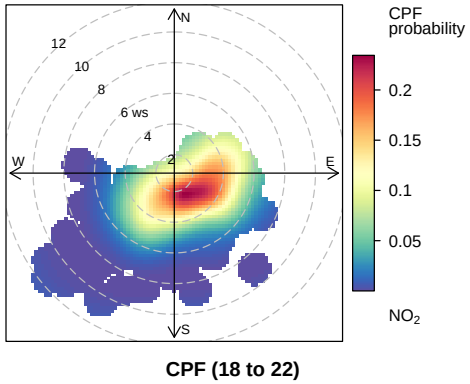

E.8(b): 50-75th percentile

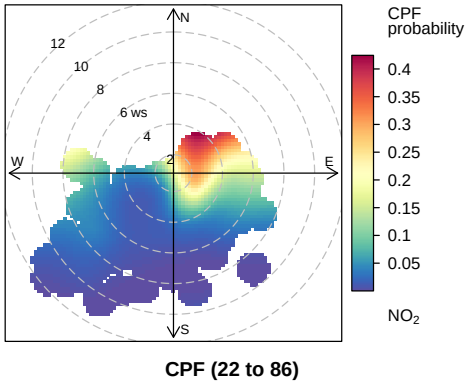

E.8(c): 75-100th percentile

Figure E.8: Conditional bivariate probability function plot of criteria pollutants at the SE site for (a) NO_2 concentrations between 13 and 18 μg m^{-3}, (b) NO_2 concentrations between 18 and 22 μg m^{-3}, and (c) NO_2 concentrations between 22 and 86 μg m^{-3}.

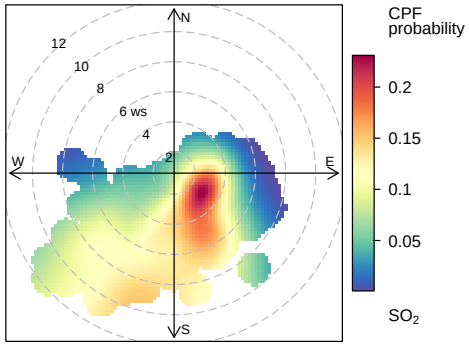

E.9(a): 0-25th percentile

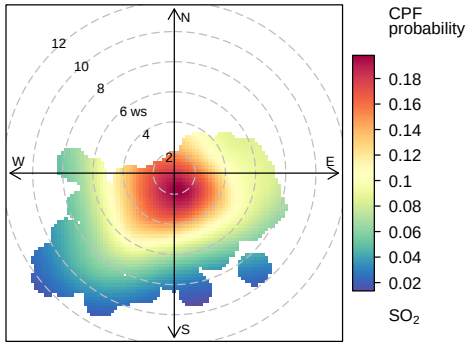

E.9(b): 25-50th percentile

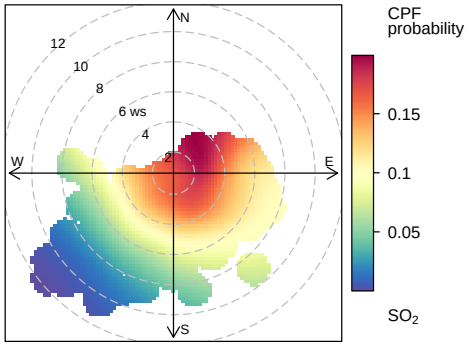

E.9(c): 50-75th percentile

Figure E.9: Conditional bivariate probability function plot of criteria pollutants at the SE site for (a) SO_2 concentrations between 0.68 and 1.5 μg m^{-3}, (b) SO_2 concentrations between 1.5 and 2.3 μg m^{-3}, and (c) SO_2 concentrations between 2.3 and 4 μg m^{-3}.

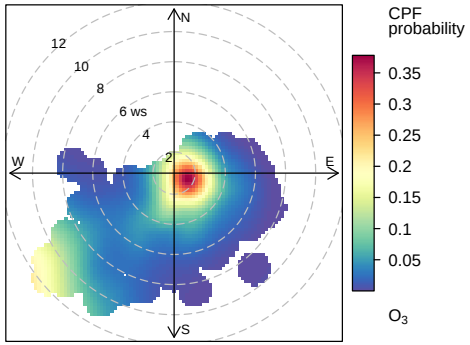

E.10(a): 0-25th percentile

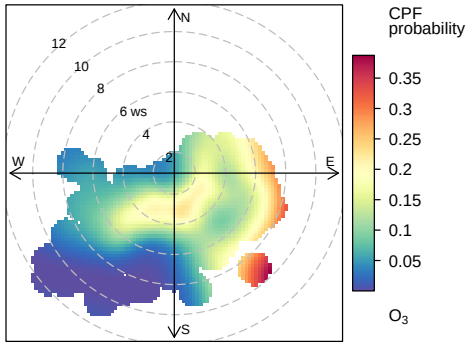

E.10(b): 25-50th percentile

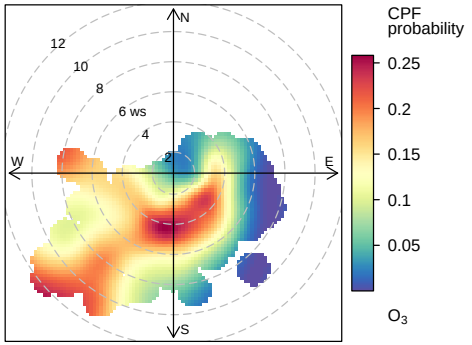

E.10(c): 75-100th percentile

Figure E.10: Conditional bivariate probability function plot of criteria pollutants at the SE site for (a) O_3 concentrations between 2.6 and 24 μg m^{-3}, (b) O_3 concentrations between 24 and 33 μg m^{-3}, and (c) O_3 concentrations between 44 and 100 μg m^{-3}.

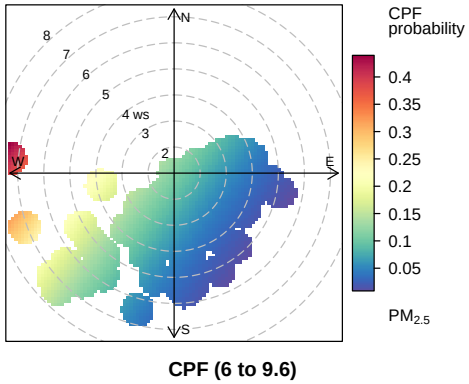

E.11(a): 25-50th percentile

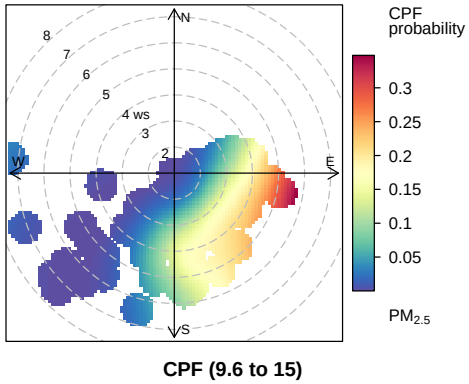

E.11(b): 50-75th percentile

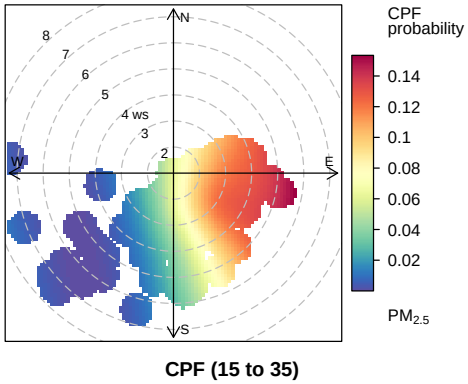

E.11(c): 75-100th percentile

Figure E.11: Conditional bivariate probability function plot of criteria pollutants at the SE site for (a) $PM_{2.5}$ concentrations between 6 and 9.6 μg m^{-3}, (b) $PM_{2.5}$ concentrations between 9.6 and 15 μg m^{-3}, and (c) $PM_{2.5}$ concentrations between 15 and 35 μg m^{-3}.

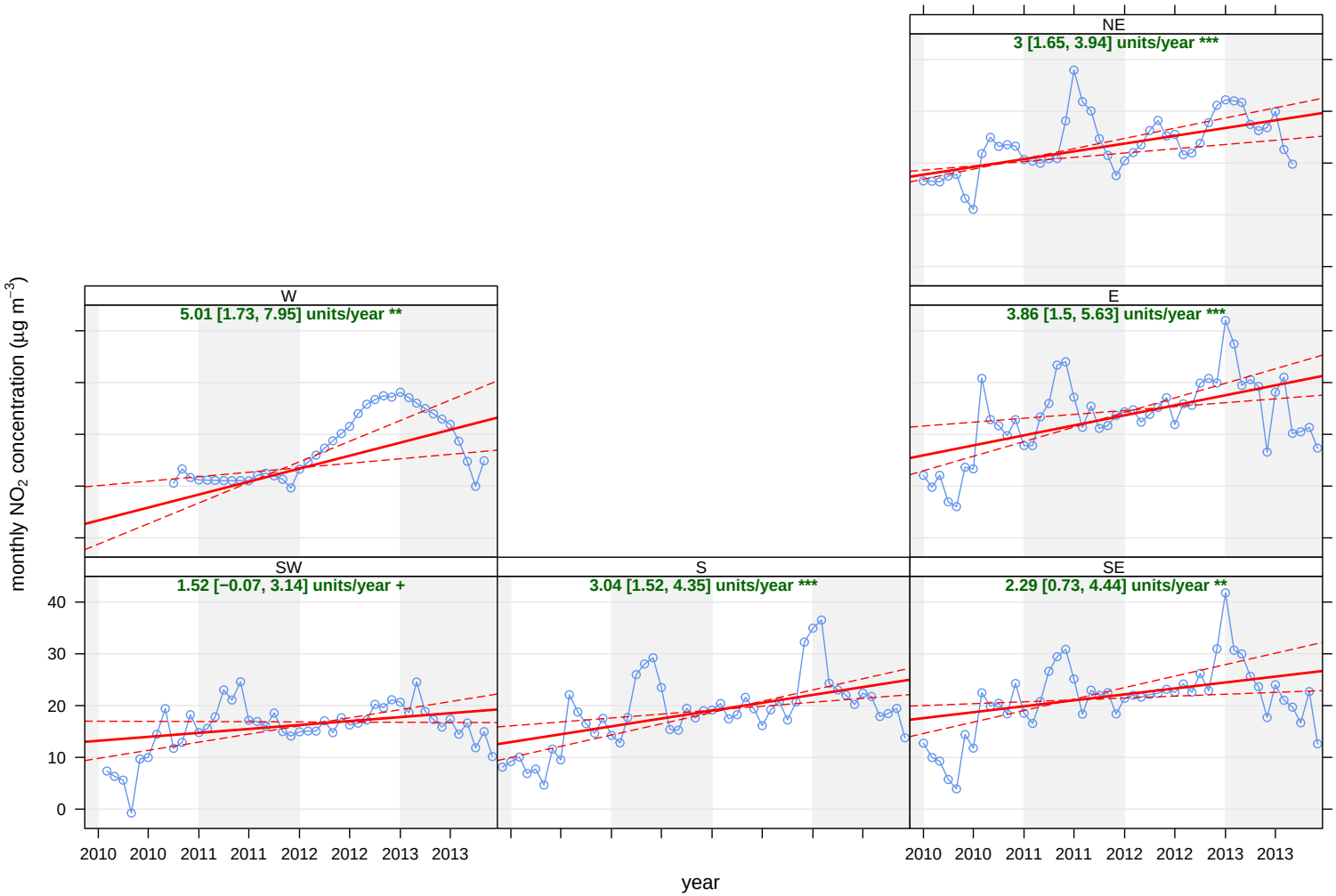

Figure E.12: Trend analysis of NO_2 at the industrial region of Santa Cruz according to wind sectors. The solid red line shows the trend estimate and the dashed red lines show the 95 % confidence intervals for the trend. The overall trend per year is shown at the top, before brackets, and the 95 % confidence intervals between brackets. $p < 0.001 = ***$, $p < 0.01 = **$, $p < 0.1 = +$

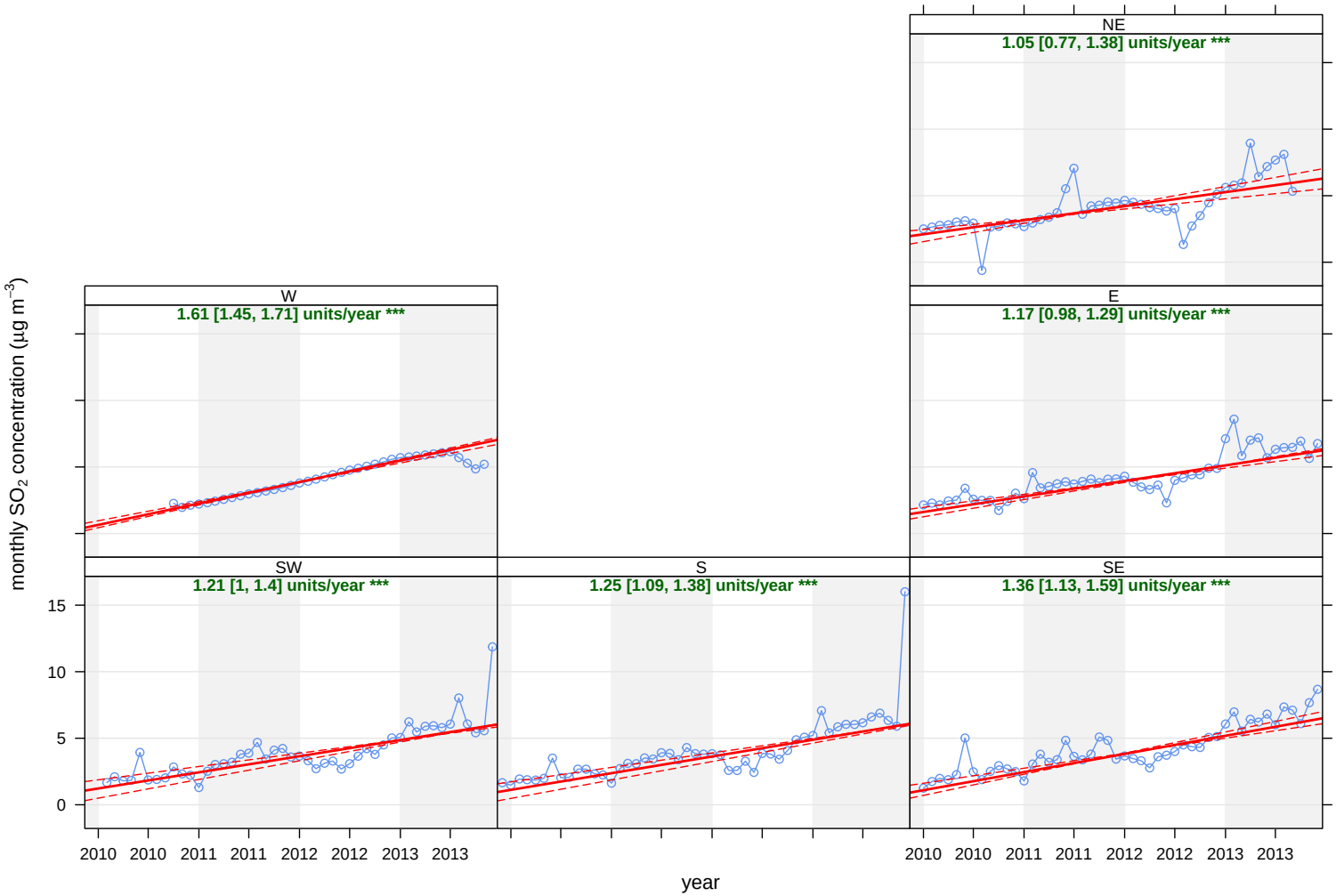

Figure E.13: Trend analysis of SO_2 at the industrial region of Santa Cruz according to wind sectors. The solid red line shows the trend estimate and the dashed red lines show the 95 % confidence intervals for the trend. The overall trend per year is shown at the top, before brackets, and the 95 % confidence intervals between brackets. $p < 0.001 = ***$

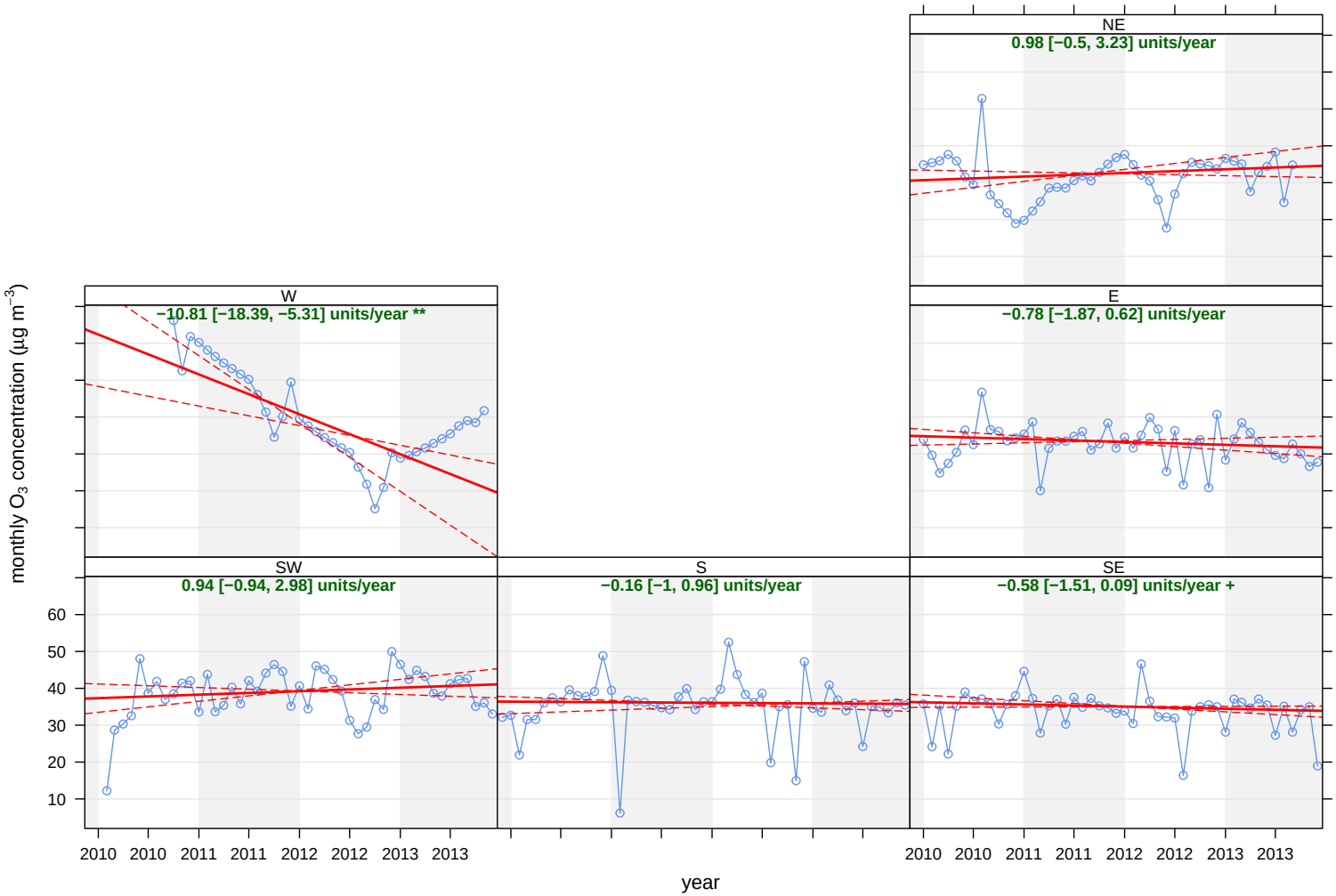

Figure E.14: Trend analysis of O_3 at the industrial region of Santa Cruz according to wind sectors. The solid red line shows the trend estimate and the dashed red lines show the 95 % confidence intervals for the trend. The overall trend per year is shown at the top, before brackets, and the 95 % confidence intervals between brackets. $p < 0.01$ = **, $p < 0.1$ = +

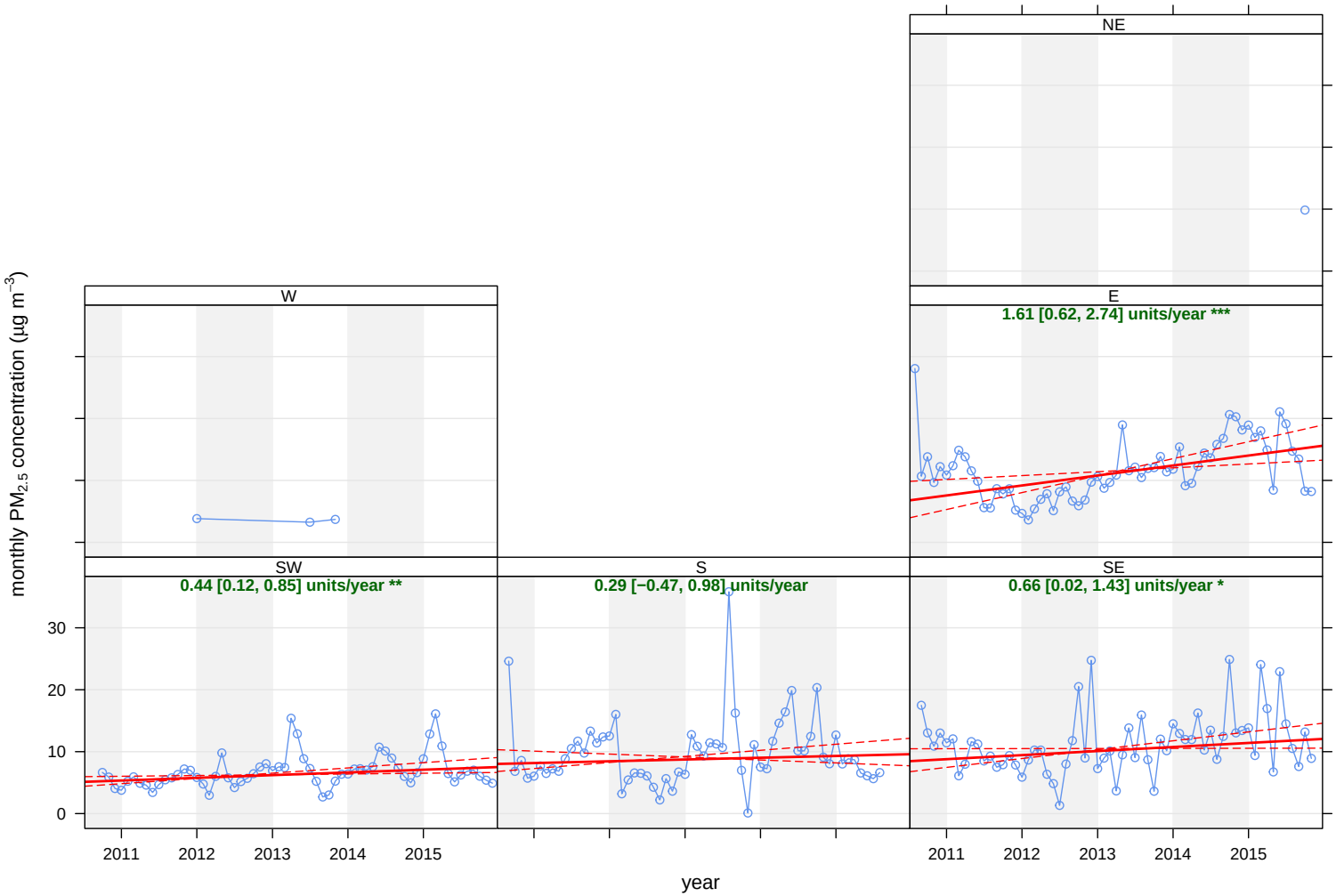

Figure E.15: Trend analysis of $PM_{2.5}$ at the industrial region of Santa Cruz according to wind sectors (2010-2015). The solid red line shows the trend estimate and the dashed red lines show the 95 % confidence intervals for the trend. The overall trend per year is shown at the top, before brackets, and the 95 % confidence intervals between brackets. $p < 0.001 = ***$, $p < 0.01 = **$, $p < 0.05 = *$

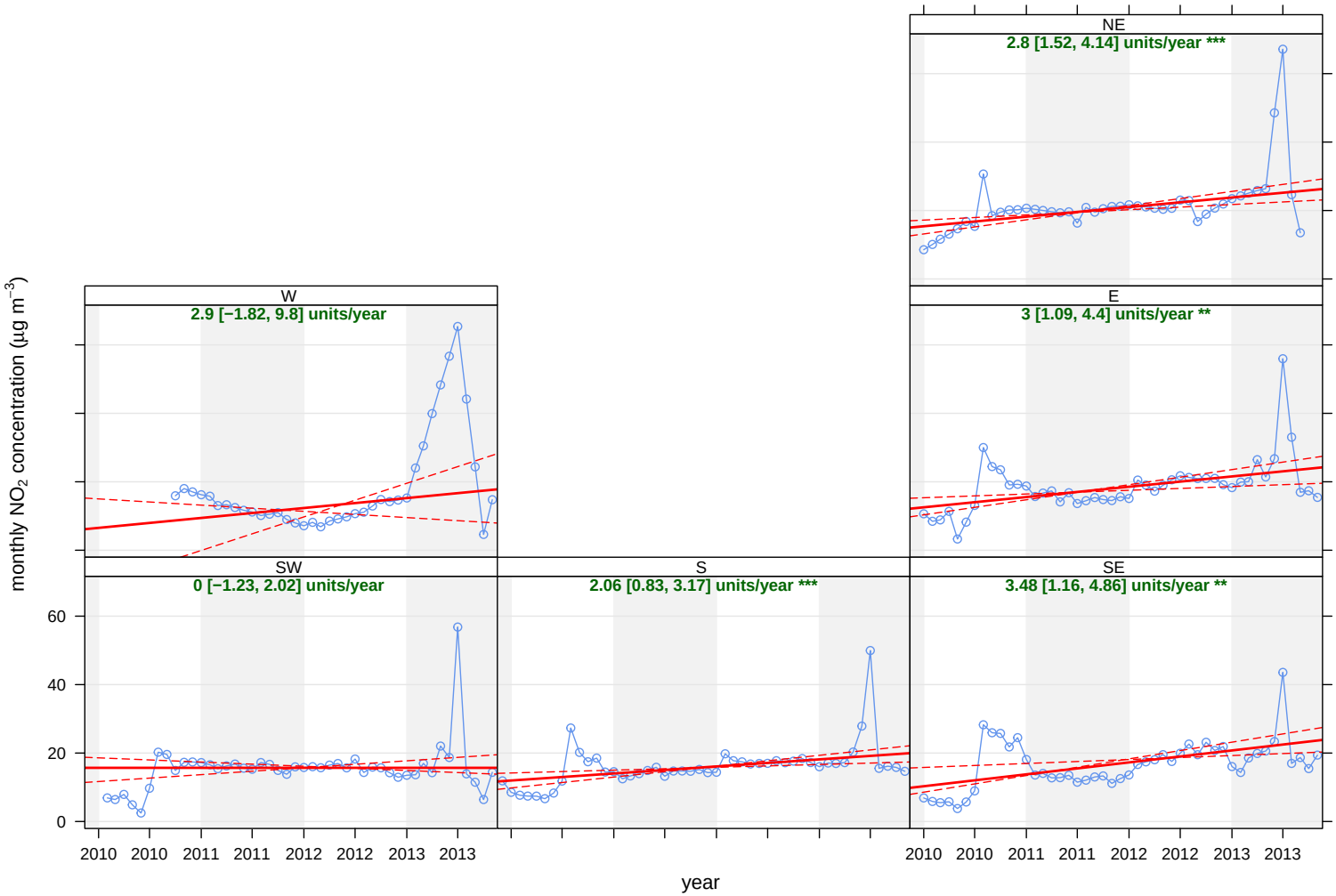

Figure E.16: Trend analysis of NO_2 at the reference site (Seropédica) according to wind sectors. The solid red line shows the trend estimate and the dashed red lines show the 95 % confidence intervals for the trend. The overall trend per year is shown at the top, before brackets, and the 95 % confidence intervals between brackets. p < 0.001 = ***, p<0.01 = **

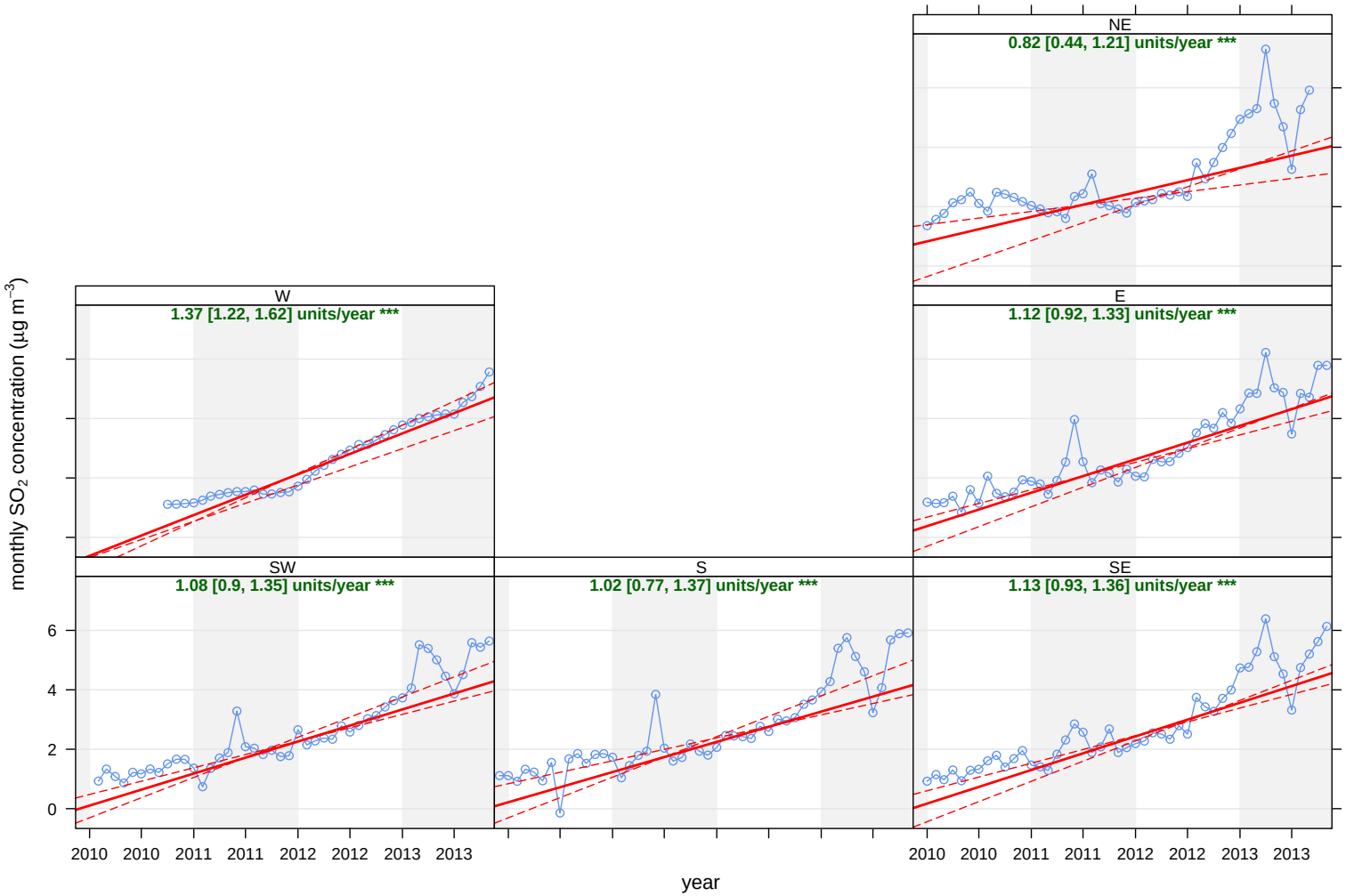

Figure E.17: Trend analysis of SO_2 at the reference site (Seropédica) according to wind sectors. The solid red line shows the trend estimate and the dashed red lines show the 95 % confidence intervals for the trend. The overall trend per year is shown at the top, before brackets, and the 95 % confidence intervals between brackets. $p < 0.001 = ***$

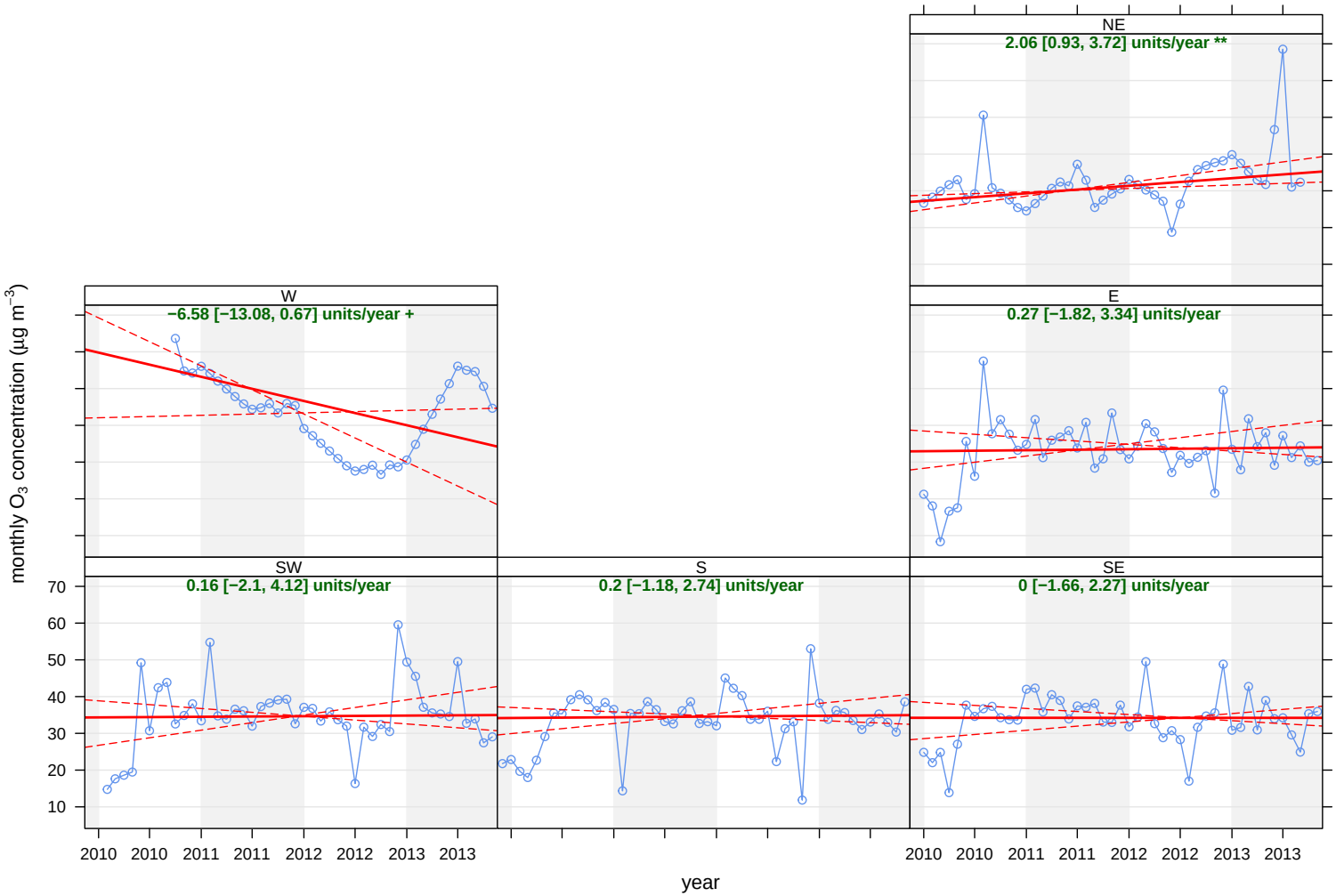

Figure E.18: Trend analysis of O_3 at the reference site (Seropédica) according to wind sectors. The solid red line shows the trend estimate and the dashed red lines show the 95 % confidence intervals for the trend. The overall trend per year is shown at the top, before brackets, and the 95 % confidence intervals between brackets. $p < 0.01 = **$, $p < 0.1 = +$

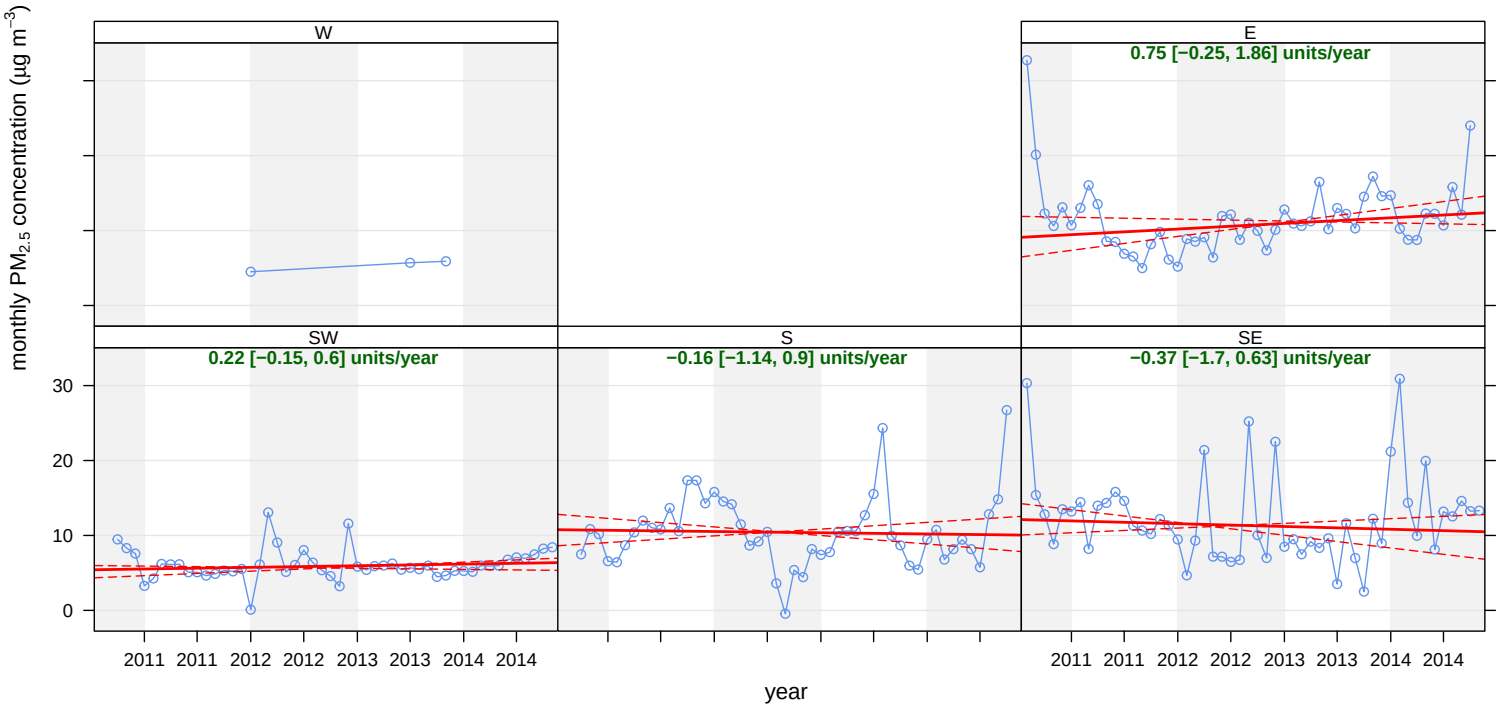

Figure E.19: Trend analysis of $PM_{2.5}$ at the reference site (Seropédica) according to wind sectors (2010-2014). The solid red line shows the trend estimate and the dashed red lines show the 95 % confidence intervals for the trend. The overall trend per year is shown at the top, before brackets, and the 95 % confidence intervals between brackets.

Table E.1: Detection limits (DL) for the determination of total water-soluble carbon (TWSC), water-soluble inorganic carbon (WSIC), water-soluble cations and anions, and elemental concentration in $PM_{2.5}$ samples.

Detection limit (ng m^{-3})	Analyzed species
0.01-1	Ag, Co, Ni, Sb, Sn, Th, Ti, Tl
1-10	Bi, Cd, Cr, Cu, V, Mg^{2+}, NH_4^+, NO_2^-
10-30	Mn, Pb, Oxalate
30-100	Ca^{2+}, K^+, NO_3^+
100-1000	Fe, Cl^-, SO_4^{2-}, WSIC
> 1000	Al, Zn, Na^+, TWSC

Table E.2: Measured concentrations (average ± standard deviation, mg kg^{-1}) and extraction efficiencies (%) for the analysis by ICP-MS of the certified reference material NIST-SRM 1648a.

Element	Measured	Reference	Extraction efficiency
Ag	6.4 ± 0.5	6.0 ± 0.3	98
Al	5229 ± 166	34,300 ± 1300	15
Cd	72.1 ± 8.0	73.7 ± 2.3	98
Co	11.62 ± 1.69	17.93 ± 0.68	65
Cr	81 ± 5	402 ± 13	20
Cu	509 ± 65	610 ± 70	84
Fe	29,996 ± 3261	39,200 ± 2100	69
Mn	583 ± 81	790 ± 44	74
Ni	81.5 ± 7.3	81.1 ± 6.8	100
Pb	6553 ± 1025	6550 ± 330	100
Sb	13.1 ± 1.8	45.4 ± 1.4	29
Ti	785 ± 84	4021 ± 86	20
V	95 ± 11	127 ± 11	75
Zn	2275 ± 300	4800 ± 270	53

Table E.3: Average (range in parentheses) concentration of speciated $PM_{2.5}$ components (μg m^{-3}) in the first (Aug/10-Jul/11) and second evaluation period (Jan-Dec/13).

Variable	CA		CJ		SE	
	Aug/10-Jul/11	Jan-Dec/13	Aug/10-Jul/11	Jan-Dec/13	Aug/10-Jul/11	Jan-Dec/13
Ag	*	<DL	*	<DL	*	<DL
Al	<DL	<DL	<DL	<DL	<DL	<DL
Bi	*	<DL	*	<DL	*	<DL

Continuation of Table E.3

Variable	CA		CJ		SE	
	Aug/10-Jul/11	Jan-Dec/13	Aug/10-Jul/11	Jan-Dec/13	Aug/10-Jul/11	Jan-Dec/13
Cd	<DL	<DL	<DL	<DL	<DL	<DL
Co	*	<DL	*	<DL	*	<DL
Cr	<DL	<DL	<DL	<DL	<DL	<DL
Cu[a]	62.11 (11.61-189.9)	19.78 (9.96-40.20)	13.35 (7.59-22.84)	11.35 (8.01-13.69)	50.96 (11.50-530.6)	18.39 (1.66-40.79)
Fe	<DL	<DL	<DL	<DL	<DL	<DL
Mn[a]	21.68 (13.17-37.81)	<DL	19.33 (12.76-21.63)	<DL	18.39 (14.37-20.93)	<DL
Ni[a]	1.82 (0.03-13.79)	1.26 (0.16-3.96)	2.07 (0.10-9.61)	0.98 (0.06-2.48)	1.77 (0.07-7.05)	0.90 (0.18-2.87)
Pb	<DL	<DL	<DL	<DL	<DL	<DL
Sb[b]	1132 (235.7-5924)	<DL	1276 (245.7-4858)	<DL	1580 (251.5-9374)	<DL
Sn	*	<DL	*	<DL	*	<DL
Th	*	<DL	*	<DL	*	<DL
Ti[a]	7.99 (0.18-44.92)	7.08 (1.00-15.97)	8.34 (0.21-33.87)	7.55 (1.14-17.49)	7.70 (0.16-44.18)	6.88 (1.06-16.76)
Tl	*	<DL	*	<DL	*	<DL
V[a]	5.07 (2.37-14.45)	<DL	6.06 (2.98-18.23)	<DL	4.82 (2.65-9.77)	<DL
Zn	<DL	<DL	<DL	<DL	<DL	<DL
Ca^{2+}	0.24 (0.07-0.65)	0.28 (0.07-0.81)	0.24 (0.08-0.51)	0.24 (0.07-0.85)	0.24 (0.07-0.58)	0.23 (0.07-0.74)
Mg^{2+}	0.23 (0.01-1.07)	0.07 (0.01-0.23)	0.29 (0.02-1.24)	0.07 (0.01-0.24)	0.23 (0.01-1.16)	0.06 (0.01-0.23)
NH_4^+ [a]	*	9.84 (2.94-52.44)	*	10.71 (3.35-50.281)	*	6.61 (2.97-13.02)
K^+	0.09 (0.08-0.11)	0.18 (0.08-0.53)	0.09 (0.08-0.10)	0.24 (0.10-0.64)	0.11 (0.08-0.21)	0.20 (0.08-0.60)
Cl^-	0.93 (0.14-4.95)	0.50 (0.18-1.15)	1.05 (0.13-3.14)	0.50 (0.13-1.13)	1.17 (0.15-6.43)	0.36 (0.15-1.07)

Continuation of Table E.3

Variable	CA		CJ		SE	
	Aug/10-Jul/11	Jan-Dec/13	Aug/10-Jul/11	Jan-Dec/13	Aug/10-Jul/11	Jan-Dec/13
NO_2^- [a]	*	0.07 (0.01-0.23)	*	0.07 (0.01-0.24)	*	0.06 (0.01-0.23)
NO_3^-	1.30 (0.11-4.72)	0.90 (0.13-3.41)	1.64 (0.19-4.22)	1.11 (0.17-4.03)	1.69 (0.21-9.27)	0.79 (0.14-1.84)
SO_4^{2-}	3.21 (1.00-10.58)	2.85 (1.20-5.92)	4.17 (0.98-12.62)	2.57 (1.25-6.70)	3.71 (1.29-10.52)	2.70 (1.19-6.38)
Oxalate	*	0.31 (0.05-0.74)	*	0.30 (0.05-0.75)	*	0.32 (0.03-0.83)
WSOC	1.83 (0.29-9.38)	1.11 (0.75-1.45)	1.28 (0.30-5.19)	1.13 (0.40-1.92)	1.67 (0.31-4.17)	0.89 (0.24-1.61)

*: not analyzed; <DL: lower than the detection limit

[a]: ng m^{-3}; [b]: pg m^{-3}

F
Supplementary material - 2

Table F.1: Average (range in parentheses) concentration of speciated TSP and PM_{10} components (elements) (μg m^{-3}) at Mário Xavier National Florest (FLONA) and Serra dos Órgãos National Park (PARNA), respectively. Other sites from the literature are added for comparison purposes.

Variable	FLONA	PARNA	TSP Ref.(125)	PM_{10} Ref.(125)	PM_{10} Ref.(174)	TSP Ref.(176)
Al	4.24 (0.24-22.9)	3.39 (0.05-18.4)	1.09 (0.31-1.80)	0.43 (0.12-0.66)	0.12 (0.06-0.21)	*
Cd	31.7 (0.06-77.4) [a]	9.00 (0.13-55.1) [a]	*	*	0.19 (0.10-0.35) [a]	2.33 (0.16-6.31) [a]
Cr	2.19 (0.63-5.57) [a]	3.98 (0.39-12.4) [a]	13 (8-19) [a]	<DL	1.60 (0.56-3.5) [a]	10.2 (1.36-22.6) [a]
Cu	13.1 (1.84-56.6) [a]	117.1 (3.84-1030) [a]	179 (130-253) [a]	87 (58-167) [a]	9.2 (6.6-14.8) [a]	76.5 (10.9-198) [a]
Fe	402.0 (0.95-2385) [a]	505.0 (5.10-1822) [a]	4101 (2479-6490) [a]	994 (418-1779) [a]	330 (175-550) [a]	2820 (133-6401) [a]
Mn	31.4 (3.43-111.6) [a]	17.1 (0.33-47.9) [a]	54 (30-90) [a]	14 (5-24) [a]	8.9 (4.7-16.1) [a]	72.9 (3.22-170) [a]
Ni	20.7 (0.71-111.0) [a]	3.11 (0.15-10.6) [a]	*	*	2.9 (1.57-4.7) [a]	6.61 (0.36-18.1) [a]
Pb	7.79 (1.28-47.8) [a]	16.5 (0.90-51.7) [a]	*	*	8.9 (6.2-14.4) [a]	73.0 (12.1-173) [a]
Sb	0.05 (0.04-0.08)	0.12 (0.00-2.23)	*	*	1.45 (1.04-2.4) [a]	*

Continuation of Table F.1

Variable	FLONA	PARNA	TSP Ref.(125)	PM_{10} Ref.(125)	PM_{10} Ref.(174)	TSP Ref.(176)
Si	0.42 (0.03-1.78)	0.94 (0.07-3.00)	*	*	*	*
Ti	53.9 (3.21-221.8) [a]	20.3 (0.93-74.2) [a]	*	*	6.7 (3.7-13.1) [a]	*
V	4.84 (0.24-24.0) [a]	5.69 (0.01-41.3) [a]	7 (4-16) [a]	5 (1-10) [a]	2.1 (1.08-3.6) [a]	6.91 (0.22-22.8) [a]
Zn	7.01 (0.17-44.4)	4.43 (0.14-26.6)	0.13 (0.07-0.18)	0.04 (0.02-0.09)	0.03 (0.02-0.05)	0.22 (0.01-0.80)
Ca^{2+}	1.26 (0.00-7.29)	0.55 (0.00-3.22)	*	*	0.40 (0.23-0.62)	1.97 (0.17-6.94)
Mg^{2+}	0.42 (0.03-1.57)	0.14 (0.00-0.56)	*	*	0.11 (0.06-0.17)	0.23 0.02-0.85
Na^{+}	5.64 (0.11-18.5)	3.76 (0.10-16.2)	*	*	0.57 (0.26-0.96)	0.56 (0.20-1.16)
NH_4^{+} [a]	462.7 (5.5-87.0)	33.8 (0.05-184.6)	*	*	1180 (510-2900)	4200 (99.7-13100)
K^{+}	0.44 (0.04-2.28)	0.33 (0.00-2.04)	*	*	0.11 (0.08-0.15)	0.51 (0.06-1.54)
Li^{+} [a]	34.3 (27.5-39.4)	6.87 (0.03-38.6)	*	*	*	*

Continuation of Table F.1

Variable	FLONA	PARNA	TSP Ref.(125)	PM_{10} Ref.(125)	PM_{10} Ref.(174)	TSP Ref.(176)
Br^-	0.11 (0.05-1.87)	0.21 (0.00-0.57)	*	*	*	*
F^-	0.05 (0.00-0.10)	0.07 (0.00-0.18)	*	*	*	0.08 9.32E-4-0.35
Cl^-	2.01 (0.16-11.0)	1.13 (0.00-9.59)	*	*	0.56 (0.18-1.07)	0.71 (0.02-3.24)
NO_3^-	2.20 (0.26-15.0)	1.70 (0.02-16.1)	*	*	3.7 (1.88-7.5)	7.63 (0.39-27.6)
PO_4^{3-}	0.10 (0.02-0.23)	0.21 (0.00-1.13)	*	*	*	*
SO_4^{2-}	3.53 (0.75-13.7)	4.92 (0.03-25.6)	*	*	2.1 (1.51-3.7)	9.64 (0.26-31.1)
Acetate	0.03 (0.02-0.06)	0.15 (0.00-1.17)	*	*	*	*
Formate	0.22 (0.07-0.54)	0.04 (0.00-0.25)	*	*	*	*
Malonate	0.08 (0.02-0.16)	0.14 (0.01-1.80)	*	*	*	*
Oxalate	0.57 (0.14-1.14)	0.67 (0.11-2.65)	*	*	*	*

Continuation of Table F.1

Variable	FLONA	PARNA	TSP Ref.(125)	PM_{10} Ref.(125)	PM_{10} Ref.(174)	TSP Ref.(176)
WSOC	1.90 (0.88-3.78)	2.95 (1.32-4.69)	*	*	*	*

*: not analyzed; <DL: lower than the detection limit

[a]: ng m^{-3}

G
Supplementary material - 3

Table G.1: Summary of socio-demographic characteristics of the respondents ($n = 454$) and NH_3 exposures (Retrieved from Blanes-Vidal et al. 2014 (34))

	n(%)
Gender	
Male	245 (54)
Female	209 (46)
Age [a]	
$<$ 40 years	80 (18)
40-60 years	210 (46)
$>$ 60 years	164 (36)
Smoking	
No	389 (86)
Yes	65 (14)
Years living in the household [a]	
$\leq$ 25 years	218 (48)
$>$ 25 years	236 (52)
Children at home	
No	343 (76)
Yes	111 (24)
Time spent at home [a]	
$\leq$ 100 h/week	184 (41)
$>$ 100 h/week	270 (59)

[a] Mean $\pm$ Standard deviation:
- Age: 54 ± 14 years
- Years living in the area: $30 + 20$ years
- Time spent at home: 114 ± 37 h/week

[b] Source-related jobs are jobs related to animal production, agriculture or farming.

[c] The most common self-reported health conditions were diabetes, cardiovascular conditions and digestive diseases.

TableG.1 – continued from previous page

	n(%)
Job [a]	
Not source-related	412 (91)
Source-related	42 (9)
Health conditions	
Acute respiratory	46 (10)
Chronic respiratory	41 (9)
Other health conditions [c]	67 (15)
NH_3 exposures: Range (mean $\pm$ standard deviation), $\mu g\ m^{-3}$	
$< 0.5 (0.15 \pm 0.00)$	14 (3)
$0.5 - 1 (0.89 \pm 0.09)$	37 (8)
$1 - 1.5 (1.27 \pm 0.15)$	91 (20)
$1.5 - 2 (1.74 \pm 0.16)$	101 (22)
$2 - 2.5 (2.24 \pm 0.16)$	74 (16)
$2.5 - 3 (2.69 \pm 0.14)$	45 (10)
$3 - 3.5 (3.21 \pm 0.13)$	43 (9)
$> 3.5 (5.10 \pm 1.67)$	49 (11)

[a] Mean $\pm$ Standard deviation:

- Age: 54 ± 14 years
- Years living in the area: $30 + 20$ years
- Time spent at home: 114 ± 37 h/week

[b] Source-related jobs are jobs related to animal production, agriculture or farming.

[c] The most common self-reported health conditions were diabetes, cardiovascular conditions and digestive diseases.

Table G.2: PSY, measured by one indicator: Explained variance (R^2) for both observed and latent variables.

Variable		R^2
Class	Name	
Observed covariate		
	NH_3 exposure	1.000
Observed response		
	Eyes itching dryness or irritation	0.844
	Nose itching dryness or irritation	0.856
	Runny nose	0.678
	Nausea	0.767
	Cough	0.648
	Chest wheezing or whistling	0.501
	Difficulty breathing	0.563
	Fatigue	0.775
	Headache	0.701
	Difficulty concentrating	0.809
	Dizziness	0.696
	Odor annoyance	0.901
Endogenous latent		
	SIS	0.163
	RNS	0.063
	PSY	0.240

Table G.3: PSY - measured by odor annoyance, behavioral interference, and health risk perception: Explained variance per variable, R^2.

Variable		R^2
Class	Name	
Observed covariate		
	NH_3 exposure	1.000
Observed response		
	Eyes itching dryness or irritation	0.847
	Nose itching dryness or irritation	0.850
	Runny nose	0.676
	Nausea	0.760
	Cough	0.650
	Chest wheezing or whistling	0.512
	Difficulty breathing	0.555
	Fatigue	0.771
	Headache	0.695
	Difficulty concentrating	0.813
	Dizziness	0.701
	Odor annoyance	0.740
	Behavioral interference	0.720
	Health risk perception	0.825
Endogenous latent		
	SIS	0.171
	RNS	0.157
	PSY	0.249